

USE OF TIME DOMAIN (TD) AND FAST FIELD CYCLING (FFC) NMR  
RELAXOMETRY TO DESIGN AND CHARACTERIZE SOFT CANDY  
PRODUCTS

A THESIS SUBMITTED TO  
THE GRADUATE SCHOOL OF NATURAL AND APPLIED SCIENCES  
OF  
MIDDLE EAST TECHNICAL UNIVERSITY

BY

PELİN POÇAN

IN PARTIAL FULFILLMENT OF THE REQUIREMENTS  
FOR  
THE DEGREE OF DOCTOR OF PHILOSOPHY  
IN  
FOOD ENGINEERING

AUGUST 2021



Approval of the thesis:

**USE OF TIME DOMAIN (TD) AND FAST FIELD CYCLING (FFC) NMR  
RELAXOMETRY TO DESIGN AND CHARACTERIZE SOFT CANDY  
PRODUCTS**

submitted by **PELİN POÇAN** in partial fulfillment of the requirements for the degree of Doctor of Philosophy in Food Engineering, **Middle East Technical University** by,

Prof. Dr. Halil Kalıpçılar  
Dean, Graduate School of **Natural and Applied Sciences**

Prof. Dr. Serpil Şahin  
Head of the Department, **Food Engineering**

Assoc. Prof. Dr. Mecit Halil Öztop  
Supervisor, **Food Engineering, METU**

Prof. Dr. Behiç Mert  
Co-Supervisor, **Food Engineering, METU**

**Examining Committee Members:**

Prof. Dr. Gülüm Şümnü  
Food Engineering, METU

Assoc. Prof. Dr. Mecit Halil Öztop  
Food Engineering, METU

Prof. Dr. Hami Alpas  
Food Engineering, METU

Prof. Dr. Hussnain A. Janjua  
Industrial Biotechnology, ASAB-NUST

Assist. Prof. Dr. Nadide Seyhun  
Food Technology, Kocaeli University

Date: 20.08.2021

**I hereby declare that all information in this document has been obtained and presented in accordance with academic rules and ethical conduct. I also declare that, as required by these rules and conduct, I have fully cited and referenced all material and results that are not original to this work.**

Name Last name : Pelin Poçan

Signature :

## **ABSTRACT**

### **USE OF TIME DOMAIN (TD) AND FAST FIELD CYCLING (FFC) NMR RELAXOMETRY TO DESIGN AND CHARACTERIZE SOFT CANDY PRODUCTS**

Poçan, Pelin

Doctor of Philosophy, Food Engineering  
Supervisor: Assoc. Prof. Dr. Mecit Halil Öztop  
Co-Supervisor: Prof. Dr. Behiç Mert

August 2021, 287 pages

Confectionary gels are considered as composite gel systems consisting of high amount of sugar and gelling agents such as gelatin or starch. Production of low-calorie soft confectionery products has been the interest of the industry in recent years. D-allulose is classified as one of the rare sugar; sugars which are found in rare amounts in nature. It is a C-3 epimer of fructose and has 70% of the sweetness of sucrose with much less caloric value of 0.39 kcal/g compared to common sugars. Utilization of D-allulose in food products is gaining particular interest due to its low caloric value. In this study, D-Allulose was used to formulate soft candies.

NMR Relaxometry based methods are known as nondestructive techniques and can be used to obtain significant information on the physiochemical properties of many food systems. Time Domain (TD) and Fast Field Cycling (FFC) NMR Relaxometry are the two methods that can be used for characterization purposes. Time domain methods mostly rely on the interpretation of spin-spin ( $T_2$ ) and spin-lattice ( $T_1$ )

relaxation times at a fixed magnetic field strength whereas FFC NMR uses a changing magnetic field to obtain information at molecular level.

In this dissertation, allulose containing soft candies were formulated using different gelling agents and gels were characterized by different relaxometry techniques.

In the 1<sup>st</sup> part of the study, effect of D-allulose substitution was explored on the quality of the gelatin-based candies by using Time Domain NMR methods. For characterization of the soft candies, moisture content, water activity, color, hardness, and glass transition temperature of samples were investigated. X-ray diffraction analysis was also performed to explain the crystallization tendency of jelly candies. Results showed that, the softest sample with the highest moisture content and the smallest crystallization tendency was the sample that included the highest amount of D-allulose. Time domain (TD) NMR relaxometry experiments were conducted on gel samples through the measurement of  $T_2$  and  $T_1$  relaxation times at a 20.35 MHz system.  $T_2$  results showed the presence of three distinct proton populations in the relaxation spectrum for all formulations. Spin-lattice relaxation times obtained through mono-exponential fitting ( $T_1$ ) were also obtained to explain some quality parameters.

In the second part of the study, again effect of D-allulose substitution on gelatin based confectionery gels were studied by using Fast Field Cycling (FFC) NMR relaxometry. . For this part of the study,  $^1\text{H}$  spin-lattice relaxation ( $T_1$ ) experiments for gelatin-based candies prepared by different amounts of D-allulose have been performed in the frequency range of 4 kHz–40 MHz. In addition, physical properties such as moisture content and hardness were also measured. Analysis of NMR dispersion profiles showed the presence of two fractions of water: *confined and free-water*. The relaxation data have been associated with parameters characterizing translation diffusion and rotation of the confined-water molecules and dynamics of the free-water fraction. The translation dynamics has turned out to be about three orders of magnitude slower compared to bulk water; the time scale of the rotational

dynamics was similar to that of translation diffusion. Moreover, quantitative analysis of the relaxation data provided a unique parameter, the number of water molecules undergoing translation dynamics within the confined-water fraction per unit volume. On this basis, the influence of D-allulose on the mechanisms of water motion were discussed.

In the 3<sup>rd</sup> part of the dissertation, starch based confectionery gels were examined by using both TD-NMR and FFC NMR relaxometry experiments. This time allulose was not used but focus was the use of relaxometry techniques on the starch based candies formulated using different corn syrup types. As the system of interest, Turkish delights (*lokum*) being starch based confectionery gels were formulated.

Turkish delights are traditional confectionery products that contains mainly sucrose as the sugar source and starch as the gelling agent. However, manufacturers sometimes might prefer to use corn syrup instead of sucrose to decrease the cost. This case jeopardizes the originality of Turkish delights and led to production of adulterated samples. In this part of the study, Turkish delights were formulated by using sucrose (original one) and different type of corn syrups (SBF10, SCG40 and SCG60). For all samples, moisture content measurements, texture profile analysis (TPA), X-ray Diffraction Analysis, color analysis, TD-NMR and FFC-NMR experiments were performed. FFC experiments were also performed at two different temperature: 4 °C and 25 ° to understand the water dynamics of the samples at different temperatures. Results clearly indicated that, corn syrups containing samples had improved textural properties and were less prone to crystallization. However, this case affected the authenticity of the products. Both TD-NMR and FFC-NMR techniques were found to be effective to discriminate the original samples from the corn syrup containing ones. According to the results of TD-NMR experiments, two distinct proton population was observed for all formulations. In addition, quantitative analysis of FFC-NMR showed that, apart from the rotational motions, molecules in Turkish delights (mainly water but also sugar molecules) undergo two types of translational dynamics.

To summarize, this dissertation enlightens the possible application areas of TD-NMR and FFC-NMR to characterize the soft candy products as an alternative to the commonly used well-known methods such as *X-ray Diffraction*, *Thermo-gravimetric Analysis (TGA)* or *Texture Profile Analysis (TPA)*. In addition, it gives deep insight to the researchers about the utilization of TD-NMR and FFC-NMR Relaxometry as an authenticity and quality detection tool for the analysis of confectionery gels.

**Keywords:** Confectionery Gels, Time Domain (TD) NMR Relaxometry, Fast Field Cycling (FFC) NMR Relaxometry, Water Dynamics, D-allulose



## ÖZ

### ZAMANSAL ALANLI VE HIZLI ALAN DÖNGÜLÜ NMR RELAKSOMETRE KULLANILARAK YUMUŞAK ŞEKERLEME ÜRÜNLERİNİN TASARIM VE KARAKTERİZASYONU

Poçan, Pelin  
Doktora, Gıda Mühendisliği  
Tez Yöneticisi: Doç. Dr. Mecit Halil Öztop  
Ortak Tez Yöneticisi: Prof. Dr. Behiç Mert

Ağustos 2021, 287 sayfa

Jelly şekerlemeler, yüksek miktarda şeker, jelatin veya nişasta gibi jelleştirici maddelerden oluşan kompozit jel sistemleri olarak kabul edilir. Son zamanlarda kalorisiz düşük şekerleme üretimine olan talep artmıştır. Nadir şekerler doğal kaynaklarda miktarda az bulunan şekerlerdir. 'D-alüloz, fruktozun C-3 epimeri olan ve 0.39 kcal/g kalori değeri ile sakkarozun tatlılığının %70'ine sahip olan bir nadir şeker türü olarak sınıflandırılmaktadır. D-alülozun gıda ürünlerinde kullanımı, düşük kalori değeri nedeniyle özel ilgi görmektedir.

NMR Relaxometri tabanlı yöntemler, tahribatsız teknikler olarak bilinir ve birçok gıda sisteminin fizyokimyasal özellikleri hakkında önemli bilgiler elde etmek için kullanılabilir. Zaman Alanlı (TD) ve Hızlı Alan Döngülü (FFC) NMR metotları, karakterizasyon amacıyla kullanılabilir iki yöntemdir. Zaman alanlı yöntemler genellikle sabit bir manyetik alan kuvvetinde  $T_2$  ve  $T_1$  relaksasyon sürelerinin yorumlanmasına dayanırken, FFC NMR moleküler düzeyde bilgi elde etmek için değişen bir manyetik alan kullanır.

Çalışmanın 1. bölümünde D-alüloz ikamesinin ürünlerin kalitesine etkisi araştırılmıştır. Yumuşak şekerlerin karakterizasyonu için numunelerin nem içeriği, su aktivitesi, rengi, sertliği ve cam geçiş sıcaklığı incelenmiştir. Yumuşak şekerlerin kristalleşme eğilimini açıklamak için X-ışını kırınım analizi de yapılmıştır. Sonuçlar, en yüksek nem içeriğine ve en düşük kristalleşme eğilimine sahip en yumuşak numunenin, en yüksek miktarda D-alüloz içeren numune olduğunu göstermiştir. Jel numuneleri üzerinde zamansal alanlı NMR relaksometre deneyleri de yapılmış ve tüm formülasyonlar için relaksasyon spektrumunda üç farklı proton havuzu gözlenmiştir.

Çalışmanın ikinci bölümünde yine D-alüloz ikamesinin jelatin bazlı şekerleme jelleri üzerindeki etkisi incelenmiş ancak bu sefer “Zamansal alanlı NMR (TD-NMR)” yerine “Hızlı Alan Döngülü NMR (FFC-NMR)” kullanılmıştır. Tezin bu bölümü için, farklı miktarlarda D-alüloz ile hazırlanan jelatin bazlı şekerler için FFC-NMR deneyleri 4 kHz-40 MHz frekans aralığında çalışılarak yapılmıştır. Ayrıca nem içeriği ve sertlik gibi fiziksel özellikler de ölçülmüştür. FFC deneyleri sonucunda elde edilen NMR dispersiyon profillerinin analizi, suyun iki fraksiyonunun varlığını göstermiştir: sınırlı su ve serbest su. Relaksasyon verileri, sınırlı su moleküllerinin translasyon difüzyonunu ve rotasyonunu ve serbest su fraksiyonunun dinamiklerini karakterize eden parametrelerle ilişkilendirilmiştir. Bu temelde, D-alülozun su hareketinin mekanizmaları üzerindeki etkisi tartışılmıştır.

Tezin 3. bölümünde nişasta bazlı şekerleme jellerine örnek olarak lokum formüle edilmiştir. Türk lokumu, şeker kaynağı olarak sükröz, jelleştirici madde olarak ise nişasta içeren geleneksel şekerleme ürünlerinden biridir. Ancak üreticiler bazen maliyeti düşürmek için sakkaroz yerine mısır şurubu kullanmayı tercih edebilirler. Bu durum Türk lokumunun orijinalliğini tehlikeye atmakta ve tağşişli lokumların üretilmesine neden olmaktadır. Bu çalışmanın ilk kısmında, lokumlar sükröz (orjinal) ve farklı mısır şurupları (SBF10, SCG40 ve SCG60) kullanılarak formüle edilmiştir. Tüm numuneler için nem içeriği ölçümleri, Tekstür Profil Analizi (TPA), X ışını Kırınım Analizi, renk analizi, TD-NMR ve FFC-NMR deneyleri yapılmıştır.

FFC deneyleri ayrıca numunelerin su dinamiklerini daha detaylı anlamak için 4°C ve 25 olmak üzere iki farklı sıcaklıkta gerçekleştirilmiştir. Sonuçlar, mısır şurubu içeren örneklerin gelişmiş dokusal özelliklere sahip olduğunu ve kristalleşmeye daha az yatkın olduğunu açıkça göstermiştir. Ancak bu durum ürünlerin orijinalitesini olumsuz etkilemiştir. Hem TD-NMR hem de FFC-NMR tekniklerinin, orijinal örnekleri (sükroz içeren) mısır şurubu içerenlerden ayırt etmede etkili olduğu bulundu. TD-NMR deneylerinin sonuçlarına göre, tüm formülasyonlar için iki farklı proton popülasyonu gözlemlendi. Ek olarak, FFC-NMR tekniğinin kantitatif analizi, dönme hareketlerinden ayrı olarak, Türk lokumlarındaki moleküllerin (esas olarak su ve ayrıca şeker moleküllerinin) iki tür dönüşüm dinamiğine maruz kaldığını göstermiştir.

Özetlemek gerekirse, bu tez, X-ışını Kırınımı, Termo-gravimetrik Analiz (TGA) veya Doku Profili Analizi (TPA) gibi yaygın olarak kullanılan iyi bilinen yöntemlere alternatif olarak yumuşak şekerleme ürünlerini karakterize etmek için TD-NMR ve FFC-NMR tekniğinin olası uygulama alanlarını aydınlatmaktadır. Ayrıca, şekerleme jellerinin analizi için bir özgünlük ve kalite tespit aracı olarak TD-NMR ve FFC-NMR Relaxometre tekniklerinin kullanımı hakkında araştırmacılara fikir vermektedir.

**Anahtar Kelimeler:** Şekerleme Jelleri, Zamansal Alanlı NMR Relaxometre (TD-NMR), Hızlı Alan Döngülü NMR Relaxometre (FFC-NMR), Su Dinamiği, D-Aluloz

To the memory of my grandmother...

## ACKNOWLEDGMENTS

I would like to express deepest gratitude to my supervisor Assoc. Prof. Dr. Mecit Halil Öztop for his continuous support, motivation and kind interest during my PhD study. It was a chance for me to study under his guidance in such a productive and successful team. I could not succeed without your help and support. Thank you very much for accepting me as a member of your team.

I would like acknowledge and thank to TUBITAK 2211-C National Priority Areas Doctoral Scholarship program and YOK 100/2000 Priority Areas Doctoral Scholarship program. It was an honor for me to be the first of the fellows of these scholarships' programs in food science and food engineering area.

I also gratefully acknowledge the financial support of National and Scientific Technological Council of Turkey under the COST Program (2515) with proposal number 1160759. The role of COST Action CA15209 (European Network on NMR Relaxometry) is also acknowledged.

My special thanks also go to Dr. Adam Rachocki for his help and support in learning FFC-NMR technology in Institute of Molecular Physics, Poznan Poland. The time that I spent in Poznan was short but really productive and it has a high contribution to this dissertation. I'm also very thankful to Assoc. Prof. Dr. Rachocki for his hospitality and kind interest during the days I spent in Poznan. I also gratefully acknowledge the help and support of Prof. Dr. Danuta Kruk for her help in analysis of FFC data and contribution to this dissertation.

Very special thanks go to my best lab mate, Esma Ilhan, for her continuous help and support during my PhD studies. It was a really big chance for me to work with you in the same project. Thank you very much for your friendship, being with me whenever I am happy or whenever I am sad and all enjoyable laboratory days that we spent together.

I would like to thank to other Oztop lab members especially Derya Ucbas, Sevil Cıkrıkçı, Selen Güner and Barış Özel for their help and support whenever I need. I also thank to Berkay Berk, Bilge Baştürk and Serap Namlı for their help during my experiments.

In addition, I really would like to thank Derya Ucbas and Tuğçe Topaloğlu for their friendship and continuous support especially during the anxious pandemic days that I spent in Ankara.

I would like to express my deepest appreciation to my best friend Helin Karaçam. Starting from our college days, you were always with me and supported me. Your lifetime friendship is a big chance for me.

Last but not least, I would like to express my deepest appreciation to my family, my mother Hülya Poçan, my father Ali Kemal Poçan and my sister Pınar Poçan. Thank you very much being with me during the most difficult and most enjoyable times that I spent during my PhD journey. I could not succeed without your help and support and thank you very much for supporting all my ideas in my life whatever my decision is.

## TABLE OF CONTENTS

ABSTRACT .....	iii
ÖZ.....	ix
ACKNOWLEDGMENTS .....	xiii
LIST OF TABLES.....	xix
LIST OF FIGURES .....	xxi
CHAPTERS	
1 INTRODUCTION .....	1
1.1 Confectionery Gels .....	1
1.1.1 Gelatin based Confectionery Gels .....	3
1.1.2 Starch based Confectionery Gels .....	5
1.1.2.1 Turkish Delights ( <i>Lokum</i> ).....	6
1.1.3 Other biopolymers used in the formulations of confectionery gels ....	9
1.2 Sugar Types Used in Confectionery Gels .....	9
1.2.1 Sucrose.....	9
1.2.2 Corn Syrup .....	12
1.2.3 Rare Sugars .....	15
1.3 Characterization of Confectionery Gels .....	18
1.3.1 Physical Characterization of Confectionery Gels .....	18
1.3.1.1 Moisture Content Determination.....	18
1.3.1.2 Water Activity ( $a_w$ ) Determination.....	20
1.3.1.3 Texture Profile Analysis (TPA) .....	20
1.3.2 Advanced Characterization Methods of Confectionery Gels .....	22

1.3.2.1	Thermo-gravimetric Analysis (TGA) .....	22
1.3.2.2	Differential Scanning Calorimetry (DSC) .....	24
1.3.2.3	X-Ray Diffraction (XRD) Analysis.....	26
1.4	Characterization of Gel Systems with NMR Relaxometry .....	28
1.4.1	Characterization of Gel Systems with Time Domain (TD) NMR Relaxometry.....	38
1.4.2	Characterization of Gel Systems with Fast Field Cycling (FFC) NMR Relaxometry.....	44
1.5	Objective of the Study .....	48
2	MATERIALS AND METHODS.....	51
2.1	Materials.....	51
2.1.1	Gelatin based Soft Candies .....	51
2.1.2	Turkish Delights .....	51
2.2	Methods.....	52
2.2.1	Gelatin based Soft Candies .....	52
2.2.1.1	Preparation of Gelatin based Soft Candies .....	52
2.2.1.2	Brix Measurement .....	53
2.2.1.3	Moisture Content Determination.....	53
2.2.1.4	Water Activity .....	54
2.2.1.5	Color .....	54
2.2.1.6	X-Ray Diffraction.....	54
2.2.1.7	Textural Analysis .....	55
2.2.1.8	Glass Transition Temperature Determination ( $T_g$ ).....	55
2.2.1.9	Time Domain (TD) NMR Relaxometry Experiments.....	55



2.2.1.10	Fast Field Cycling (FFC) NMR Relaxometry.....	56
2.2.1.11	Thermo gravimetric Analysis (TGA) .....	56
2.2.2	Turkish Delights .....	57
2.2.2.1	Preparation of Turkish Delights .....	57
2.2.2.2	Moisture Content Determination.....	58
2.2.2.3	Color Analysis.....	58
2.2.2.4	Texture Profile Analysis (TPA) .....	59
2.2.2.5	X-ray Diffraction.....	59
2.2.2.6	TD-NMR Relaxometry Experiments .....	59
2.2.2.7	Fast Field Cycling NMR Relaxometry Experiments.....	60
	Statistical Analysis .....	61
3	RESULTS AND DISCUSSION.....	63
3.1	Gelatin based Soft Candies .....	63
3.1.1	Moisture Content Determination.....	63
3.1.2	Water Activity Determination ( $a_w$ ).....	65
3.1.3	Color Measurements.....	67
3.1.4	X-ray Diffraction Analysis .....	69
3.1.5	Textural Analysis .....	73
3.1.6	Glass Transition Temperature ( $T_g$ ).....	75
3.1.7	Time Domain (TD) NMR Relaxometry .....	76
3.1.7.1	$T_1$ (Spin-Lattice) Relaxation Time .....	76
3.1.7.2	$T_2$ Relaxation Spectra .....	79
3.1.8	Fast Field Cycling (FFC) NMR Relaxometry.....	87
3.1.8.1	Theoretical Model .....	87

3.1.8.2	Effect of D-Allulose substitution on relaxation rates.....	94
3.1.9	Effect of D-allulose substitution on thermo gravimetric analysis (TGA) Thermograms .....	98
3.2	Turkish Delights .....	102
3.2.1	Moisture Content .....	102
3.3	Color Analysis .....	104
3.4	Texture Profile Analysis (TPA) .....	107
3.5	X-ray Diffraction Analysis.....	110
3.6	Time Domain (TD) NMR Relaxometry .....	112
3.6.1	$T_2$ (Spin-spin) Relaxation Spectra .....	112
3.7	Fast Field Cycling (FFC) NMR Relaxometry.....	116
4	CONCLUSION AND RECOMMENDATIONS .....	129
	REFERENCES .....	133
	APPENDICES.....	153
A.	Statistical Analysis Results for the Gelatin Based Confectionery Gels (Formulation & Storage Experiments).....	153
B.	Statistical Analysis Results of the TGA Experiments for the Gelatin Based Confectionery Gels .....	264
C.	Statistical Analysis Results for the Turkish Delights.....	268
	CURRICULUM VITAE .....	285

## LIST OF TABLES

### TABLES

Table 2.1. Specifications of corn syrup types that were used in the production of Turkish delights .....	52
Table 2.2. Gelatin based soft candies formulated with different D-Allulose substitution (wt (%)) .....	53
Table 2.3. Turkish delights formulated with different type of sugar type (corn syrup or sucrose) (w/w) (%) .....	58
Table 3.1. L*, a*, b* values of gelatin based soft candies at the first day of storage .....	69
Table 3.2. T <sub>2</sub> (spin-spin) relaxation results of each compartment observed in relaxation spectrum for gelatin based soft candies .....	84
Table 3.3. Relative area (%) (RA) of each peak observed in relaxation spectrum for gelatin based soft candies .....	85
Table 3.4. Gelatin based soft candies with different D-allulose substitution (wt %) .....	87
Table 3.5. Parameters obtained from the fits presented in Figure 3.11 .....	93
Table 3.6. Moisture content (%) and hardness values for gelatin based soft candies containing different amount of D-allulose .....	94
Table 3.7. Mass loss at first decomposition and peak temperatures.....	100
Table 3.8. L, a, b values of Turkish delights formulated with different type of sugar source (corn syrup or sucrose).....	106
Table 3.9. TPA Results of Turkish Delights .....	109
Table 3.10. Proton spin-spin relaxation (T <sub>2</sub> ) times (ms) of each compartment observed in relaxation spectrum for Turkish delights formulated with different type of sugar source (corn syrup or sucrose) .....	113

Table 3.11. Relative area (%; RA) of each peak observed in relaxation spectrum for Turkish delights formulated with different type of sugar source (corn syrup or sucrose) .....	114
Table 3.12. Parameters obtained from the fits presented in Equation 7 .....	127

## LIST OF FIGURES

### FIGURES

Figure 1.1. Sol-gel transition in gelatin system (Burey et al., 2009).....	4
Figure 1.2. The mechanism of starch gelatinization a) Starch granules b) Swelling of starch granules upon exposing heat and moisture c) Leaching of amylose from the granules d) Formation of starch gel matrix (Burey et al., 2009) .....	5
Figure 1.3. Crystals of fructose (A), sucrose (B), glucose (C), and Mannitol (D) (10x magnification) (Roos et al., 2012).....	11
Figure 1.4. Production steps of corn syrup .....	13
Figure 1.5. Linkage of ketohexoses by D-tagatose-3-epimerase (Izumori, 2006) ..	16
Figure 1.6. Representative TPA curve for the starch based confectionery product (Turkish delight).....	21
Figure 1.7. X -ray diffraction patterns of starch based confectioneries.....	27
Figure 1.8. Flipping of $M_0$ (longitudinal magnetization $90^\circ$ into x-y plane leading to formation of $M_{xy}$ (transverse magnetization) after RF pulse is turned ON (Hashemi et al., 2010).....	30
Figure 1.9. Decaying and recovering of transverse magnetization ( $M_{xy}$ ) vector longitudinal magnetization vector ( $M_z$ ), respectively after RF pulse is turned OFF (Hashemi et al., 2010).....	31
Figure 1.10. Representative graph for the magnetization recovery curve with the growth rate of $T_1$ .....	32
Figure 1.11. Representative graph for the magnetization decaying curve with the decay rate of $T_2$ .....	33
Figure 1.12. Schematic representation of a typical cycle of the main magnetic field $B_0$ employed with field-cycling NMR relaxometry (Kimmich & Anoardo, 2004)	36
Figure 3.1. Moisture content (%) of gelatin based soft candies at the first day (■), 14 <sup>th</sup> day (▣) and 28 <sup>th</sup> day (▤) of storage.....	65
Figure 3.2. Water activity of gelatin based soft candies at the first day (■), 14 <sup>th</sup> day (▣) and 28 <sup>th</sup> day (▤) of storage .....	66

Figure 3.3. X-Ray Diffraction Pattern of gelatin based soft candies at the first day of storage: P0 (—) and P40 (—)	72
Figure 3.4. X-Ray Diffraction Pattern of gelatin based soft candies at the 28 <sup>th</sup> day of storage: P0 (—) and P40 (—)	72
Figure 3.5. Hardness values of gelatin based soft candies at the first day (■), 14 <sup>th</sup> day (▣) and 28 <sup>th</sup> day (▢) of storage	74
Figure 3.6. Glass transition temperature of gelatin based soft candies at the first day (■) and 28 <sup>th</sup> day (▢) of storage	76
Figure 3.7. T <sub>1</sub> (spin-lattice) relaxation times of gelatin based soft candies at the first day (■), 14 <sup>th</sup> day (▣) and 28 <sup>th</sup> day (▢) of storage	77
Figure 3.8. T <sub>2</sub> Relaxation Spectrum graph of gelatin based soft candies at the first day of storage: P0 (—) and P40 (—)	86
Figure 3.9. T <sub>2</sub> Relaxation Spectrum graph of gelatin based soft candies at the 28 <sup>th</sup> day of storage: P0 (—) and P40 (—)	86
Figure 3.10. Representative NMRD profiles of gelatin based soft candies containing different amount of D-allulose; indices 1, 2 denote two replicates of each composition.	88
Figure 3.11. <sup>1</sup> H spin-lattice relaxation dispersion profiles, $R1, H\omega$ , for different gelatine composition. Red lines – theoretical fits decomposed into the individual contributions: $R1, Hconfined, rot\omega$ (brown lines), $R1, Hconfined, trans\omega$ (orange lines), $A$ (light blue lines)	92
Figure 3.12. Thermogravimetric Analysis (TGA) thermogram of different formulations	100
Figure 3.13. Derivative weight loss curves for different formulations	101
Figure 3.14. Moisture contents (%) of Turkish delights formulated with different type of sugar source (corn syrup or sucrose)	103
Figure 3.15. X-ray diffraction pattern of Turkish delights formulated with different type of sugar source (SUC: — , SCG60: — , SCG40: — , SBF10: — )	110
Figure 3.16. Proton spin-lattice relaxation dispersion profiles of Turkish delights formulated with different type of sugar source (corn syrup or sucrose) obtained	

with a FFC NMR relaxometer in the range of 10 kHz-20 MHz at 25°C (a) and 4°C (b); additional points were obtained at 500 MHz with a conventional NMR spectrometer ..... 118

Figure 3.17. Proton spin-lattice relaxation dispersion profiles obtained at 25°C for SUC (a), SBF10 (b), SCG40 (c), and SCG60 (d); the solid lines are the best fits of equations (3), (6), (7) to the experimental data (see text); deconvolution of the overall fits: rotational contributions (dot lines), two translational contributions (dash and dot-dash lines)..... 123

Figure 3.18. Proton spin-lattice relaxation dispersion profiles obtained at 4°C for SUC (a), SBF10 (b), SCG40 (c), and SCG60 (d); the solid lines are the best fits of equations (3), (6), (7) to the experimental data (see text); deconvolution of the overall fits: rotational contributions (dot lines), two translational contributions (dash and dot-dash lines)..... 125





## CHAPTER 1

### INTRODUCTION

#### 1.1 Confectionery Gels

Gels could be defined as consistent systems composed of two main components and formed by dissolving solid substances in liquid phase. (Burey, Bhandari, Rutgers, Halley, & Torley, 2009). As well as various systems such as polymers or plant and animal tissues, the majority of food products also comprise of gels (Burey et al., 2009).

Most of the food gels that were found in the market could be classified as composite gels including two or more gelling agents in their formulations (Burey et al., 2009). In addition, it was also indicated that, different biopolymer mixtures such as proteins, starch and polysaccharides are generally used to design composite gels (Stokes, 2012). Due to having wide range of melting profiles and textures, composite gels are utilized in various type of food such as cheeses and margarines (Stokes, 2012).

Soft candy products could be also considered as perfect examples for the composite gels due to high amount of sugar together with several types of gelling agents affecting the microstructure and texture of the final products (Ilhan, Pocan, Ogawa, & Oztop, 2020b). Texture of the soft candies mainly depend on the formation of the gel network which is strongly affected from the type of the biopolymers used on the formulation (Pocan, Ilhan, & Oztop, 2019b). Burey et al. (2009) compared the aqueous gel systems and composite confectionery gel systems and showed that that addition of sugars directly affects the high solid network of composite confectionery

gels resulting in a significant difference from the aqueous gel systems (Burey et al., 2009).

There are two important factors that affect the gelation of aqueous systems: the 1<sup>st</sup> one is the minimum critical gelling concentration ( $C_0$ ) denoting the minimum concentration of biopolymer that is necessary for the formation of gel network. The 2<sup>nd</sup> one is the concentration of coil which results from the entanglement and overlapping of the chains of biopolymers ( $C^*$ ) affecting the density of gel network (Burey et al., 2009). However, once sugars are introduced to this aqueous gel system, a different mechanism is observed as in the case of confectionery gel systems. Sugars alters the microstructure of aqueous gel systems by affecting the phase separation. (Burey et al., 2009). Although the main textural properties of confectionery gels are governed by the gelling agents such as starch or gelatin, sugar components also have a strong contribution on the formation and behaviors of composite gels (Burey et al., 2009).

Soft candies can also be classified as gummy confections. The main ingredients of the gummy confections are composed of sucrose and/or glucose syrup, gelling agents such as starch, gelatin or pectin and water (Pocan, Kaya, Mert, & Oztop, 2021). Pocan et al. (2021) indicated that gummy candies might also include citric acid, coloring and flavoring agents as additional ingredients (Pocan, Kaya, et al., 2021).

One of the most important components of confectionery gels is water as in the case of most food products (R Ergun, Lietha, & Hartel, 2010). It is a vital component found in confectionery gels since gel formation occurs with the help of plasticizing effect of water (Pocan et al., 2019b). The main function of water in the formation of confectionery gel is to enable the dissolving of other ingredients such as sucrose and/or corn syrup leading to the formation of a homogeneous slurry. Nearly 20%-35% of water by weight of sugars is needed to complete the dissolution of slurry in confectionery products (R Ergun et al., 2010). As well as its plasticizing effect, the properties of water utilized in the formulation of confectionery product is also

important since it directly affects the quality of final product (R Ergun et al., 2010). It has also an important role to determine the textural properties of confectionery gels (R Ergun et al., 2010). Confectionery gels can be prepared by using gelling agents as stated. Gelatin, starch, pectin, carrageenan are the polymers used to formulate soft candies.

### **1.1.1 Gelatin based Confectionery Gels**

Gelatin is a protein obtained from the hydrolysis of collagen with the help of alkaline or acid hydrolysis. Porcine (pig), bovine (cow) and piscine (fish) gelatins are the examples of the most common gelatin origins with wide application areas (Burey et al., 2009). A typical gelatin is composed of 84% protein, 14% moisture and 2% ash. The main amino acid types that are present in the structure of gelatin are *proline*, *hydroxyproline* and *glycine* (Burey et al., 2009).

Gelatin undergoes thermo-reversible gelation (with lowering the temperature) when protein concentrations in the aqueous environment is higher than 2%-3%. Gelatin when dissolved in water behaves similar to the synthetic polymers having random-coil configurations. These random-coils contain polypeptide chains known as  $\alpha$ -chains which might expose to entanglement. After the cooling step, these aforementioned coils might expose to coil-helix transition resulting in gelation of gelatin with the help of a process named as “sol-gel transition” (Burey et al., 2009) (Fig. 1.1).

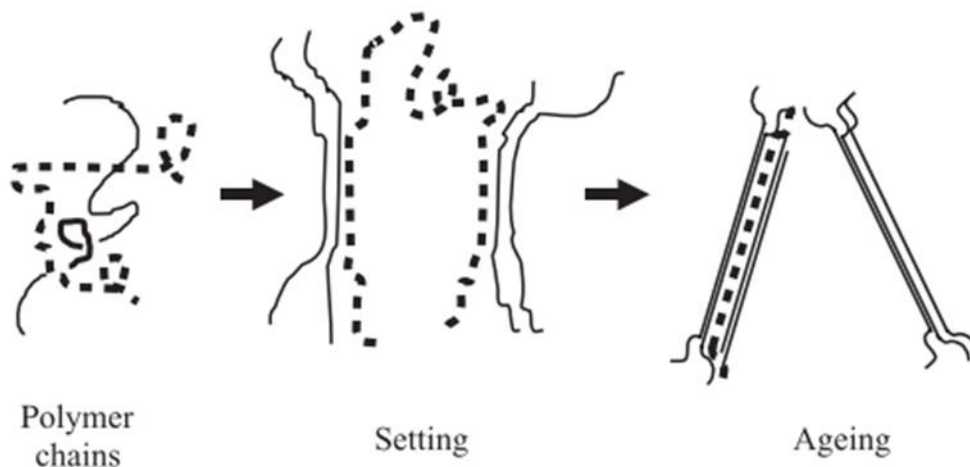


Figure 1.1. Sol-gel transition in gelatin system (Burey et al., 2009)

As seen in Fig.1.1, during the gelation of gelatin (sol-gel transition of gelatin), two important step occurs: setting and aging. During the setting step, irregular parts found in the triple helices form gel network from the gelatin solution. On the other hand, during the last step known as aging, development of gel strength takes place.

The aging process normally takes a long time in confectionery gels. However, it was hypothesized that, interactions occurring between gelatin and other compounds such as sucrose and/or glucose syrup might slow down this process since sugars are known with their stabilizing properties on the structure of gelatins (Burey et al., 2009; Ilhan et al., 2020b). It is known that, sugars improve the stability of junction zones found in gelatin gels leading to formation of strong and elastic gels (Burey et al., 2009; Kasapis, Al-Marhoobi, Deszczynski, Mitchell, & Abeysekera, 2003).

Stability of gelatin based confectionery gels were also mentioned in various publications proving the improved stability of gelatin network in the presence of high sugar content (Ilhan et al., 2020b; Otálora, de Jesús Barbosa, Perilla, Osorio, & Nazareno, 2019; Pohan, Ilhan, et al., 2021; Pohan et al., 2019b).

### 1.1.2 Starch based Confectionery Gels

Along with its important role in plant physiology, starch could be also considered as a vital source of carbohydrate in terms of nutrition aspects (Marfil, Anhê, & Telis, 2012). Normal starch types generally contain nearly 25% amylose and 75% amylopectin while waxy types of starches consist of higher amount of amylopectin compared to the normal starch types (Huang, Kennedy, Li, Xu, & Xie, 2007).

Upon exposing of starch molecules to the high temperature (generally higher than 50 °C) in the presence of water, the swelling and rupturing of starch granules occurs which is stemmed from the disruption of double helices of amylopectin. In the meantime, amylose molecules leached out from the starch granules leading to dramatic increase in the viscosity of solution. All these events are known as “starch gelatinization” (Huang et al., 2007) as indicated in Fig. 1.2.

When gelatinized starch is stored at low temperatures, “retrogradation” ‘ the recrystallization of dispersed amylose and amylopectin chains of starch molecules’ takes place (Huang et al., 2007).

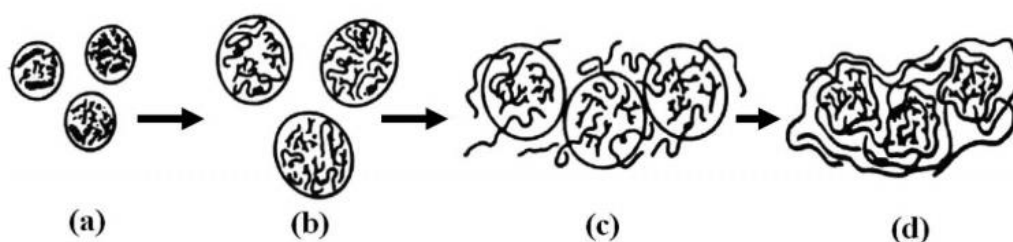


Figure 1.2. The mechanism of starch gelatinization a) Starch granules b) Swelling of starch granules upon exposing heat and moisture c) Leaching of amylose from the granules d) Formation of starch gel matrix (Burey et al., 2009)

Due to its gelling properties, starch is a commonly used a gelling agent (alone or with other gelling agents) to produce various types of soft candy products (Ilhan et al., 2020b; Marfil et al., 2012; Pohan, Knapkiewicz, Rachocki, & Oztop, 2021; Siegwein, Vodovotz, & Fisher, 2011).

However native starch is usually not the starch type preferred for soft candy production. Acid-thinned starches are the most common types that are utilized in confectionery industry due to their low viscosity resulting in easier agitation of the slurries with minimum energy requirement (Siegwein et al., 2011). Besides these advantages of starch as a gelling agent, it has some drawbacks which limits its utilization in confectionery industry. For example, use of starch in confectionery gels might have sometimes result in products with undesirable textural characteristics such as higher firmness and brittleness. These type of starch based soft candies with undesirable attributes are called as “short” (Siegwein et al., 2011). Starch based confectionery gels also have some disadvantages compared to the gelatin based confectionery gels. For instance, at high sugar concentrations in the range of 40%-60% gelatin can lead to the formation of a network with improved characteristics. On the other hand, such a high sugar content used in starch based confectionery gels can decrease the chain-chain associations which might be stemmed from the increase in critical gelling concentration leading to the formation of a weak starch gel network and obtaining products with undesirable textural properties (Burey et al., 2009; Ilhan et al., 2020b; Kasapis et al., 2003).

#### **1.1.2.1 Turkish Delights (*Lokum*)**

Turkish delights (lokum) is also an example for these soft candy products and it is known as traditional sugar-based jelly confection which contains starch as the main gelling agent (A. Batu & Kirmaci, 2009). In accordance with Turkish food legislations, Turkish delight (lokum) is prepared by using sucrose, starch, drinking

water, citric acid or tartaric acid as the main ingredients (Uslu, Erbas, Turhan, 2010). As its name implies, it is a well-known traditional confectionery product especially in Turkey but it is also popular in Greece, Middle Eastern countries and in the Balkans (Kavak & Akpunar, 2018).

The type of starch utilized in the production of Turkish delights is very important since it directly affects the starch gelatinization and thereby textural properties and quality of the final products (A. Batu & Kirmaci, 2009). In previous studies, it was mentioned that using corn starch in lokum formulations led to the formation of Turkish delights with more opaque appearance and harder texture, which could be considered as a poor quality indication for the final products (A. Batu & Kirmaci, 2009). In order to prevent this opaque appearance and hard texture, lokum manufacturers generally prefer to use acid modified starch since this type of starch needs less water for the gelatinization compared to the natural starch types such as corn starch leading to the formation of delights with more desirable quality properties (A. Batu & Kirmaci, 2009). Since acid modified starch does not solidify immediately like natural starch, it does not cause difficulties during processing (A. Batu & Batu, 2016). For this reason, use of acid modified starch is more preferable in the production of Turkish delights.

Acid type that is utilized to produce Turkish delights is also an important factor in determining the quality of the products since use of the acids prevents the crystallization of Turkish delights with the help of inversion reaction in which sucrose is converted to invert sugar (A. Batu & Kirmaci, 2009). According to the Turkish food legislation, as an acid type, only citric acid or tartaric acid could be utilized in the production of Turkish delights (A. Batu & Kirmaci, 2009). Batu et al. (2009) also indicated that use of tartaric acid in the formulation led to the formation of lokum samples with a softer texture compared to the samples containing citric acid.

Although lokum manufacturers do not have certain and common decisions about the quality properties of products such as texture and color, they agreed that elasticity and softness are the most important textural parameters to determine the quality of Turkish delights (A. Batu & Kirmaci, 2009). Moreover, as indicated by Batu et al. (2009), Turkish delights should not be too soft or too hard. In addition, it should preserve its shape during the storage (A. Batu & Kirmaci, 2009).

As well as its quality, authenticity of Turkish delights is also very important since they are vital confectionery products in terms of their economic value and market share in Turkey. Therefore, they are protected under Turkish legislation covering the ingredients and production methods. So, it is vital to determine the originality and authenticity of the production of Turkish delights especially in terms of the ingredients. According to the national legislations (Reference Number:2013/55), the only sugar type that can be utilized to produce *lokum* is defined as the white sugar which is sucrose (Uslu, Erbas, Turhan, 2010). However, confectionery manufacturers prefer to use corn syrup instead of sucrose for various purposes such as crystallization inhibition (Porter & Hartel, 2013). As it was known from the previous studies, corn syrup can be utilized as a crystallization inhibitor to improve the shelf life of the confectionery products (Labuza et al., 2004). It was also stated that, as the amount of corn syrup increased in the formulations, the smaller crystals were obtained leading to the formation of more desirable confectionery products in terms of both textural and sensorial properties (Hartel & Shastry, 2009). In addition, manufacturers might prefer corn syrups to decrease the cost of ingredients. However, utilization of corn syrups (especially high fructose corn syrups) as a sweetener is a controversial issue since it directly affects the authenticity of the products that are protected by legislations as mentioned before and Turkish delights that are produced by using corn syrup can be considered as even “adulterated”.



### **1.1.3 Other biopolymers used in the formulations of confectionery gels**

In addition to the gelatin and starch, other biopolymers such as pectin and carrageenan could be also utilized to formulate confectionery gels.

Pectin is known as a water-soluble complex polysaccharide and it was found in mainly plant cell walls. It is composed of D-galacturonic acid units that are linked by  $\alpha$ -1-4 glycosidic linkages. There are two main types of pectin: Low Methoxyl Pectin (LMP) and High Methoxyl Pectin (HMP) (Ates, Ozvural, & Oztop, 2020). While divalent ions such as calcium chloride are required to form LMP gels, sugars and acidic conditions are needed to form HMP gels. (Ates et al., 2020). In previous studies, soy protein and pectin was used together to formulate the composite confectionery gels and their physicochemical properties were examined (Ates et al., 2020)

$\kappa$ -carrageenan (KC) is a negatively charged and sulphated biopolymer which is obtained from the red seaweed. It has been widely used in food industry as a thickener, stabilizer and gelling agent (Sow, Nicole Chong, Liao, & Yang, 2018). In previous studies, KC was utilized together with Fish Gelatin (FG) as the gelling agents and it was observed that melting temperature ( $T_m$ ) and gelling temperature ( $T_g$ ) of FG increased in the presence of KC. Moreover, it was mentioned that, formation of KC network led to enhancement of physicochemical properties (Sow et al., 2018).

## **1.2 Sugar Types Used in Confectionery Gels**

### **1.2.1 Sucrose**

Sugar type used in the formulations has a vital role in both flavor and structural properties of the confectionery gels (Su et al., 2021). Most of the confectionery gels

include sucrose and /or glucose syrup as the sugar source in their formulation (Burey et al., 2009).

The main and the most widely used sugar source in confectionery industry is sucrose which is produced from the sugar cane or sugar beet through extraction and crystallization processes (Hartel & Shastry, 2009; Roos et al., 2013). Besides acting as a sweetener, sucrose is also used to contribute to the texture and sensorial properties of the confectionery products by increasing bulk weight of the products and giving desirable mouth-feel (Burey et al., 2009). In addition, it improves the functional and physical properties of the confectionery products such as humectancy, freezing point depression, osmotic stability and flavor enhancement (Zavala, Roberti, Piermaria, & Abraham, 2015). As indicated by Zavala et al. (2015), sucrose led to changes in mechanical and physical properties of food gels by changing the intermolecular interactions and conformational ordering (Zavala et al., 2015).

Sucrose is generally used together with the glucose syrup in the formulation of confectionery gels since syrup improves the solubility of sucrose and inhibit sucrose crystallization in confectionery products (Roja Ergun, Hartel, & Noda, 2009)

Large quantities of sucrose is produced at a purity level (>99.9%) from the sugar cane or sugar beet with the help of extractions and crystallization steps (Roos et al., 2013). Although there are some differences between two plant sources regarding the refining processes, for both of the sugar source (beet or cane), similar extraction procedure was applied to remove the sucrose from the beet or cane and produce dilute liquid with high amount of impurities (Hartel & Shastry, 2009). These impurities are mainly composed of organic matter and minerals and show changes according the type of sugar source (beet or cane) resulting in application of slightly different clarification steps for each source (Hartel & Shastry, 2009).

Crystalline sucrose products differing in terms of their particle sizes are available from the refiners for commercial purposes. Regardless of the plant source, pure

crystalline sucrose have always same structure since its molecular structure depends on physical constraints. On the other hand, due to presence of some impurities, the natural sucrose obtained from the normal refining process could not be totally pure (Hartel & Shastry, 2009). Depending on the plant source, these small impurities could be different in terms of size and morphology. Due to the importance of impurities having a key role in the crystallization process, differences in impurities are vital to control the formation of sucrose crystals in food products along with confectionery gels (Hartel & Shastry, 2009).

In order to produce highly purified and refined sucrose crystals having uniform sizes, industrial sucrose crystallization processes were developed. Even though refined sucrose crystals have high chemical purity, perfectly uniform and defect-free crystals cannot be produced (Roos et al., 2013).

Impurities found in the crystal lattice are called as “inclusions”. Compared to the other commercially available sugars such as fructose and glucose, sucrose crystals have larger size as seen in Fig. 1.3, increasing the incidence of inclusions (Roos et al., 2013).

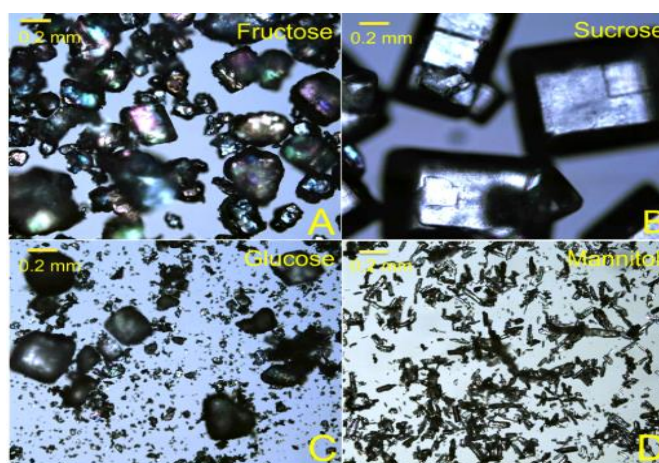


Figure 1.3. Crystals of fructose (A), sucrose (B), glucose (C), and Mannitol (D) (10x magnification) (Roos et al., 2012)

Moreover, in previous studies, crystallinity degree (%) of sucrose was found to be higher compared to the other sugar types such as glucose and lactose (Grunin, Oztop, Guner, & Baltaci, 2019). Therefore, the presence of sucrose in confectionery products can lead to the formation of some defects related with the crystallinity which might be stemmed from both larger size of sucrose crystals and higher crystallinity degree (%) of sucrose.

Control of sucrose crystallization in confectionery products is important to keep the desired textural properties of the final products. Therefore, in order to control crystallization, maintaining sucrose in solution phase or controlling the solid crystalline phase formation are important factors that should be considered by soft candy manufacturers (Hartel & Shastry, 2009).

### **1.2.2 Corn Syrup**

As its name implies, corn is the major source that is used in the production of corn syrups (Parker, Salas, & Nwosu, 2010). As seen in Fig.1.4, in order to produce High Fructose Corn Syrup (HFCS), firstly corn starch containing amylose and amylopectin subunits undergoes chemical and enzymatic hydrolysis leading to formation of corn syrup including mostly glucose. As the second step, this glucose syrup is converted to HFCS with the help of isomerization reaction by the action of glucose isomerase enzyme (Parker et al., 2010).

There are also three main subtypes of HFCS which are categorized according to their glucose and fructose amounts (%). The first one is HFCS-90 containing 90% fructose and 10% glucose and generally blended with glucose syrup to produce HFCS-42 (42% fructose and 58% glucose) and HFCS-55 (55% fructose and 45% glucose). Among these three types, the most well-known and commonly used one is HFCS - 42 including 42% fructose and 58% glucose in its formulation and it was generally

utilized as a stability and functionality enhancement in various food products including beverages and confectionery products (Parker et al., 2010).

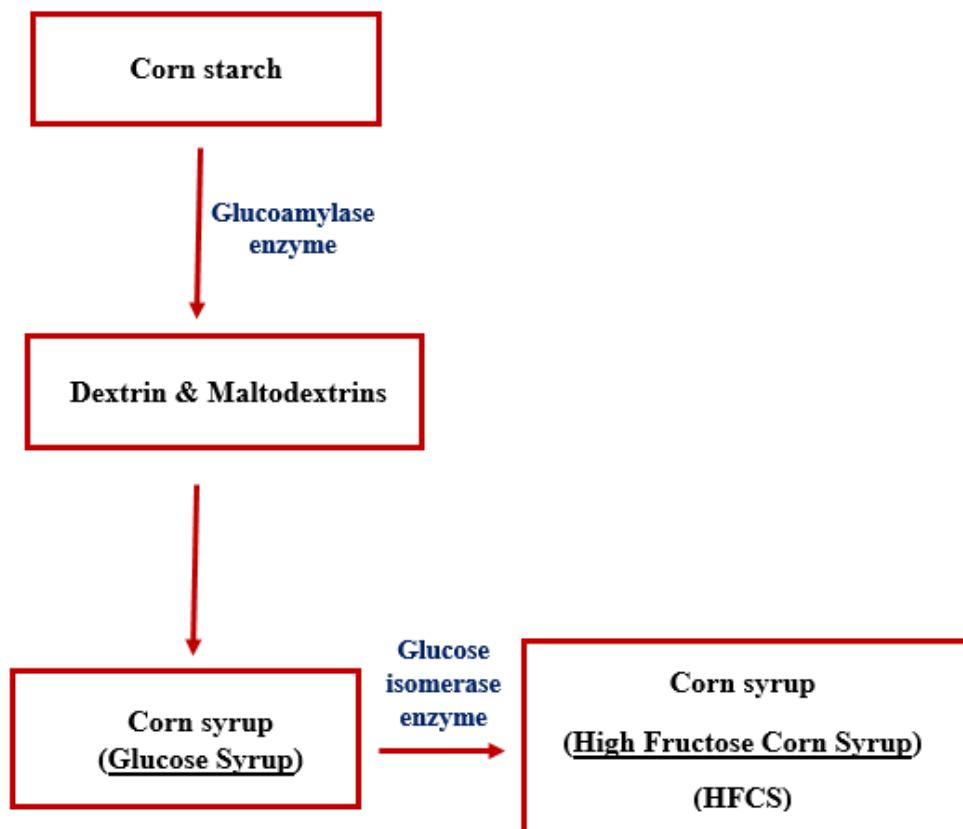


Figure 1.4. Production steps of corn syrup

HFCS has become a promising alternative to both sucrose and other natural sugars in a very short time due to its lower cost and higher sweetness (Parker et al., 2010).

Corn syrups especially HFCS and glucose syrups generally with high Dextrose Equivalent (DE) values were utilized in the production of confectionery gels as the common humectants (R Ergun et al., 2010).

Glucose syrups are generally categorized according to their DE values changing between 20 and 80 (DE: 100 indicates syrups containing solely glucose while DE:0 indicates absence of glucose in the syrup) (Burey et al., 2009). Glucose syrups having DE smaller than 20 are called as maltodextrins while the ones having DE higher than 80 are categorized as hydrols or hydrolysates (Burey et al., 2009). Generally, glucose syrup having 42 DE value is preferred in the production of confectionery gels due to its crystallization inhibition property.

In addition to its crystallization inhibition property, glucose syrup also decreases the water activity of confectionery gels due to the presence of higher solid content leading to the formation of shelf stable products in which microbial growth is prevented (Burey et al., 2009). Therefore, glucose syrup is widely used in the formulation of jelly and gummy confectioneries as a sweetener and stabilizer. It is also worth mentioning that, confectionery products generally include higher amount of glucose syrup compared to the amount of sucrose in their formulation (Burey et al., 2009).

Despite of all these advantages of corn syrups like crystallization inhibition nature and lower cost, their utilization in the production of some certain types of confectioneries such as Turkish delights (lokum) is not accepted by local manufacturers since they affect the authenticity and originality of these traditional confectionery products negatively as mentioned in a recent study (Pocan, Knapkiewicz, et al., 2021). In their study, it was indicated that, corn syrup containing samples had improved textural properties and were less prone to crystallization, although this case affected the authenticity of the products leading to production of “adulterated” Turkish delights (Pocan, Knapkiewicz, et al., 2021).

### 1.2.3 Rare Sugars

Due to the high sugar amount of soft candies, utilization of sweeteners with low caloric values in these products is gaining particular interest. Nevertheless, the expensiveness or chemical origin of the sweeteners restricts their use. At this point, rare sugars emerge as an alternative to sweeteners (Pocan et al., 2019b). The International Rare Sugar Institute (ISRS) defines rare sugars as monosaccharides and their derivatives that are found in nature as small quantities (Granström, Takata, Tokuda, & Izumori, 2004). D-Tagatose, the C-4 epimer of fructose, is one of these rare sugars with a sweetness of 92% of sucrose and a caloric value of 1.5 kcal/g (Levin, 2002). The inhibitory effect of tagatose on postprandial glucose increase in blood showed that this sugar can be used in the treatment of type 2 diabetes (Roberts & Wright, 2012). D-Allulose (formerly known as D- Psicose) which is also classified as a rare sugar has 70% of the sweetness of sucrose and a caloric value of 0.39 kcal/g (O'Charoen, Hayakawa, Matsumoto, & Ogawa, 2014). Inhibitory effect of D-Allulose (D- Psicose) on blood glucose levels and fat accumulation in the body (Fig.1.5) was also indicated in various studies (Chen, Huang, Zhang, Lu, & Jiang, 2019; Chung, Oh, & Lee, 2012).

D-Tagatose was accepted as “Generally Recognized as Safe (GRAS)” in 2002 (Levin, 2002) while D-Allulose was accepted as “GRAS” in 2012 (Mu, Zhang, Feng, Jiang, & Zhou, 2012) by the U.S. Food and Drug Administration (FDA). In addition, D-allose, the C-3 epimer of D-Glucose, is also classified as a rare sugar. Unlike D-Tagatose and D-Allulose, it is an aldohexose as it is an epimer of glucose and can be produced from D-Allulose by the enzyme L-rhamnose isomerase (Chattopadhyay, Raychaudhuri, & Chakraborty, 2014).

Among these three types of rare sugars, D-Allulose is the most well-known one because of the benefits of its applications in foods and its easier mass production. D-Allulose is produced from D-Fructose using the enzyme D-tagatose-3-epimerase,

which is produced by utilizing the recombinant enzyme technology and used in immobilized form (Granström et al., 2004). The first mass production of D-Allulose began in 1994, when Professor Ken Izumori of Kagawa University in Japan obtained the enzyme D-tagatose-3-epimerase. Ken Izumori later proposed the “Izumoring” strategy, which showed that all hexo-sugars could be synthesized using this enzyme as illustrated in Figure 1.6. (Izumori, 2006).

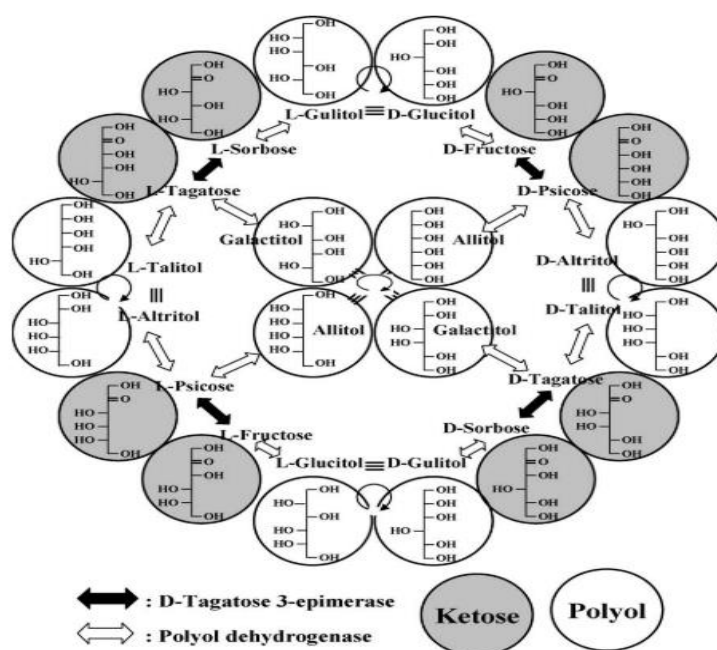


Figure 1.5. Linkage of ketohexoses by D-tagatose-3-epimerase (Izumori, 2006)

Mass production of D-Allulose at the Kagawa Rare Sugar Research center is currently ongoing. It was also mentioned in various studies, the cost of D-Allulose produced with the help of “Izumoring” technology is quite low compared to the other sweeteners (O’Charoen et al., 2014; O’Charoen, Hayakawa, & Ogawa, 2015), which will pave the way of utilization of D-allulose in the production of various type of food products as a promising sweetener.



The first commercial production of D-Allulose was performed by Japanese company, Matsunami and they produced D-allulose in different forms such as syrup and table sugar. Today, various companies carry out the production of D-Allulose such as Tate and Lyle (UK), Bonumose (USA), Savanna Ingredients GmbH (Germany) and Ingredion (USA) conducts the commercial production and sale of D-allulose products in the form of syrup and crystal sugar (Ilhan, 2019)

There are numerous studies that have explored the effect of D-Allulose addition on food products. Enhanced color formation as a result of accelerated non-enzymatic browning reactions was observed during the processing of cookies leading to higher antioxidant capacity (Sun, Hayakawa, Ogawa, Fukada, & Izumori, 2008). In addition to the antioxidant capacity, it was also revealed that, emulsification (Puangmanee, Hayakawa, Sun, & Ogawa, 2008), foaming capacity (Sun et al., 2008), gelling ability (Sun, Hayakawa, Puangmanee, & Izumori, 2006) and textural properties (S. Ikeda, Furuta, Fujita, & Gohtani, 2014) of food products noticeably enhanced with the utilization of D-Allulose in various studies.

In recent studies, D-allulose was also utilized in the production of low-calorie gelatin based (Pocan, Ilhan, et al., 2021; Pocan et al., 2019b), starch based (Ilhan et al., 2020b) and pectin based (Ates et al., 2020; Ates, Ozvural, & Oztop, 2021) confectionery gels. In all these studies, it was observed that, use of D-allulose led to drastic changes in the textural and quality attributes of the soft candies by changing the water binding properties of the products. Crystallization inhibition property of D-allulose was found to be promising for the gelatin based (Pocan et al., 2019b) and starch based confectionery gels (Ilhan et al., 2020b). On the other hand, surprisingly, for the pectin based soft candies, crystallization of the samples were triggered when D-Allulose was utilized in the formulations (Ates et al., 2020). Moreover, regarding all these soft candy products, accelerated Maillard reaction rate was observed in the presence of D-allulose leading to formation of confectionery products with brownish

color (Ates et al., 2020; Ilhan et al., 2020b; Pohan, Ilhan, et al., 2021; Pohan et al., 2019b).

As well as confectionery gels, D-allulose was also found to be effective to increase the caramelization rate of sugar solutions compared to glucose and fructose (Ertugrul, Tas, Namli, & Oztop, 2021). In addition, accelerated Maillard reaction rate was also observed during the glycation of various type of proteins such as pea (Ertugrul, Namli, et al., 2021) and soy protein (Namli, Sumnu, & Oztop, 2021; Zia, Namli, & Oztop, 2021) when D-allulose used in the sugar solutions.

### **1.3 Characterization of Confectionery Gels**

#### **1.3.1 Physical Characterization of Confectionery Gels**

##### **1.3.1.1 Moisture Content Determination**

The main moisture content determination methods used for the confectionery products can be classified in three categories (R Ergun et al., 2010):

- Loss on drying
- Karl Fischer Titration
- Refractometry

Among these methods, the most commonly used one for the analysis of confectionery products is the first one: Loss of drying. For this method, vacuum oven drying is generally used in which weighed sample is placed in oven at reduced pressure and lower temperature (~ 70 °C ) (R Ergun et al., 2010). This method is more advantageous compared to atmospheric drying method for the moisture content determination of confectionery products since it is less destructive for the heat sensitive ingredients. Due to the high temperature that was used during atmospheric

drying method (100-135 °), decomposition stemmed from caramelization reactions or Maillard reactions might be observed resulting in production of water and this case may increase the weight loss during drying leading to less accurate measurement (R Ergun et al., 2010) However, the important point that should be considered while performing vacuum-oven drying is the duration of drying which should be sufficiently long for allowing confectionery product to reach the steady state (R Ergun et al., 2010).

Another well-known method to determine the moisture content of confectionery products is Karl Fischer titration. This method is based on two-step chemical reaction to identify the amount of water in the products.  $I_2$  is used as a titrating reagent to determine the end-point. The reagent reacts with only water and eliminating the error that comes from the volatile components (R Ergun et al., 2010). It is useful method to determine the moisture content of certain type of foods such as candies, roasted coffee, dried fruit & vegetables and fats. Although it is not as fast as spectroscopic techniques such as NIR and NMR spectroscopy, it is still promising and it can be considered as a fast method (20-25 minutes) and easily used in the online processing (R Ergun et al., 2010).

Water content (inverse of solid contents) of the liquid samples like sugar syrups can be measured by means of refractive index. The refractive index is directly correlated to concentration for the pure sucrose solutions. However, most of the confectionery syrups are composed of mixtures of sucrose and other sweeteners such as corn syrup or invert sugar. For this case, the refractive index of the solution changes according to the relative ratios of the component ingredients (R Ergun et al., 2010). Refractometer reading is called as “°Brix”. Although Brix value does not represent the actual amount of total solids or water content, in most of the confectionery applications °Brix value is directly used without needing any correction factor and it is assumed as true total solid concentration or inversely water content (Pocan, Kaya, et al., 2021)

### **1.3.1.2 Water Activity ( $a_w$ ) Determination**

Water activity ( $a_w$ ) is an important parameter, which is mainly affected by the presence of dissolved sugars, humectants, and sweeteners in confections (Pocan et al., 2019b)

During the storage time of confections, upon moisture gain or loss, changes in textural and quality characteristics can be observed, so measuring water activity is a crucial step to check the stability of the samples (Pocan et al., 2019b). Basically, water activity can be defined as the ratio of partial pressure of water vapor to the pressure of pure water at a specified temperature (Pocan, Kaya, et al., 2021). As well as physicochemical parameters, it is also an important parameter to characterize the microbial stability of confectionery products (R Ergun et al., 2010). It was indicated that, water activity of jelly candies should be changed in the range of 0.5-0.7 to prevent the mold growth and achieve desirable quality characteristics (Pocan, Kaya, et al., 2021). In addition, it was known that, gummy candies are known as moisture intermediate foods which is rich in hygroscopic compounds such as sugars leading to decrease in  $a_w$  of the confectionery products and making them difficult to dry (Delgado & Bañón, 2015).

### **1.3.1.3 Texture Profile Analysis (TPA)**

Textural changes in gummy confectioneries can be monitored by utilizing Texture Profile Analysis (TPA) and different descriptors are measured by evaluating deformation under the applied force (Delgado & Bañón, 2015). TPA mimics the first two bites of the food mastication process and this method makes the technique very suitable to examine the deformation of viscoelastic material like gummy jellies. Chewiness and gumminess are examples to the TPA descriptors which are commonly used to define textural properties of gelled confections (Delgado & Bañón, 2015). Other descriptors such as hardness, cohesiveness, springiness, etc. can

be also found by evaluating TPA curve which shows force deformation. An example to the TPA curve was shown in Figure 1.6.

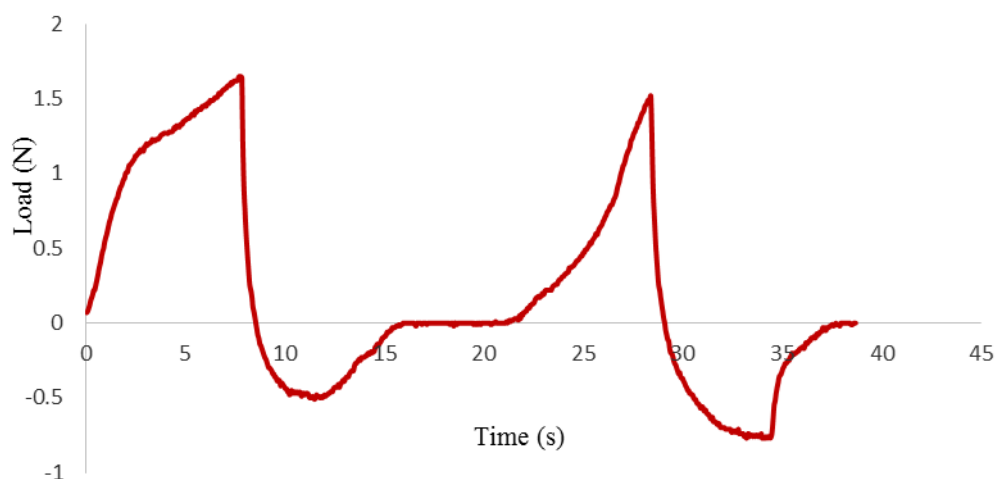


Figure 1.6. Representative TPA curve for the starch based confectionery product (Turkish delight)

According to this curve, hardness is defined as the first peak that formed during the first compression cycle and it is attributed to the strength of the gel structure (Chandra & Shamasundar, 2015).

Adhesiveness can be defined as the negative force area for the first bite and represents the work needed to overcome the attractive forces between the surface of the gel and the surface of other materials with which the sample comes into contact. The higher adhesiveness value indicates the soft structure and increases the stickiness which might be undesirable for the certain types of gummy confectioneries (Chandra & Shamasundar, 2015).

Cohesiveness could be defined as the ratio of positive force area obtained during the second compression to that of the first compression. It is also known as “consistency” and indicates the strength of internal bounds that are found in the gel network. It indicates the ability of the gel to hold its structure together (Chandra & Shamasundar, 2015).

Springiness is also known as elasticity and it is defined as the height to which the food recovers during the time elapsing between the end of the first bite and start of the second bite. It also can be defined as the distance or length of the compression cycle during the second bite (Sahin & Sumnu, 2006).

Gumminess is defined as the product of the hardness and cohesiveness. Regarding the sensorial approach, it indicates the necessary energy to disintegrate the confectionery gel and making it ready for the swallowing (Sahin & Sumnu, 2006). The higher hardness value resulted in higher gumminess of the samples.

The last textural parameter, chewiness is defined as the product of gumminess and springiness that is equal to product of hardness, cohesiveness and springiness. It is the measure of energy that is required to masticate the food and it is generally reported for the solid type foods (Chandra & Shamasundar, 2015).

### **1.3.2 Advanced Characterization Methods of Confectionery Gels**

#### **1.3.2.1 Thermo-gravimetric Analysis (TGA)**

The main objective of the Thermo gravimetric Analysis (TGA) is to measure the weight of a sample in a specified atmosphere in which the temperature of the sample is programmed (Robinson, Frame, & Frame, 1987). The most common program that is utilized in the TGA experiment is to increase the temperature linearly with time. There are also some other programs such as stepped temperature and isothermal programs (Robinson et al., 1987). During the most widely used TGA experiment,

the temperature of the sample is increased linearly and weight (%) of the sample is recorded simultaneously. The typical output of a TGA experiment is the plot of mass (%) the sample versus temperature.

Looking the TGA thermograms, one can easily determine the temperature at which the sample loses or gains weight (Robinson et al., 1987). Weight loss indicates evaporation or decomposition of the sample while weight gain demonstrates adsorption of some component from the atmosphere by the sample or occurrence of chemical reaction such as oxidation. Secondly, if no weight change occurs in the material although temperature is increased, the information on the temperature stability of the sample might be detected (Robinson et al., 1987).

Moreover, in a typical TGA thermogram, first two stages can be related with the removal of volatiles and plasticizers. Water can be considered as both volatile and a plasticizer in food systems since it can be found in free and bound form. Therefore, TGA thermogram can be used to determine the state of water in a food matrix (Pocan, Ilhan, et al., 2021).

As well as polymer systems, TGA can also be conducted to characterize various type of food matrices by providing simple thermogram and “derivative weight loss curves” at the end of the experiment (Botosoa, Chéné, Blecker, & Karoui, 2015; Fisher, Ahn-Jarvis, Gu, Weghorst, & Vodovotz, 2014; Gu, Ahn-jarvis, & Vodovotz, 2015; Siegwein et al., 2011). Especially “derivative weight loss curves” obtained as a result of the TGA experiments could be utilized in the estimation of strength of the interactions between water and polymer existing in the formulations by means of peak temperatures. For example, while the peak temperature shifted to right indicates strong water association (in other words hard to lose moisture due to strong polymer-water interaction), temperature shifted to left shows lower water association meaning easy to lose moisture due to weaker interaction (Ilhan, 2019).

Applications of TGA were also found to be promising for the confectionery products. For instance, Fisher et al. (2014) utilized TGA to detect storage stability of strawberry confections. Gu et al. (2015) formulated black raspberry confections by using pectin and starch as the gelling agents and they showed the differences in these samples by using TGA. Similarly, Siegwein et al. (2011) studied the addition of soy protein isolate on the properties of starch based confections again by using TGA. In these studies, it was stated that mass loss (%) up to 150 °C can be assumed to be water while mass loss above that temperature is mostly related with decomposition (Fisher et al., 2014). Therefore, mass loss up to 150 °C was used to determine the water content of samples.

#### **1.3.2.2 Differential Scanning Calorimetry (DSC)**

Differential Scanning Calorimetry (DSC) measures the heat flow as a function of temperature and it is found as a suitable tool to measure specific heat and phase transitions. In confectionery products, measurement of the glass transition temperature; gelatinization, denaturation are important changes to be observed by using DSC.

The measurements are performed by heating sample at a fixed rate depending on nature of the sample (Sahin & Sumnu, 2006). Commercial DSC equipment are capable to work at the temperature ranges changing between -180 ° to 725 ° with specific instruments which are also capable to reach 2000 °C (Robinson et al., 1987). During DSC experiments, as well as heating step, cooling step should be also performed in a controlled manner.

During DSC experiments, firstly, an empty sample pan is used to obtain a “baseline”. Then, the sample is weighed and put into the pan and same procedure is applied as in the case of empty pan to obtain the thermogram that shows the rate of input versus temperature.



DSC is the most widely used device to measure the phase transitions taking place in the sample. When a material experiences changes on its physical state, heat might be absorbed or liberated and phase transitions lead to the formation of peaks in a thermogram (Sahin & Sumnu, 2006). As well as endothermic peaks which could be related with the melting, gelatinization or denaturation, exothermic peaks associated with the crystallization, oxidation or freezing could be observed in DSC thermograms (Sahin & Sumnu, 2006).

Glass transition temperature ( $T_g$ ) is another important parameter obtained from DSC thermograms and observed as a change in the heat capacity of the polymer ( $c_p$ ) that is seen as a step change in the DSC thermal curve (Robinson et al., 1987). It is worth mentioning that, since no change is observed in the enthalpies of the samples at  $T_g$ , a peak is not observed in the DSC thermogram (Robinson et al., 1987).

Levine and Slade (1988) indicated that polymer science approach might be also used in food science, demonstrating that parameters obtained from DSC curve especially the glass transition temperature ( $T_g$ ) is worth to examine considering the food stability (R Ergun et al., 2010). Therefore, as well as its applications in polymeric materials, DSC is also widely used in the characterization of food samples such as staling characteristics and retrogradation behavior of gluten free breads (Demirkesen, Campanella, Sumnu, Sahin, & Hamaker, 2014), monitoring honey crystallization and melting (Berk, Grunin, & Oztop, 2021) and characterization of different types of goats' cheese (Tomaszewska-Gras et al., 2019).

Many types of food samples demonstrate a specific  $T_g$  in which various type of transitions occur. Recently, this approach had started to be used widely to characterize the confectionery products including confectionery gels (R Ergun et al., 2010). For example, in recent studies,  $T_g$  of the gelatin based (Pocan et al., 2019b) and starch based (Ilhan et al., 2020b) soft candies were found and evaluated in terms of the stability of the products during the one month of storage time.

The definition of  $T_g$  becomes important at this point to understand its effect on confectionery products. Various type of food materials especially dried foods and confectionery products having low water content are in the amorphous metastable state in which compounds do not have long-range molecular order. The amorphous state could be divided into two main group: Glassy state and rubbery state. Glass transition temperature ( $T_g$ ) is called as the temperature where transition occurs between the glassy state and more-fluid like rubbery state (R Ergun et al., 2010).  $T_g$  is strongly depend on molecular weight, degree of cross-linking of polymer and amount of plasticizer (e.g water content) found in the confectionery products. It was indicated that, even a few percent of water can result in dramatic decrease in  $T_g$  of confectionery products. Especially the higher  $T_g$  values of hard candies might have stemmed from this case knowing that hard candies normally found in stable glassy state as long as their storage temperature is lower than their  $T_g$ . For the hard candies, if too high  $T_g$  can cause the formation of too hard and brittle candy production (R Ergun et al., 2010).

### **1.3.2.3 X-Ray Diffraction (XRD) Analysis**

X-ray diffraction (XRD) is a useful method to analyze the solid-crystalline or semi-crystalline samples (Robinson et al., 1987). It is widely used in the analysis of metals, alloys, minerals and various types of polymers to detect their crystallinity. XRD can be exploited both qualitatively and quantitatively to identify the crystallinity of the samples (Robinson et al., 1987).

If the ions or molecules which make up crystals are arranged in a regular form, this structure is called as “crystal lattice”. In a material, there are distinct types atomic planes that are composed of distinct “crystal lattice” structures. If X-ray beam falls on a crystal, each planes existing on the material reflects this beam differently. Each beam interact with other beams. Although some of them are not in phase and destroy

each other, some beams coming from crystal planes enhance each other and lead to the formation of “diffraction pattern” (Robinson et al., 1987).

Along with information about the crystallinity, XRD pattern also gives information about the average grain size, texture, strain and crystal defects (Kohli, 2012). The peak intensities obtained from XRD pattern also gives valuable information about the crystallinity of the samples and they are detected by the atomic positions found in lattice planes (Kohli, 2012). Worth to mentioning that, XRD patterns could be considered as a fingerprint of atomic arrangements that are periodically ordered and they change from sample to sample indicating differences in their crystallinity (Kohli, 2012). An example for the X-Ray Diffraction (XRD) patterns for the starch based confectioneries (Turkish delights) containing different type of sugar source (sucrose and corn syrup) was shown in Fig. 1.7.

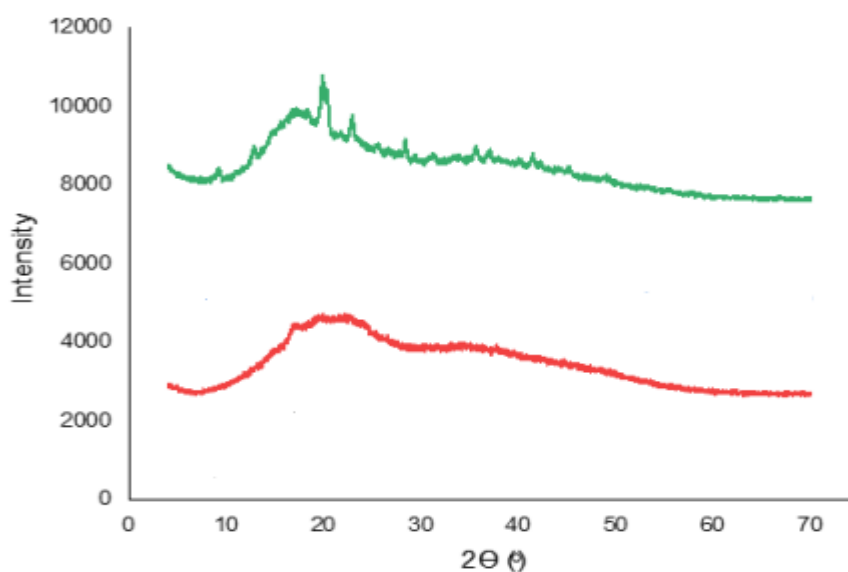


Figure 1.7. X -ray diffraction patterns of starch based confectioneries (Turkish delights) containing different type of sugar source (sucrose:— and corn syrup:—)

As well as polymeric materials and characterization of composite films (Qiao, Ma, Zhang, & Yao, 2017; Shi, Tao, & Cui, 2017), XRD patterns are also widely used to detect the crystallinity of food samples such as spray or freeze-dried milk powders (Hartel & Shastry, 2009), powder sugars like sucrose, lactose and glucose (Grunin et al., 2019), to monitor the staling and retrogradation of gluten free bread samples (Demirkesen et al., 2014) and to detect the crystallinity of cocoa butter samples (Ladd Parada, Povey, Vieira, Rappolt, & Ries, 2019). In addition to these food samples, it was also used to detect the crystallinity of gelatin based (Pocan et al., 2019b) and pectin based (Ates et al., 2020, 2021) confectionery gels. Moreover, in a previous study related with the starch based soft candies, XRD utilized with a purpose of both monitoring retrogradation of the samples due to the presence of starch in a gel network followed by the sugar crystallization process (Ilhan et al., 2020b).

#### **1.4 Characterization of Gel Systems with NMR Relaxometry**

NMR (Nuclear Magnetic Resonance) was firstly applied to the polymeric materials in 1970s and since then it has been considered one of the main characterization techniques for the polymers. Especially, solid-state NMR enables researchers to examine polymers at a molecular level and with minimal sample preparation procedure, in a non-destructive and solvent-free technique (Besghini, Mauri, & Simonutti, 2019). In addition to the analysis of polymeric materials, low field NMR relaxometry has also widely been used in the analysis of various food products such as fruits and vegetables, dairy products, cereals and confectionery products as well as monitoring food processing (Kirtil & Oztop, 2016).

As indicated by Besghini et al. (2019), utilization of high field instruments gives information about the chemical and structural composition of materials, but these instruments are expensive and require great maintenance cost which limits their

application in industry. At this point, powerful alternative that comes to mind is low field bench-top devices operating in time domain which draws the attention as an affordable and rapid analysis method especially for the food samples (Kirtil, Cikrikci, McCarthy, & Oztop, 2017). These low field alternatives are definitely easy to handle due to its less laborious nature (Kirtil, Cikrikci, et al., 2017) and they allow the researchers to perform experiments fast since they do not need any special sample preparation method (Besghini et al., 2019). Although they cannot be utilized to make compositional analysis as in the case of their “high field” counterparts, they are becoming more popular due to their capacity to make quick and easy analysis which makes them preferable as a standard quality control technique (Kirtil, Cikrikci, et al., 2017).

It is worth to point out that, the systems having field higher than 5.8 T (or alternatively  $> 250$  MHz) were recognized as “high field systems” while low field NMR systems generally known as compact “benchtop” NMR spectrometers and they have permanent magnets with typical magnetic field strength of 20-80 MHz (0.46-1.88 T) (Chakrapani, Minkler, & Beckingham, 2019). Due to its time saving and less laborious nature, low field time domain NMR (TD-NMR) was mostly utilized as a routine quality control tool to determine the oil & moisture content (Cobo et al., 2017) and solid fat content (Ziegler, MacMillan, & Balcom, 2003) of food samples.

Utilization of radio frequency (RF) pulse could be considered as the basic of NMR techniques. RF pulse is a kind of electromagnetic wave and with the help of this pulse, temporary disturbance on a sample could be created. As a result, excited signal from the sample was obtained and then relaxation of this excited signal was recorded yielding the spin-spin and spin lattice relaxations times (Hashemi, Bradley, & Lisanti, 2010).

In TD- NMR experiments, the sample is placed into a static magnetic field which is also known as ‘external magnetic field’ ( $B_0$ ) to obtain a signal. In response to this

strong magnetic field in z direction, the spins line up resulting in net magnetization  $M_0$ . This magnetization is called as longitudinal magnetization. After the application of an external RF pulse,  $M_0$  (longitudinal magnetization) flipped  $90^\circ$  into x-y plane leading to formation of  $M_{xy}$  (transverse magnetization) as shown in Fig.1.12. (Hashemi et al., 2010). Upon removal of RF pulse, spins turn back to their previous and the lowest energy stages. This phenomena is called as relaxation and relaxation of both transverse and longitudinal magnetization is utilized in NMR experiments to provide insights about the microstructure of food sample. Measuring the relaxation times and making interpretations based on relaxation times is what we call as ‘NMR Relaxometry’.

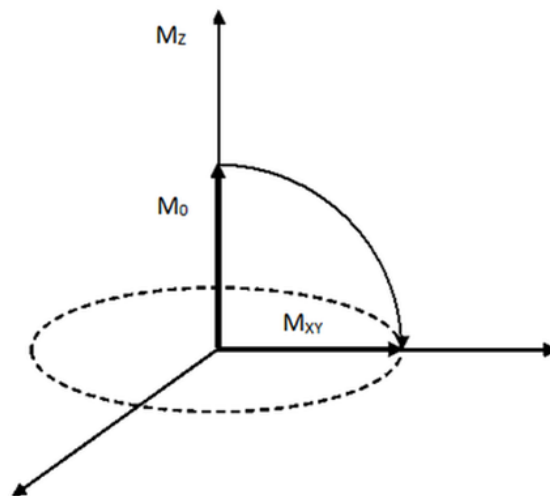


Figure 1.8. Flipping of  $M_0$  (longitudinal magnetization  $90^\circ$  into x-y plane leading to formation of  $M_{xy}$  (transverse magnetization) after RF pulse is turned ON (Hashemi et al., 2010)

$T_1$  time constant is called as longitudinal relaxation time. As it could be understood from its name, it indicates the time that necessary for the spins to realign along the longitudinal z-axis. Longitudinal relaxation time ( $T_1$ ) is also called as spin-lattice relaxation time referring the necessary time for the spins giving back to the energy which they obtained as a result of exposing RF pulse to their surrounding lattice. After flipping the magnetization vector  $90^\circ$  into the xy plane, RF pulse is turned off leading relaxation of spins. After RF pulse is turned off, transverse magnetization ( $M_{xy}$ ) vector begins to decay while longitudinal magnetization vector ( $M_z$ ) starts to recover as demonstrated in Fig.1.13.

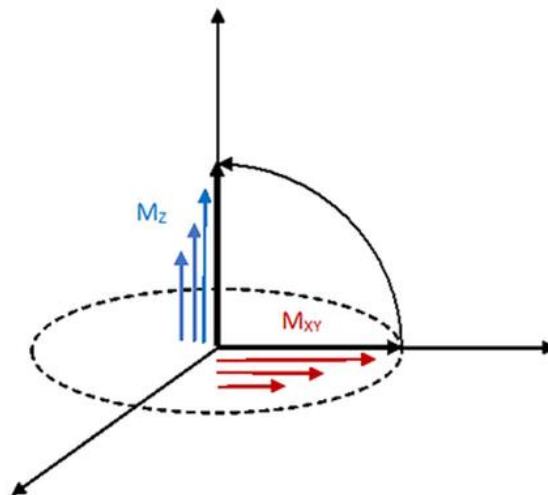


Figure 1.9. Decaying and recovering of transverse magnetization ( $M_{xy}$ ) vector longitudinal magnetization vector ( $M_z$ ), respectively after RF pulse is turned OFF (Hashemi et al., 2010)

This recovery in longitudinal component is shown by below equation 1:

$$M_z(t) = M_0 \left( 1 - e^{-\frac{t}{T_1}} \right) \quad (1)$$

where  $T_1$  denotes the time constant of magnetization recovery curve (demonstrated in Fig.1.14,  $M_z(t)$  is the component of magnetization along the z- axis (longitudinal magnetization vector) and  $M_0$  refers the initial magnetization.

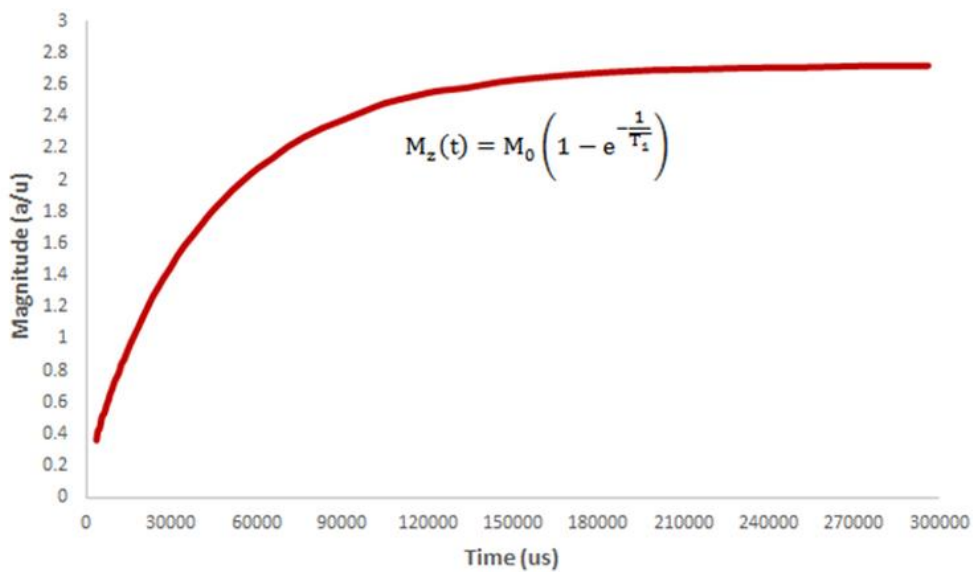


Figure 1.10. Representative graph for the magnetization recovery curve with the growth rate of  $T_1$

It is important to keep in mind that the recovery of magnetization vector along the z axis and decaying of magnetization vector in xy plane occurs simultaneously with two distinct rates. While the longitudinal magnetization component ( $M_z$ ) recovers, the transverse component of magnetization ( $M_{xy}$ ) starts to decay (displayed in Fig.1.15).



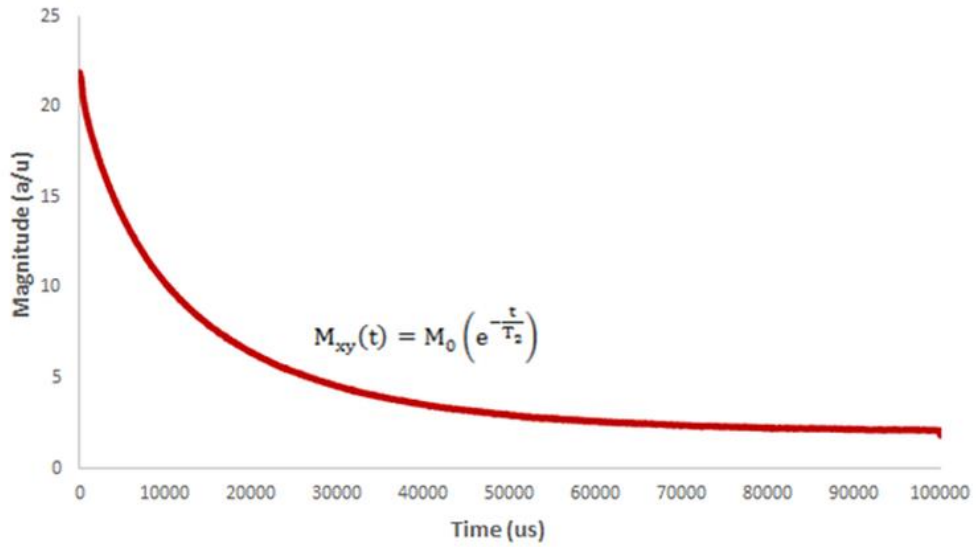


Figure 1.11. Representative graph for the magnetization decaying curve with the decay rate of  $T_2$

This decay in longitudinal component was denoted by below equation 2:

$$M_{xy}(t) = M_0 \left( e^{-\frac{t}{T_2}} \right) \quad (2)$$

where  $T_2$  shows the time constant of magnetization decay curve,  $M_{xy}(t)$  is the component of magnetization on the xy plane while  $M_0$  denotes the initial magnetization (Hashemi et al., 2010).

$T_2$  relaxation time was generally measured by using Carr-Purcell-Meiboom-Gill (CPMG) which is a well-known pulse sequence. This sequence is a modified form of Spin Echo (SE) sequence and it is composed  $90^\circ$  RF pulse followed by echo induced by the  $180^\circ$  pulses (Cikrikci & Oztop, 2016).  $T_1$  relaxation times was generally measured through Saturation Recovery (SR) or Inversion Recovery (IR) pulse sequences. In SR pulse sequence, all longitudinal magnetization is tried to be recovered before applying another  $90^\circ$  RF pulse. After each  $90^\circ$  RF pulse, Free

Induction Decay (FID) was measured (Hashemi et al., 2010). On the other hand, in IR sequence, firstly 180 °RF pulse was applied then waited a period time called as “inversion time (TI)”. After that, 90 °RF pulse was applied followed by 180 °RF pulse (Hashemi et al., 2010)

Both of these relaxation time constants ( $T_1$  and  $T_2$ ) could be used to give insight about the microstructures of food samples in TD-NMR based studies as a complementary method to well-known traditional methods. For example,  $T_1$  (spin-lattice) relaxation times was generally attributed to crystal structures found in samples (Le Botlan, Casseron, & Lantier, 1998). On the other hand,  $T_2$  (spin-spin) relaxation times was utilized to explain the presence of different compartments in gels (Ozel, Uguz, Kilercioglu, Grunin, & Oztop, 2016a) and emulsions (Akkaya, Ozel, Oztop, Yanik, & Gogus, 2020) systems, as well as to understand the polymer-water and polymer-polymer interactions in these systems (Ozel, Aydin, & Oztop, 2020). It was also used to understand the gelation behavior of different type of proteins (Bolat, Ugur, Oztop, & Alpas, 2021) and emulsification behavior of various hydrocolloids in food systems (Pocan, Ilhan, & Oztop, 2019a). Especially, regarding the multi-compartment nature of gel systems, multi-exponential analysis of relaxation decays were found to be more useful approach to get information about the different proton pools that exist in gel matrices and these proton pools can be used as a fingerprint to analyze the quality and microstructure of the gel systems (Ozel, Dag, Kilercioglu, Sumnu, & Oztop, 2017). In that regard, it is worth to hypothesize that, utilization of  $T_2$  relaxation times is an important tool to characterize gel systems. These relaxation times was also utilized to characterize soft candy confectionery products based on gelatin (Pocan et al., 2019b), starch (Ilhan et al., 2020b) and pectin (Ates et al., 2020) which can be considered as perfect examples for the composite food gels. In addition to the analysis of gel systems, TD-NMR is also important method to determine the originality and adulteration in food samples. For example, it was used in various studies to detect the adulteration in several type of food products such as honey (Ribeiro et al., 2014), milk (Santos, Pereira-Filho, &

Colnago, 2016), olive oil (Ok, 2017), frankfurter (Uguz, Ozvural, Beira, Oztop, & Sebastião, 2019), wine and fruit juices (Ogrinc, Košir, Spangenberg, & Kidrič, 2003).

In addition to the conventional low field TD-NMR methods that were mentioned above, Fast Field Cycling (FFC) NMR is also promising method in terms of its wide application areas including food science. FFC-NMR relaxometry is the only low-field NMR technique that measures the longitudinal spin relaxation rate ( $1/T_1$ ) as a function of the magnetic field strength, spanning a wide range of frequencies (from a few kilohertz to 42 MHz (1 T) or higher regarding the limitation such as the size of the magnet and the FFC technique that was used (Steele, Korb, Ferrante, & Bubici, 2016). As indicated by Besghini et al. (2019), this can be performed by two different ways: the 1<sup>st</sup> one is the utilization of a single instrument which is capable to perform fast electrical switching of the field while the second one is moving the sample physically in instruments with different magnetic fields (Besghini et al., 2019).

FFC technology has improved significantly after the installation of the first version of the SPINMASTER FFC 0.5 T relaxometry, from Stelar s.r.l. (Mede, Italy) at the University of Lund in 1997 and this NMR relaxomet having a two-layer air-core solenoid magnet was capable to switch the magnetic field strengths from 10 kHz to 20 MHz (Steele et al., 2016). Upon utilization of these commercial FFC NMR Relaxometers exploiting the principle of  $T_1$  dependency on magnetic field strength, NMR Dispersion (NMRD) profiles could be obtained quickly without altering the instruments due to the fast electronic switching time ( $\sim 150\mu\text{s}$ ) (Steele et al., 2016).

Regarding the basic principle of fast field cycling NMR as shown in Fig.1.16, the sample is firstly polarized in a magnetic field with a flux density  $B_p$ . The relaxation occurs in the low field interval and it changes according to the length and flux density known as  $B_r$ . The remaining signal from this last relaxation process is determined at a fixed flux  $B_d$ . In other words, regardless of chosen relaxation field, signals obtained via RF unit are tuned to the frequency which is predetermined. In order to detect the

signals, the simple free induction decay (FID) after a 90° RF pulse or a spin echo combined by several pulses is recorded as seen in Fig. 1.16 (Kimmich & Anardo, 2004).

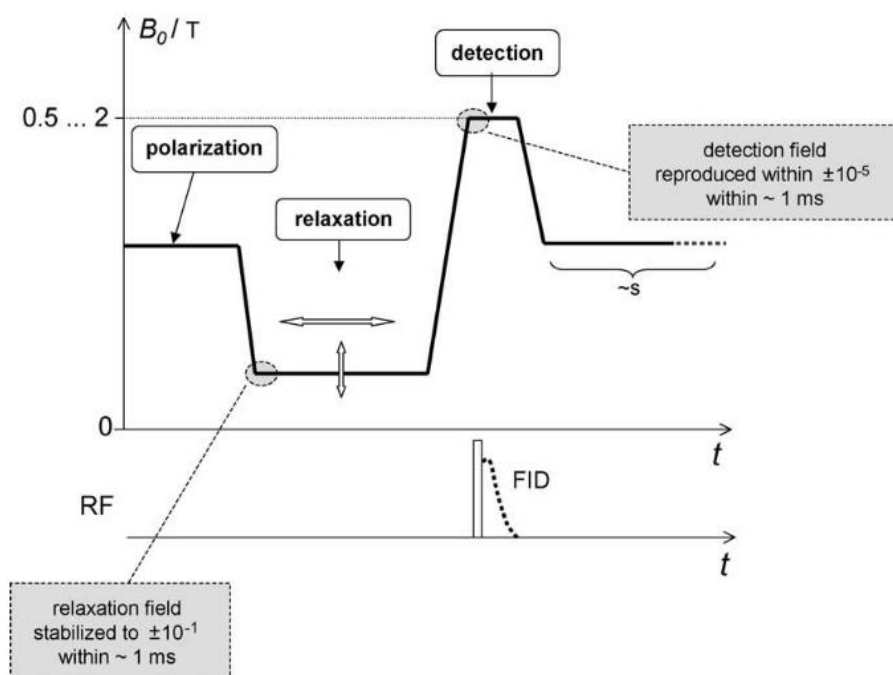


Figure 1.12. Schematic representation of a typical cycle of the main magnetic field  $B_0$  employed with field-cycling NMR relaxometry (Kimmich & Anardo, 2004)

As indicated by Besghini et al. (2019), the magnitude of  $T_1$  (spin-lattice) relaxation time is depend on how the interaction between spins and with their environment (in other words “lattice”) is regulated by the molecular mobility (Besghini et al., 2019). Actually, the magnitude of  $T_1$  also depends on motional correlation time ( $\tau_c$ ) which is described by the BPP (Bloembergen–Purcell–Pound) equation which was shown in below as equation 3:

$$\frac{1}{T_1} = \frac{3}{10} \frac{\gamma^4 \hbar^2}{r^6} \tau_c \left( \frac{1}{1 + \omega_0^2 \tau_c^2} + \frac{1}{1 + 4\omega_0^2 \tau_c^2} \right) \quad (3)$$

Where  $T_1$  denotes spin-lattice relaxation time,  $\gamma$  is gyromagnetic ratio,  $\hbar$  denotes Planck's constant while  $r$  denotes mean distance between coupling proton pairs within the molecule.  $\omega_0$  denotes Larmor angular frequency while  $\tau_c$  denotes motional correlation time.

Determination of these correlation times can be utilized to differentiate distinct dynamical regimes inside the material which is related with its morphology and structure (Besghini et al., 2019). Since motional correlation times affect dynamical behavior of the samples associated with viscoelasticity and mechanical response, evaluation of these correlation times becomes the main concern for specific applications (Besghini et al., 2019). Referring back to the Equation 3, analysis of dispersion curves of ( $T_1$  vs  $\omega_0$  (Larmor frequency)) enables researchers to differentiate distinct correlation times defining distinct dynamics inside the material (Besghini et al., 2019) leading to make quantitative analysis about the molecular dynamics of the materials (Danuta Kruk et al., 2019). Moreover, thanks to FFC technology, it makes possible to obtain detailed analysis of molecular dynamics in a single experiment and helps to understand the mechanism of motion (R. Meier, Kruk, Gmeiner, & Rössler, 2012) such as dimensionality of translation diffusion (Danuta Kruk et al., 2019). In addition, since FFC relaxometry is capable to describe water dynamics, it is suitable to characterize gel systems such as renewable ionic gels (Bielejewski, Rachocki, Kaszyńska, & Tritt-Goc, 2018), supramolecular gels (Kowalczyk, Rachocki, Bielejewski, & Tritt-Goc, 2016) and hyaluronic dermal fillers (Danuta Kruk et al., 2019). Recently, it was also utilized to explore the water mobility in food gels such as gelatin based soft candies (Pocan, Ilhan, et al., 2021) and different kind of cheese samples (Danuta Kruk, Florek-Wojciechowska, Masiewicz, & Oztop, 2021). FFC NMR relaxometry has also promising applications as a quality control tool in food science and processing such as discriminating the spoiled milk samples from the fresh (unspoiled) ones (Steele et al., 2016), determining the shelf life of fruits (Capitani et al., 2014), detecting the geographical

origins of vinegars (Baroni, Consonni, Ferrante, & Aime, 2009), characterization of wine (Bodart et al., 2020), honey (Płowaś-Korus et al., 2018), cocoa butter (Ladd-Parada, Povey, Vieira, & Ries, 2019) and vegetable oils (A. Rachocki & Tritt-Goc, 2014).

#### **1.4.1 Characterization of Gel Systems with Time Domain (TD) NMR Relaxometry**

There are numerous studies in the literature that utilized TD-NMR to characterize hydrogels such as exploring the effect of different polysaccharides on swelling of composite whey protein hydrogels (Ozel, Uguz, Kilercioglu, Grunin, & Oztop, 2016b), monitoring the synthesis of polyacrylamide hydrogels (Rodrigues, Sebastião, & Tavares, 2017) and designing of pH sensitive Alginate/Gum Tragacanth based hydrogels for oral insulin delivery (Cikrikci, Mert, & Oztop, 2018).

Ozel and coworkers used a 0.32 T (13.52 MHz) low field NMR system to investigate the effect of different polysaccharides such as xanthan (XN), pectin (PC) and alginate (AL) addition on the swelling of whey protein hydrogels (Ozel et al., 2016a). For this purpose, they measured  $T_2$  (spin-spin) relaxation times. In their study, firstly, the relation between swelling ratio (SR) and mono-exponential  $T_2$  relaxation times was discussed and  $T_2$  percent changes (%) were calculated during the 0-6 h time interval of the experiments. The results of their experiments indicated that there was a high correlation between the water uptake and  $T_2$  relaxation times of the gels ( $r > 0.99$ ). It was also demonstrated that, although XN gels uptake lower amount of water compared to its counterparts, high increase in  $T_2$  times of these gels validated that polymer-water interaction are predominant factor on the swelling behavior of these gels and this case was explained with the high viscosity and decreased permeability of XN gel network (Ozel et al., 2016a). In the same study, in order to get more

information about the hydrogels, a multi-exponential approach was utilized while interpreting the  $T_2$  relaxation times and for this purpose NNLS analysis was used to obtain the relaxation spectrum of the hydrogels. As a result of this analysis, for all type of hydrogels three distinct peaks with different proton populations were found excluding the control one containing only whey protein. Among these peaks, the first one was attributed to the polymer-polymer interactions, the second one was explained with the polymer-water interactions while the third one was associated with water entrapped in gel network during swelling of the hydrogels. On the other hand, for the control hydrogel which contains solely whey protein, only one peak was observed in the spectrum indicating polymer-water interactions dominated the system (Ozel et al., 2016a).

In another study performed by the same research group, release behavior of insulin from the alginate-gum tragacanth (ALG-GT) hydrogels containing different amount of ALG ratio (100,75, 50,25) during the 0-6 h time interval was studied by utilizing TD-NMR (Cikrikci et al., 2018). For this study, again 0.32 T (13.52 MHz) low resolution TD-NMR system was utilized to measure spin lattice ( $T_1$ ) and spin-spin ( $T_2$ ) relaxation times.  $T_1$  relaxation times was measured by using saturation recovery pulse sequence while  $T_2$  relaxation time was measured by a CPMG pulse sequence. In addition to these classical approach, they also measured the self-diffusion coefficients (SDCs) of hydrogels by using pulse gradient spin echo sequence. In their study, it was illustrated that, as a result water uptake after immersion in intestinal fluid during 6 h,  $T_1$  relaxation times increased for all samples compared to their initial values (0 h). Results of  $T_2$  relaxation times were also found to be consistent with the  $T_1$  relaxation times and swelling of samples absorbing solvent and having abundant hydrogen molecules led to longer  $T_2$  relaxation times of the hydrogels. It was also demonstrated that as the GT amount increased in hydrogels,  $T_2$  times also increased significantly ( $p < 0.05$ ) (Cikrikci et al., 2018). In the same study, as a more quantitative approach, SDCs of the hydrogels were measured as mentioned previously and they were found in the range of  $2 \times 10^{-9}$ - $1 \times 10^{-9}$  m<sup>2</sup>/s and found to be

similar as a result of 6 h immersion in intestinal media ( $p < 0.05$ ). It was highlighted that SDCs showed the average of water molecules that come from different compartments of the gels and it was associated with the self-diffusion of water molecules in the gel matrix and mobility of water molecules (Cikrikci et al., 2018).

In addition to these studies related with the gels systems, Rodrigues et al. (2017) studied the synthesis reactions of polyacrylamide based hydrogels and monitored these reactions by using  $^1\text{H}$  TD-NMR system operating at 0.54 T (23.4 MHz, proton Larmor frequency) equipped with an air flow temperature control unit ( $\pm 0.1^\circ\text{C}$ ). However, this time, instead of utilizing traditional pulse sequences like CPMG or Saturation Recovery as mentioned previously, steady state pulse sequence called as “Carr-Purcell Continuous Wave Free Precession pulse sequence (CP-CWFP)” was used to determine the relaxation constants. Structure-property relations of the hydrogel samples was also examined by using “Multiple Quantum ( $^1\text{H}$  MQ)” probing (Rodrigues et al., 2017). For the experiments, four hydrogel samples containing different amounts of crosslinking agents and monomers were examined. Results of CP-CWFG experiments indicated that detectable correlation was observed between the signal behavior and formulations of the samples demonstrating the powerful sensitivity of CP-CWFG to differentiate the samples prepared by using different amount of crosslinking agents. The results obtained from the TD-NMR experiments were also compared with the traditional methods such as UV-Vis spectroscopy and very similar results were obtained suggesting that utilization of TD-NMR by using advanced pulse sequences such as CP-CWFP and MQ could be considered as a promising technique to monitor polymerization reactions of hydrogels as well as conventional methods such as UV-Vis spectroscopy (Rodrigues et al., 2017).

In recent years, characterization of confectionery gels with the low field NMR systems are becoming more common as well as ordinary gel systems. Regarding the similarities between gel systems and soft candy products, very similar approaches



are utilized by using TD-NMR systems to explore structural properties of soft candy products such as water binding and water holding behavior, crystallinity, solid-solid and solid-water interactions, etc. as in the case of gel system characterization.

In previous studies, TD-NMR was utilized to characterize gelatin based low calorie soft candies (Efe, Bielejewski, Tritt-Goc, Mert, & Oztop, 2019), effect of D-allulose substitution on starch based (Ilhan et al., 2020b) & pectin based (Ates et al., 2020, 2021) soft candies and detection of the optimum drying conditions for gelatin based soft candies (Pocan, Kaya, et al., 2021).

In the study of Efe et al. (2019), gelatin based low calorie soft candies were formulated by using isomalt, stevia and maltitol and they were substituted with sucrose at increasing concentration level (30%, 50% and 70%). Low field TD-NMR experiments were performed by using 0.52 T (22.34 MHz) system at 23 °C.  $T_2$  relaxation times were measured through Carr–Purcell–Meiboom–Gill (CPMG) sequence with 2 ms echo time and 150 echoes while  $T_1$  relaxation times were measured by using Inversion Recovery (IR) sequence with 1s repetition delay. Mono-exponential model was used to express  $T_1$  spin-lattice relaxation times while bi-exponential model was utilized to measure the  $T_2$  spin-spin lattice relaxation times. In their study, authors mentioned that, most probably due to the rigid and strong structure of gelatin network, mono-exponential behavior of  $T_1$  relaxation times is expected. It was also found that, different sucrose concentration and sweetener type used in the formulations led to detectable changes in  $T_1$  relaxation times, indicating power of  $T_1$  relaxation times to differentiate the gelatin based soft candies regarding the source of sugar they contain. Among the samples with different formulations, the highest  $T_1$  was found for the maltitol containing samples while similar and lower  $T_1$  relaxation times were found for the ones containing stevia and isomalt (Efe et al., 2019). In the same study, unlike  $T_1$  relaxation times, bi-exponential fitting was applied to  $T_2$  relaxation times leading to obtain two distinct proton pools with different relaxation times ( $T_{21}$  and  $T_{22}$ ) with different contributions

of proton populations. Similar to the results of  $T_1$  relaxation times,  $T_{21}$  and  $T_{22}$  results were found to be the longest for the samples containing maltitol whereas they were found shorter for the ones including stevia and isomalt in their formulations. (Efe et al., 2019).

Ilhan et al. (2020) studied the effect of D-allulose and soy protein isolate (SPI) substitution in starch based candies by using TD-NMR (Ilhan et al., 2020b). TD-NMR experiments were conducted by using 0.5 T (20.34 MHz) low resolution system. For  $T_1$  measurements, saturation recovery sequence was utilized with 300 ms relaxation time (TR) and 400 ms observation time while  $T_2$  relaxation times were measured through CPMG sequence with the parameters of 40 us echo time and 400-700 echoes. Mono-exponential fitting was applied for  $T_1$  measurements while  $T_2$  relaxation times were defined by multi exponential approach. In their study, upon SPI addition, longer  $T_1$  relaxation times were obtained which could be attributed to the collapse of starch gel matrix resulting in higher mobility of water molecules. Moreover, it was also observed that as the D-allulose substitution was increased, significant decrease was observed for the  $T_1$  relaxation times of starch based soft candies, indicating the improved starch gel network formation in the presence of D-allulose resulting in mobility of water and thereby shorter  $T_1$  relaxation time. In addition, higher  $T_1$  relaxation times of the samples only containing sucrose as the sugar source compared to the samples including D-allulose was attributed higher crystallinity of these samples, proving crystallization inhibition behavior of D-allulose (Ilhan et al., 2020b). In the same study, Ilhan et al. (2020) also demonstrated  $T_2$  relaxation spectra for the starch based gels and at least 3 peaks with distinct  $T_2$  relaxation times and relative areas (RA) were observed for the starch based soft candies depending on formulation. According to the spectra results, the shortest  $T_2$  with highest RA1 was obtained for the samples containing soy protein, starch and 10% D-allulose containing samples due to improved solid-solid interactions for this sample which might be stemmed from the competitive environment for water molecules. In addition, for the SPI containing starch gels, proton population with

higher relative area was observed and this case was attributed to enhanced Maillard reaction rate in the presence of SPI. In this study, authors followed the changes upon D-allulose and/or SPI addition in starch gel network as a result of retrogradation, sugar crystallization or occurrence of Maillard reaction and they concluded that TD-NMR is a promising method to monitor gelation behavior of starch based soft candies (Ilhan et al., 2020b).

In another study performed by the same research group, again effect of D-allulose and SPI addition was studied but this time for the pectin based soft candies (Ates et al., 2020). For the TD-NMR experiments, same low resolution system working at 0.5 T (20.34 MHz) was used.  $T_2$  relaxation times of the samples were measured through CPMG sequence with 40  $\mu$ s echo time and echo numbers changing in the range of 400-900 depending on the formulation of pectin based soft candies. In their study, both mono-exponential and bi-exponential approaches were used to in the analysis of  $T_2$  relaxation times but bi-exponential model was found to be more suitable to define the characteristics of the samples. According to the results, two distinct proton pools with different  $T_2$  relaxation times and relative areas (contribution of signal intensity) were found in the relaxation spectra. While the first proton pool with the shortest relaxation times changing in the range of 0.7-2.5 ms were found to be associated with the solid-solid interactions in the sample, the second proton pool showing higher  $T_2$  (longer than 1.5 ms) was found to be related with the entrapment of bulk water in gel network. For the pectin based soft candies without SPI addition, as the sugar source only sucrose containing samples showed one peak in the spectra while solely allulose containing samples demonstrated two distinct peaks related with different proton populations in the spectra, indicating use of different type of sugar (allulose or sucrose) lead to detectable changes in spectra which could be related with the different gelation properties of pectin in the presence of different type of sugars. Moreover, in the same study, it was observed that, addition of SPI resulted in new peak formation for the samples containing solely

sucrose, proving occurrence of possible new interactions between pectin-water or SPI-pectin (Ates et al., 2020).

In a very similar study conducted by the same researchers, *in vitro* digestibility of D-allulose containing pectin-soy based soft candies were explored by using low resolution TD-NMR system with the same properties that were mentioned above (Ates et al., 2021). This time mono-exponential  $T_2$  relaxation times were utilized to investigate the changes in pectin based soft candies during *in vitro* digestion since  $T_2$  data were found to be well-fitted to a mono-exponential model. In the same study, significant increase in  $T_2$  relaxation times was observed for all samples after 2 h digestion. In addition, it was found that both D-allulose and SPI concentration led to detectable changes in mono-exponential  $T_2$  relaxation times. Regarding SPI concentration, the longest  $T_2$  relaxation time was found for the samples including 2.5% SPI in its formulation compared to the ones containing 1% SPI and non-soy samples. On the other hand,  $T_2$  relaxation times were found to be increased as the sucrose content increased in the samples, indicating confirmation of higher water binding ability of sucrose compared to the D-allulose (Ates et al., 2021).

#### **1.4.2 Characterization of Gel Systems with Fast Field Cycling (FFC) NMR Relaxometry**

In addition to the TD-NMR techniques, FFC NMR also seems as a powerful technique to characterize gel systems. In previous studies, FFC NMR technique utilized in numerous studies like exploring the water dynamics in hyaluronic dermal fillers (Danuta Kruk et al., 2019), revealing the effect of gel matrix confinement in supramolecular gels (Kowalczyk et al., 2016) and investigating the influence of gelation on diffusion and conductivity enhancement effect in ionic renewable gels (Bielejewski et al., 2018).

Kruk and coworkers performed spin–lattice nuclear magnetic resonance relaxation experiments by using a FFC NMR Relaxometer (Stelar S.r.l., Mede, Italy, model SPINMASTER FFC2000) by collecting the data over a frequency range changing between 4 kHz to 40 MHz for the five different type of commercially available dermal fillers (DF1-DF5) composed of hyaluronic acid (Danuta Kruk et al., 2019). FFC experiments were performed for the dermal fillers at 37° to mimic the body temperature. It was also found that, the relaxation data fitted to mono-exponential model for all samples and at all magnetic fields and dispersion profiles of all samples showed detectable differences.

On the other hand, translational ( $\tau_{trans}$ ) and rotational correlation times ( $\tau_{rot}$ ) were found to be very similar for the dermal fillers. In addition, dipolar relaxation constants of the samples were found to be in concordance with the hyaluronate contents indicating that these dermal fillers have very similar water binding capacities. Moreover, translational diffusion coefficient ( $D_{trans}$ ) values were found around  $1 \times 10^{-12}$  m<sup>2</sup>/s which is nearly  $3 \times 10^3$  times smaller than the diffusion coefficient of bulk water. On the other hand, for these samples, rotational correlation times ( $\tau_{rot}$ ) of the water molecules that was in confined region were found in the order of  $4 \times 10^{-9}$  s producing the ratio of ( $\tau_{trans}$ )/( $\tau_{rot}$ ) which is changing in the range of 17-21, which is a typical ratio for the liquid samples. Finally, for this group of samples frequency independent term (A) was found in the range of 0.32-0.34 s<sup>-1</sup> which is close to the bulk water 's relaxation rate (Danuta Kruk et al., 2019). For all samples, it was indicated that, there is a pool for the confined water molecules which exposed to rotational dynamics characterized by ( $\tau_{rot}$ ) which is equal to  $4 \times 10^{-9}$  s. It was concluded that, FFC NMR relaxometry was found to be powerful tool to reveal both time scales of molecular motion and mechanism of molecular motions leading to obtain valuable information from the water dynamics of different dermal fillers (Danuta Kruk et al., 2019).

Kowalczuk et al. (2016) investigated the gel matrix confinement together with solvent dynamics in supramolecular gels (Kowalczuk et al., 2016). In their study, supramolecular gels were prepared by using sugar gelator of methyl-4, 6-O- $\alpha$ -D-glucopyranoside (labeled through the text as “**1**”) at 4% concentration with certain types of solvents with the name of 1-butanol (BU) and 1,3-propanediol (PG), respectively.. The measurements of FFC NMR Relaxometry was conducted as a function of magnetic field  $B_L$  and it was expressed in terms of Larmor frequency ( $\omega = \gamma B_L$ ). In their study, the results of the FFC experiments were reported as Nuclear Magnetic Resonance Dispersion (NMRD) profiles indicating the plot of relaxation rate ( $R_1=1/T_1$ ) versus Larmor frequency. In their study, NMRD profiles demonstrated for both bulk solvents (PG) and BU) and for the gel systems formulated by using 4% **1** with PG solvent ( labeled as “**1**/PG”) and 4% **1** and BU solvent (labeled as “**1**/BU”) (Kowalczuk et al., 2016). According to the results of NMRD profiles, higher viscosity of PG related with the stronger dipole-dipole interactions resulted in shorter spin-lattice relaxation times ( $T_1$ ) resulting in higher relaxation rate ( $R_1$ ). In the same study, it was also found that, bulk BU and PG solvents’ NMRD profiles are frequency independent at the frequencies ranging from 0.01 to 5 MHz and their profiles followed a steady trend. On the other hand, it was also demonstrated that, below 0.1 MHz detectable alterations were observed in NMRD profiles of gels that were formed in the presence of PG solvent and gelator **1**, which could be considered as a fingerprint of molecular interaction between PG and gelator **1**. Unlike PG gels, detectable alterations were not observed in NMRD profiles of BU gels, indicating weak gelator-solvent interactions, which can be stemmed from lower polarity of BU solvent compared to the PG solvent (Kowalczuk et al., 2016). In the same study, quantitative analysis of relaxation data was also applied by using RMTD (reorientations mediated by translational displacements) model which is suitable for the analysis and explanation of liquid confinement in nanopores (Kowalczuk et al., 2016). According to the results of analysis, rotational correlation times ( $\tau_{rot}$ ) were found as  $1.32 \times 10^{-9}$  and  $1.45 \times 10^{-9}$  s for the PG and BU

solvents, respectively. On the other hand, translational correlation times ( $\tau_{trans}$ ) were found as  $2.32 \times 10^{-8}$  s for PG and  $4.31 \times 10^{-9}$  for the BU solvent. Authors also concluded that, dynamical parameters such as correlation times and surface diffusion could be obtained to define the solvent dynamics in supramolecular gels (Kowalczyk et al., 2016).

In another study conducted by the same research group, FFC NMR was utilized to investigate the local motions of the electrolyte that was found at the surface of gelator matrix in renewable ionic gels (Bielejewski et al., 2018). In their study, FFC NMR was utilized to investigate the molecular dynamics of both water (solvent) and tetramethylammonium cations (TMABr) (solute) at changing molar concentrations, which were found in both pure electrolyte and ionogel state. According to the NMRD results, authors stated that, increasing molar concentrations of TMABr solutions resulted in increase in relaxation rates ( $R_1$ ) or in a same manner, decrease in  $T_1$  spin-lattice relaxation times. It was stated that, this situation might have stemmed from two reason: The first one is viscosity effect. As the TMABr increased in the solutions, viscosity of the solutions also ascended resulting in longer  $R_1$  and shorter  $T_1$  most probably due to the slower molecular motions and enhanced dipole-dipole couplings. The second reason is existence of paramagnetic ions such as bromide anion in the solutions. As the molar concentrations of solutions increased, paramagnetic ion concentrations (bromide) were also increased in the solution leading to more effective nuclear-electron spin-spin interactions and longer  $R_1$  or shorter  $T_1$  (Bielejewski et al., 2018). In the same study, NMRD profiles of ionogels were also investigated and more complicated profiles were observed compared to the ones which contains solely electrolyte solutions. Unlike solutions, two distinct values of  $R_1$  were obtained for the ionogels: The first one was found as  $0.7 \text{ s}^{-1}$  for the ionogels composed of the lowest electrolyte concentration while the second  $R_1$  was found as  $0.6 \text{ s}^{-1}$  for the ones consisting of higher electrolyte concentration. In order to analyze the relaxation data quantitatively, two different suitable models were used: The first model is RMTD and it was used to explain the contribution of water which

interacts within the gel network to the overall relaxation. The second model is BPP and it was utilized to define the contributions from water fractions that were found in other environments. As a result of the analysis, it was concluded that water fraction which was adsorbed at the gel matrixes is defined with reduced diffusion coefficient which is related with the RMTD contribution compared to the bulk water. In addition, it was concluded that, regarding the water fraction which creates shell of solvation in vicinity of ions, its dynamics does not rely on to molar concentrations of electrolytes since correlation times ( $\tau_c$ ) were found in the range of  $7.8 \times 10^{-9}$  s-  $7.8 \times 10^{-8}$  s, which is valid case at all molar concentrations of electrolytes (Bielejewski et al., 2018).

As well as characterization of hydrogels and ionogels, FFC NMR technique also becoming common and seems as a promising method to characterize the food gels such as cheese (Conte et al., 2020; Danuta Kruk, Florek – Wojciechowska, et al., 2021). However, there are still few studies to explore the application areas of FFC-NMR of soft candies which could be also considered as an example to the perfect composite gel systems.

## **1.5 Objective of the Study**

Understanding the quality and authenticity problems of confectionery products require a deep understanding of the science behind. Confectionary research is usually based on classical physical measurements such as moisture content, water activity, texture and rheology. Use of advanced characterization techniques for a better understanding of the system is an issue of interest

The main objective of this dissertation is to use TD-NMR and FFC-NMR relaxometry techniques for the characterization of different confectionery formulations and complement the results with the conventional techniques.. For this purpose, the study was divided into three main parts.



For the first and the second part, D-Allulose was utilized in gelatin based confectionery gels to formulate the low calorie soft candy products. The candies were investigated by TD-NMR and FFC NMR Relaxometry respectively and results were supported with other complementary methods such as DSC, XRD and TGA.

For the third part, starch based confectionery gels (Turkish delights) are formulated by using sucrose and different types of corn syrups to understand the quality changes and the presence of corn syrup by using both TD-NMR and FFC NMR Relaxometry.

The most important objectives of this dissertation could be summarized as shown in below:

- *To design and formulate D-allulose containing low calorie gelatin based confectionery gels*
- *To determine the effect of D-allulose substitution on the quality characteristics of gelatin based confectionery gels such as texture, crystallinity, etc.*
- *To determine the effect of D-allulose substitution on the relaxation behavior of gelatin based confectionery gels by evaluating  $T_1$  (spin-lattice) and  $T_2$  (spin-spin) relaxation times obtained through TD-NMR experiments*
- *To assess the effect of D-allulose substitution on the water dynamics of gelatin based confectionery gels by using FFC-NMR Relaxometry together with Thermo-gravimetric analysis (TGA) as a complementary method*
- *To reveal the potential of TD-NMR and FFC-NMR techniques to detect the authenticity and quality of Turkish delights as an alternative to well-known techniques such as X-ray Diffraction Analysis*



## CHAPTER 2

### MATERIALS AND METHODS

#### 2.1 Materials

##### 2.1.1 Gelatin based Soft Candies

Sucrose (Bal K p , Aksaray, Turkey) was purchased from a local market in Ankara, Turkey. D-Allulose was used as the rare sugar supplement (All-u-lose, Downers Grove, U.S.A). Bovine gelatin with a blooming index of 200 and corn syrup (DE=42) were kindly provided from Kervan Gıda (Istanbul, Turkey). Distilled water was used in all preparations. Sodium azide (Sigma Chemical Co., St Louis, Mo., U.S.A.) was added at a final concentration of 0.02% (w/w) to all sugar solutions as the antimicrobial agent.

##### 2.1.2 Turkish Delights

Sucrose (Bal K p , Aksaray, Turkey) was purchased from a local market in Ankara, Turkey. Corn syrups with commercial names SBF10, SCG40 and SCG60) were kindly provided by Sunar Mısır A.Ş (Adana, Turkey). Total soluble solid content (Brix) and glucose or glucose/fructose content of these corn syrups are given in Table 2.1. Acid modified starch was kindly provided by Kervan Gıda A.Ş (İstanbul, Turkey). Citric acid monohydrate was purchased from Sigma-Aldrich Chemical Co. (St. Louis, MO, USA). Distilled water was used in all formulations.

Table 2.1. Specifications of corn syrup types that were used in the production of Turkish delights

<b>Corn Syrup Name</b>	<b>Brix(°)</b>	<b>Glucose (%)</b>	<b>Fructose (%)</b>
<b>SBF10 (Glucose/Fructose Syrup)</b>	<b>79</b>	<b>36</b>	<b>10</b>
<b>SCG40 (Glucose Syrup)</b>	<b>83</b>	<b>40</b>	<b>-</b>
<b>SCG60 (Glucose Syrup)</b>	<b>82</b>	<b>60</b>	<b>-</b>

## **2.2 Methods**

### **2.2.1 Gelatin based Soft Candies**

#### **2.2.1.1 Preparation of Gelatin based Soft Candies**

The gelatin concentration was determined as 8% by considering the study of Marfil et al., 2012. 8 gram of gelatin was dissolved in 15 ml of distilled water at 100°C using a magnetic stirrer. For the sugar mixture, 20 grams of corn syrup (DE = 42) and 40 grams of powdered sugar (sucrose / sucrose + rare sugar mixture) were mixed in 17 ml of water at 400 rpm until the temperature of the mixture reached 100 ° C. Afterwards, this mixture was added to the gelatin solution and mixed using a magnetic stirrer at 85° and 350 rpm. The mixture was taken when the brix value reached nearly 70° for all formulations and poured into molds with dimensions 3x3x2 cm. They were kept at room temperature for 1 day and then taken from the molds and stored at an incubator having 25°C temperature and 60% relative humidity. Analysis of all samples were carried out at the first, 14<sup>th</sup> and 28<sup>th</sup> day of storage. Samples containing only sucrose (40 wt% sucrose) as a powdered sugar were

prepared for control purposes (P0). For the other samples, D-Allulose was replaced with sucrose in increasing amounts (10%, 20%, 30%, 40%) (wt). Formulations of all samples are shown in Table 2.2.

Table 2.2. Gelatin based soft candies formulated with different D-Allulose substitution (wt (%))

<b>Sample Name</b>	<b>Formulation</b>
<b>P0</b>	40% sucrose
<b>P10</b>	30% sucrose + 10% D-Allulose
<b>P20</b>	20% sucrose + 20% D-Allulose
<b>P30</b>	10% sucrose + 30% D-Allulose
<b>P40</b>	40 % D-Allulose

### 2.2.1.2 Brix Measurement

Brix measurements were performed by using a Digital Refractometer (HANNA, Cluj, Romania) for all candy solutions before molding to ensure that all samples reached similar brix values.

### 2.2.1.3 Moisture Content Determination

Moisture Content of the different formulations of gelatin-based confections were measured by keeping small amount of samples at 70 °C for 4 hours in a vacuum oven (DAIHAN, Germany). Weight loss from samples were recorded and the moisture content (MC) of each sample was calculated on a wet basis. MC was analyzed in the samples during the 0, 14, 28 days aging period.

#### **2.2.1.4 Water Activity**

An Aqualab 4TE (METER Group, Pullman, WA) was used to measure water activities of the prepared samples. Experiments were conducted at 25 °C in replicates during the 0, 14, 28 days of storage.

#### **2.2.1.5 Color**

L\* (brightness), a\* (red/green ratio) and b\* (yellow/blue ratio) values of the gummy candies were measured with a bench-top spectrophotometer (model CM-5, Konica Minolta Inc., Japan). Color measurements were performed for the samples at the first day of storage.

Chroma (C) which indicates colour intensity, and hue angle (H°) which shows visual colour appearance were also calculated as indicated in a previous study (Kamiloglu, Pasli, Ozcelik, Van Camp, & Capanoglu, 2015) by the following equations:

$$C = (a^{*2} + b^{*2})^{1/2} \quad (1)$$

$$H^{\circ} = \tan^{-1}(b^{*}/a^{*}) \quad (2)$$

#### **2.2.1.6 X-Ray Diffraction**

XRD Patterns of samples containing only sucrose (P0) and only D-Allulose (P40) were measured by using Rigaku Ultima-IV X-Ray Diffractometer. All the samples were measured within 2h in a temperature range of 5–50 °C with a scan rate of 1°/min according to the method of Qoiao et al. (2017). X-ray analysis was performed at the first and last day of the storage. Experiments were carried out at METU Central Laboratory.

### **2.2.1.7 Textural Analysis**

Hardness of the gelatin-based confections was measured by using a Texture Analyzer (Lloyd Instruments, TA Plus, Hants, UK). A 35 mm cylinder shape probe having a diameter of 1 cm and load cell of 50N was attached to the instrument for the measurement of hardness. Samples were compressed twice with 100 mm/min pre-test speed. Extension distance was adjusted as 0.68 cm. NEXIGEN Texture Analysis software was used for data analysis.

### **2.2.1.8 Glass Transition Temperature Determination ( $T_g$ )**

A Differential Scanning Calorimeter DSC 4000 (Perkin Elmer, MA, USA) was used to determine the changes in the glass transition temperature of gelatin based soft candies at the first and last day of storage. Approximately 10 mg samples were measured in hermetically sealed pans, by taking an empty aluminum pan as a reference. Pure nitrogen gas was applied to the system with a flow rate of 19.8 ml/min and samples were cooled from 25 °C to -65 °C with a rate of 5 °C/min and heated from -65 °C to 35 °C at a rate of 5 °C/min. The Pyris Manager software was used to calculate glass transition temperature ( $T_g$ ).

### **2.2.1.9 Time Domain (TD) NMR Relaxometry Experiments**

TD NMR relaxometry experiments were carried out using 0.5 T (20.34 MHz) system (Spin Track, Russia) at Middle East Technical University (METU), Department of Food Engineering, Ankara, Turkey. For  $T_1$  measurements, Saturation Recovery Sequence was used with a 300 ms relaxation period (TR) and 400 ms observation time and 4 scans.

For  $T_2$  measurements, the Carr-Purcell- Meiboom-Gill (CPMG) sequence was used with parameters of 40  $\mu$ s echo time, 2,500 echoes and 4 scans.  $T_1$  and  $T_2$  measurements were performed for all samples at each sampling day in duplicates.

The  $T_1$  and  $T_2$  data were analyzed by 2 different approaches as indicated in the study of Ozel et al. (2017). Firstly, mono-exponential fitting was conducted on the relaxation curves using MATLAB. Non-negative-Least-Square analysis was conducted on  $T_2$  curves to obtain a relaxation spectrum. Relative areas (%), number and amplitudes of peaks of the samples were recorded by using this method with the PROSPA software (Magritek Inc., WellingtonNew Zealand). For  $T_1$  relaxation time, only mono-exponential approach was used.

#### **2.2.1.10 Fast Field Cycling (FFC) NMR Relaxometry**

This part of the study was performed at University of Warmia and Mazury (UWM), Olstyn, Poznan. Samples were cut into smaller pieces to fit into 10 mm NMR tubes. Spin-lattice relaxation times of samples have been collected in the frequency range of 4 kHz-40 MHz (expressed in terms of  $^1\text{H}$  Larmor frequency) with a Spinmaster 2000 Relaxometer. (Stelar, Mede, Italy). The switching time was set to 3 ms. In order to simulate the storage conditions, temperature was set to 25 °C. The FFC measurements have been performed for two samples (replicates) for each composition for only freshly prepared samples (0 day).

#### **2.2.1.11 Thermo gravimetric Analysis (TGA)**

Thermo gravimetric analysis was conducted by using Perkin Elmer Pyris1 (Perkin Elmer, MA, USA). The experiment was operated from 30 °C to 400 °C at a heating rate of 5 °C/min under nitrogen. Mass loss at first decomposition stage (up to 150 °C) and derivative weight loss (%) curve was analyzed determine state of water in different formulations. Mean of 4 replicates were reported for these experiments.



## **2.2.2 Turkish Delights**

### **2.2.2.1 Preparation of Turkish Delights**

Turkish delights were prepared according to the method of Ilhan et al. (2020) with some modifications.

10 g starch was mixed with 2 times the amount of water (20 g) by its weight and gelatinized in an oil bath at 140 °C for 5 min until it was dissolved completely. During this time, 54 g sugar (sucrose or corn syrup) and 16 ml water boiled up to 115 °C before mixed with starch water. 0.1 g citric acid was also added to this sugar mixture for all formulations. Cooking was continued at 125 °C in oil bath. Afterwards, the mixture was poured into starch molds with dimensions of 2.5×2.5×2 cm and kept at room temperature (25 °C) for 48 hours. Composition (w/w) (%) of the Turkish delights were given in Table 2.3 Original Turkish delights samples (SUC) were prepared by using only powder sugar (sucrose) while other samples were prepared by using different type of corn syrups as the sugar source. They were classified with the same name with the corn syrups that they contain (SBF10, SCG40, and SCG60).

Table 2.3. Turkish delights formulated with different type of sugar type (corn syrup or sucrose) (w/w) (%)

<b>Sample Name</b>	<b>Starch (%)</b>	<b>Sucrose (%)</b>	<b>Corn Syrup (%)</b>	<b>Citric Acid (%)</b>
SUC	10	54	-	0.1
SBF10	10	-	54	0.1
SCG40	10	-	54	0.1
SCG60	10	-	54	0.1

#### **2.2.2.2 Moisture Content Determination**

Moisture Content of the different formulations were measured at 70 °C for 4 hr in a vacuum oven (DAIHAN, Germany). Weight loss from the samples was recorded, and the MC of each sample was calculated on a wet basis.

#### **2.2.2.3 Color Analysis**

L\* (brightness), a\* (red/green ratio), and b\* (yellow/blue ratio) values of the Turkish delights were measured with a bench-top spectrophotometer (Datacolor 110<sup>TM</sup>, Lawrenceville, NJ, USA). The sample that did not contain corn syrup (SUC) was selected as the reference. Total color change ( $\Delta E$ ) was calculated as follows:

$$\Delta E = \sqrt{(L^* - L_{ref}^*)^2 + (a^* - a_{ref}^*)^2 + (b^* - b_{ref}^*)^2}. \quad (1)$$

#### **2.2.2.4 Texture Profile Analysis (TPA)**

TPA test was performed by using Texture Analyzer (Brookfield Ametek CT3, TA44 probe, Middleboro, MA, USA) by following the method of Delgado & Banon (2015) with some modifications. The samples were compressed twice with a cylindrical probe (4 mm in diameter). The testing conditions were: two consecutive cycles of 50% deformation; cross-head moved at a constant speed of 1 mm/s and a trigger point of 0.05 N (Delgado & Bañón, 2015). Hardness, adhesiveness, cohesiveness, springiness, gumminess and chewiness values of the Turkish delights were calculated by using TPA curves.

#### **2.2.2.5 X-ray Diffraction**

X-Ray Diffraction experiments were conducted by using a Rigaku Ultima-IV X-Ray Diffractometer (Japan) at 40 kV and 30 mA. Data were collected by the method of (Ilhan et al., 2020) between 4-70° with a scan rate of 1°/min.

#### **2.2.2.6 TD-NMR Relaxometry Experiments**

TD NMR relaxometry measurements were conducted by using 0.5 T (20.34 MHz) NMR instrument (Spin Track, Resonance Systems GmbH, Kirchheim/Teck, Germany) at METU, Department of Food Engineering in Ankara, Turkey.  $T_1$  (spin-lattice) and  $T_2$  (spin-spin) relaxation times were measured for different formulations. For  $T_1$  measurements, saturation-recovery sequence was used with 300-ms relaxation period (TR) and 300 ms observation time and four scans. For  $T_2$  measurements, Carr-Purcell-Meiboom-Gill (CPMG) sequence was used with parameters of 100 us echo time, 128 echoes, and four scans.

The  $T_1$  and  $T_2$  data were analyzed by two different approaches as indicated in the study of Pocaan et al (2019). First, mono-exponential fitting was conducted on the

relaxation curves using MATLAB. Nonnegative least square analysis was also conducted on  $T_2$  curves to obtain a relaxation spectrum. Relative areas (RAs; %), number, and amplitudes of peaks of the samples were recorded by using this method with the XPFit (Softonics Inc., Israel). For  $T_1$  relaxation time, only mono-exponential approach was used.

### 2.2.2.7 Fast Field Cycling NMR Relaxometry Experiments

This part of the study was performed in Institute of Molecular Physics, Poznan, Poland. Fast Field Cycling Nuclear Magnetic Resonance (FFC NMR) measurements were performed and proton  $T_1$  (spin-lattice) relaxation times were measured over different range of magnetic field strengths (covering the Larmor frequencies from 10 kHz to 20 MHz) by a Fast Field Cycling NMR Relaxometer (Spinmaster FFC2000, Stelar s.r.l., Mede, Italy) to detect the differences in NMRD profiles of the samples prepared with different sugar types. In the proton Larmor frequency range below 10 MHz, the pre-polarized (PP) sequence with the polarizing magnetic field corresponding to 20 MHz was applied for a time  $5T_1$ , whereas for experimental conditions above 10 MHz, the non-polarized (NP) sequence was used. As a result of a mono-exponential decay/recovery of the amplitude of magnetization versus time (including 22 logarithmically scaled points) the single  $T_1$  relaxation times were calculated for each sample under investigation. The error of the relaxation rates ( $R_1 \equiv 1/T_1$ ) does not exceed 5%. The NMR signal measured in the samples by FFC came only from the “mobile” protons associated mainly with water molecules undergoing different molecular dynamics depending on local surroundings. The “rigid” protons associated with a part of the gel candy composition that are not exposed to water were undetectable under the applied measuring conditions because of short FID signal. The FFC NMR experiments were conducted at 2 different temperatures, i.e., at room temperature (25 °C) to simulate storage conditions, and additionally at 4 °C to see the effect of temperature on molecular dynamics and confirm the theoretical

model applied for analysis. All samples were cooled using a liquid nitrogen (LN2) Dewar and temperature was stabilized within  $\pm 0.1$  °C. Additional  $T_1$  measurements at 500 MHz were performed with a Bruker Avance III HD spectrometer coupled to a superconducting Ascend magnet operating at 11.74 T.  $T_1$  relaxation times were determined by the zero-method ( $t(M_z = 0) = T_1 \ln 2$ ). OriginPro software with implemented functions was used for fitting theoretical models to NMRD experimental data.

### **Statistical Analysis**

All measurements were carried out in replicates (two and three depending on the measurement) and reported as means and standard errors. Statistical analysis for all the experimental results were performed by analysis of variance with the one-way model tool of Minitab (Minitab Inc., Coventry, UK). For the comparison of results, Tukey's comparison test was applied at a 95% confidence interval. The correlation coefficients were also expressed by Pearson correlation at a 95% confidence level.



## CHAPTER 3

### RESULTS AND DISCUSSION

#### 3.1 Gelatin based Soft Candies

##### 3.1.1 Moisture Content Determination

Moisture content (MC) is one of the most important criteria for the confections and most food since it directly affects the quality of the final product. The final moisture content has an important effect on shelf life and texture of the products (R Ergun et al., 2010). As shown in Figure 3.1, P30 and P40 had the highest moisture content (15.2% and 15.1%, respectively) at the first day of storage and an ascending trend was observed in MC as the D-allulose amount (wt%) increased in the formulations for each day. For this study, bovine gelatin was used in all formulations as the gelling agent. As indicated in previous studies, gelatin is a polypeptide produced from the animal protein collagen and it is used as a main ingredient for most confectionery products (Jiamjariyatam, 2017). It is capable of forming junction zones and forms a three-dimensional gel network. Sugars also have stabilizer effect on the structure of gelatin by providing hydration of proteins or strengthening hydrophobic interactions (Jiamjariyatam, 2017). In our study, it was hypothesized that, since gelatin was used as the only gelling agent, a stable gel network was obtained for the all formulations and an increasing trend in MC was associated with increasing replacement of sucrose with D-Allulose. To the best of our knowledge, there is very limited studies in literature related with the moisture uptake behavior of rare sugars. However, it was known from the previous studies that D-Allulose (formerly known as D- Psicose) has higher solubility which makes it preferable for food processing (Sun et al., 2008). Solubility of D-Allulose was reported as 74 wt% at 25 °C while solubility of fructose

was given as 80% wt% at the same temperature (Fukada et al., 2010). In another study, solubility of sucrose was reported as 67.4 wt % at 25 ° C (R Ergun et al., 2010). Therefore, it could be concluded that, D-Allulose has higher solubility than sucrose and comparable solubility with fructose which is known for its high hygroscopic property. In the light of such information, high moisture content of samples that contain 30% and 40 % D-Allulose could be attributed to high hygroscopicity of D-Allulose and their tendency to absorb more water.

It was also worth to note that, a noticeable increase was observed for the MC of P0 and P10 at the end of 28 day storage period ( $p < 0.05$ ) whereas detectable changes were not appeared for the P20, P30 and P40. Since it was known that , sucrose crystallization triggers moisture uptake (Kirtil, Aydogdu, & Oztop, 2016), high MC and a sandy appearance of the control samples containing only sucrose as the sugar could be attributed to increased crystallization of the control samples (P0) at the end of the 28 days storage. Storage experiments were performed at 60% relative humidity and therefore there is a strong possibility for samples to take up moisture from the environment and consequently the highest moisture uptake was found to belong to P0 and P10 which are considered to exhibit high crystallinity. On the other hand, for the samples that contain increased amounts of D-Allulose, this sandy appearance was not observed at the end of the 28 day period and it was seen that they are capable to protect their soft and elastic structure during the storage experiments. Although samples including high amounts of D-Allulose remained soft during the storage, an increase in surface stickiness was observed. This case could be associated with the slow diffusion of water molecules in candy matrices. Ergun et al. (2017) demonstrated that as a result of slow diffusion of water into the candy matrices, a surface layer with increased moisture content forms first leading to elevated stickiness on the surface of the soft candies. This incident was not observed for the P0 samples and instead of a sticky and moist layer, a stiff structure was observed on



the surface of candies. This might have stemmed from the higher crystallinity of these samples leading to the formation of stiff layer on the surface of the candies.

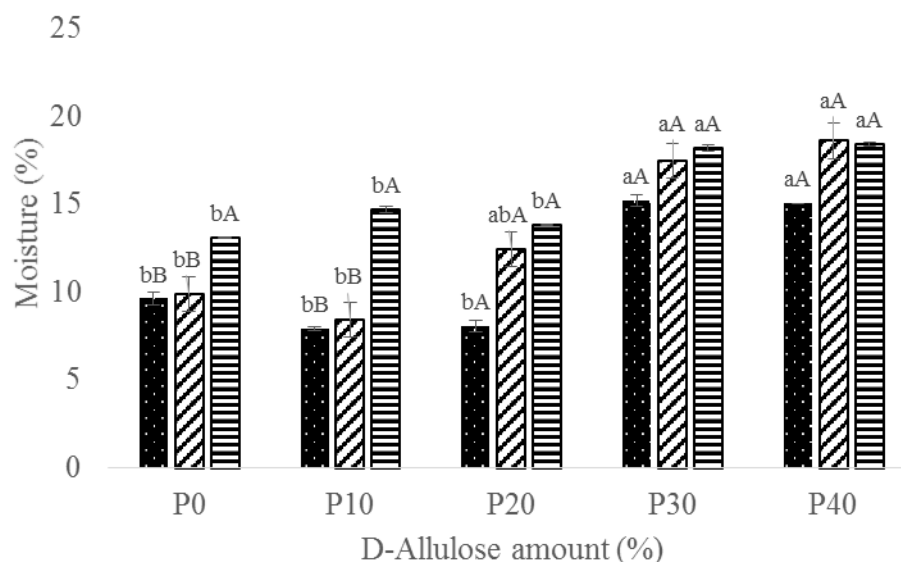


Figure 3.1. Moisture content (%) of gelatin based soft candies at the first day (■), 14<sup>th</sup> day (▨) and 28<sup>th</sup> day (▩) of storage

*Different small letters indicate significant difference ( $p < 0.05$ ) for each sample with different D-Allulose amount (%) at the same storage days.*

*Different capital letters indicate significant difference ( $p < 0.05$ ) for each sample that stored at different storage day with the same D-Allulose amount (%).*

### 3.1.2 Water Activity Determination ( $a_w$ )

Water activity ( $a_w$ ) is an important parameter which is mainly affected by the presence of dissolved sugars, humectants and sweeteners in confections (R Ergun et al., 2010). During the storage time of confections, upon moisture gain or loss, changes in textural and quality characteristics can be observed so understanding

water activity is a crucial step to check the stability of the samples (R Ergun et al., 2010) As seen in Fig.2, significant changes were not observed among the formulations in terms of their water activities and they changed in the range of 0.72-0.75 at the first day of storage ( $p>0.05$ ). However, during the 28 day storage time, a decreasing trend in water activities was observed for the candies.

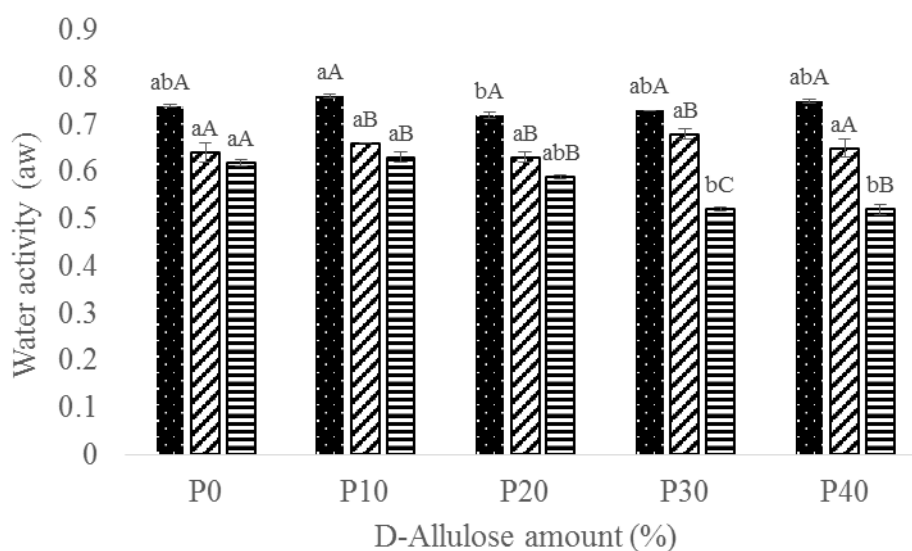


Figure 3.2. Water activity of gelatin based soft candies at the first day (■), 14<sup>th</sup> day (▨) and 28<sup>th</sup> day (▩) of storage

*Different small letters indicate significant difference ( $p<0.05$ ) for each sample with different D-Allulose amount (%) at the same storage days.*

*Different capital letters indicate significant difference ( $p<0.05$ ) for each sample that stored at different storage day with the same D-Allulose amount (%).*

As stated in previous studies, water activity of confections having gummy or jelly structures generally changes between 0.50-0.75 (R Ergun et al., 2010). Therefore, it could be concluded that water activity results of gelatin based soft candies

formulated in this study were consistent with the literature results and even addition of D-Allulose to the formulations did not alter the results significantly ( $p>0.05$ ). Since D-Allulose acts as a humectant, it was expected to decrease the water activity based upon the previous studies (R Ergun et al., 2010). The reason not to see significant changes in terms of water activities could be associated with the stable gel matrices of gelatin as discussed in previous section. In consequence of the formation of a stable gel network of gelatin, all formulations were able to protect their stability by preserving their water activities. The water activity ( $a_w$ ) decreased significantly ( $p<0.05$ ) during the storage period for all samples, except the control samples (P0), as a result of the reduction in mobility of water (free water).

### **3.1.3 Color Measurements**

Color changes among the samples were observed as a result of the cooking process. Color analysis was performed on the first day of storage and  $L^*$ ,  $a^*$  and  $b^*$  values of the samples are shown in Table 3.1. In addition to these values, Chroma (C) and Hue Angle ( $H^\circ$ ) values were also determined for the samples and shown in Table 3.1. P0 samples had the highest  $L^*$  value meaning that they are the lightest ones. Although,  $L^*$  values decreased as the D-Allulose replacement increased, significant changes were not observed between the P0 and P40 samples' lightness values ( $p>0.05$ ). On the other hand, for the " $a^*$ " values which indicated redness, a different scenario existed. It was observed that, P0 and P10 samples had negative " $a^*$ " values meaning that greener color is predominated over reddish color for those samples. With P20 samples, the " $a^*$ " value reached positive values and increased gradually for the P30 and reached its highest value (0.31) for the P40 samples which contains totally D-Allulose as the sugar. The " $b^*$ " values were all positive and it was seen that as the D-Allulose replacement increased,  $b^*$  value also increased and reached its maximum value for the P40 soft candies. To sum up, by considering the  $L^*$ ,  $a^*$  and  $b^*$  values of all samples, candies containing D-Allulose were browner than the control (P0)

and the P40 samples which contained the highest amount of rare sugar was the brownest one. This strong brownish color was attributed to highest rate of Maillard reaction of P40 samples that occurred between gelatin and the D-Allulose since it was known from the previous studies, compared to glucose and fructose, all rare hexoses revealed enhanced covalent linking and faster reaction rate during the condensation reactions with amines (Sun et al., 2006). Maillard reactions occur between carbonyl groups of reducing sugar and amino groups of protein and begin with condensation reactions to produce Schiff base products that will further degrade to Amadori compounds (O'Charoen et al., 2014). These Amadori compounds expose degradation to produce water insoluble, brown pigments known as Melanoidins (O'Charoen et al., 2014). Since sucrose is a non-reducing sugar, it could not be involved in Maillard reactions. Therefore, Amadori compounds which were further degraded to form brown Melanoidin pigments could not be formed during the processing of P0 soft candies. Enhanced reaction rates of Maillard reactions in the presence of rare sugars are also widely reported in literature. During the baking of meringues (O'Charoen et al., 2014), processing cookies (Sun et al., 2008) and production of custard pudding dessert (Sun, Hayakawa, Ogawa, & Izumori, 2007), D-Allulose was replaced with sucrose and in all studies and it was demonstrated that rare hexoses were capable to increase the Maillard reaction rate leading to the formation of products with brownish color.

Considering chroma values, significant increase was observed when the D-Allulose substitution was increased ( $p < 0.05$ ). Since chroma value is directly related with the color intensity, it could be concluded that the samples containing highest amount of D-Allulose (P40) have the highest color intensity.

On the other hand Hue angle ( $H^\circ$ ) is directly related with visual color appearance and generally an angle  $0^\circ - 360^\circ$  represents red-purple hues while  $90^\circ$ ,  $180^\circ$  and  $270^\circ$  indicate yellow, green and blue colors, respectively (Dag, Kilercioglu, & Oztop, 2017). According to the results that were shown in Table 2, for the P0 and P10

samples yellowish color is predominated since their hue angles are very close to the yellow hue (90°). As the D-Allulose substitution was increased in samples, it was investigated that H° values shifted towards red hue significantly as a result of the Maillard reaction.

Table 3.1. L\*, a\*, b\* values of gelatin based soft candies at the first day of storage

Samples	L* value	a* value	b* value	Chroma	Hue Angle (°)
P0	52±0.4 <sup>a</sup>	-0.27±0.0 <sup>c</sup>	12.49±0.1 <sup>d</sup>	12.49±0.1 <sup>d</sup>	91.22±0.0 <sup>b</sup>
P10	49.56±0.1 <sup>b</sup>	-0.33±0.0 <sup>c</sup>	13.9±0.0 <sup>c</sup>	13.92±0.0 <sup>c</sup>	92.27±0.0 <sup>a</sup>
P20	48.96±0.1 <sup>b</sup>	0.11±0.0 <sup>b</sup>	14.37±0.0 <sup>bc</sup>	14.37±0.0 <sup>bc</sup>	89.56±0.0 <sup>c</sup>
P30	49.22±0.4 <sup>b</sup>	0.13±0.0 <sup>b</sup>	14.48±0.1 <sup>b</sup>	14.48±0.1 <sup>b</sup>	89.55±0.0 <sup>c</sup>
P40	50.42±0.1 <sup>ab</sup>	0.31±0.0 <sup>a</sup>	17.66±0.0 <sup>a</sup>	17.66±0.0 <sup>a</sup>	88.99± 0.0 <sup>d</sup>

\* Different letters represent significant difference ( $p \leq 0.05$ )

### 3.1.4 X-ray Diffraction Analysis

X-ray Diffraction Analysis was performed for the P0 and P40 samples to predict the crystallization behavior during storage experiments. Results were shown in in Fig. 3.3 and Fig.3.4 for the first day and 28<sup>th</sup> day of the storage respectively. Vertical axis shows the intensity of the peak while horizontal axis represents the Bragg 2-theta angle (Labuza et al., 2004). When the diffraction peaks were examined, it was observed that P0 samples containing only sucrose had narrower peaks with higher intensity compared to its P40 counterpart which comprised 40% D-Allulose at the first day of storage. From previous studies, it was known that, for the X-ray Diffraction analysis, peaks intensity is related with the more crystalline regions. For instance, raffinose containing cookies revealed 25% less peak intensity compared to

sucrose containing ones in their X-ray diffraction pattern and this incident was attributed to crystallization inhibition behavior of raffinose (Belcourt & Labuza, 2007). Similar to the raffinose, it was hypothesized that D-Allulose might also have crystallization inhibition effect on soft candies. As seen in Fig. 3.3, P0 and P40 samples showed the typical amorphous glass halo pattern. Although, intensity and size of peaks are different from each other, these patterns mostly indicated amorphous regions since peaks are broad and distributed in a wide-angle range. From previous studies, it was known that crystal sucrose has discrete peaks at 11.6, 13.1, 18.8, 19.6 and 24.6 degrees (Leinen & Labuza, 2006). As seen in Fig. 3.3, even P0 samples containing only sucrose did not demonstrate these peaks in its diffraction pattern. This incidence might have stemmed from proper melting of sucrose crystals during the preparation of soft candies leading to formation of an amorphous gelatin-sucrose system. The halo pattern of peaks might also have been attributed to the gelatin network of soft candies. Qiao et. al. (2017) investigated the crystal structure of gelatin/chitosan composite films by using X-ray diffraction and they revealed that gelatin gives diffraction peaks at 8 and 20 degrees respectively (Qiao et al., 2017). When diffraction pattern of P40 sample in Fig. 3.3 were examined, it was seen that a halo pattern which consists of broad peaks with less intensity was predominating in the system, which could be associated with the amorphous gelatin network as indicated in previous studies (Qiao et al., 2017). Diffraction patterns of composite gels composed of gelatin that found by Quiao et.al. (2017) were also very similar to the one observed for P40 samples.

Diffraction patterns of soft candies at the end of the 28-day storage is shown in Fig.3.4. As it could be clearly seen from the figure, that P0 samples have numerous narrow and sharp peaks that could be attributed to the crystal regions. Moreover, this sample demonstrated all distinct crystal peaks which appear at 11.6, 13.1, 18.8, 19.6 and 24.6 degrees as previously indicated. Therefore, it could be hypothesized that at the end of the 28 day storage, the diffraction pattern of the P0 samples transformed from the amorphous halo pattern to a crystalline pattern as a result of sucrose

crystallization. On the other hand, for the P40 samples that were stored during the 28-day period a different hypothesis was proposed. The diffraction pattern of this sample did not demonstrate sharp and narrow peaks. In addition to this incident, it was revealed that the diffraction pattern of the P40 samples did not change remarkably during the storage. All these results provided evidence that D-Allulose had a crystallization inhibition effect on gelatin based soft candies and retarded crystallization over the time frame of the 28 day storage. A sandy appearance of P0 samples at the end of 28-day storage could be also accepted as an evidence for the sucrose crystallization while this was not observed for P40 samples as indicated previously. It is worth to note that, crystallization results were also observed to be consistent with water activity and moisture content results for the samples that were stored for 28 days. A significant increase was observed in MC of the samples as the amount of D-Allulose was increased to 40% for each storage day. As indicated in previous studies, it is known that crystal structures hold less water (Labuza et al., 2004). This was also valid for our study since it was obvious that the crystallinity of the P0 samples with low moisture content was higher than P40 samples at the end of the 28-day storage according to their X-Ray diffraction patterns. As a result of keeping a high amount of water, the water activity diminished for the P40 samples compared to P0 ones as expected at the end of the 28-day storage ( $p < 0.05$ ). Harnkarnsujarit and Charoenrein (2011) studied the impact of water activity on sugar crystallization of freeze-dried mango powder and reported that elevated  $a_w$  led to higher sugar crystallization (Harnkarnsujarit & Charoenrein, 2011). This observation was also valid for the P0 samples which gained crystal structure at the end of 28 days.

Crystallization inhibition mechanism of D-Allulose was also validated in the literature. The effect of D-Allulose addition on gelatinization and retrogradation of rice flour was studied, and it was found that peaks that belonged to crystalline structure in starch disappeared in the presence of D-Allulose in X-Ray diffraction pattern (S. Ikeda et al., 2014).

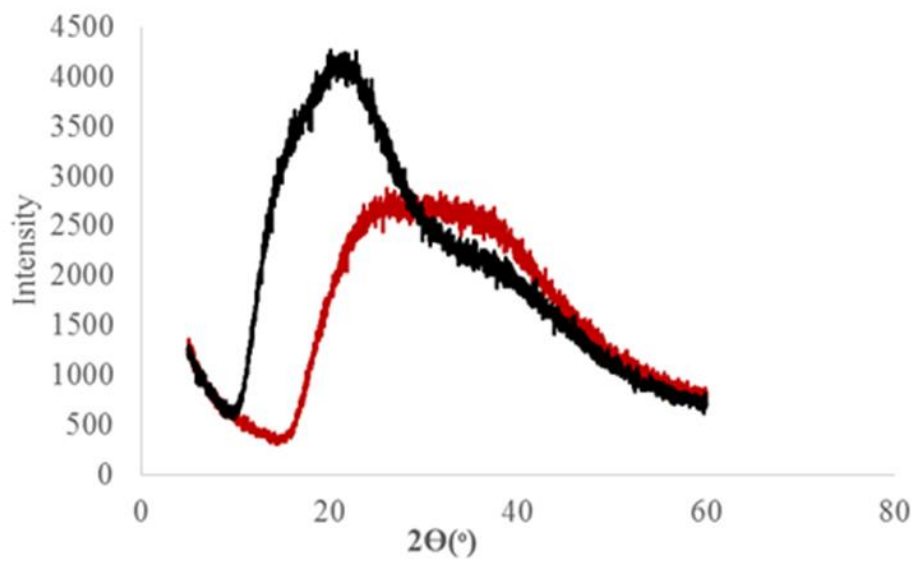


Figure 3.3. X-Ray Diffraction Pattern of gelatin based soft candies at the first day of storage: P0 (—) and P40 (—)

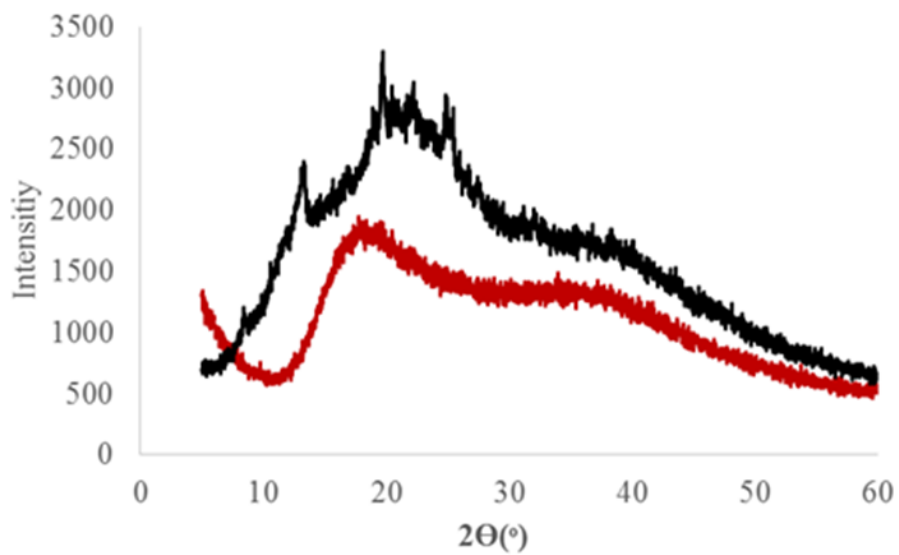


Figure 3.4. X-Ray Diffraction Pattern of gelatin based soft candies at the 28<sup>th</sup> day of storage: P0 (—) and P40 (—)



### 3.1.5 Textural Analysis

The effects of D-Allulose concentration and storage time on hardness values of gelatin based soft candies are shown in Fig. 3.5. For all samples, a drastic increase was observed over the course of the 28-day storage ( $p < 0.05$ ). Moreover, by considering changes on the D-Allulose concentration, it was found that gradual decrease was valid for the hardness values of specimens, as the D-Allulose substitution increased for each storage day ( $p < 0.05$ ). This was an expected result since it was known that moisture loss is accepted as the predominant factor in hardening of confectionary products (Tan & Lim, 2008). As discussed in the “Moisture content determination” section, due to the hygroscopic effect of D-Allulose, P40 samples absorbed more moisture than its counterparts leading to softer gel structure. This outcome was also consistent with literature since it was demonstrated that D-Allulose is capable of suppressing hardening of rice cake samples (S. Ikeda et al., 2014). With the exception of the first day of storage, a strong inverse correlation between hardness and moisture of the samples was observed (Pearson correlation coefficients were -0.65 and -0.73 for the samples stored for 14 days and 28 days, respectively). It is worth to mention that, increase in hardness values for all samples at the end of 28 day storage, might be directly related with the increased crystallinity of the samples. Considering composition changes, a correlation between the hardness and water activity was obtained ( $r = 0.65$ ,  $p < 0.05$ ) at the last day of storage whereas no such correlation was observed at the first and 14<sup>th</sup> day of storage ( $p > 0.05$ ). As mentioned in the previous section, elevated water activity values were generally associated with higher crystallinity (Harnkarnsujarit & Charoenrein, 2011). Therefore, it could be concluded that at the last day of storage, as the D-Allulose substitution increased, hardness and water activity of the specimens decreased which could be accepted as an indication of a less crystalline gel structure. Another noticeable result related with hardness values was the drastic rise of hardness of the P0 samples over the course of the 28 days storage ( $p < 0.05$ ).

Although moisture uptake occurred for this sample during the storage, hardness values increased leading to a sandy appearance. This could be explained with the enhanced crystallinity of samples rather than the moisture uptake mechanism. Belcourt & Labuza (2007) demonstrated that use of raffinose, which is known for its crystallization inhibition behavior, led to production of softer cookies compared to control recipes that contained only sucrose. A similar analogy was valid for our study. Since the sample that had the most crystalline structure is the P0 that was stored for 28 days, it exhibited the highest hardness value (25.3 N), while the P40 sample which contained only D-Allulose was the softer one (5.6 N) as a result of less crystalline gel structure.

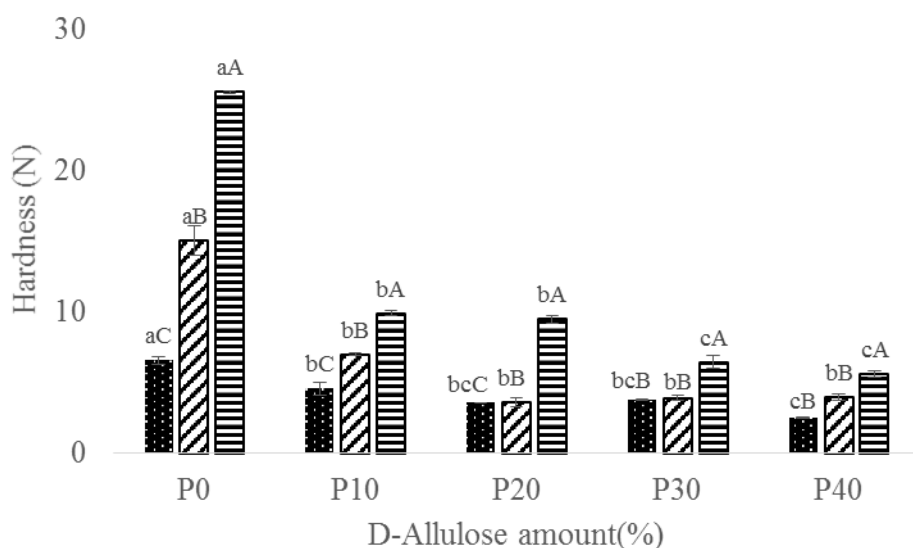


Figure 3.5. Hardness values of gelatin based soft candies at the first day (■), 14<sup>th</sup> day (▨) and 28<sup>th</sup> day (▩) of storage

*Different small letters indicate significant difference ( $p < 0.05$ ) for each sample with different D-Allulose amount (%) at the same storage days.*

*Different capital letters indicate significant difference ( $p < 0.05$ ) for each sample that stored at different storage day with the same D-Allulose amount (%).*

### 3.1.6 Glass Transition Temperature ( $T_g$ )

Many food systems especially dried foods and confections having a low water content are in the amorphous metastable state where long range molecular order are not observed (R Ergun et al., 2010). The amorphous phase could be classified as a glassy state having a low internal mobility and a rubbery state that can be defined as a more fluid-like state. Glass transition temperatures are defined as the transition between the glassy state and rubbery state (R Ergun et al., 2010). Glass transition temperatures of the D-Allulose containing soft candies were demonstrated in Fig.3.6. It was observed that all  $T_g$ 's has negative values and ranged between -19 and -22, indicating that all formulations were far away from the amorphous glassy state and keep their rubbery-gel structure. As clearly seen from the graphs, at the first day of storage, noticeable alterations were not observed regarding different D-Allulose substitution concentrations. On the other hand, at the last day of storage, a gradual decrease was detected as the D-Allulose concentration was increased in the formulations ( $p < 0.05$ ). The glass transition temperature generally depends on the degree of cross-linking polymers, the molecular weight and the plasticizer (water) concentration (R Ergun et al., 2010). Although a stable trend was observed for the first day, the descending order of  $T_g$ 's at the 28<sup>th</sup> day could be attributed to an enhanced moisture content, thereby leading to decreased hardness. Results also indicated that there is a strong correlation between  $T_g$  and moisture and hardness values, respectively, for the samples that were stored for 28 days. Pearson's correlation coefficients of -0.77 and 0.66 were observed for the moisture and hardness results, respectively, ( $p < 0.05$ ). To conclude, as a result of the high water association of D-Allulose and due to the plasticizer effect of water,  $T_g$  diminished and the candies became capable to preserve their soft texture till the end of 28 day.

Considering the aging of samples, significant alterations were not deduced for each formulation which enabled us to conclude that the gelatin based candies are capable to preserve their gel.

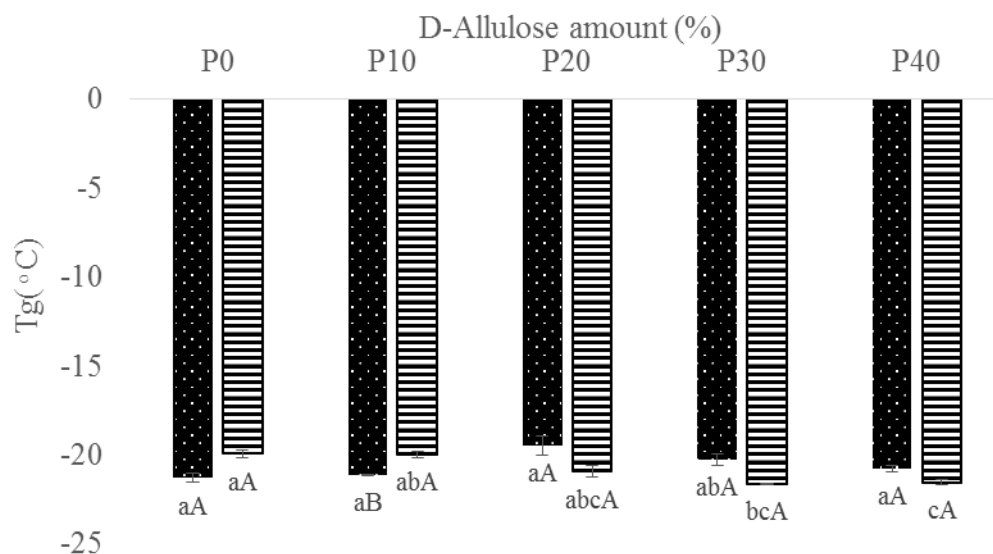


Figure 3.6. Glass transition temperature of gelatin based soft candies at the first day (■) and 28<sup>th</sup> day (▨) of storage

*Different small letters indicate significant difference ( $p < 0.05$ ) for each sample with different D-Allulose amount (%) at the same storage days.*

*Different capital letters indicate significant difference ( $p < 0.05$ ) for each sample that stored at different storage day with the same D-Allulose amount (%).*

### 3.1.7 Time Domain (TD) NMR Relaxometry

#### 3.1.7.1 T<sub>1</sub> (Spin-Lattice) Relaxation Time

Longitudinal relaxation time T<sub>1</sub> is also called as spin-lattice relaxation time since it indicates the time necessary for the spins to give the energy they obtained from the radio frequency pulse back in order to return to their initial equilibrium state (Ozel et al., 2017). It is known that that T<sub>1</sub> is highly dependent on the mobility of protons that come from water in the gel (Ozel et al., 2017). Therefore, it could be deduced

that the spin-lattice relaxation time could give an idea about the moisture distribution of food products.  $T_1$  (spin-lattice) relaxation times of soft candies are shown in Fig.3.7.

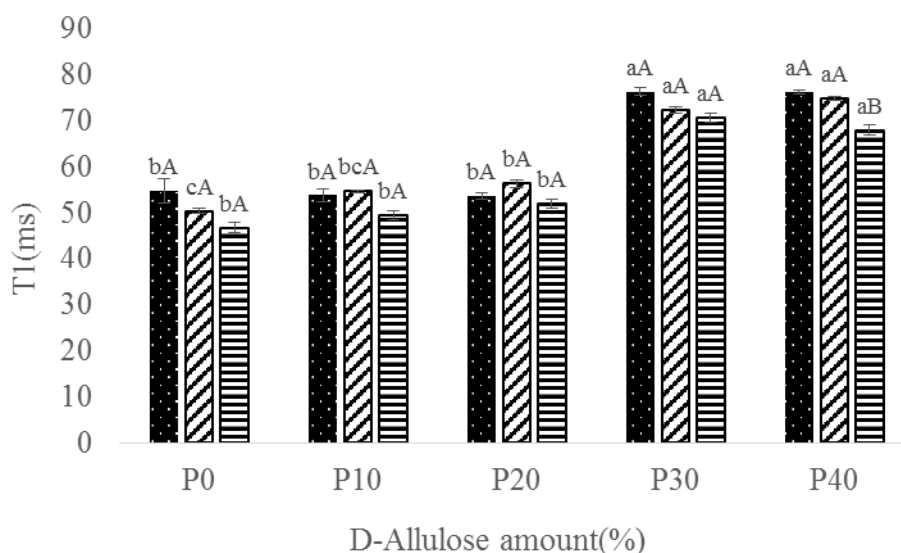


Figure 3.7.  $T_1$  (spin-lattice) relaxation times of gelatin based soft candies at the first day (■), 14<sup>th</sup> day (▨) and 28<sup>th</sup> day (▩) of storage

*Different small letters indicate significant difference ( $p < 0.05$ ) for each sample with different D-Allulose amount (%) at the same storage days.*

*Different capital letters indicate significant difference ( $p < 0.05$ ) for each sample that stored at different storage day with the same D-Allulose amount (%).*

As clearly seen from the results,  $T_1$  was highly affected by D-Allulose substitution and demonstrated an ascending trend as the D-Allulose substitution was increased in the formulations for each day of storage ( $p < 0.05$ ). On the other hand, significant changes were not observed when the whole storage time was considered for each sample with different D-Allulose substitution ( $p > 0.05$ ). This might be related to the

relative humidity of the soft candies which reached an equilibrium condition with its surroundings in the incubator. Similar steadiness of  $T_1$  values was also observed in another study which examined the  $T_1$  values of cereals that were stored at a constant relative humidity (58%) over the course of 16 days (Cornillon & Salim, 2000).

By considering the only concentration changes of samples, considerable correlations were observed between the MC and  $T_1$  values of samples with different D-Allulose substitution for each storage day (Pearson correlation coefficients were 0.97, 0.9 and 0.92 for the first, 14<sup>th</sup> and 28<sup>th</sup> day of storage, respectively for the soft candies with different formulations,  $p < 0.05$ ). Therefore, it is worth to note that mobility of water is directly related to the  $T_1$  time and moisture distribution of soft candies. It was thought that due to the humectant effect of D-Allulose, mobility of water in the gel network was enhanced, thereby leading to an increase in  $T_1$  values. In previous studies, NMR relaxometry has also used to detect the moisture distribution of food products such as sponge cake and similar correlations were observed between the MC and  $T_1$  values as in this work (Botosoa et al., 2015). In the same study, it was also mentioned that strong correlations were detected between the hardness and  $T_1$  values of sponge cakes (Botosoa et al., 2015). Similar results were also valid for our study. With the exception of the first day of storage,  $T_1$  and hardness values were inversely correlated (Pearson correlation coefficients were -0.78 and -0.69 for the 14<sup>th</sup> and 28<sup>th</sup> day of storage for the samples with different formulations,  $p < 0.05$ ). It is also worth to mention that in addition to moisture distribution, information about the crystal structure could be obtained from the spin-lattice relaxation times. According to the study of Botlan et al. (1998), longer  $T_1$  relaxation times are associated with the more crystalline regions (Le Botlan et al., 1998). Although higher crystallinity was observed especially for the P0 samples in their X-Ray diffraction pattern as a result of the 28 day storage, noticeable changes were not observed in their  $T_1$  relaxation times during the storage experiments as mentioned previously ( $p > 0.05$ ). This phenomenon might be explained with the dominant effect of moisture. If the MC of the samples were the same, the effect of crystallinity could be dominant by

leading to higher  $T_1$  values. However, since the MC follows an ascending trend the  $T_1$  relaxation time was stated to be mostly related to the mobility of water as mentioned previously.  $T_1$ -MC correlation thus became dominant for this study.

Considering the whole data set, (regarding the effect of both storage time and different D-Allulose substitution), Pearson correlation coefficients between  $T_1$  and moisture and hardness 0.67 and -0.61, respectively ( $p < 0.05$ ), were obtained. To conclude, NMR  $T_1$  relaxation might also be a noticeable indicator to define quality parameters of gelatin based soft candies.

### **3.1.7.2 $T_2$ Relaxation Spectra**

In previous studies, in order to get a detailed idea about the moisture distribution of food products having a multi-compartment nature such as fresh cut and frozen thawed mangoes (Kirtil, Oztop, Sirijariyawat, Ngamchuachit, Barrett, & McCarthy, 2014), gluten-free cakes (Yildiz, Guner, Sumnu, Sahin, & Oztop, 2018) and Pintado fish (Pitombo & Lima, 2003) a multi-exponential approach was the best option for interpreting  $T_2$  (transverse relaxation) times. For this reason, by using inverse Laplace transformations, the decaying magnetization curve could be converted into a continuous one-dimensional distribution of transverse magnetization, thereby obtaining a  $T_2$  relaxation spectra (Kirtil, Dag, Guner, Unal, & Oztop, 2017). The changes in the relaxation spectrum could be attributed to several proton related variations in food systems such as alteration in moisture content, exchange of protons between compartments or physiological factors that may give rise to formation of new proton pools (Kirtil, Oztop, Sirijariyawat, Ngamchuachit, Barrett, & McCarthy, 2014).

In our study,  $T_2$  curves yielded three distinct peaks (P1, P2 and P3) with different  $T_2$  (spin-spin) relaxation times and relative areas (RA) as seen from the Table 3.2 and Table 3.3. The RA's are calculated considering magnitude of signal intensity which

is related with each proton pool (Kirtil, Oztop, Sirijariyawat, Ngamchuachit, Barrett, & McCarthy, 2014). And they indicate the contribution of these proton pools to the whole signal (Kirtil, Oztop, Sirijariyawat, Ngamchuachit, Barrett, & McCarthy, 2014). Each peak represented different proton compartments indicating distinct regions in the gel network with a different moisture distribution. Results were consistent with literature. In a previous study, water uptake behavior of whey protein composite hydrogels was investigated and three distinct proton population was observed (Ozel et al., 2016b). In their study, it was reported that the first peak and second peak represented solid-solid interactions and polymer-water interactions, respectively, whereas the third peak showed the entrapment of bulk water in the gel matrix (Ozel et al., 2016b). Since gelatin based soft candies might also be considered as composite gel systems, a very similar analogy was thought to be valid for our study. The first peak (P1) is generally attributed to rigid proton interactions that were not generally exposed to water (Ozel et al., 2017). Compared to the other peaks, the smallest area with the shortest relaxation time was observed to belong to the first peak for all formulations of the soft candies as seen in Table 3.2 and Table 3.3. It was an expected outcome since jelly candies comprise high amounts of sugar, thereby leading to the formation of sugar-sugar interactions in the system. Considering the relaxation times of the first peaks (Table 3.2), very short  $T_2$  relaxation times were observed that varied in the range of 0.25-0.37 milliseconds (ms) for all specimens. It was obvious that such a short relaxation time belonged to protons associated with the solid component in the matrix. Indeed, this outcome was not surprising since a very short echo time was used (40  $\mu$ s). The shorter the echo time, the more information about the various proton populations could be obtained. Thanks to TD NMR relaxometry, it enables us to utilize low echo times (40  $\mu$ s), thereby leading to get an idea about the multi-exponential proton populations of gelatin based soft candies where solid-solid interactions was also thought to be vital to analyze the gel system. Referring back to the  $T_2$  relaxation data, noticeable changes were not observed for the  $T_2$  times and RA of the first peaks for each day of



storage indicating that D-Allulose substitution did not alter the solid-solid interactions significantly ( $p < 0.05$ ).

As mentioned previously, the second peak (P2) is generally assigned as polymer-water interactions since relaxation times of this peak stand between the P1 and P3 in the relaxation spectrum as represented in Fig. 3.8 and Fig.3.9. For this study, since bovine gelatin was used as the only gelling agent, gelatin-water interactions are likely to stand for the polymer-water interactions for all formulations. Since the soft candies formulated in this study have high sugar concentrations, in addition to the gelatin-water interactions, sugar-water interactions have also a vital role in the emerging second peak. Therefore, it could be concluded that P2 represents both gelatin-water and sugar-water interactions. Regarding the use of gelatin in all formulations with the same amount, changes in the  $T_2$  relaxation time and the relative areas of P2 might have come from mainly different sugar-water interactions which could stem from the use of different D-Allulose concentration in the formulations. To conclude, protons belonging to the P2 might have come from a more mobile environment, in which water interacts with the hydroxyl groups of gelatin and sugar as indicated in similar studies (Ozel et al., 2017). Considering the  $T_2$  relaxation times of P2, it was deduced that as the D-Allulose substitution increased in the formulations, the  $T_2$  time also increased for each storage day, excluding the first day. This change between the  $T_2$  times of the peaks could be attributed to the distinct characteristics of sucrose and D-Allulose. In a previous study, hydration properties and proton exchange of different aqueous sugar solutions (glucose, fructose and sucrose) were studied and results of this study were striking (Aroulmoji, Mathlouthi, Feruglio, Murano, & Grassi, 2011). According to this study, such a decreasing trend in  $T_2$  relaxation times was observed for the aqueous solutions: D-fructose > D-glucose > sucrose. The shortest  $T_2$  value of sucrose was attributed to a higher molecular weight (dipolar contribution) in addition to the existence of a higher amount of exchangeable OH groups compared to the ones of glucose (Aroulmoji et al., 2011). In the same study, alterations of  $T_2$  relaxation times of glucose and

fructose were explained as measures of the interaction of water with sugars. Since the glucose and fructose interaction with water is higher than sucrose, they gave longer  $T_2$  relaxation times (Aroulmoji et al., 2011). Considering that D-Allulose is also a monosaccharide similar to fructose and glucose with known hygroscopic effects, a similar scenario could be valid for explaining increase in relaxation times for P2 as the D-Allulose substitution was increased. A similar trend was also notable for the relaxation times of P3 as will be discussed later. Contrary to the  $T_2$  relaxation times of P2, descending trend was detected for the RA (%) of all samples on each storage day. This incident could be related with the higher crystallization tendency of sucrose compared to D-Allulose as discussed in previous sections. Since the P0 sample contains only sucrose as sugar and crystal sucrose holds less water resulting in emergence of more protons coming from the free water state, P2 RA(%) of this samples was significantly higher compared to its counterparts for each storage day ( $p < 0.05$ ). Higher water activity of this control sample may lead to formation of higher RA (%) of P2. As the D-Allulose substitution was increased, RA of the P2 peak diminished and reached a minimum value for the P40 sample.

Remembering that the third peak (P3) was assigned to the entrapment of bulk water in the gelatin network, the relaxation time of this peak was observed to be longer compared to the other peaks as expected since the signal came from the more mobile proton pools. An increasing trend of the relaxation time of P3 could be explained with the same analogy as for P2 since hydration of sugar also occurs within the gelatin network. Considering the relaxation times of P3, it was seen that they ranged between 12-32 ms meaning they were still far from the  $T_2$  relaxation time of pure water which has a  $T_2$  (spin-spin) reported around 3s (Kirtil, Dag, et al., 2017). Although the mobility of water that is entrapped in a gel network is higher than in other compartments, its mobility is still restricted due to dissolution of sugars. By comparing the changing trend of RA of P2 and P3 as D-Allulose substitution increased for each day, it was observed that peak 2 became more dominant in the system. Gradual increase in the RA (%) of the P3 on concentration basis could be

explained with the increment in moisture content of the samples as D-Allulose substitution was enhanced. This is strongly related to the humectant effect of D-Allulose as discussed previously. The other hypothesis that comes to mind is the Maillard reaction. As discussed in the “Color determination” section, as the D-Allulose amount was elevated in the formulations, a brownish color was observed due to a non-enzymatic browning reaction. Together with the color development, water release was also observed in the presence of proteins and reducing sugars (Yildiz et al., 2018). This water release related with the Maillard reaction might have promoted an increase in RA of P3. It is worth to note that, the descending trend of hardness values of samples resulting from enhanced D-Allulose substitution was also strongly related to an ascending trend of RA3 for each storage day. Due to presence of an elevated portion of bulk water that remained in the gel network, the P40 samples preserved their softness during 28 day storage leading to decrease in hardness values. Noticeable variations generally were not detected for the T2 and RA of the samples during storage. This might be originated from a continuous exchange of protons between the distinct proton pools. The stable trends in the relaxation times and RA's over the course of the 28 day storage time, could be attributed to the compact gelatin network that preserve their stability for all formulations.

To conclude, for all formulation that were stored during the 28 day period, three distinct peaks (P1,P2 and P3) with different relaxation times were observed in the relaxation spectra representing different proton pools (Fig.3.8 and Fig.3.9). It could be clearly seen from the graphs that D-Allulose replacement gave rise to shifting of the all peaks towards longer relaxation times and an increase in RA of the P3.

Table 3.2. T<sub>2</sub> (spin-spin) relaxation results of each compartment observed in relaxation spectrum for gelatin based soft candies

		(ms)	Time (days)		
		Name	0	14	28
Peak 1	P0	0.35±0.00 <sup>a,A</sup>	0.25±0.00 <sup>b,C</sup>	0.28±0.00 <sup>b,B</sup>	
	P10	0.34±0.01 <sup>a,A</sup>	0.34±0.01 <sup>a,A</sup>	0.35±0.00 <sup>ab,A</sup>	
	P20	0.37±0.01 <sup>a,A</sup>	0.32±0.01 <sup>a,A</sup>	0.37±0.01 <sup>a,A</sup>	
	P30	0.36±0.02 <sup>a,A</sup>	0.32±0.01 <sup>a,A</sup>	0.37±0.01 <sup>a,A</sup>	
	P40	0.36±0.02 <sup>a,A</sup>	0.29±0.01 <sup>ab,A</sup>	0.36±0.02 <sup>ab,A</sup>	
Peak 2	P0	5.00±0.35 <sup>a,B</sup>	3.00±0.07 <sup>c,B</sup>	3.60±0.00 <sup>c,AB</sup>	
	P10	4.65±0.11 <sup>a,A</sup>	3.85±0.18 <sup>c,A</sup>	5.00±0.14 <sup>ab,A</sup>	
	P20	5.00±0.14 <sup>a,B</sup>	7.70±0.21 <sup>b,A</sup>	5.50±0.00 <sup>a,B</sup>	
	P30	5.20±0.00 <sup>a,AB</sup>	6.90±0.35 <sup>ab,A</sup>	4.80±0.00 <sup>b,B</sup>	
	P40	6.45±0.32 <sup>a,B</sup>	9.25±0.46 <sup>a,A</sup>	4.80±0.00 <sup>b,B</sup>	
Peak 3	P0	19.0±2.12 <sup>b,A</sup>	12.0±0.00 <sup>d,A</sup>	13.0±0.00 <sup>c,A</sup>	
	P10	19.0±0.71 <sup>b,A</sup>	15.5±0.00 <sup>cd,A</sup>	18.5±0.00 <sup>b,A</sup>	
	P20	22.0±0.00 <sup>b,A</sup>	21.5±1.77 <sup>bc,A</sup>	20.0±0.00 <sup>b,A</sup>	
	P30	29.5±1.77 <sup>ab,A</sup>	29.0±0.00 <sup>ab,A</sup>	30.5±1.06 <sup>a,A</sup>	
	P40	33.0±0.71 <sup>a,A</sup>	28.0±0.71 <sup>a,A</sup>	32.0±0.00 <sup>a,A</sup>	

Means within the same row, followed by the different small letters (a–d) are significantly different for each sample ( $p < 0.05$ )

Means within the same column, followed by the different capital letters (A–B) are significantly different for each storage day ( $p < 0.05$ )

Table 3.3. Relative area (%) (RA) of each peak observed in relaxation spectrum for gelatin based soft candies

		(%)	Time (days)		
		Name	0	14	28
RA 1(%)	P0		7.92±0.19 <sup>a,A</sup>	7.65±0.04 <sup>a,A</sup>	8.53±0.01 <sup>a,A</sup>
	P10		7.47±0.08 <sup>a,A</sup>	7.32±0.11 <sup>a,A</sup>	7.60±0.03 <sup>a,A</sup>
	P20		7.37±0.22 <sup>a,A</sup>	6.79±0.54 <sup>a,A</sup>	7.70±0.21 <sup>a,A</sup>
	P30		7.00±0.31 <sup>a,A</sup>	7.68±0.02 <sup>a,A</sup>	7.59±0.05 <sup>a,A</sup>
	P40		6.95±0.22 <sup>a,A</sup>	6.03±0.13 <sup>a,B</sup>	7.52±0.40 <sup>a,A</sup>
RA 2(%)	P0		22.18±1.35 <sup>a,A</sup>	19.49±1.56 <sup>ab,A</sup>	22.21±0.30 <sup>a,A</sup>
	P10		17.86±0.07 <sup>ab,A</sup>	10.64±1.15 <sup>c,B</sup>	20.45±0.01 <sup>b,A</sup>
	P20		16.28±0.26 <sup>b,B</sup>	23.87±0.49 <sup>a,A</sup>	16.94±0.24 <sup>c,B</sup>
	P30		10.73±0.04 <sup>c,B</sup>	17.18±1.06 <sup>abc,A</sup>	10.43±0.09 <sup>d,B</sup>
	P40		9.71±0.32 <sup>c,B</sup>	15.35±0.51 <sup>bc,A</sup>	9.21±0.09 <sup>d,B</sup>
RA 3(%)	P0		69.90±1.54 <sup>d,A</sup>	72.86±1.52 <sup>bc,A</sup>	69.27±0.27 <sup>d,A</sup>
	P10		74.67±0.16 <sup>cd,B</sup>	82.03±1.26 <sup>a,A</sup>	71.96±0.02 <sup>c,B</sup>
	P20		76.36±0.48 <sup>bc,A</sup>	69.36±0.05 <sup>c,B</sup>	75.36±0.64 <sup>b,A</sup>
	P30		82.27±0.36 <sup>ab,A</sup>	75.15±1.09 <sup>abc,B</sup>	81.99±0.14 <sup>a,A</sup>
	P40		83.34±0.00 <sup>a,A</sup>	78.65±0.39 <sup>ab,A</sup>	83.27±0.30 <sup>a,A</sup>

*Means within the same row, followed by the different small letters (a–d) are significantly different for each sample ( $p < 0.05$ )*

*Means within the same column, followed by the different capital letters (A–B) are significantly different for each storage day ( $p < 0.05$ )*

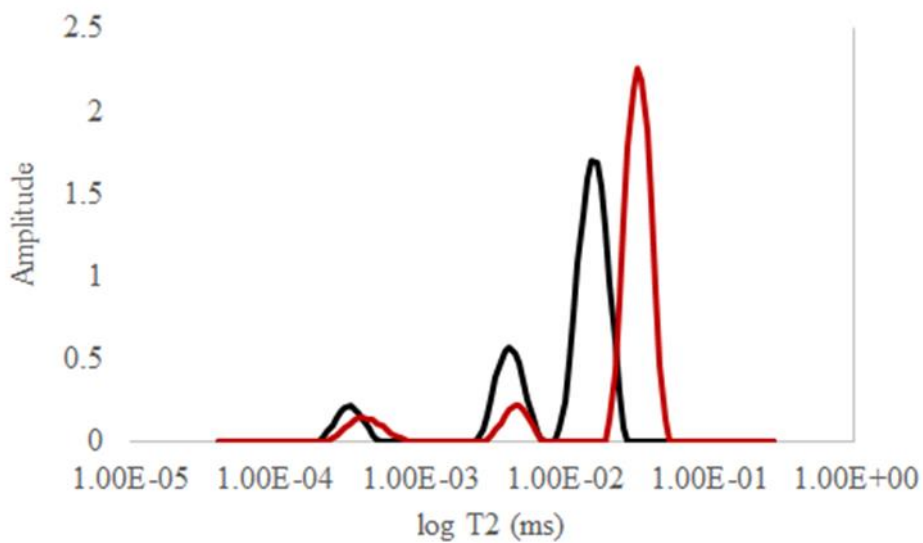


Figure 3.8.  $T_2$  Relaxation Spectrum graph of gelatin based soft candies at the first day of storage: P0 (—) and P40 (—)

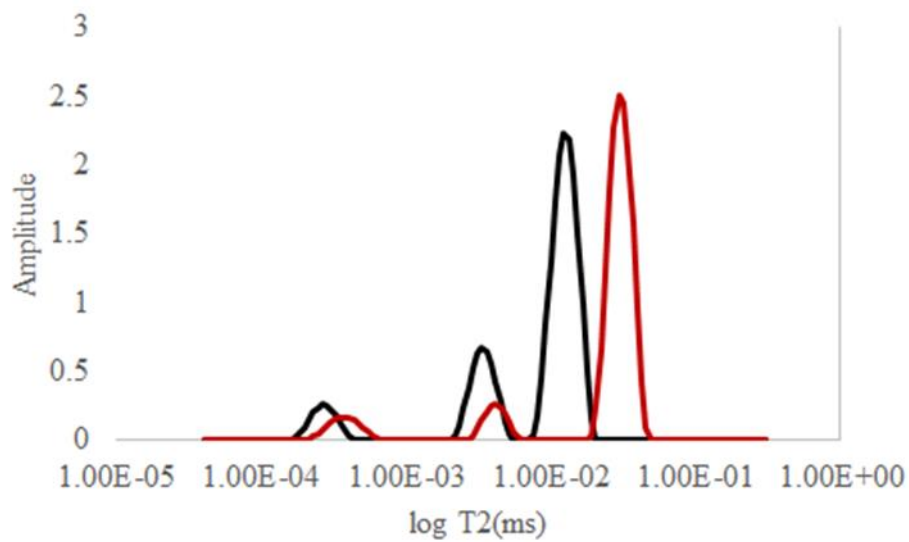


Figure 3.9.  $T_2$  Relaxation Spectrum graph of gelatin based soft candies at the 28<sup>th</sup> day of storage: P0 (—) and P40 (—)

### 3.1.8 Fast Field Cycling (FFC) NMR Relaxometry

#### 3.1.8.1 Theoretical Model

For this part of the dissertation, storage experiments were not performed and only freshly prepared gelatin based soft candies was used as indicated below table

Table 3.4. Gelatin based soft candies with different D-allulose substitution (wt %)

Sample *	Composition
S0	40% sucrose
S10	30% sucrose + 10% D-allulose
S20	20% sucrose + 20% D-allulose
S30	10% sucrose + 30% D-allulose
S40	40% D-allulose

\* In addition to sucrose samples also included corn syrup at a fixed % as described by Pohan et. al (2019).

The NMRD profiles obtained at different frequencies (in the range of 0.004-40 MHz) for the gelatin based soft candies containing different amount of D-allulose were represented in Figure 3.10.

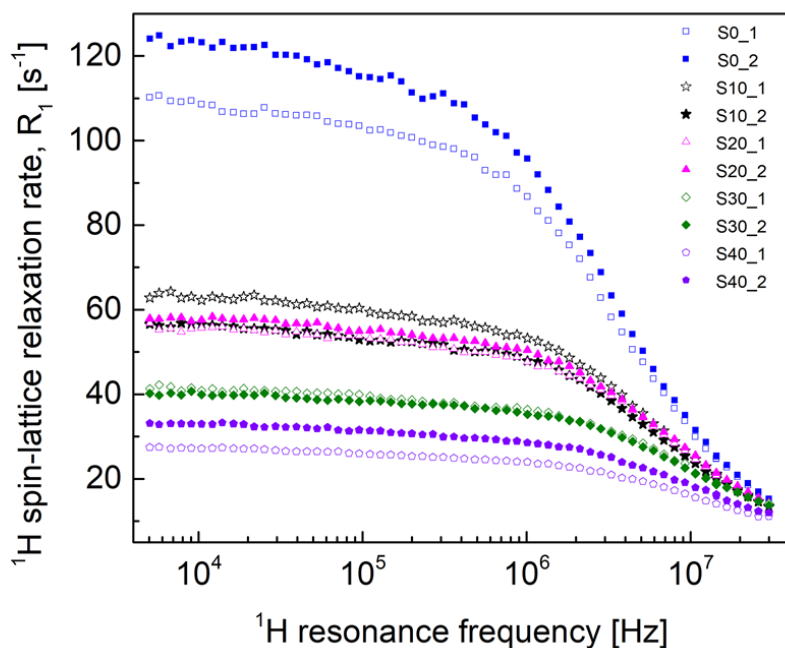


Figure 3.10. Representative NMRD profiles of gelatin based soft candies containing different amount of D-allulose; indices 1, 2 denote two replicates of each composition.

The relaxation rates have been obtained as a single-exponential fit of  $^1\text{H}$  magnetization curves (*the amplitude of the magnetization versus time*) including 16 logarithmically scaled points. The error of the relaxation rates does not exceed 5%. The  $^1\text{H}$  spin-lattice relaxation data reflected the water dynamics in these materials. Two observations can immediately be made. The first one is that the relaxation rates converge at high magnetic fields (resonance frequencies), while at low and intermediate frequencies they were found to be considerably different. The second observation concerns the relationship between the values of the relaxation rates and the composition of the gels. The relaxation process became slower (the relaxation rates become lower) almost in the whole frequency range (at the highest frequencies the data tend to coincide) with the increasing amount of D-allulose, starting from 0%



(S0) up to 40% (S40). The measurements have been performed for two samples (replicates) for each composition.

One can distinguish two pools (fractions) of water in the gels: a fraction of water *confined* in the gel matrix and, hence, undergoing a much slower dynamics compared to bulk water, and a fraction of water that exhibits *dynamics comparable with bulk water*. We shall refer to these two water pools as *confined-water* and *free-water* fractions. This implies that the overall  $^1\text{H}$  spin-lattice relaxation rate,  $R_{1,H}(\omega)$ , (where  $\omega$  denotes the  $^1\text{H}$  resonance frequency in angular frequency units) is given as a sum of the relaxation contributions associated with the confined-water and free-water fractions:

$$R_{1,H}(\omega) = R_{1,H}^{confined}(\omega) + R_{1,H}^{free}(\omega) \quad (1)$$

As the dynamics of the free-water pool is fast, the corresponding relaxation contribution can be approximated by a frequency independent term:  $R_{1,H}^{free}(\omega) = A$ . The water in confinement undergoes translational and rotational diffusion. The translational diffusion modulates inter-molecular  $^1\text{H}$ - $^1\text{H}$  dipole – dipole interactions, while the intra-molecular coupling between water protons fluctuates in time due to the molecular tumbling. This leads to the following expression for the overall relaxation rate:

$$R_{1,H}(\omega) = R_{1,H}^{confined,rot}(\omega) + R_{1,H}^{confined,trans}(\omega) + A \quad (2)$$

The relaxation rate originating from the intra-molecular dipole-dipole interactions,  $R_{1,H}^{confined,rot}(\omega)$ , can be expressed as (D. Kruk, Meier, & Rössler, 2012)

$$R_{1,H}^{confined,rot}(\omega) = C_{DD} \left[ \frac{\tau_{rot}}{1+(\omega\tau_{rot})^2} + \frac{4\tau_{rot}}{1+(2\omega\tau_{rot})^2} \right] \quad (3)$$

where  $\tau_{rot}$  denotes the rotational correlation time of the water molecules in the confinement, while  $C_{DD}$  is referred to as a dipolar relaxation constant. The relaxation contribution associated with the inter-molecular interactions mediated by translation diffusion,  $R_{1,H}^{confined,trans}(\omega)$ , can be described as (Hwang & Freed, 1975; Ayant, Belorizky, Aluzon & Gallice, 1975)

$$R_{1,H}^{confined,trans}(\omega) = C_{trans} \left[ \int_0^\infty \frac{u^4}{81+9u^2-2u^4+u^6} \left( \frac{\tau_{trans}}{u^4+(\omega\tau_{trans})^2} + \frac{4\tau_{trans}}{u^4+(2\omega\tau_{trans})^2} \right) du \right] \quad (4)$$

The translational correlation time,  $\tau_{trans}$ , is defined as:  $\tau_{trans} = \frac{d^2}{2D_{trans}}$ , where  $D_{trans}$  denotes the translational diffusion coefficient of the confined-water molecules, while  $d$  is referred to as the distance of closest approach for the interacting molecules – it can be approximated by the diameter of water molecule,  $2.75\text{\AA}$ . The quantity  $C_{trans}$  is defined as:

$C_{trans} = \frac{108}{5} \left( \frac{\mu_0}{4\pi} \gamma_H^2 \hbar \right)^2 \frac{N_H}{d^3}$ , where  $N_H$  denotes the number of  $^1\text{H}$  nuclei (hydrogen atoms) per unit volume, *i.e.* the number of the confined water molecules per unit volume, after dividing it by 2.

This model has been applied to analyse the relaxation data. Fig.3.11 shows the outcome, including the individual relaxation contributions:  $R_{1,H}^{confined,rot}$ ,  $R_{1,H}^{confined,trans}$  and  $A$ .

The presented model has been applied to reproduce the  $^1\text{H}$  spin-lattice relaxation data. The results of the analysis were revealed in Fig.3.11 which includes a decomposition into the individual relaxation contributions while Table 3.5 represented the obtained parameters. The values of the translational diffusion coefficients for the confined-water fraction have been calculated from the

relationship:  $D_{trans} = \frac{d^2}{2\tau_{trans}}$ , while  $N_H$  has been obtained from the definition of  $\mathcal{C}_{trans}$ .

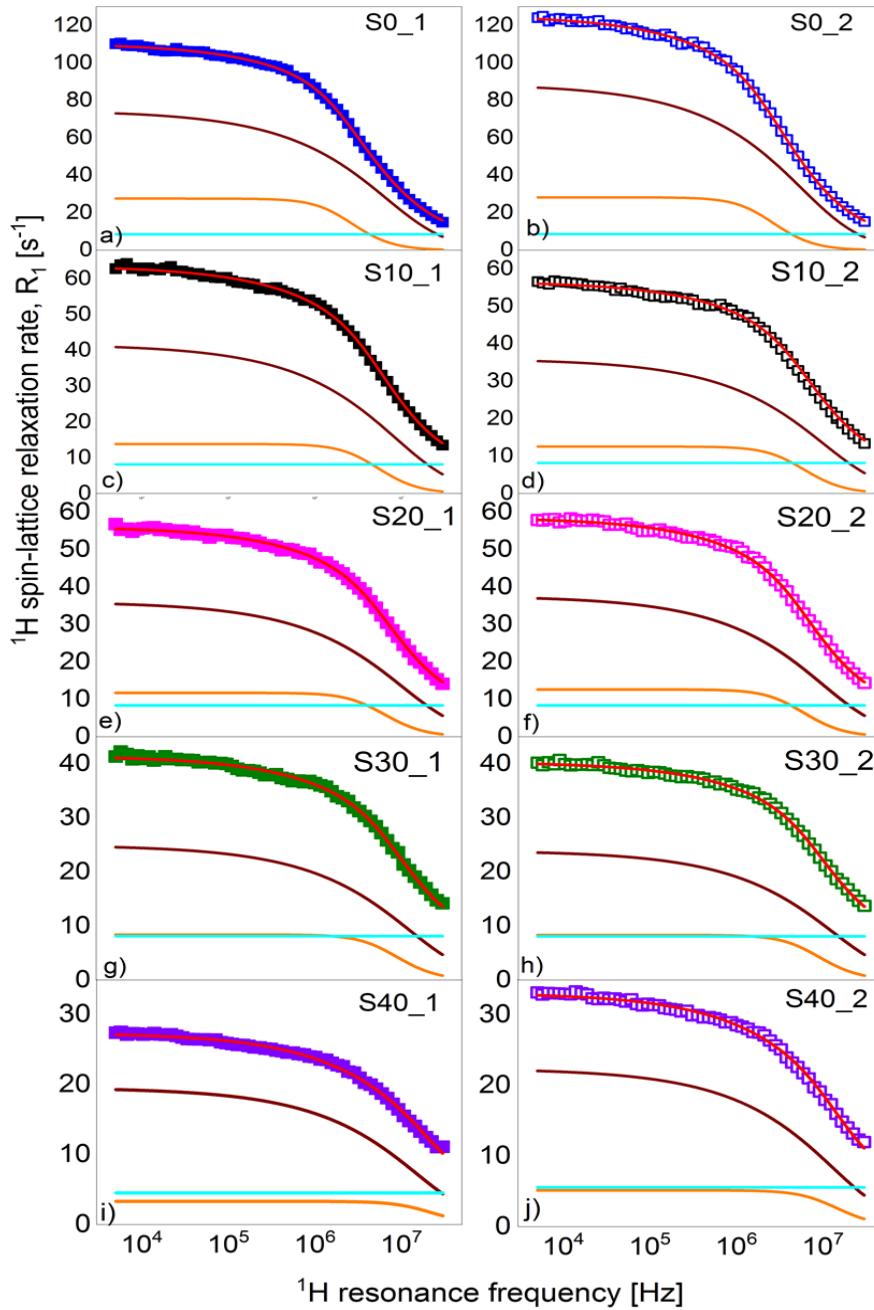


Figure 3.11.  $^1\text{H}$  spin-lattice relaxation dispersion profiles,  $R_{1,H}(\omega)$ , for different gelatine composition. Red lines – theoretical fits decomposed into the individual contributions:  $R_{1,H}^{\text{confined,rot}}(\omega)$  (brown lines),  $R_{1,H}^{\text{confined,trans}}(\omega)$  (orange lines),  $A$  (light blue lines)

Table 3.5. Parameters obtained from the fits presented in Fig. 3.11

Sample	$C_{trans}$ [ $10^{10}$ Hz $^2$ ]	$\tau_{trans}$ [ $10^{-8}$ s]	$\tau_{rot}$ [ $10^{-8}$ s]	$A$ [ $s^{-1}$ ]	$*D_{trans}$ [ $10^{-12}$ m $^2$ /s]	** $N_H$ [ $10^{23}$ m $^{-3}$ ]	Relative error [%]
S0_1		2.60±0.06	3.25 ± 0.09	8.4	1.45		0.96
S0_2	2.22 ± 0.09	3.10±0.06	2.85	3.29	1.22	3.78	0.69
S10_1		2.02 ± 0.06	1.63 ± 0.07	8.1	1.87		0.87
S10-2	1.59 ± 0.07	1.74 ± 0.07	1.88	1.56	2.17	2.72	1.53
S20_1		1.69 ± 0.04	1.39 ± 0.05	8.4	2.24		0.73
S20_2	1.65 ± 0.07	1.76 ± 0.05	1.72	1.44	2.15	2.81	0.77
S30_1		1.40 ± 0.07	0.99 ± 0.06	8.1	2.69		0.94
S30_2	1.37 ± 0.08	1.35 ± 0.05	1.38	0.98	2.81	2.34	0.76
S40_1		1.16 ± 0.02	0.39 ± 0.04	4.5	3.27		1.12
S40_2	1.31 ± 0.08	1.32 ± 0.03	1.24	0.56	2.86	2.23	1.13

\*Calculated from the relationship:  $D_{trans} = \frac{d^2}{2\tau_{trans}}$

\*\* Calculated from the relationship:  $C_{trans} = \frac{108}{5} \left( \frac{\mu_0}{4\pi} \gamma_H^2 \hbar \right)^2 \frac{N_H}{d^3}$

### 3.1.8.2 Effect of D-Allulose substitution on relaxation rates

Table 3.4 includes the moisture content, hardness and water activity ( $a_w$ ) values for the investigated samples. Hardness of the samples was calculated by using compression test consisting of two consecutive cycles. The peak force during the first compression cycle in Texture Profile Analysis Curve (TPA) was utilized to detect the hardness of the soft candies. D-allulose substitution had a significant effect on moisture and hardness values ( $p < 0.05$ ) (Table 3.4). Increase in allulose concentration increased the moisture content and decreased the hardness values. On the other hand, it was observed that D-allulose substitution did not affect  $a_w$  results significantly.

Table 3.6. Moisture content (%) and hardness values for gelatin based soft candies containing different amount of D-allulose

Sample label	Moisture content (%)	Water activity ( $a_w$ )	Hardness (N)
S0	9.18 <sup>b</sup> ±0.18*	0.74 <sup>ab</sup> ±0.24	6.75 <sup>a</sup> ±0.29
S10	7.51 <sup>b</sup> ±0.13	0.76 <sup>a</sup> ±0.46	4.48 <sup>b</sup> ±0.0.65
S20	8.22 <sup>b</sup> ±0.33	0.72 <sup>b</sup> ±0.02	3.45 <sup>bc</sup> ±0.12
S30	15.44 <sup>a</sup> ±0.39	0.73 <sup>ab</sup> ±0.06	3.62 <sup>bc</sup> ±0.16
S40	15.23 <sup>a</sup> ±0.12	0.75 <sup>ab</sup> ±0.04	2.72 <sup>c</sup> ±0.21

\* Data were recorded with standard errors. Lower case letters denote significance difference between the samples @ 95% confidence level between the parameters.

As previously indicated in the related study of Pohan et al. (2019), the reason not to see detectable alterations in terms of  $a_w$  values could be linked with stable gel matrices that formed by gelatin and it could be concluded that even addition of D-

allulose to the gels did not change the  $a_w$  results significantly ( $p>0.05$ ). In addition, as already pointed out, the  $^1\text{H}$  spin-lattice relaxation rates decreased with increasing the amount of D-allulose (Fig.3.10). This effect is seen at low and intermediate frequencies, while at higher frequencies the relaxation rates tend to converge. One should also, notice that the relaxation rates for the samples containing 10% and 20% of D-allulose are relatively close compared to the differences observed for higher concentrations of D-allulose. Although the lowest relaxation rates correspond to the highest moisture content and relatively low hardness, the decreasing of the relaxation rates does not monotonically follow neither the moisture content nor the hardness values. This indicates a complex mechanism of the water dynamics.

The translational as well the rotational dynamics of the confined-water molecules (*characterized by the correlation times  $\tau_{trans}$  and  $\tau_{rot}$ , respectively*) is slower for the sample containing only sucrose as the sugar source compared to the other samples. Comparing the estimated translation diffusion coefficient  $D_{trans} = 1.34 \cdot 10^{-12} \text{ m}^2/\text{s}$  (for S0 samples) with the diffusion coefficient of bulk water at room temperature,  $2.3 \cdot 10^{-9} \text{ m}^2/\text{s}$  ((Mills, 1973), one can immediately conclude that the translation diffusion slows down by three orders of magnitude in the confinement. The value of the diffusion coefficient should be considered together with  $N_H$  ; the quantity describing the number of water molecules per unit volume.  $N_H$  values for bulk water yields  $6.68 \cdot 10^{28}/\text{m}^3$ , while for the sample without D-allulose  $N_H=3.78 \cdot 10^{28}/\text{m}^3$  (about 0.6 of the value for bulk water) has been obtained. This indicates that a fraction of the confined-water molecules is bound to the gel matrix and, hence, it does not effectively participate in the translational motion. Moreover,  $N_H$  decreased with increasing D-allulose concentration so less confined-water molecules contributed to the translational motion in the presence of allulose. Following this line, one should note that the  $N_H$  parameter actually reaches the highest value for the sample containing only sucrose as the sugar source.

It is important to point out (to avoid confusion) that the  $N_H$  is not necessarily related in any way to the moisture content – the content can be low, yet a majority of the molecules can perform translational dynamics leading to a large  $N_H$  number. It is also worth to say that the analysis does not allow to determine the relationship between the confined-water and free-water fractions in terms of their relative populations. There is an exchange dynamic between the two fractions. One can say that when the free-water fraction is more populated the “average dynamics” becomes more faster, but this is a vague statement not allowing to determine the populations. As far as the free-water fraction is concerned, the frequency independent term,  $A$ , reaches the value of about  $8.5 \text{ s}^{-1}$  for the sample containing solely sucrose (S0) and  $\sim 5 \text{ s}^{-1}$  for only allulose samples (S40).  $^1\text{H}$  spin-lattice relaxation rate for water in bulk at room temperature is about  $0.5 \text{ s}^{-1}$ . This indicates that the dynamics of the free-water fraction is by about 17 times slower in S0 samples compared to bulk water. Thus, the term “free-water fraction” should be treated with caution, because the dynamics in this fraction is considerably slower than in bulk water (yet much faster than in the confined-water pool).

Previous studies showed that in different food systems, water binding ability of D-allulose was lower than sucrose despite the high solubility of D-allulose (S. I. Ikeda, Gohtani, Ukada, & Mo, 2011; Ilhan, Pocan, Ogawa, & Oztop, 2020a; Pocan et al., 2019b). Actually, “water binding” is related with the hydration behavior of the sugars. Polar groups such as hydroxyl groups can readily form H-bonds with water molecules. According to a previous study, these interactions occur for all types of sugar but for the D-allulose, they occur in lesser extent compared to sucrose (Ikeda et al., 2011). Decrease in ‘ $A$ ’ values also confirms this finding. There could also be another factor that can result in a decrease on the  $A$  values. Maillard reaction that occurs between reducing sugar and proteins is a complex reaction and in the initial step of this reaction namely condensation step, water is generated (Yildiz et al., 2018). The presence of D-allulose increases the efficiency of the Maillard reaction



as reported for various food products including soft candies (Ilhan et al., 2020b; Pohan et al., 2019b; Sun et al., 2008). Increase in moisture contents and decrease in  $A$  value further confirm this hypothesis.

In a previous study, Pohan et al. (2019) investigated the effect of D-allulose substitution on gelatin based soft candies and evaluated the impact of Maillard reaction from several aspects. It was shown that the rate of Maillard reaction was found to be the fastest for the samples that contained the highest amount of D-allulose (S40) considering their color changes. In the same study, it was also observed that together with color development, water release also occurred as a result of Maillard reaction (Pohan et al., 2019b; Yildiz et al., 2018) leading to the formation of new proton pool which was assessed by a  $T_2$ -CPMG experiment conducted at system operating @ 20.34 MHz frequency.

It is also of interest to inquire into the ratio between the *translational* and *rotational* correlation times,  $\frac{\tau_{trans}}{\tau_{rot}}$ . According to the Stokes-Einstein equation, the ratio for spherical, non-interacting molecules is equal to 9. It has been found that for “real” molecules the ratio typically ranges between 20 and 40 (D. Kruk, Meier, & Rössler, 2011; Roman Meier, Kruk, & Rössler, 2013) ; values between 17 and 21 have been found for water in hyaluronic dermal fillers matrices (Kruk et al. (2019)). In the present case the ratio is below 1 ( $\tau_{rot}$  is longer than  $\tau_{trans}$ ) for S0 samples and it increases with increasing allulose concentration. But still values reached maximum 2.2 that is considerably low. The relation between the translational and rotational correlation times showed that the gelatin confinement led to a very considerable slowing down of the rotational dynamics of the confined- water molecules.

From S0  $\rightarrow$  S40,  $\frac{\tau_{trans}}{\tau_{rot}}$  increased almost 3-fold ( $\sim 2.21$ ) which indicated that translational dynamics was slower with respect to rotational dynamics with increasing allulose concentration. Translational correlation times decreased by half from S0  $\rightarrow$  S40 whereas the decrease was much higher in rotational correlation

times (~17 times less). So, it is obvious that both translational and rotational dynamics was affected from the presence of D-Allulose. Rotational and translational dynamics being faster at high allulose concentrations are also accompanied by the decrease in hardness and increase in moisture contents and translational diffusion coefficients (*almost 2-fold*) of the gels. In other words, faster motion was associated with softer confectionery gels. These textural properties have become more important especially during the storage of soft candies. Pohan et al. (2019) stated that, compared to the control one that contains only sucrose as the sweetener, as the D-allulose substitution increased, gelatin based soft candies preserved their softness even at the end of 28 days of storage. It was hypothesized that, this outcome was expected due to the crystallization inhibition mechanism of D-allulose (Belcourt & Labuza, 2007; Pohan et al., 2019b). Pohan et al. (2019) also indicated that control samples (S0) gained a sandy appearance at the end of 28 days of storage, which was considered as a poor quality indicator. On the other hand, samples containing D-allulose did not gain this sandy appearance. To sum up, regarding the storage time of the products which is a very important parameter that directly affects the quality of the confectionery gels, products that resists crystallization and remain softer could be considered as favorable. In the present study, thanks to FFC-NMR Relaxometry, detailed analysis of water dynamics within the confectionery gels was achieved and results enabled us to put a link between the water dynamics and textural properties of the gelatin based confectionery gels.

### **3.1.9 Effect of D-allulose substitution on thermo gravimetric analysis (TGA) Thermograms**

TGA experiments were also performed for the soft candies. Results are shown in Fig.3.12 and Table 3.7. In a typical TGA thermogram, first two stages are related with the removal of volatiles and plasticizers. Water can be considered as both volatile and a plasticizer in food systems since it can be found in free and bound

form. Therefore, TGA thermogram can be used to determine the state of water in a food matrix (Botosoa et al., 2015; Fisher et al., 2014; Gu et al., 2015; Siegwein et al., 2011). Botosoa et al. (2015) utilized low field NMR relaxometry, TGA and DSC together to monitor the changes of sponge cakes during storage. Fisher et al. (2014) utilized TGA to detect storage stability of strawberry confections. Gu et al. (2015) formulated black raspberry confections by using pectin and starch as the gelling agents and they explained the differences in these samples by using TGA. Similarly, Siegwein et al. (2011) studied the addition of soy protein isolate on the properties of starch based confections again by using TGA. In these studies, it was stated that mass loss (%) up to 150 °C can be assumed to be water while mass loss above that temperature is mostly related with decomposition (Fisher et al., 2014). Therefore, mass loss up to 150 °C was used to determine the water content of samples.

In our study, it was observed that weight losses at the first decomposition stage varied between 13.89 (%) and 18.60 (%) for the different formulations. Thermogram for the samples and the weight loss (%) values are given in Fig.3.7 and Table 3.7, respectively. According to the results, regular trend could not be observed in the weight loss of samples and significant changes could not be detected ( $p>0.05$ ).

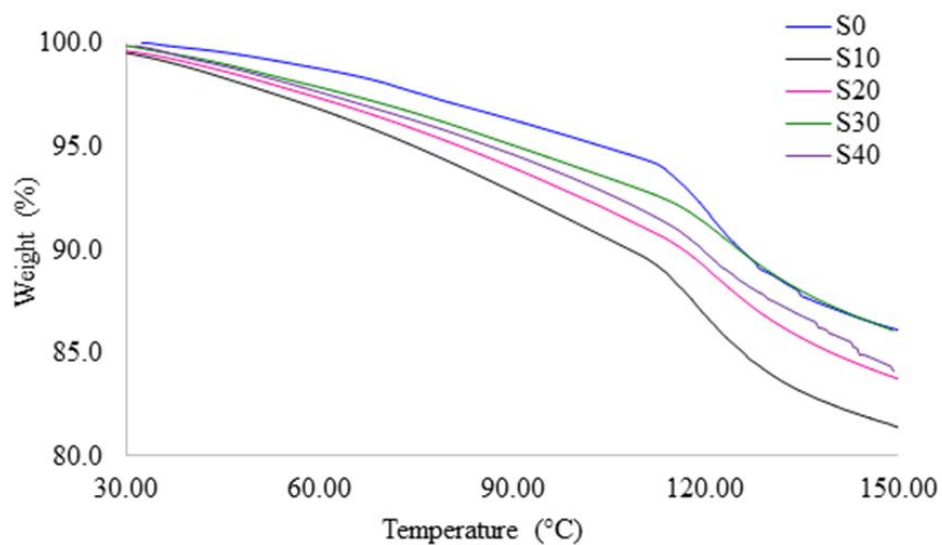


Figure 3.12. Thermogravimetric Analysis (TGA) thermogram of different formulations

Table 3.7. Mass loss at first decomposition and peak temperatures

Sample	Moisture Loss (%)	Peak Temperature (°C)
S0	13.92 <sup>b</sup> ± 0.61	122.26 <sup>a</sup> ± 0.13
S10	19.10 <sup>a</sup> ± 1.73	121.55 <sup>a</sup> ± 0.23
S20	16.24 <sup>ab</sup> ± 0.49	118.77 <sup>b</sup> ± 0.35
S30	14.01 <sup>b</sup> ± 0.10	118.38 <sup>b</sup> ± 0.11
S40	15.03 <sup>b</sup> ± 1.03	115.47 <sup>c</sup> ± 0.41

In addition, derivative weight loss curves can be interpreted for the determination of strength of the water- polymer interaction in formulations. This approach is based on the identifying peak temperatures. While high peak temperatures indicates strong

water association, low peak temperatures indicates lower water association (Siegwein et al., 2011; Tian, Li, Xu, & Jin, 2011). Figure 3.13 shows the derivative weight loss (%) curves of investigated samples. Derivative weight loss curves showed that D-allulose substitution had a significant effect on peak temperatures ( $p < 0.05$ ). Considering the first peak temperatures (related with water loss), increase in allulose concentration decreased the peak temperature by indicating lower water interaction with the system, whereas higher sucrose concentration increased the peak temperature.

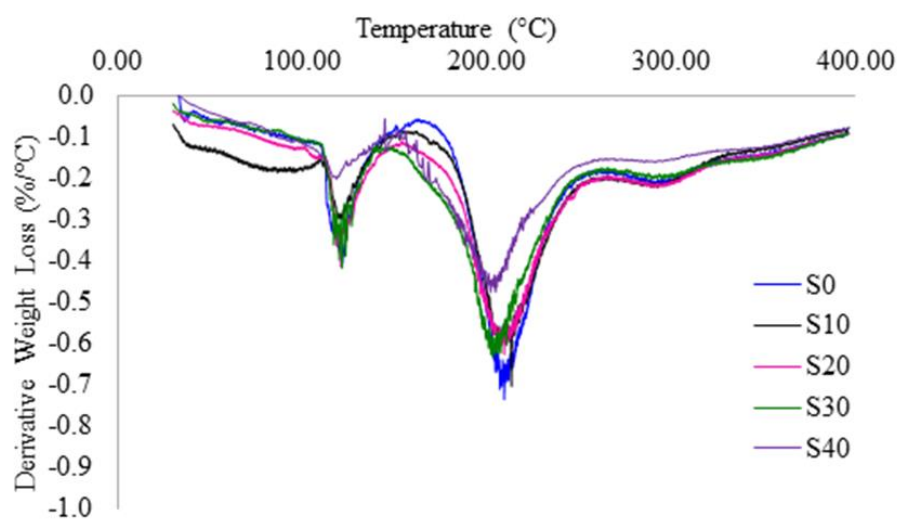


Figure 3.13. Derivative weight loss curves for different formulations

As already pointed out in relaxation studies, the translational as well the rotational dynamics of the confined water molecules was slower, and the 'A' values was higher for the sample containing only sucrose as the sugar source compared to the other samples. Increase in peak temperatures obtained by thermogravimetric analysis also confirmed these findings. This was explained by less interaction of D-allulose with

water molecules, (S. Ikeda, Gohtani, Fukada, & Amo, 2011). Therefore, it was concluded that, there was a good relation between the FFC NMR Relaxometry and TGA to explain the water dynamics by utilizing derivative weight loss (%) curves and peak temperatures. However, TGA was found to be still inefficient compared to the FFC NMR Relaxometry, to understand how composition changes affected the dynamics of water pools within the confectionery gels.

## **3.2 Turkish Delights**

### **3.2.1 Moisture Content**

Moisture content is one of the most important criteria for the confectionery products since it directly affects the textural and sensorial properties of the products leading to changes in their shelf life (Pocan et al., 2019b). This case is also valid for the Turkish delights which can be classified as a traditional confectionery product. As shown in Figure 3.14, utilization of corn syrup led to significant changes of the moisture content of the original (SUC) Turkish delights ( $p < 0.05$ ). The lowest moisture content (4%) was found for the original Turkish delights containing only powder sucrose as the sugar source. However, when the corn syrup types were used instead of sucrose, dramatic increase in moisture content was observed compared to the original ones. It was worth to mention that, use of different type of corn syrups (SBF10, SCG40 and SCG60) led to similar changes in the moisture content of the products ( $p > 0.05$ ) and it was found in the range of 7.5-9%.

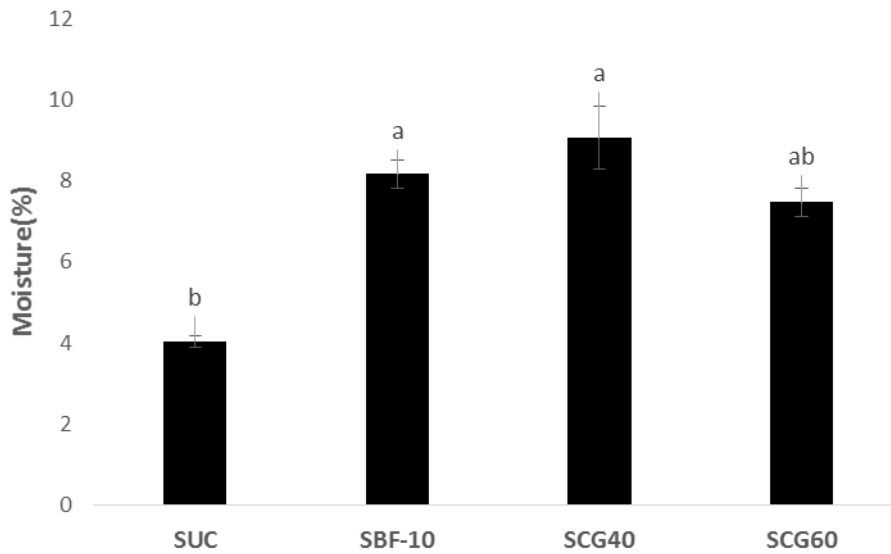


Figure 3.14. Moisture contents (%) of Turkish delights formulated with different type of sugar source (corn syrup or sucrose)

*\* Data were recorded with standard errors. Lower case letters denote significance difference between the samples @ 95% confidence level between the parameters. Analysis was done based on the 2 replicates*

It was an expected trend since it was very well known fact that candies produced with using corn syrup can readily pick up moisture due to their hygroscopic (water binding) nature (R Ergun et al., 2010). Hygroscopic substances are also known as humectants and they promote the retention of water and capable to keep the confections moist (R Ergun et al., 2010). Ergun et al (2010) stated that humectants can be considered as molecules containing hydroxyl groups which have an affinity to form hydrogen bounds with the molecules of water. Actually, these interactions related with “hydration” occur for all types of sugar (Pocan, Ilhan, et al., 2021) but for the corn syrups (especially with high DE value (e.g SCG40 and SCG60) and containing fructose ones (e.g SBF10), they occur in higher extent compared to

sucrose (R Ergun et al., 2010). Especially for our case, since SBF10, SCG40 and SCG60 samples produced by using only corn syrup as the sugar source, higher moisture content of these samples is not a surprising outcome.

In addition, corn syrups are generally preferred by the manufactures due to their crystallization inhibiting properties which is a desirable case for the confectionery gels (Porter & Hartel, 2013). Therefore, confectionery products generally consist of more glucose syrup than sucrose (Burey et al., 2009). Unlike the crystallization inhibition feature of corn syrup, confectionery gels containing sucrose generally have higher crystallinity degree and lower moisture content (Pocan et al., 2019b) which is consistent with the fact that crystal structures hold less water (Labuza et al., 2004). For example, sucrose can be considered as one of the pure crystalline ingredients and for these substances, water is only able to interact by hydrogen bounding at the surface of the crystal structure because of the packing arrangement of crystal lattice excluding foreign molecules like water (R Ergun et al., 2010). Therefore, the lower moisture content of original sample (SUC) could be attributed to sucrose which is prone to more crystallization compared to its counterparts containing corn syrups. Moreover, for these samples (SUC), sandy appearance which can be considered as poor quality indicator was observed most probably due to higher crystallization tendency of sucrose. On the other hand, for its counterparts containing different types of corn syrup, this sandy appearance was not observed.

### **3.3 Color Analysis**

The color is an important sensorial and physical property which affects the perceived quality of the products directly (Kavak & Akpunar, 2018). It is an also important quality parameter for the Turkish delights. Color analysis was performed for all samples and  $L^*$ ,  $a^*$ , and  $b^*$  and  $\Delta E$  values were reported as shown in Table 3.8.



SBF10 samples had the highest L\* value meaning that they are the lightest ones ( $p < 0.05$ ) while SCG40 samples were the darkest ones. Similar to the lightness (L\*) values, the highest a\* (refers to redness) and b\* values (refers to yellowness) were found also for the SBF10 samples ( $p < 0.05$ ) meaning that reddish and yellowness were predominated for these samples. As expected, total color change ( $\Delta E$ ) was also significantly higher for SBF10 compared to its counterparts indicating that this sample were browner than the others ( $p < 0.05$ ). This intense color of SBF10 sample could be attributed to the enhanced rate of caramelization reaction. Since, Turkish delights that used in this study was prepared at 125 °C and it was known that caramelization reactions likely to occur above 120° C (Kocadağlı & Gökmen, 2018), this was an expected result. According to the study of Kocadagli & Gokmen (2018), it was known that contribution of fructose to browning development is generally higher than glucose during the caramelization reactions. Therefore, considering the SBF10 is the only sample that contains fructose (10%), browner color of this sample actually is not surprising. Although, SCG60 sample is not as brown as the SBF10 one, it was worth to mention that, its total color change ( $\Delta E$ ) was higher than SCG40 sample. It was an also expected result since SCG60 contains higher amount of glucose (60%) compared to SCG40 one (40%). Although glucose is not as reactive as fructose during caramelization reactions, it also takes place in caramelization reactions as a reactant. Therefore, relatively higher amount of glucose (60%) found in SCG60 sample might have contributed to the formation of browner appearance compared to SCG40 sample consisting of 40% glucose.

Another important point that should be mentioned here is that, relatively higher a\* and b\* values were observed for the original samples (SUC) compared to SCG40 and SCG60 ones. This was an unexpected result since this sample contains only sucrose as the sugar source. At this point, the hypothesis that comes to mind is the “inversion reaction”. It was a very well-known fact that, in the presence of acid, sucrose degrades into fructose and glucose with the help of high cook temperature and low pH (Hartel, Ergun, & Vogel, 2011). Sucrose inversion is also important

reaction that should be considered during the production of lokum (Turkish delights) since acidification is generally used to improve the quality, texture and flavor of the Turkish delights (P. A. Batu, Gör, Arslan, & Batu, 2018). In this study, Turkish delights were also produced by using citric acid (0.1%). Therefore, inversion of sucrose to glucose and fructose is an expected result leading to formation of yellowish and reddish color of this sample compared to samples containing only glucose syrup (SCG40 and SCG60) since fructose is a more reactive sugar than glucose in caramelization reactions as mentioned previously (Kocadağlı & Gökmen, 2018).

Considering the quality of Turkish delights in terms of color parameters, one can conclude that SBF10 samples that composed of corn syrup consisting of 10% fructose and 36% glucose were samples with higher quality since they have the lightest ones which is an important quality indicator for Turkish delights (A. Batu & Batu, 2016).

Table 3.8. L, a, b values of Turkish delights formulated with different type of sugar source (corn syrup or sucrose)

Samples	L* value	a* value	b* value	ΔE
SUC	30.98 <sup>c</sup>	0.18 <sup>c</sup>	1.05 <sup>b</sup>	-
SBF10	37.35 <sup>a</sup>	0.38 <sup>a</sup>	1.29 <sup>a</sup>	6.38 <sup>a</sup>
SCG40	30.20 <sup>d</sup>	0.14 <sup>d</sup>	0.38 <sup>d</sup>	1.03 <sup>c</sup>
SCG60	33.67 <sup>b</sup>	0.25 <sup>b</sup>	0.65 <sup>c</sup>	2.72 <sup>b</sup>

\*Data were recorded with standard errors. Lower case letters denote significance difference between the samples @ 95% confidence level between the parameters. Analysis was done based on the 2 replicates.

### 3.4 Texture Profile Analysis (TPA)

In addition to the color analysis, TPA also gives valuable information about the quality of confectionery gels. Therefore, TPA was performed for the Turkish delights composing of different types of sugar source and the result were represented in Table 3.9. All textural parameters (hardness, adhesiveness, cohesiveness, etc.) were calculated considering the TPA curve.

The hardness is an important textural parameter which is related to the strength of gel structure under compression and it is defined as the peak force during the first compression cycle (Chandra & Shamasundar, 2015). As seen in Table 3.9, the highest hardness value (2.60 N) was found for the SCG40 sample whereas the lowest hardness was found for the original (SUC) sample ( $p < 0.05$ ). Regarding the desirable textural properties, confectionery gels should not be neither too hard nor too soft (Ates et al., 2020). This case is also valid for the Turkish delights and consumers usually do not prefer too rough products (Kavak & Akpunar, 2018). In this context, it was worth to mention that, such a low hardness value of SUC samples is not a desirable textural property and it might be considered as an indication of weak gel formation. Decrease in hardness values of starch based confectionery gels is generally associated with the phase separation that occurred as a result of release of water from the gel network resulting in softening the sample (Ilhan et al., 2020b).

Adhesiveness is another textural parameter and it is defined as the capacity of a material to stick another substance so it depends on the surface characteristics of the material (Slavutsky & Bertuzzi, 2019). It can be calculated as the negative area between two compression cycle (Slavutsky & Bertuzzi, 2019). It usually considered as an undesirable characteristic for the confectionery gels since it is related with the stickiness of the food materials (Delgado & Bañón, 2015). For the SUC sample, adhesiveness value could not be reported since negative area could not be observed in its TPA curve. On the other hand, the highest adhesiveness value was found for

the SBF10 samples whereas the lowest one was found for the SCG60 sample ( $p < 0.05$ ). This outcome might be stemmed from the different stickiness behavior of corn syrups used in this study. In a previous study, effect of saccharide distribution on the stickiness of various type of syrups was studied and it was revealed that allulose syrups had higher stickiness compared to other common type of corn syrups (Wang & Hartel, 2020). Remembering, allulose is C-3 epimer of fructose having very similar properties with it, the highest adhesiveness value for the SBF10 which was the only sample containing fructose (10%) was not surprising.

The cohesiveness is also known as consistency and it indicates the strength of internal bonds that makes up the body of food and the degree to which a food can be deformed before it breaks (Chandra & Shamasundar, 2015). As indicated by Chandra et al (2015), it was also defined as the ratio of the positive force area during the second compression to that of the first compression that observed in TPA curve. Since cohesiveness indicates the ability of the food to hold together (Chandra & Shamasundar, 2015), higher cohesiveness values could be considered as formation of strong gel network which resist rupturing. Referring back to the results that were shown in Table 4, the cohesiveness values of lokum samples were found in the range of 0.19-0.43. Cohesiveness of SBF10 sample was found to be higher than others while the smallest cohesiveness was found for the SUC samples. This outcome is consistent with the hardness results that was mentioned above and low cohesiveness could be also considered as an indication of weak gel formation.

The springiness is another textural parameter, which is related to elasticity of the sample. Springiness in TPA is related to the height that the food recovers during the time that elapses during the end of first bite and the start of the second bite (Chandra & Shamasundar, 2015). Higher springiness values were obtained for the SBF10 and SCG40 samples indicating enhanced elastic properties of these products while the lowest elasticity was obtained for the SUC samples.

As indicated by Delgado & Banon (2015), gumminess and chewiness are generally utilized as the texture descriptors particularly applicable to jelly confections together with hardness. Gumminess is defined as the product of hardness and cohesiveness so higher hardness have led to high gumminess in confectionery gels and it is considered as an important textural parameter for the semisolid foods (Chandra & Shamasundar, 2015). In our study, the highest gumminess was found for the SCG40 samples while the lowest one was found for the SUC samples ( $p < 0.05$ ). Since the same trend was also observed for the hardness results, expected trend was seen in the gumminess of the Turkish delight samples.

The last textural parameter seen in Table 3.9 was the chewiness and in it was defined as the measure of energy which is necessary to masticate the food and it is generally reported for the solid foods (Chandra & Shamasundar, 2015). It is calculated as the products of gumminess and springiness that is equal to hardness  $\times$  cohesiveness  $\times$  springiness (Chandra & Shamasundar, 2015). As seen in Table 4, the highest chewiness values were found for the SBF10 and SCG40 samples (49.00 g.cm).

Table 3.9. TPA Results of Turkish Delights

Sample	Hardness(N)	Adhesiveness(g.cm)	Cohesiveness	Springiness(mm)	Gumminess(N)	Chewiness(g.cm)
SUC	0.64 <sup>c</sup>	-	0.19 <sup>c</sup>	2.08 $\pm$ 0.04 <sup>c</sup>	0.13 $\pm$ 0.04 <sup>d</sup>	-
SBF10	1.78 $\pm$ 0.07 <sup>b</sup>	23.50 $\pm$ 0.29 <sup>a</sup>	0.43 $\pm$ 0.02 <sup>a</sup>	6.36 $\pm$ 0.05 <sup>a</sup>	0.76 <sup>b</sup>	49.00 $\pm$ 0.58 <sup>a</sup>
SCG40	2.60 $\pm$ 0.03 <sup>a</sup>	11.00 $\pm$ 0.58 <sup>b</sup>	0.37 $\pm$ 0.01 <sup>ab</sup>	5.08 $\pm$ 0.19 <sup>ab</sup>	0.95 $\pm$ 0.03 <sup>a</sup>	49.00 $\pm$ 2.89 <sup>a</sup>
SCG60	1.92 $\pm$ 0.05 <sup>b</sup>	5.50 $\pm$ 0.29 <sup>c</sup>	0.28 $\pm$ 0.02 <sup>bc</sup>	3.74 $\pm$ 0.40 <sup>bc</sup>	0.53 $\pm$ 0.02 <sup>c</sup>	20.00 $\pm$ 2.89 <sup>b</sup>

To conclude, regarding the TPA analysis of the samples, it is definite that textural property of Turkish delights is following this order: SBF10  $\geq$  SCG40 > SCG60 > SUC. According to this trend, it was worth to mention that, utilization of corn syrups especially SBF10 and SCG40 led to the formation of desirable textural

characteristics in Turkish delights. In previous studies, it was also revealed that higher values of textural properties except adhesiveness were found to be an indicator of production of Turkish delights with enhanced textural properties which was also found parallel with the sensory analysis results (Çam & Topuz, 2018). However, it should be kept in mind that, although utilization of corn syrup in Turkish delights led to the formation of high-quality products with enhanced textural properties, it will also affect the authenticity of this traditional confectionery negatively.

### 3.5 X-ray Diffraction Analysis

X-ray diffraction analysis of Turkish delights was performed and patterns of the samples obtained as seen in Figure 3.15. While interpreting XRD pattern, it is important to keep in mind that, the narrower and more concentrated peaks are associated with the crystal regions, whereas the larger and less dense peaks are associated with the amorphous regions (Ilhan et al., 2020b).

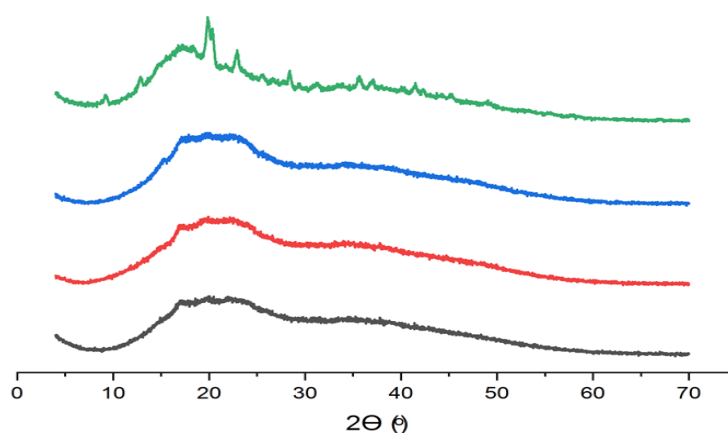


Figure 3.15. X-ray diffraction pattern of Turkish delights formulated with different type of sugar source (SUC: —, SCG60: —, SCG40: —, SBF10: —)

In that regard, it is obvious that, SUC samples are the ones with the highest crystallinity degree compared to its corn syrup containing counterparts by demonstrating various sharper and narrower peaks in its X-ray pattern. This case is an expected outcome because corn syrups have a crystallization inhibition nature as mentioned previously and that is why manufacturers prefer to use corn syrups in the production of Turkish delights even this case jeopardize the originality of the products. On the other hand, X-ray pattern of the corn syrup containing samples (SBF10, SCG40 and SCG60) indicated less crystallinity since they demonstrated broader peaks which distributed in a wide-angle range and they all showed similar patterns. From previous studies, it was known that starch gives diffraction peaks in the range of 15-24° (Shi et al., 2017). These peaks were also observed for all samples in our study and the results are not surprising since all samples that were used in our study contains starch as the gelling agent. In addition to these peaks, SUC samples also demonstrated the characteristic diffraction pattern of sucrose crystals (11.6-24.6°) band (Pocan et al., 2019b).

Referring back to diffraction pattern of the corn syrup containing samples, amorphous halo pattern is more dominant as seen in Figure 3.15 This incident might be stemmed from the existence of maltose in the formulation of corn syrups which found normally in amorphous state in its native form (Wu, Huang, Cui, & Fan, 2020). Although similar diffraction patterns were obtained for the corn syrup containing samples, there were also small changes. For example, diffraction pattern of SCG40 and SCG60 sample is very similar as expected because these specimens are composed of similar corn syrup. Only difference is SCFG40 contains 40% glucose while SCG60 contains 60% glucose. However, it should be considered that, SCG40 contains higher amount of maltose compared to SCG60 since small amount of maltose was converted to glucose (40%) during the production of corn syrup which SCG40 sample contains. This case also affected the diffraction pattern of these samples. As indicated by Wu et al (2020), native maltose gives peak at 12.7°. This peak was also observed in our study for all the samples that contains corn syrup due

to the existence of maltose residues. However, important result that should be mentioned at this point is the different intensities of this peak that were seen among the SCG40 and SCG60. Aforementioned peak's intensity was found to be higher for the SCG40 sample compared to SCG60 one. This case could be related with the quantity of maltose crystal as mentioned in previous studies (Wu et al., 2020). According to this study, increase in the quantity of maltose crystals resulted in increase in the intensity of related peaks. The similar case might be valid for our study. Since SCG40 sample includes higher amount of maltose, existence of higher amount of maltose crystals is also possible for this sample indicating that it has more crystalline and ordered structure compared to its corn syrup containing counterparts.

For the SBF10 sample, all peaks were found to have less intensity compared to its counterparts indicating SBF10 had the least crystal structure. It was an expected trend since as indicated by Pocan et al. (2019), allulose (which is C-3 epimer of fructose and showing very similar properties with it) was found to have crystallization inhibition effect on gelatin based soft candies. Therefore, similar effect might be also valid in our study and even low amount of fructose that was found in SBF10 sample might have led to formation of less crystals.

Consequently, it is worth to note that sucrose containing original samples had the highest crystallinity while corn syrups containing adulterated ones have lesser crystallinity degree. Results also revealed that adulterated samples could be easily discriminated from the original ones with the help of X-ray diffraction analysis.

### **3.6 Time Domain (TD) NMR Relaxometry**

#### **3.6.1 $T_2$ (Spin-spin) Relaxation Spectra**

Regarding the multi-compartment of gel systems including soft candies, multi-exponential approach was generally used for interpreting  $T_2$  (transverse relaxation)



times (Pocan et al., 2019b). With the help of inverse Laplace transformations, the decaying magnetization curve could be converted into a continuous one-dimensional distribution of transverse magnetization, resulting in obtaining a  $T_2$  relaxation spectra (Pocan et al., 2019b). Multi-exponential approach was used in various studies related with soft candy products previously such as gelatin (Efe et al., 2019), starch (Ilhan et al., 2020b) and pectin (Ates et al., 2020) based soft candies concluding bi-exponential model is better compared to mono-exponential model for comparing  $T_1$  relaxation times.

In our study, with the help of XPFit software, discrete component analysis of decaying  $T_2$  curves was performed and two distinct peak (P1 and P2) with different relaxation times ( $T_{2a}$  and  $T_{2b}$ ) and different relative areas (RAs) were found for all samples as seen in Table 3.10 and 3.11. The RAs are calculated regarding magnitude of signal intensity, which was related with each proton pool and they showed the contribution of these proton pools to the whole signal(Pocan et al., 2019b).

Table 3.10. Proton spin-spin relaxation ( $T_2$ ) times (ms) of each compartment observed in relaxation spectrum for Turkish delights formulated with different type of sugar source (corn syrup or sucrose)

<b>Sample</b>	<b>T<sub>2a</sub>(ms)</b>	<b>T<sub>2b</sub>(ms)</b>
<b>SUC</b>	2.31±0.04 <sup>a</sup>	13.17±0.18 <sup>a</sup>
<b>SBF-10</b>	1.14±0.05 <sup>b</sup>	7.38±0.19 <sup>b</sup>
<b>SCG-40</b>	0.51±0.01 <sup>c</sup>	5.59±0.11 <sup>c</sup>
<b>SCG-60</b>	0.58±0.01 <sup>c</sup>	5.17±0.12 <sup>c</sup>

*\* Data were recorded with standard errors. Lower case letters denote significance difference between the samples @ 95% confidence level between the parameters. Analysis was done based on the 2 replicates*

Table 3.11. Relative area (%; RA) of each peak observed in relaxation spectrum for Turkish delights formulated with different type of sugar source (corn syrup or sucrose)

<b>Sample</b>	<b>RA1(%)</b>	<b>RA2(%)</b>
<b>SUC</b>	54.5±1.06 <sup>d</sup>	45.5±1.06 <sup>a</sup>
<b>SBF-10</b>	59.5±0.35 <sup>c</sup>	40.5±0.35 <sup>b</sup>
<b>SCG-40</b>	67.5±0.35 <sup>b</sup>	32.5±0.35 <sup>c</sup>
<b>SCG-60</b>	74.5±0.35 <sup>a</sup>	25.5±0.35 <sup>d</sup>

*\* Data were recorded with standard errors. Lower case letters denote significance difference between the samples @ 95% confidence level between the parameters. Analysis was done based on the 2 replicates*

As in the case of previous studies, P1 was generally associated with non-exchanging proton pool (Efe et al., 2019) and it was attributed to the rigid proton interactions which were not exposed to water (Pocan et al., 2019b) while P2 was thought to be associated with relatively more mobile water which was entrapped in gel network (Efe et al., 2019). Therefore, RA1 (%) indicates contribution of non-exchanging proton pool while RA2 (%) shows contribution of signal coming from more mobile water that entrapped in gel network to the whole signal.

Compartments with the lowest relaxation times were generally associated with solid-solid interactions (Ilhan et al., 2020b) which might be stemmed from sugar-starch or sugar-sugar interactions in our case. As seen in Table 5a, use of corn syrups in Turkish delights' formulation led to significant decrease in  $T_2$  relaxation times of the P1 compared to original SUC sample. ( $p < 0.05$ ). On the other hand, similar  $T_{2a}$  relaxation times were found for the SCG40 and SCG60 sample. Regarding RA1 (%) of the samples, detectable increase was observed for the corn syrup containing ones

and all RA1 results were found to be significantly different ( $p < 0.05$ ). Ascending trend of RA1 (%) actually is not surprising since it indicates the enhanced solid-solid interactions which is expected for the corn syrup containing samples since they include various type of solutes such as maltose, oligosaccharides, etc. in addition to sugar. Contrary to RA1, descending trend of  $T_{2a}$  was also expected since existing of more solid result in competitive environment for water leading to decrease in  $T_{2a}$  as in the case of similar studies (Ilhan et al., 2020b). At this point, it was also worth to mention that, significant high correlation ( $r = -0.94$ ) was found between the hardness values and  $T_{2a}$  relaxation times of the samples indicating that as the solid-solid interactions increases, hardness of the samples decreases. Increased hardness of corn syrup containing samples was also mentioned previously in “Texture Profile Analysis (TPA)” section. Therefore, it could be concluded that enhanced solid-solid interactions led to increase in hardness values of samples indicating formation of strong gel formation which is validated by  $T_{2a}$  relaxation times.

As mentioned previously, second compartment (P2) was attributed to the water having higher mobility that was entrapped in gel network. Similar decreasing trend was also found for the  $T_{2b}$  as in the case of  $T_{2a}$  and the shortest  $T_{2b}$  relaxation times were found for the SCG40 and SCG60 samples. ( $p < 0.05$ ). The decrease in  $T_{2b}$  relaxation times for the corn syrup containing ones could be explained with hygroscopic (water binder) nature of corn syrups. It could be hypothesized that, corn syrups bound more water compared to sucrose leading to decrease in mobility of water that entrapped in gel network. RA2 also validated this case since it decreased for the corn syrup containing ones revealing signal coming from more mobile water pool decreased for the corn syrup containing samples. On the other hand, the highest  $T_{2b}$  was found for the SUC sample indicating weak gel formation as mentioned in earlier sections. Most probably, due to weak gel formation free water fraction in gel network increased leading to increase in  $T_{2b}$  and RA2 of SUC samples.

In addition to these findings, it is also very important to mention the power of  $T_2$  relaxation spectra to discriminate corn syrup containing samples from the original SUC sample. As clearly indicated in Table 3.10-3.11, use of different type of corn syrups in Turkish delights gave rise to shifting of both peaks towards shorter relaxation times and an increase in RA of the P1 while decrease in RA of P2. Similar adulteration detection studies also exist in literature. Therefore, it could be considered that  $T_2$  relaxation spectra obtained from low resolution system could be used as an authenticity and quality detection tool for Turkish delights and spin-lattice relaxation times ( $T_{2a}$  and  $T_{2b}$ ) and signal contribution of each pool (RA1 and RA2) could be used as a fingerprint to differentiate the samples.

### 3.7 Fast Field Cycling (FFC) NMR Relaxometry

The measurements of proton  $T_1$  (spin-lattice) relaxation times as a function of magnetic field strength were performed to give insight for discriminating the Turkish delight samples in relation to dynamic processes undergoing over the molecular scale. Bearing in mind a board range of timescale of molecular motions occurring in gel-based systems, the FFC NMR experimental points obtained in the frequency range from 10 kHz to 20 MHz were additionally completed with the points obtained at 500 MHz. The latter are essential not only as evidence for proper analysis of the NMRD profiles at high frequency range but also because of appropriate evaluation of low-frequency components to the overall relaxation.

In Figure 3.16, the experimental spin-lattice relaxation rates ( $R_1 \equiv 1/T_1$ ) of protons in the samples composing of different types of sugar source are presented as a function of Larmor frequency (the so-called NMRD profiles) at two different temperatures (25 °C and 4° C). As can be seen, at low frequency range (below a few MHz) the amplitude of the relaxation rate is significantly lower ( $T_1$  relaxation times are longer) in the original SUC sample at 25° C, than that observed in other samples

in the same frequency range and temperature (Figure 3.16-a). Differentiation of  $R_1$  amplitude in SUC sample and others becomes even more pronounced at 4 °C (Figure 3.16-b). On the other hand, the NMRD profiles recorded for SBF10, SCG40, and SCG60 seem to be similar, except for an enhancement of the relaxation rate observed in the range of 0.15-2 MHz in SCG40 and SCG60 samples at 25 °C. The explanation of this effect requires to conduct additional study; therefore the effect will not be discussed in this paper. However, on the basis of the FFC relaxometry results so far, we can unambiguously distinguish the original Turkish delight samples (sucrose containing ones) from the corn syrup containing (adulterated) ones. The obtained results indicate that adulterated samples could be easily discriminated from the original ones when conducting even a cursory qualitative analysis of the NMRD profiles recorded at low frequency range (below a few MHz) and at temperature below storage temperature for these food products. Ultimately, a single FFC NMR measurement performed under proper conditions, i.e. at low Larmor frequency (below 1 MHz) and below storage temperature (e.g. at 4 °C), can be sufficient to confirm with certainty the authenticity of Turkish delights.

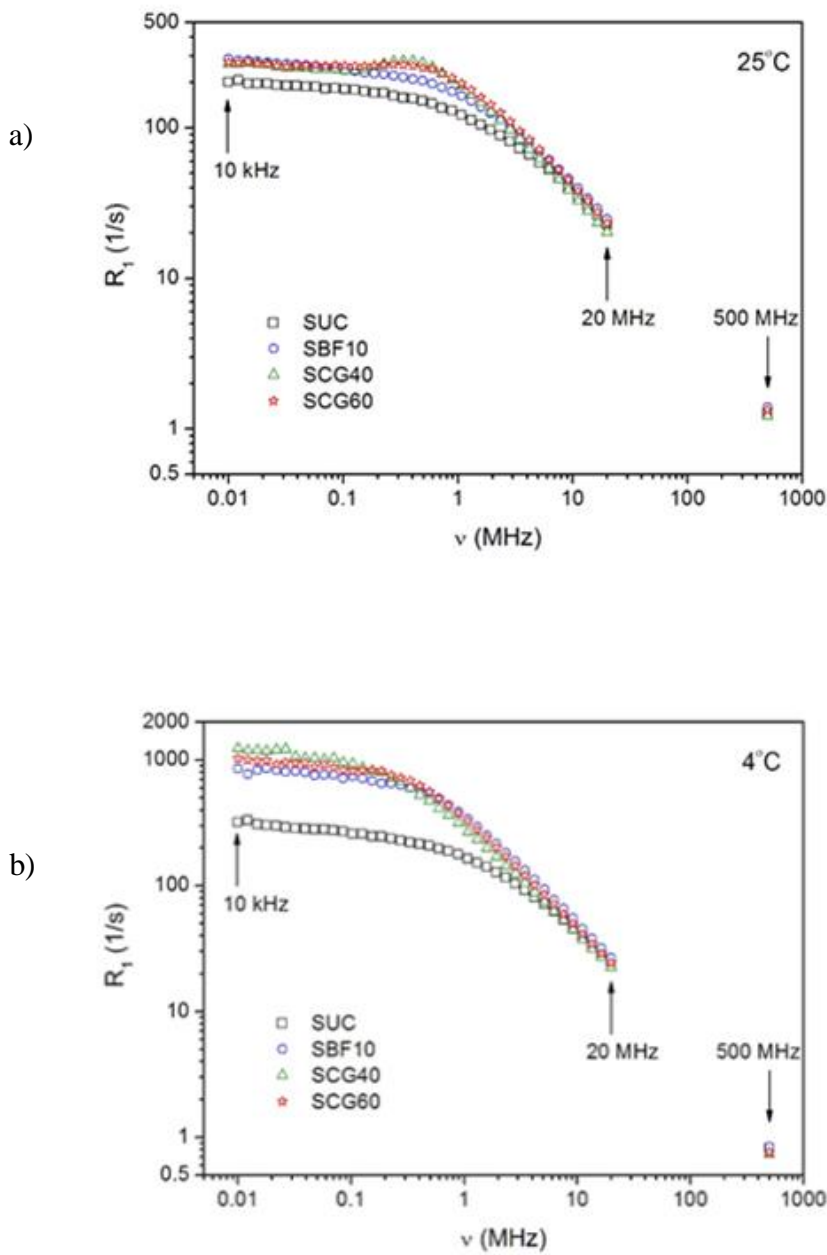


Figure 3.16. Proton spin-lattice relaxation dispersion profiles of Turkish delights formulated with different type of sugar source (corn syrup or sucrose) obtained with a FFC NMR relaxometer in the range of 10 kHz-20 MHz at 25°C (a) and 4°C (b); additional points were obtained at 500 MHz with a conventional NMR spectrometer

To provide a thorough quantitative analysis of the NMRD profiles, a theoretical approach has been carried out related with the molecular dynamics depending on microstructure of the food gels. As mentioned previously, different proton fractions can be considered in the systems under investigation. The first fraction of protons (containing “rigid” protons) is associated with the gelator (starch) molecules forming the gel network. These protons, especially protons which are not involved in chemical exchange, are undetectable under the FFC NMR measuring conditions, and thus, they can be neglected for the present study. The second proton fraction (containing “mobile” protons) is associated with mobile molecules of water (as well as mobile sugar molecules). Thinking about a complex microstructure of gel these molecules, and their protons, it is wise to make a distinction into more and less mobile ones depending on their placement in the local gel structure. The molecules moving within the large pools undergo faster dynamics compared to those entrapped in small pools where due to space-confined effect the molecular dynamics is slower. The described behavior of molecules can apply to both rotational and translational dynamics that modulates intramolecular and intermolecular dipolar interactions between coupled protons. Consequently, the overall spin-lattice relaxation rate could be expressed by the sum of the individual contributions associated with different proton fractions distinguished in the systems under investigation:

$$R_1(\omega) = R_{1,MM}^{rot}(\omega) + R_{1,LM}^{rot}(\omega) + R_{1,MM}^{trans}(\omega) + R_{1,LM}^{trans}(\omega), \quad (2)$$

where *MM* and *LM* index denotes, respectively, *more mobile* and *less mobile* fraction of protons associated with molecules undergoing rotational (*rot*) and translational (*trans*) diffusion,  $\omega = \gamma B_0$  is the Larmor angular frequency ( $B_0$  is the external magnetic flux density and  $\gamma$  is the gyromagnetic ratio).

For simplicity and applicability of the above expression to the collected FFC NMR data, the first two terms in equation (2) can be approximated by one *rot* contribution reflecting average rotational dynamics. With this assumption, the resulting expression for the proton spin-lattice relaxation rate simplifies to the following form:

$$R_1(\omega) = R_1^{rot}(\omega) + R_{1,MM}^{trans}(\omega) + R_{1,LM}^{trans}(\omega). \quad (3)$$

From a NMR spin-lattice relaxation theory point of view, the rotational and translational dynamics in a different timescale modulates in time dipolar interactions in the spin system, i.e. the former and latter is the main source of fluctuations for the dipolar spin interactions, respectively, within the same molecules (intramolecular contribution) and between neighboring ones (intermolecular contribution). For this reason, two molecular correlation times  $\tau_{rot}$  and  $\tau_{trans}$  should be considered in terms of two theoretical models describing, respectively, rotational and translational contribution in equation (3).

In simple molecular systems, the model associated with the rotational motion (rotational diffusion or molecular tumbling) is commonly given by combination of Lorentzian-shape spectral density,  $J(\omega)$ , which is a Fourier transform of normalized exponential correlation function  $G(t) = \exp(-t/\tau_{rot})$  with a single molecular correlation time  $\tau_{rot}$  (Bloembergen, Purcell, & Pound, 1948):

$$R_1^{rot}(\omega) = C_{intra} [J(\omega) + 4J(2\omega)] = C_{intra} \left[ \frac{\tau_{rot}}{1+(\omega\tau_{rot})^2} + \frac{4\tau_{rot}}{1+(2\omega\tau_{rot})^2} \right], \quad (4)$$

where  $C_{intra} \propto 1/\langle r \rangle^6$  is referred as the intramolecular dipolar relaxation constant ( $\langle r \rangle$  denotes the mean distance between coupling proton pairs within the molecule). However, in many complex molecular systems, including molecular gels, a distribution of correlation times is desired. Applying the log-Gaussian distribution form (Noack, 1971):

$$g(\ln \tau) = \frac{1}{\sqrt{2\pi}\delta} \exp\left(-\frac{\ln^2(\tau/\tau_{rot})}{2\delta^2}\right), \quad (5)$$

where  $\tau_{rot}$  is the correlation time corresponding to the center of the distribution and  $\delta$  is the width of the distribution, equation (4) can be rewritten as follows (Noack, 1971; A. Rachocki, Latanowicz, & Tritt-Goc, 2012):



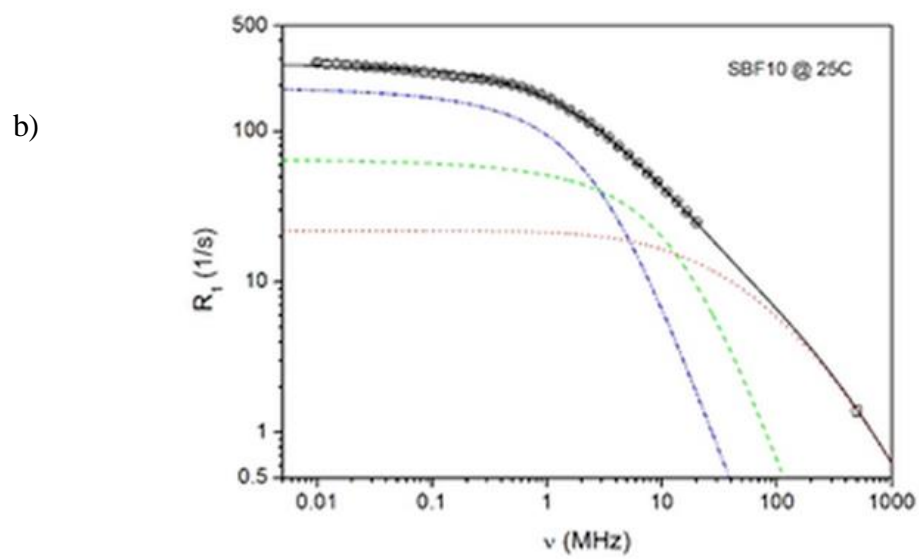
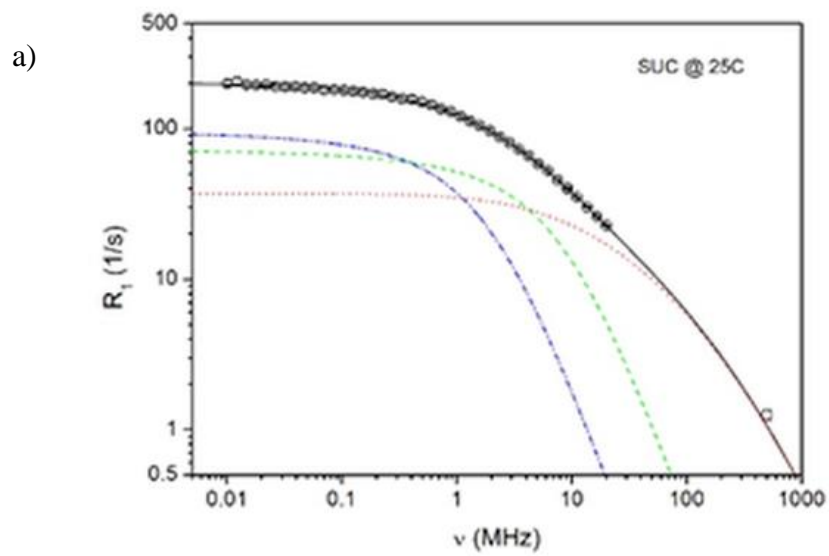
$$R_1^{rot}(\omega) = C_{intra} \left[ \int_0^\infty \frac{g(\tau_{rot})\tau_{rot}}{1+(\omega\tau_{rot})^2} d\tau_{rot} + 4 \int_0^\infty \frac{g(\tau_{rot})\tau_{rot}}{1+(2\omega\tau_{rot})^2} d\tau_{rot} \right]. \quad (6)$$

The form of the  $J(\omega)$  function applying for translational diffusion is dependent on the model assumed (Abragam, 1961; Bloembergen et al., 1948). The one frequently used in viscous liquids is proposed by Torrey (Torrey, 1953). The contribution to the overall relaxation is given by (Knapkiewicz, Rachocki, Bielejewski, & Sebastião, 2020; Adam Rachocki, Andrzejewska, Dembna, & Tritt-Goc, 2015; Torrey, 1953):

$$R_1^{trans}(\omega) = C_{inter} \frac{N\tau_{trans}}{d^3} [f(\delta, \omega\tau_{trans}) + 4f(\delta, 2\omega\tau_{trans})], \quad (7)$$

where  $C_{inter} = (9/8)(\mu_0\gamma^2\hbar/(4\pi))^2$ ,  $d$  is the closest distance between the interacting molecules,  $\tau_{trans}$  is the average time between molecular translational jumps,  $N$  is the number of protons (spin density) per unit volume,  $\delta = \langle a \rangle^2 / (12d^2)$  with  $\langle a \rangle^2 = 6D\tau_{trans}$  being the mean-square root of the molecular jump distance,  $D$  is the translational self-diffusion constant, and  $f(\delta, x)$  are analytical functions (Torrey, 1953).

The application of the presented theoretical models in combination with equation (3) allowed to reproduce the proton NMRD profiles obtained in all studied samples in the broad frequency range of 0.01-500 MHz, and determine the molecular parameters characterizing the rotational and translational dynamics of molecules in the gel systems. The results of the conducted analysis are presented in Figure 3.17 and Figure 3.18 for the FFC NMR experimental data collected at 25 °C and 4 °C, respectively. The solid lines are the best fits of equation (3) – after insertion of equations (6) and (7), to the experimental points, whereas the dot, dash, and dash-dot lines represent the individual relaxation contributions associated with rotational (dot line) and two translational motions (dash and dash-dot lines) detected by FFC NMR relaxometry.



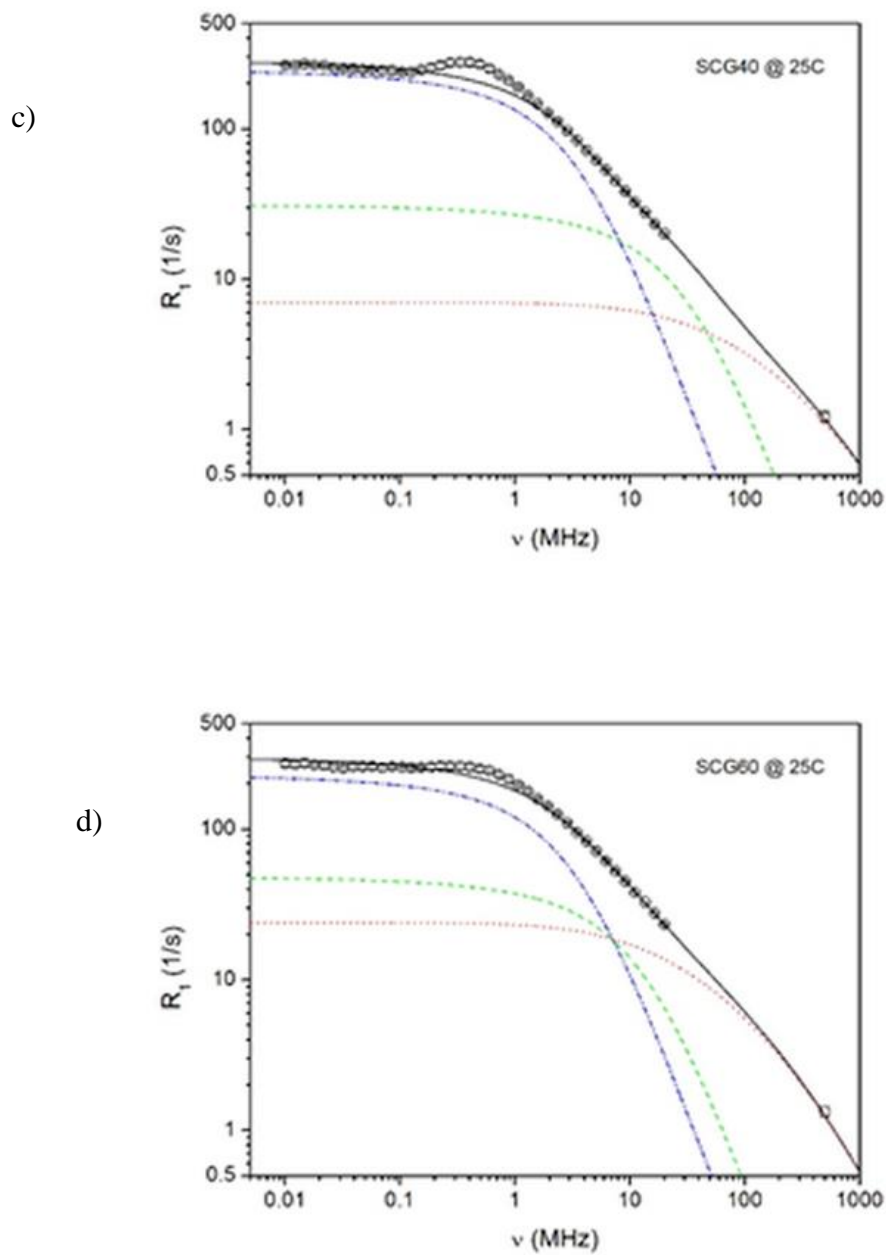
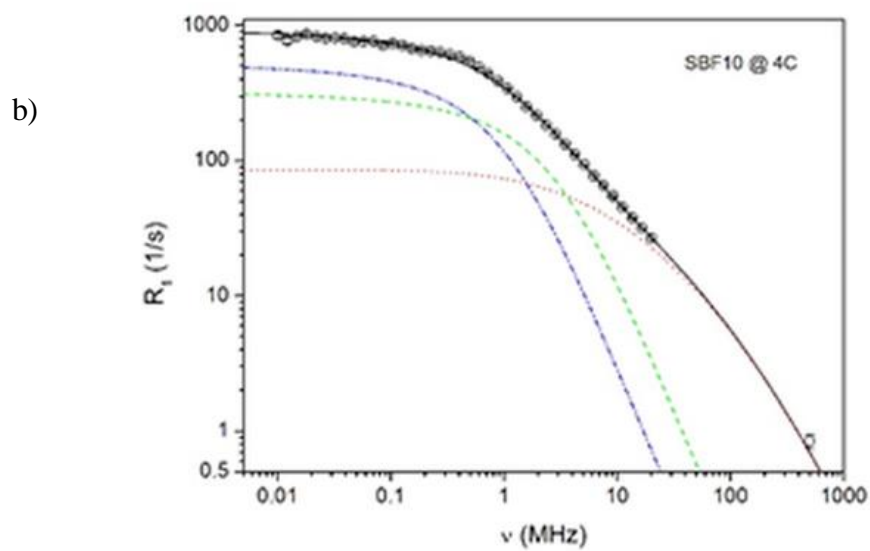
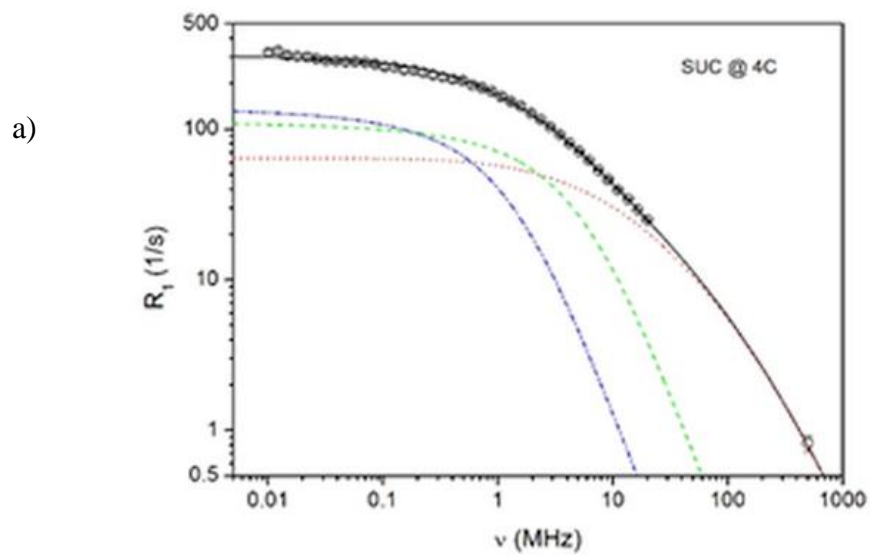


Figure 3.17. Proton spin-lattice relaxation dispersion profiles obtained at 25°C for SUC (a), SBF10 (b), SCG40 (c), and SCG60 (d); the solid lines are the best fits of equations (3), (6), (7) to the experimental data (see text); deconvolution of the overall

fits: rotational contributions (dot lines), two translational contributions (dash and dot-dash lines)



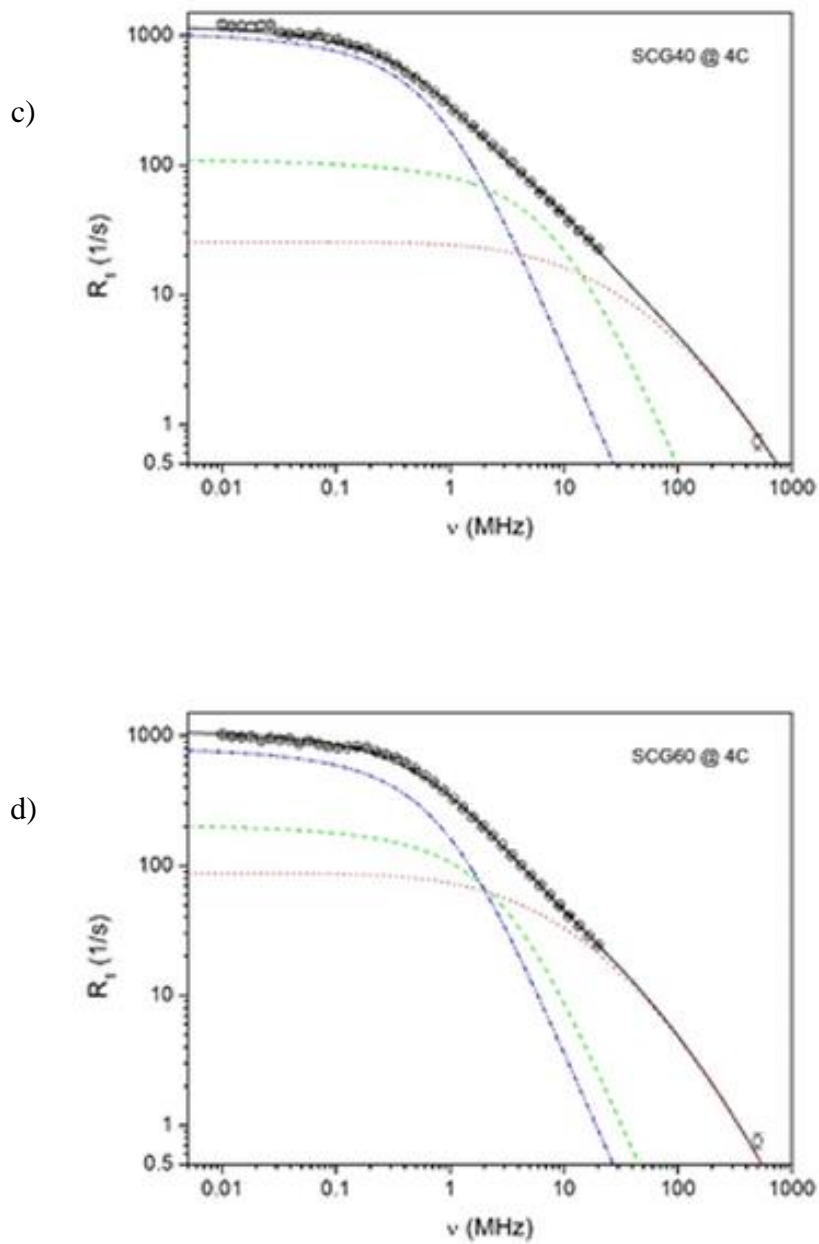


Figure 3.18. Proton spin-lattice relaxation dispersion profiles obtained at 4°C for SUC (a), SBF10 (b), SCG40 (c), and SCG60 (d); the solid lines are the best fits of equations (3), (6), (7) to the experimental data (see text); deconvolution of the

overall fits: rotational contributions (dot lines), two translational contributions (dash and dot-dash lines)

The multi-parameter fits are satisfactory and reasonable fitting parameters were obtained as seen in Table 3.12. It is worth to note that for translational contributions the closest distance  $d$  between the interacting molecules was kept constant during fitting procedure. In relation to diameter of water (2.75 Å) and sugar molecule (~4.5 Å), the average value  $d = 3.6$  Å was assessed and  $a = d$  (the mean jump length of molecules corresponds to the value  $d$ ) was assumed for simplification. For rotational contributions the width  $\delta$  of the log-Gaussian distribution was kept at the level of 1.5 decade. Finally, two parameters for rotational component ( $\tau_{\text{rot}}$  and  $C_{\text{intra}}$ ) and two parameters for each translational component ( $D$  and  $N$ ) were fitted to the experimental data at 4 and 25 °C, whereas spin densities  $N_{\text{MM}}$  and  $N_{\text{LM}}$ , respectively, for more mobile molecules (MM) and less mobile (LM) fraction, were fitted only to the experimental data at 25 °C whilst for fits at lower temperature they were kept as constant parameters.

The following major conclusions can be made from our FFC NMR data analysis. First, it has not been found before that in the soft candy products, apart from the rotational motions, the molecules (mainly water but also sugar molecules) undergo two types of translational dynamics. The observed two self-diffusion processes are possible to distinguish by FFC NMR relaxometry due to significantly different diffusion constants (see Table 6). For instance, for the original Turkish delight sample containing sucrose (SUC), the two diffusion coefficients are of the order of  $1.7 \cdot 10^{-12}$  m<sup>2</sup>/s and  $3.9 \cdot 10^{-13}$  m<sup>2</sup>/s at 25 °C. For this reason a complex microstructure of these food gels is filled with pools containing more and less mobile molecules which due to topological limitations of the gel network (confined effect) are not able to average the timescale of two distinguished translational dynamic processes.

The second important fact is that the carried out analysis has provided the spin (proton) densities within the pools with different molecular dynamics. Unexpectedly, the relative change in moisture of SUC, SBF10, SCG40, and SCG60 samples is in good agreement with the relative change in total proton densities ( $N = N_{MM} + N_{LM}$ ) as seen in Table 3.12. This leads to the conclusions that the observed translational molecular dynamics is mainly determined by water molecules entrapped in the gel network, however, the interactions of water with sugar molecules cannot be neglected. Referring the ratio  $N_{MM}/N_{LM}$  to the number (or even size) of the corresponding proton pools in the studied samples, it is possible to find out the following quantitative correlations: i) for SUC almost 3 times more protons are associated with pools containing more mobile molecules in contrast to these with less mobile ones, ii) for SBF10 the ratio  $N_{MM}/N_{LM}$  increases to  $\sim 2$ , and iii) for SCG40 and SCG60 the proton densities in two considered pools are comparable. Although this analysis requires additional microstructure study, the results obtained with the use of FFC NMR relaxometry give a direct indication of differentiation between local microstructure of the studied food gels containing deferent type of sugar.

Table 3.12. Parameters obtained from the fits presented in Equation 7

Sample	Moisture (%) & rel. change	Temp. (°C)	$C_{intra} \cdot 10^9$ (s <sup>2</sup> )	$\tau_{rot}$ (ns)	$D_{MM} \cdot 10^{-12}$ (m <sup>2</sup> /s)	$D_{LM} \cdot 10^{-13}$ (m <sup>2</sup> /s)	$N_{MM} \cdot 10^{28}$ (m <sup>-3</sup> )	$N_{LM} \cdot 10^{28}$ (m <sup>-3</sup> )	$N$	Relative change in $N$	Ratio $N_{MM}/N_{LM}$
SUC	4 / -	25	4.20 ±0.03	0.57 ±0.06	1.70 ±0.09	3.90 ±0.09	4.39 ±0.07	1.33 ±0.04	5.72	-	3.3
		4	3.86 ±0.07	1.08 ±0.04	1.11 ±0.04	2.71 ±0.08					
SBF10	8.2 / 2.05	25	4.95 ±0.05	0.29 ±0.04	2.83 ±0.09	5.43 ±0.06	6.57 ±0.19	3.79 ±0.16	10.36	1.81	1.7
		4	3.86 ±0.04	1.44 ±0.03	0.58 ±0.06	2.06 ±0.04					
SCG40	7.5 / 1.87	25	4.45 ±0.11	0.35 ±0.17	2.67 ±0.43	6.65 ±0.12	4.48 ±0.14	5.37 ±0.15	9.85	1.72	0.8
		4	3.43 ±0.08	1.66 ±0.07	0.62 ±0.02	1.84 ±0.03					
SCG60	9.1 / 2.27	25	4.01 ±0.09	0.11 ±0.08	6.51 ±0.11	7.11 ±0.07	7.24 ±0.16	6.2 ±0.12	13.44	2.35	1.2
		4	3.19 ±0.03	0.52 ±0.03	1.83 ±0.06	1.62 ±0.02					





## CHAPTER 4

### CONCLUSION AND RECOMMENDATIONS

This dissertation highlighted the potential use of TD-NMR Relaxometry and FFC-NMR Relaxometry to characterize the soft candy products in terms of quality and authenticity attributes and gave deep insight to the researchers for understanding water dynamics and water mobility in different confectionery gel systems.

In the 1<sup>st</sup> part of the dissertation, gelatin based confectionery gels were formulated by using D-Allulose and it was concluded that D-allulose substitution led to the formation of products with enhanced textural properties, which were exposed to less crystallization during the studied aging period. Regarding the economic aspects of utilization of D-allulose, further optimization studies might be necessary to extend the utilization of rare sugars in the confectionery industry. This study also revealed that interpreting  $T_1$  and  $T_2$  relaxation times is a perfect tool to characterize confectionery systems, which will pave the way for the utilization of TD NMR relaxometry in confectionery industry.

In the 2<sup>nd</sup> part of the study, for the same samples that were mentioned in the 1<sup>st</sup> part, we moved one step further and with the analysis of NMRD curves obtained by an FFC experiment and it was shown that increase in moisture content and decrease in hardness values with D-allulose substitution in fact changes the translational and rotational dynamics of the system. Increase on the concentration of D-allulose led to an increase on the relative population of the pool of water molecules (within the confined-water fraction) that are bound to the gelatin network and therefore fastened the translational and rotational dynamics and increased the contribution of the relative population of the free-water fraction which was also reflected as softer

confectionery gels. Therefore, it could be elucidated that, there is a direct relation between the water dynamics and the textural properties of the confectionery gel systems. Peak temperatures that were obtained from TGA thermograms also confirmed the results obtained from FFC experiments.

In the last part of this dissertation, this time Turkish delights were formulated as a starch based confectionery gel by using sucrose and different type of corn syrups. In this part, firstly, the effect of different type corn syrup substitution on Turkish delights was examined by using important quality parameters like moisture content, color, crystallinity and textural parameters (hardness, springiness, adhesiveness, etc.). Secondly, the adulterated (corn syrup) containing Turkish delights were discriminated from the original ones (sucrose containing) by using TD-NMR and FFC-NMR techniques. Results clearly indicated that, corn syrups containing samples had improved textural properties and less prone to crystallization although this case affected the authenticity of the products negatively. Both TD-NMR and FFC-NMR techniques were found to be effective to discriminate the original samples from the corn syrup containing ones. Thanks to FFC technology, we moved one step further and quantitative analysis of relaxation behavior of Turkish delights was performed by considering the water dynamics of different proton pools that found in samples. Results clearly indicated that, apart from the rotational motions, molecules in Turkish delights (mainly water but also sugar molecules) undergo two types of translational dynamics. In addition, it was demonstrated that, translational molecular dynamics is mainly determined by water molecules entrapped in the gel network. This study revealed that, both FFC and TD-NMR technique are promising methods enabling researchers to detect the authenticity and quality of soft candy products which will pave the way for utilization of low-resolution NMR techniques in confectionery industry and R&D laboratories.

For the future studies, by using more advanced statistical approaches such as “Multivariate Analysis” and “Chemometrics” and by utilizing more advanced pulse

sequences in NMR Relaxometry studies, more comprehensive studies could be performed to determine the authenticity and quality of the confectionery gels and other confectionery products.



## REFERENCES

- Abragam, A. (1961). *The Principles of Nuclear Magnetism*. American Journal of Physics. London,UK: Oxford University Press.  
<https://doi.org/10.1119/1.1937646>
- Akkaya, S., Ozel, B., Oztop, M. H., Yanik, D. K., & Gogus, F. (2020). Physical characterization of high methoxyl pectin and sunflower oil wax emulsions: A low-field <sup>1</sup>H NMR relaxometry study. *Journal of Food Science*, 0.  
<https://doi.org/10.1111/1750-3841.15560>
- Aroulmoji, V., Mathlouthi, M., Feruglio, L., Murano, E., & Grassi, M. (2011). Hydration properties and proton exchange in aqueous sugar solutions studied by time domain nuclear magnetic resonance. *Food Chemistry*, 132(4), 1–7.  
<https://doi.org/10.1016/j.foodchem.2011.01.110>
- Ates, E. G., Ozvural, E. B., & Oztop, M. H. (2020). Understanding the role of d-Allulose and soy protein addition in pectin gels. *Journal of Applied Polymer Science*, (August), 1–10. <https://doi.org/10.1002/app.49885>
- Ates, E. G., Ozvural, E. B., & Oztop, M. H. (2021). In vitro digestibility of rare sugar (D-allulose) added pectin–soy protein gels. *International Journal of Food Science and Technology*, 1–11. <https://doi.org/10.1111/ijfs.14966>
- Baroni, S., Consonni, R., Ferrante, G., & Aime, S. (2009). Relaxometric studies for food characterization: The case of balsamic and traditional balsamic vinegars. *Journal of Agricultural and Food Chemistry*, 57(8), 3028–3032.  
<https://doi.org/10.1021/jf803727d>

- Batu, A., & Batu, H. S. (2016). Türk Tatlı Kültüründe Türk Lokumunun Yeri (The Place of Turkish Delight (Lokum) in Turkish Sweet Culture). *Journal of Tourism and Gastronomy Studies*, 4(1), 42–52.  
<https://doi.org/10.21325/jotags.2016.5>
- Batu, A., & Kirmaci, B. (2009). Production of Turkish delight (lokum). *Food Research International*, 42(1), 1–7.  
<https://doi.org/10.1016/j.foodres.2008.08.007>
- Batu, P. A., Gör, Ö., Arslan, A., & Batu, H. S. (2018). Delight (Lokum) During Production. *Aydın Gastronomy*, 2(2), 9–20.
- Belcourt, L. A., & Labuza, T. P. (2007). Effect of raffinose on sucrose recrystallization and textural changes in soft cookies. *Journal of Food Science*, 72(1). <https://doi.org/10.1111/j.1750-3841.2006.00218.x>
- Berk, B., Grunin, L., & Oztop, M. H. (2021). A non-conventional TD-NMR approach to monitor honey crystallization and melting. *Journal of Food Engineering*, 292(August 2020), 110292.  
<https://doi.org/10.1016/j.jfoodeng.2020.110292>
- Besghini, D., Mauri, M., & Simonutti, R. (2019). Time domain NMR in polymer science: From the laboratory to the industry. *Applied Sciences (Switzerland)*, 9(9). <https://doi.org/10.3390/app9091801>
- Bielejewski, M., Rachocki, A., Kaszyńska, J., & Tritt-Goc, J. (2018). The gelation influence on diffusion and conductivity enhancement effect in renewable ionic gels based on a LMWG. *Physical Chemistry Chemical Physics*, 20(8), 5803–5817. <https://doi.org/10.1039/c7cp07740h>
- Bloembergen, N., Purcell, E. M., & Pound, R. V. (1948). Relaxation effects in nuclear magnetic resonance absorption. *Physical Review*, 73(7), 679–712.  
<https://doi.org/10.1103/PhysRev.73.679>

- Bodart, P. R., Rachocki, A., Tritt-Goc, J., Michalke, B., Schmitt-Kopplin, P., Karbowski, T., & Gougeon, R. D. (2020). Quantification of manganous ions in wine by NMR relaxometry. *Talanta*, 209(November 2019), 120561. <https://doi.org/10.1016/j.talanta.2019.120561>
- Bolat, B., Ugur, A. E., Oztop, M. H., & Alpas, H. (2021). Effects of High Hydrostatic Pressure assisted degreasing on the technological properties of insect powders obtained from *Acheta domesticus* & *Tenebrio molitor*. *Journal of Food Engineering*, 292(April 2020), 110359. <https://doi.org/10.1016/j.jfoodeng.2020.110359>
- Botosoa, E. P., Chèné, C., Blecker, C., & Karoui, R. (2015). Nuclear Magnetic Resonance , Thermogravimetric and Differential Scanning Calorimetry for Monitoring Changes of Sponge Cakes During Storage at 20 ° C and 65 % Relative Humidity. *Food and Bioprocess Technology*, 8, 1020–1031. <https://doi.org/10.1007/s11947-014-1467-7>
- Burey, P., Bhandari, B. R., Rutgers, R. P. G., Halley, P. J., & Torley, P. J. (2009). *Confectionery gels: A review on formulation, rheological and structural aspects. International Journal of Food Properties* (Vol. 12). <https://doi.org/10.1080/10942910802223404>
- Çam, İ. B., & Topuz, A. (2018). Production of soapwort concentrate and soapwort powder and their use in Turkish delight and tahini halvah. *Journal of Food Process Engineering*, 41(1), 1–8. <https://doi.org/10.1111/jfpe.12605>
- Capitani, D., Sobolev, A. P., Delfini, M., Vista, S., Antiochia, R., Proietti, N., ... Mannina, L. (2014). NMR methodologies in the analysis of blueberries. *Electrophoresis*, 35(11), 1615–1626. <https://doi.org/10.1002/elps.201300629>
- Chakrapani, S. B., Minkler, M. J., & Beckingham, B. S. (2019). Low-field 1H-NMR spectroscopy for compositional analysis of multicomponent polymer systems. *Analyst*, 144, 1679–1686. <https://doi.org/10.1039/c8an01810c>

- Chandra, M. V., & Shamasundar, B. A. (2015). Texture profile analysis and functional properties of gelatin from the skin of three species of fresh water fish. *International Journal of Food Properties*, *18*(3), 572–584. <https://doi.org/10.1080/10942912.2013.845787>
- Chattopadhyay, S., Raychaudhuri, U., & Chakraborty, R. (2014). Artificial sweeteners - A review. *Journal of Food Science and Technology*, *51*(4), 611–621. <https://doi.org/10.1007/s13197-011-0571-1>
- Chen, J., Huang, W., Zhang, T., Lu, M., & Jiang, B. (2019). Anti-obesity potential of rare sugar d-psicose by regulating lipid metabolism in rats. *Food and Function*, *10*(5), 2417–2425. <https://doi.org/10.1039/c8fo01089g>
- Chung, M.-Y., Oh, D.-K., & Lee, K. W. (2012). Hypoglycemic health benefits of D-psicose. *Journal of Agricultural and Food Chemistry*, *60*(4), 863–869. <https://doi.org/10.1021/jf204050w>
- Cikrikci, S., Mert, B., & Oztop, M. H. (2018). Development of pH Sensitive Alginate/Gum Tragacanth Based Hydrogels for Oral Insulin Delivery. *Journal of Agricultural and Food Chemistry*, *66*(44), 11784–11796. research-article. <https://doi.org/10.1021/acs.jafc.8b02525>
- Cikrikci, S., & Oztop, M. H. (2016). Mathematical Modeling and Use of Magnetic Resonance Imaging (MRI) for Oil Migration in Chocolate Confectionery Systems. *Food Engineering Reviews*, 50–70. <https://doi.org/10.1007/s12393-016-9152-4>
- Cobo, M. F., Deublein, E. J., Haber, A., Kwamen, R., Nimbalkar, M., & Decker, F. (2017). TD-NMR in Quality Control: Standard Applications. *Modern Magnetic Resonance*, (January), 1–18. <https://doi.org/10.1007/978-3-319-28275-6>
- Conte, P., Cinquanta, L., Lo Meo, P., Mazza, F., Micalizzi, A., & Corona, O.



- (2020). Fast field cycling NMR relaxometry as a tool to monitor Parmigiano Reggiano cheese ripening. *Food Research International*.  
<https://doi.org/10.1016/j.foodres.2020.109845>
- Cornillon, P., & Salim, L. C. (2000). Characterization of water mobility and distribution in low- and intermediate-moisture food systems. *Magnetic Resonance Imaging*, 18(3), 335–341. [https://doi.org/10.1016/S0730-725X\(99\)00139-3](https://doi.org/10.1016/S0730-725X(99)00139-3)
- Dag, D., Kilercioglu, M., & Oztop, M. H. (2017). Physical and chemical characteristics of encapsulated goldenberry (*Physalis peruviana* L.) juice powder. *LWT - Food Science and Technology*, 83, 86–94.  
<https://doi.org/10.1016/j.lwt.2017.05.007>
- Delgado, P., & Bañón, S. (2015). Determining the minimum drying time of gummy confections based on their mechanical properties. *CYTA - Journal of Food*, 13(3), 329–335. <https://doi.org/10.1080/19476337.2014.974676>
- Demirkesen, I., Campanella, O. H., Sumnu, G., Sahin, S., & Hamaker, B. R. (2014). A Study on Staling Characteristics of Gluten-Free Breads Prepared with Chestnut and Rice Flours. *Food and Bioprocess Technology*, 7(3), 806–820. <https://doi.org/10.1007/s11947-013-1099-3>
- Efe, N., Bielejewski, M., Tritt-Goc, J., Mert, B., & Oztop, M. H. (2019). NMR relaxometry study of gelatin based low-calorie soft candies. *Molecular Physics*, 117(7–8), 1034–1045.  
<https://doi.org/10.1080/00268976.2018.1564392>
- Ergun, R., Lietha, R., & Hartel, R. W. (2010). Moisture and Shelf Life in Sugar Confections. *Critical Reviews in Food Science and Nutrition*, 50(2), 162–192.  
<https://doi.org/10.1080/10408390802248833>
- Ergun, Roja, Hartel, R. W., & Noda, Y. (2009). Predicting Crystallization in

Confections. *The Manufacturing Confectioner*, (October), 51–60.

Ertugrul, U., Namli, S., Tas, O., Kocadagli, T., Gokmen, V., Sumnu, S. G., & Oztop, M. H. (2021). Pea protein properties are altered following glycation by microwave heating. *Lwt*, *150*(January), 111939. <https://doi.org/10.1016/j.lwt.2021.111939>

Ertugrul, U., Tas, O., Namli, S., & Oztop, M. H. (2021). A preliminary investigation of caramelisation and isomerisation of allulose at medium temperatures and alkaline pHs: a comparison study with other monosaccharides. *International Journal of Food Science & Technology*, 1–6. <https://doi.org/10.1111/ijfs.15128>

Fisher, E. L., Ahn-Jarvis, J., Gu, J., Weghorst, C. M., & Vodovotz, Y. (2014). Assessment of physicochemical properties, dissolution kinetics and storage stability of a novel strawberry confection designed for delivery of chemopreventive agents. *Food Structure*, *1*(2), 171–181. <https://doi.org/10.1016/j.foostr.2013.10.001>

Fukada, K., Ishii, T., Tanaka, K., Yamaji, M., Yamaoka, Y., Kobashi, K. I., & Izumori, K. (2010). Crystal structure, solubility, and mutarotation of the rare monosaccharide D-psicose. *Bulletin of the Chemical Society of Japan*, *83*(10), 1193–1197. <https://doi.org/10.1246/bcsj.20100148>

Granström, T. B., Takata, G., Tokuda, M., & Izumori, K. (2004). Izumoring: a novel and complete strategy for bioproduction of rare sugars. *Journal of Bioscience and Bioengineering*, *97*(2), 89–94. <https://doi.org/10.1263/jbb.97.89>

Grunin, L., Oztop, M. H., Guner, S., & Baltaci, S. F. (2019). Exploring the crystallinity of different powder sugars through solid echo and magic sandwich echo sequences. *Magnetic Resonance in Chemistry*, (March), 607–615. <https://doi.org/10.1002/mrc.4866>

- Gu, J., Ahn-jarvis, J. H., & Vodovotz, Y. (2015). Development and Characterization of Different Black Raspberry Confection Matrices Designed for Delivery of Phytochemicals, *80*(3). <https://doi.org/10.1111/1750-3841.12808>
- Harnkarnsujarit, N., & Charoenrein, S. (2011). Effect of water activity on sugar crystallization and  $\beta$ -carotene stability of freeze-dried mango powder. *Journal of Food Engineering*, *105*(4), 592–598. <https://doi.org/10.1016/j.jfoodeng.2011.03.026>
- Hartel, R. W., Ergun, R., & Vogel, S. (2011). Phase / State Transitions of Confectionery Sweeteners : Thermodynamic and Kinetic Aspects, *10*, 17–32. <https://doi.org/10.1111/j.1541-4337.2010.00136.x>
- Hartel, R. W., & Shastry, A. V. (2009). Sugar crystallization in food products. *Critical Reviews in Food Science and Nutrition*, (October 2012), 49–112.
- Hashemi, R. H., Bradley, W. G., & Lisanti, C. J. (2010). MRI: The Basics. Philadelphia: Lippincott Williams & Wilkins.
- Huang, M., Kennedy, J. F., Li, B., Xu, X., & Xie, B. J. (2007). Characters of rice starch gel modified by gellan, carrageenan, and glucomannan: A texture profile analysis study. *Carbohydrate Polymers*, *69*(3), 411–418. <https://doi.org/10.1016/j.carbpol.2006.12.025>
- Hwang, L. P., & Freed, J. H. (1975). Dynamic effects of pair correlation functions on spin relaxation by translational diffusion in liquids. *The Journal of Chemical Physics*, *63*(9), 4017–4025. <https://doi.org/10.1063/1.431841>
- Ikeda, S., Furuta, C., Fujita, Y., & Gohtani, S. (2014). Effects of D -psicose on gelatinization and retrogradation of rice flour. *Starch - Stärke*, *66*(9–10), 773–779. <https://doi.org/10.1002/star.201300259>
- Ikeda, S., Gohtani, S., Fukada, K., & Amo, Y. (2011). Dielectric Relaxation and

- Water Activity in Aqueous Solution of D -Psicose, *12*(2), 67–74.
- Ikeda, S. I., Gohtani, S. G., Ukada, K. F., & Mo, Y. A. (2011). Dielectric Relaxation and Water Activity in Aqueous Solution of D -Psicose. *Japan Journal of Food Engineering*, *12*(2), 67–74.
- Ilhan, E. (2019). Formulation and Characterization of Starch and Soy Protein Containing Low Calorie Soft Candy. *Msc Thesis, METU*, (August).
- Ilhan, E., Pocan, P., Ogawa, M., & Oztop, M. H. (2020a). Role of ‘ D-allulose ’ in a starch based composite gel matrix. *Carbohydrate Polymers*, *228*(September 2019), 115373. <https://doi.org/10.1016/j.carbpol.2019.115373>
- Ilhan, E., Pocan, P., Ogawa, M., & Oztop, M. H. (2020b). Role of ‘D-allulose’ in a starch based composite gel matrix. *Carbohydrate Polymers*, *228*, 115373. <https://doi.org/10.1016/j.carbpol.2019.115373>
- Izumori, K. (2006). Izumoring: A strategy for bioproduction of all hexoses. *Journal of Biotechnology*, *124*(4), 717–722. <https://doi.org/10.1016/j.jbiotec.2006.04.016>
- Jiamjariyatam, R. (2017). Influence of gelatin and isomaltulose on gummy jelly properties, *25*(April), 776–783.
- Kamiloglu, S., Pasli, A. A., Ozcelik, B., Van Camp, J., & Capanoglu, E. (2015). Colour retention, anthocyanin stability and antioxidant capacity in black carrot (*Daucus carota*) jams and marmalades: Effect of processing, storage conditions and in vitro gastrointestinal digestion. *Journal of Functional Foods*, *13*(October 2014), 1–10. <https://doi.org/10.1016/j.jff.2014.12.021>
- Kasapis, S., Al-Marhoobi, I. M., Deszczynski, M., Mitchell, J. R., & Abeysekera, R. (2003). Gelatin vs polysaccharide in mixture with sugar. *Biomacromolecules*, *4*(5), 1142–1149. <https://doi.org/10.1021/bm0201237>

- Kavak, D. D., & Akpunar, E. B. (2018). Quality characteristics of Turkish delight (lokum) as influenced by different concentrations of cornelian cherry pulp. *Journal of Food Processing and Preservation*, 42(7).  
<https://doi.org/10.1111/jfpp.13656>
- Kimmich, R., & Anardo, E. (2004). *Field-cycling NMR relaxometry. Progress in Nuclear Magnetic Resonance Spectroscopy* (Vol. 44).  
<https://doi.org/10.1016/j.pnmrs.2004.03.002>
- Kirtil, E., Aydogdu, A., & Oztop, M. H. (2016). Investigation of physical properties and moisture sorption behaviour of different marshmallow formulations. *Acta Horticulturae*, 10(12), 21–27.  
<https://doi.org/10.17660/ActaHortic.2017.1152.33>
- Kirtil, E., Cikrikci, S., McCarthy, M. J., & Oztop, M. H. (2017). Recent advances in time domain NMR & MRI sensors and their food applications. *Current Opinion in Food Science*, 17(August), 9–15.  
<https://doi.org/10.1016/j.cofs.2017.07.005>
- Kirtil, E., Dag, D., Guner, S., Unal, K., & Oztop, M. H. (2017). Dynamics of unloaded and green tea extract loaded lecithin based liposomal dispersions investigated by nuclear magnetic resonance T2 relaxation. *Food Research International*, 99(June), 807–814.  
<https://doi.org/10.1016/j.foodres.2017.06.064>
- Kirtil, E., & Oztop, M. H. (2016). 1H Nuclear Magnetic Resonance Relaxometry and Magnetic Resonance Imaging and Applications in Food Science and Processing. *Food Engineering Reviews*, 8(1), 1–22.  
<https://doi.org/10.1007/s12393-015-9118-y>
- Kirtil, E., Oztop, M. H., Sirijariyawat, A., Ngamchuachit, P., Barrett, D. M., & McCarthy, M. J. (2014). Effect of pectin methyl esterase (PME) and CaCl<sub>2</sub> infusion on the cell integrity of fresh-cut and frozen-thawed mangoes : An

- NMR relaxometry study. *Food Research International*, 66, 409–416.  
<https://doi.org/10.1016/j.foodres.2014.10.006>
- Kirtil, E., Oztop, M. H., Sirijariyawat, A., Ngamchuachit, P., Barrett, D. M., & McCarthy, M. J. (2014). Effect of pectin methyl esterase (PME) and CaCl<sub>2</sub> infusion on the cell integrity of fresh-cut and frozen-thawed mangoes: An NMR relaxometry study. *Food Research International*, 66, 409–416.  
<https://doi.org/10.1016/j.foodres.2014.10.006>
- Knapkiewicz, M., Rachocki, A., Bielejewski, M., & Sebastião, P. J. (2020). NMR studies of molecular ordering and molecular dynamics in a chiral liquid crystal with the SmCa\* phase. *Physical Review E*, 101(5), 52708.  
<https://doi.org/10.1103/PhysRevE.101.052708>
- Kocadağlı, T., & Gökmen, V. (2018). Caramelization in foods: A food quality and safety perspective. *Encyclopedia of Food Chemistry*, 18–29.  
<https://doi.org/10.1016/B978-0-08-100596-5.21630-2>
- Kohli, R. (2012). *Methods for Monitoring and Measuring Cleanliness of Surfaces. Developments in Surface Contamination and Cleaning: Detection, Characterization, and Analysis of Contaminants* (Vol. 4). Elsevier.  
<https://doi.org/10.1016/B978-1-4377-7883-0.00003-1>
- Kowalczuk, J., Rachocki, A., Bielejewski, M., & Tritt-Goc, J. (2016). Effect of gel matrix confinement on the solvent dynamics in supramolecular gels. *Journal of Colloid and Interface Science*, 472, 60–68.  
<https://doi.org/10.1016/j.jcis.2016.03.033>
- Kruk, D., Meier, R., & Rössler, E. A. (2011). Translational and rotational diffusion of glycerol by means of field cycling 1H NMR relaxometry. *Journal of Physical Chemistry B*, 115(5), 951–957. <https://doi.org/10.1021/jp110514r>
- Kruk, D., Meier, R., & Rössler, E. A. (2012). Nuclear magnetic resonance

relaxometry as a method of measuring translational diffusion coefficients in liquids. *Physical Review E - Statistical, Nonlinear, and Soft Matter Physics*, 85(2), 1–5. <https://doi.org/10.1103/PhysRevE.85.020201>

Kruk, Danuta, Florek-Wojciechowska, M., Masiewicz, E., & Oztop, M. H. (2021). Water mobility in cheese by means of Nuclear Magnetic Resonance relaxometry. *Journal of Food Engineering*, 135907. <https://doi.org/10.1016/j.jfoodeng.2021.110483>

Kruk, Danuta, Florek – Wojciechowska, M., Masiewicz, E., Oztop, M., Ploch-Jankowska, A., Duda, P., & Wilczynski, S. (2021). Water mobility in cheese by means of Nuclear Magnetic Resonance relaxometry. *Journal of Food Engineering*, 298(September 2020), 110483. <https://doi.org/10.1016/j.jfoodeng.2021.110483>

Kruk, Danuta, Rochowski, P., Masiewicz, E., Wilczynski, S., Wojciechowski, M., Broche, L. M., & Lurie, D. J. (2019). Mechanism of Water Dynamics in Hyaluronic Dermal Fillers Revealed by Nuclear Magnetic Resonance Relaxometry. *ChemPhysChem*, 20(21), 2816–2822. <https://doi.org/10.1002/cphc.201900761>

Labuza, T., Roe, K., Payne, C., Panda, F., Labuza, T. J., Labuza, P. S., ... Plains, M. (2004). Storage stability of dry food systems: Influence of state changes during drying and storage. *Symposium A Quarterly Journal In Modern Foreign Literatures*, A, 48–68.

Ladd-Parada, M., Povey, M. J., Vieira, J., & Ries, M. E. (2019). Fast field cycling NMR relaxometry studies of molten and cooled cocoa butter. *Molecular Physics*, 117(7–8), 1020–1027. <https://doi.org/10.1080/00268976.2018.1508784>

Ladd Parada, M., Povey, M. J., Vieira, J., Rappolt, M., & Ries, M. E. (2019). Early stages of fat crystallisation evaluated by low-field NMR and small-angle X-

- ray scattering. *Magnetic Resonance in Chemistry*, 57(9), 686–694.  
<https://doi.org/10.1002/mrc.4860>
- Le Botlan, D., Casseron, F., & Lantier, F. (1998). Polymorphism of sugars studied by time domain NMR. *Analisis*, 26(5), 198–204.  
<https://doi.org/10.1051/analisis:1998135>
- Leinen, K. M., & Labuza, T. P. (2006). Crystallization inhibition of an amorphous sucrose system using raffinose. *Journal of Zhejiang University SCIENCE B*, 7(2), 85–89. <https://doi.org/10.1631/jzus.2006.B0085>
- Levin, G. V. (2002). Tagatose, the new GRAS sweetener and health product. *Journal of Medicinal Food*, 5(1), 23–36.  
<https://doi.org/10.1089/109662002753723197>
- Marfil, P. H. M., Anhô, A. C. B. M., & Telis, V. R. N. (2012). Texture and Microstructure of Gelatin/Corn Starch-Based Gummy Confections. *Food Biophysics*, 7(3), 236–243. <https://doi.org/10.1007/s11483-012-9262-3>
- Meier, R., Kruk, D., Gmeiner, J., & Rössler, E. A. (2012). Intermolecular relaxation in glycerol as revealed by field cycling <sup>1</sup>H NMR relaxometry dilution experiments. *Journal of Chemical Physics*, 136(3).  
<https://doi.org/10.1063/1.3672096>
- Meier, Roman, Kruk, D., & Rössler, E. A. (2013). Intermolecular Spin Relaxation and Translation Diffusion in Liquids and Polymer Melts : Insight from Field-Cycling H NMR Relaxometry. *ChemPhysChem*, 14, 3071–3081.  
<https://doi.org/10.1002/cphc.201300257>
- Mills, R. (1973). Self-diffusion in normal and heavy water in the range 1-45°. *Journal of Physical Chemistry*, 77(5), 685–688.  
<https://doi.org/10.1021/j100624a025>
- Mu, W., Zhang, W., Feng, Y., Jiang, B., & Zhou, L. (2012). Recent advances on



applications and biotechnological production of D-psicose. *Applied Microbiology and Biotechnology*, 94(6), 1461–1467.  
<https://doi.org/10.1007/s00253-012-4093-1>

Namli, S., Sumnu, S. G., & Oztop, M. H. (2021). Microwave Glycation of Soy Protein Isolate with Rare Sugar (D-allulose), Fructose and Glucose. *Food Bioscience*, 40(January), 100897. <https://doi.org/10.1016/j.fbio.2021.100897>

Noack, F. (1971). Nuclear Magnetic Relaxation Spectroscopy. In P. Diehl, E. Fluck, & R. Rosfelf (Eds.), *NMR Basic Principles and Progress* (Vol. 3, pp. 83–144). Berlin: Springer-Verlag. [https://doi.org/10.1007/978-3-642-65180-9\\_2](https://doi.org/10.1007/978-3-642-65180-9_2)

O'Charoen, S., Hayakawa, S., Matsumoto, Y., & Ogawa, M. (2014). Effect of d-Psicose Used as Sucrose Replacer on the Characteristics of Meringue. *Journal of Food Science*, 79(12), E2463–E2469. <https://doi.org/10.1111/1750-3841.12699>

O'Charoen, S., Hayakawa, S., & Ogawa, M. (2015). Food properties of egg white protein modified by rare ketohexoses through Maillard reaction. *International Journal of Food Science and Technology*, 50(1), 194–202.  
<https://doi.org/10.1111/ijfs.12607>

Ogrinc, N., Košir, I. J., Spangenberg, J. E., & Kidrič, J. (2003). The application of NMR and MS methods for detection of adulteration of wine, fruit juices, and olive oil. A review. *Analytical and Bioanalytical Chemistry*, 376(4), 424–430.  
<https://doi.org/10.1007/s00216-003-1804-6>

Ok, S. (2017). Detection of olive oil adulteration by low-field NMR relaxometry and UV-Vis spectroscopy upon mixing olive oil with various edible oils. *Grasas y Aceites*, 68(1), 173. <https://doi.org/10.3989/gya.0678161>

Otálora, M. C., de Jesús Barbosa, H., Perilla, J. E., Osorio, C., & Nazareno, M. A.

- (2019). Encapsulated betalains (*Opuntia ficus-indica*) as natural colorants. Case study: Gummy candies. *Lwt*, *103*(September 2018), 222–227. <https://doi.org/10.1016/j.lwt.2018.12.074>
- Ozel, B., Aydin, O., & Oztop, M. H. (2020). In vitro digestion of polysaccharide including whey protein isolate hydrogels. *Carbohydrate Polymers*, *229*(July 2019), 115469. <https://doi.org/10.1016/j.carbpol.2019.115469>
- Ozel, B., Dag, D., Kilercioglu, M., Sumnu, S. G., & Oztop, M. H. (2017). NMR relaxometry as a tool to understand the effect of microwave heating on starch-water interactions and gelatinization behavior. *LWT - Food Science and Technology*, *83*, 10–17. <https://doi.org/10.1016/j.lwt.2017.04.077>
- Ozel, B., Uguz, S. S., Kilercioglu, M., Grunin, L., & Oztop, M. H. (2016a). Effect of different polysaccharides on swelling of composite whey protein hydrogels: A low field (LF) NMR relaxometry study. *Journal of Food Process Engineering*, *40*(3), 1–9. <https://doi.org/10.1111/jfpe.12465>
- Ozel, B., Uguz, S. S., Kilercioglu, M., Grunin, L., & Oztop, M. H. (2016b). Effect of different polysaccharides on swelling of composite whey protein hydrogels: A low field (LF) NMR relaxometry study. *Journal of Food Process Engineering*, (July), 1–9. <https://doi.org/10.1111/jfpe.12465>
- Parker, K., Salas, M., & Nwosu, V. C. (2010). High fructose corn syrup : Production , uses and public health concerns. *Biotechnology and Molecular Biology Review*, *5*(5)(December), 71–78. Retrieved from <http://www.academicjournals.org/journal/BMBR/article-abstract/41CAC0411547>
- Pitombo, R. N. M., & Lima, G. A. M. R. (2003). Nuclear magnetic resonance and water activity in measuring the water mobility in Pintado (*Pseudoplatystoma corruscans*) fish. *Journal of Food Engineering*, *58*(1), 59–66. [https://doi.org/10.1016/S0260-8774\(02\)00334-5](https://doi.org/10.1016/S0260-8774(02)00334-5)

- Płowaś-Korus, I., Masewicz, Ł., Szwengiel, A., Rachocki, A., Baranowska, H. M., & Medycki, W. (2018). A novel method of recognizing liquefied honey. *Food Chemistry*, 245(July 2017), 885–889.  
<https://doi.org/10.1016/j.foodchem.2017.11.087>
- Pocan, P., Ilhan, E., Florek–Wojciechowska, M., Masiewicz, E., Kruk, D., & Oztop, M. H. (2021). Exploring the water mobility in gelatin based soft candies by means of Fast Field Cycling (FFC) Nuclear Magnetic Resonance relaxometry. *Journal of Food Engineering*, 294, 110422.  
<https://doi.org/10.1016/j.jfoodeng.2020.110422>
- Pocan, P., Ilhan, E., & Oztop, M. H. (2019a). Characterization of Emulsion Stabilization Properties of Gum Tragacanth, Xanthan Gum and Sucrose Monopalmitate: A Comparative Study. *Journal of Food Science*, 84(5), 1087–1093. <https://doi.org/10.1111/1750-3841.14602>
- Pocan, P., Ilhan, E., & Oztop, M. H. (2019b). Effect of d-psicose substitution on gelatin based soft candies: A TD-NMR study. *Magnetic Resonance in Chemistry*, 57(9), 661–673. <https://doi.org/10.1002/mrc.4847>
- Pocan, P., Kaya, D., Mert, B., & Oztop, M. H. (2021). Determination of the Best Drying Conditions for Gelatin Based Candies. *Gıda/ The Journal of Food*, 46(2), 279–295. <https://doi.org/10.15237/gida.GD20093>
- Pocan, P., Knapkiewicz, M., Rachocki, A., & Oztop, M. H. (2021). Detection of Authenticity and Quality of the Turkish Delights (Lokum) by Means of Conventional and Fast Field Cycling Nuclear Magnetic Resonance Relaxometry. *Journal of Agricultural and Food Chemistry*.  
<https://doi.org/10.1021/acs.jafc.1c00943>
- Porter, T., & Hartel, R. W. (2013). Quantifying Sucrose Crystal Content in Fondant. *The Manufacturing Confectioner*, (January), 61–64.

- Puangmanee, S., Hayakawa, S., Sun, Y., & Ogawa, M. (2008). Application of Whey Protein Isolate Glycated with Rare Sugars to Ice Cream. *Food Science and Technology Research*, *14*(5), 457–466. <https://doi.org/10.3136/fstr.14.457>
- Qiao, C., Ma, X., Zhang, J., & Yao, J. (2017). Molecular interactions in gelatin / chitosan composite films. *Food Chemistry*, *235*, 45–50. <https://doi.org/10.1016/j.foodchem.2017.05.045>
- Rachocki, A., Latanowicz, L., & Tritt-Goc, J. (2012). Dynamic processes and chemical composition of *Lepidium sativum* seeds determined by means of field-cycling NMR relaxometry and NMR spectroscopy. *Analytical and Bioanalytical Chemistry*, *404*(10), 3155–3164. <https://doi.org/10.1007/s00216-012-6409-5>
- Rachocki, A., & Tritt-Goc, J. (2014). Novel application of NMR relaxometry in studies of diffusion in virgin rape oil. *Food Chemistry*, *152*, 94–99. <https://doi.org/10.1016/j.foodchem.2013.11.112>
- Rachocki, Adam, Andrzejewska, E., Dembna, A., & Tritt-Goc, J. (2015). Translational dynamics of ionic liquid imidazolium cations at solid/liquid interface in gel polymer electrolyte. *European Polymer Journal*, *71*, 210–220. <https://doi.org/10.1016/j.eurpolymj.2015.08.001>
- Ribeiro, R. D. O. R., Mársico, E. T., Carneiro, C. D. S., Monteiro, M. L. G., Júnior, C. C., & Jesus, E. F. O. De. (2014). Detection of honey adulteration of high fructose corn syrup by Low Field Nuclear Magnetic Resonance (LF 1H NMR). *Journal of Food Engineering*, *135*, 39–43. <https://doi.org/10.1016/j.jfoodeng.2014.03.009>
- Roberts, M. W., & Wright, J. T. (2012). Nonnutritive, low caloric substitutes for food sugars: Clinical implications for addressing the incidence of dental caries and overweight/obesity. *International Journal of Dentistry*, *2012*. <https://doi.org/10.1155/2012/625701>

- Robinson, J. W., Frame, E., & Frame, G. M. (1987). *Undergraduate Instrumental Analysis. Analytica Chimica Acta* (7th ed., Vol. 193). Taylor & Francis.  
[https://doi.org/10.1016/s0003-2670\(00\)86198-x](https://doi.org/10.1016/s0003-2670(00)86198-x)
- Rodrigues, E. J. R., Sebastião, P. J. O., & Tavares, M. I. B. (2017). 1H time domain NMR real time monitoring of polyacrylamide hydrogels synthesis. *Polymer Testing*, *60*, 396–404. <https://doi.org/10.1016/j.polymertesting.2017.04.028>
- Roos, Y. H., Franks, F., Karel, M., Labuza, T. P., Levine, H., Mathlouthi, M., ... Slade, L. (2012). Comment on the melting and decomposition of sugars. *Journal of Agricultural and Food Chemistry*, *60*(41), 10359–10362.  
<https://doi.org/10.1021/jf3002526>
- Roos, Y. H., Karel, M., Labuza, T. P., Levine, H., Mathlouthi, M., Reid, D., ... Slade, L. (2013). Melting and crystallization of sugars in high-solids systems. *Journal of Agricultural and Food Chemistry*, *61*(13), 3167–3178.  
<https://doi.org/10.1021/jf305419y>
- Sahin, S., & Sumnu, S. G. (2006). *Physical Properties of Foods*. (D. R. Heldman, Ed.) (1st ed.). New York: Springer.
- Santos, P. M., Pereira-Filho, E. R., & Colnago, L. A. (2016). Detection and quantification of milk adulteration using time domain nuclear magnetic resonance (TD-NMR). *Microchemical Journal*, *124*, 15–19.  
<https://doi.org/10.1016/j.microc.2015.07.013>
- Shi, C., Tao, F., & Cui, Y. (2017). New starch ester/gelatin based films: Developed and physicochemical characterization. *International Journal of Biological Macromolecules*. <https://doi.org/10.1016/j.ijbiomac.2017.11.073>
- Siegwein, A. M., Vodovotz, Y., & Fisher, E. L. (2011). Concentration of Soy Protein Isolate Affects Starch-Based Confections' Texture, Sensory, and Storage Properties. *Journal of Food Science*, *76*(6), 422–428.

<https://doi.org/10.1111/j.1750-3841.2011.02241.x>

Slavutsky, A. M., & Bertuzzi, M. A. (2019). Formulation and characterization of hydrogel based on pectin and brea gum. *International Journal of Biological Macromolecules*, *123*, 784–791.

<https://doi.org/10.1016/j.ijbiomac.2018.11.038>

Sow, L. C., Nicole Chong, J. M., Liao, Q. X., & Yang, H. (2018). Effects of  $\kappa$ -carrageenan on the structure and rheological properties of fish gelatin. *Journal of Food Engineering*, *239*(April), 92–103.

<https://doi.org/10.1016/j.jfoodeng.2018.05.035>

Steele, R. M., Korb, J. P., Ferrante, G., & Bubici, S. (2016). New applications and perspectives of fast field cycling NMR relaxometry. *Magnetic Resonance in Chemistry*, *54*(6), 502–509. <https://doi.org/10.1002/mrc.4220>

Stokes, J. R. (2012). Food Biopolymer Gels, Microgel and Nanogel Structures, Formation and Rheology. *Food Materials Science and Engineering*, 151–176. <https://doi.org/10.1002/9781118373903.ch6>

Su, K., Festring, D., Ayed, C., Yang, Q., Sturrock, C. J., Linforth, R., ... Fisk, I. (2021). Reducing sugar and aroma in a confectionery gel without compromising flavour through addition of air inclusions. *Food Chemistry*, *354*(March), 129579. <https://doi.org/10.1016/j.foodchem.2021.129579>

Sun, Y., Hayakawa, S., Ogawa, M., Fukada, K., & Izumori, K. (2008). Influence of a rare sugar, D-Psicose, on the physicochemical and functional properties of an aerated food system containing egg albumen. *Journal of Agricultural and Food Chemistry*, *56*(12), 4789–4796. <https://doi.org/10.1021/jf800050d>

Sun, Y., Hayakawa, S., Ogawa, M., & Izumori, K. (2007). Antioxidant properties of custard pudding dessert containing rare hexose, d-psicose. *Food Control*, *18*(3), 220–227. <https://doi.org/10.1016/j.foodcont.2005.09.019>

- Sun, Y., Hayakawa, S., Puangmanee, S., & Izumori, K. (2006). Chemical properties and antioxidative activity of glycated  $\alpha$ -lactalbumin with a rare sugar, D-allose, by Maillard reaction. *Food Chemistry*, *95*(3), 509–517. <https://doi.org/10.1016/j.foodchem.2005.01.033>
- Tan, J. M., & Lim, M. H. (2008). Effects of gelatine type and concentration on the shelf-life stability and quality of marshmallows. *International Journal of Food Science and Technology*, *43*(9), 1699–1704. <https://doi.org/10.1111/j.1365-2621.2008.01756.x>
- Tian, Y., Li, Y., Xu, X., & Jin, Z. (2011). Starch retrogradation studied by thermogravimetric analysis (TGA). *Carbohydrate Polymers*, *84*(3), 1165–1168. <https://doi.org/10.1016/j.carbpol.2011.01.006>
- Tomaszewska-Gras, J., Cais-Sokolińska, D., Bierzuńska, P., Kaczyński, Ł. K., Walkowiak, K., & Baranowska, H. M. (2019). Behaviour of water in different types of goats' cheese. *International Dairy Journal*, *95*, 18–24. <https://doi.org/10.1016/j.idairyj.2019.02.015>
- Torrey, H. C. (1953). Nuclear spin relaxation by translational diffusion. *Physical Review*, *92*(4), 962–969. <https://doi.org/10.1103/PhysRev.92.962>
- Uguz, S. S., Ozvural, E. B., Beira, M. J., Oztop, M. H., & Sebastião, P. J. (2019). Use of NMR Relaxometry to identify frankfurters of different meat sources. *Molecular Physics*, *117*(7–8), 1015–1019. <https://doi.org/10.1080/00268976.2018.1542162>
- Uslu, Erbas, Turhan, T. (2010). Effects of Starch Ratios and Soapwort Extract Addition on some Properties of Turkish delight (Turkish with English Abstract). *Gida/The Journal of Food*, *35*(5), 331–337.
- Wang, R., & Hartel, R. W. (2020). Effects of moisture content and saccharide distribution on the stickiness of syrups. *Journal of Food Engineering*,

284(March), 110067. <https://doi.org/10.1016/j.jfoodeng.2020.110067>

Wu, Y., Huang, W., Cui, T., & Fan, F. (2020). Crystallization and strength analysis of amorphous maltose and maltose/whey protein isolate mixtures. *Journal of the Science of Food and Agriculture*, (October).

<https://doi.org/10.1002/jsfa.10881>

Yildiz, E., Guner, S., Sumnu, G., Sahin, S., & Oztop, M. H. (2018). Monitoring the Effects of Ingredients and Baking Methods on Quality of Gluten-Free Cakes by Time Domain ( TD ) NMR Relaxometry. *Fabt*, *11*, 1923–1933.

Zavala, L., Roberti, P., Piermaria, J. A., & Abraham, A. G. (2015). Gelling ability of kefir in the presence of sucrose and fructose and physicochemical characterization of the resulting cryogels. *Journal of Food Science and Technology*, *52*(8), 5039–5047. <https://doi.org/10.1007/s13197-014-1577-2>

Zia, M. Bin, Namli, S., & Oztop, M. H. (2021). Physicochemical properties of wet-glycated soy proteins. *Lwt*, *142*(August 2020), 110981.

<https://doi.org/10.1016/j.lwt.2021.110981>

Ziegler, G. R., MacMillan, B., & Balcom, B. J. (2003). Moisture migration in starch molding operations as observed by magnetic resonance imaging. *Food Research International*, *36*(4), 331–340. [https://doi.org/10.1016/S0963-9969\(02\)00224-7](https://doi.org/10.1016/S0963-9969(02)00224-7)



## APPENDICES

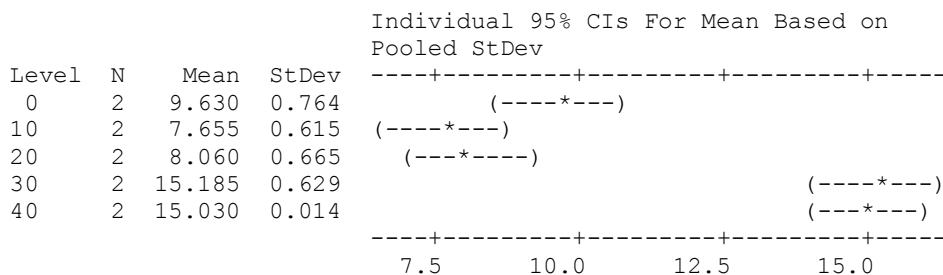
### A. Statistical Analysis Results for the Gelatin Based Confectionery Gels (Formulation & Storage Experiments)

**Table A.1.** Effect of D-Allulose Substitution on the Gelatin Based Confectionery Gels for each storage day. 1) Moisture Content (MC %), 2) Water Activity (aw), 3) Color (L, a, b), 4) Hardness, 5) T<sub>1</sub>, 6) T<sub>2</sub> Spectra, 7) Glass Transition Temperature (T<sub>g</sub>) for **Day 0**.

#### 1) One-way ANOVA: MC (%) versus D-Allulose

Source	DF	SS	MS	F	P
D-Allulose	4	110.804	27.701	76.96	0.000
Error	5	1.800	0.360		
Total	9	112.604			

S = 0.5999    R-Sq = 98.40%    R-Sq(adj) = 97.12%



Pooled StDev = 0.600

Grouping Information Using Tukey Method

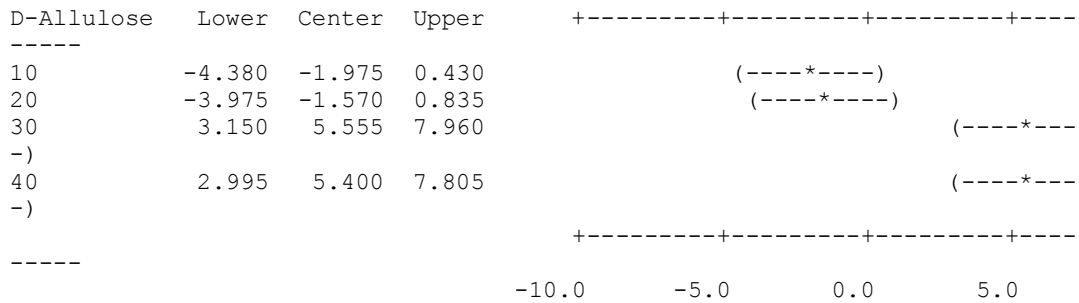
D-Allulose	N	Mean	Grouping
30	2	15.185	A
40	2	15.030	A
0	2	9.630	B
20	2	8.060	B
10	2	7.655	B

Means that do not share a letter are significantly different.

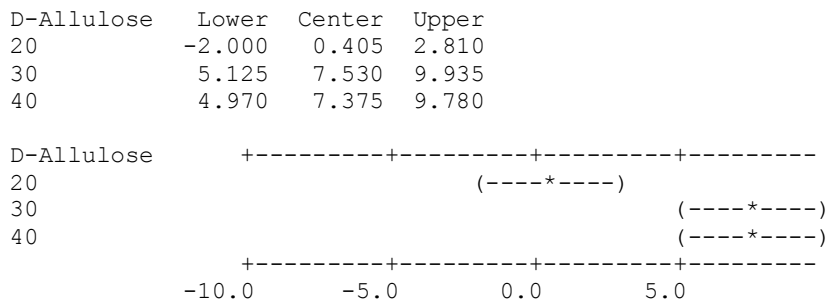
Tukey 95% Simultaneous Confidence Intervals  
All Pairwise Comparisons among Levels of D-Allulose

Individual confidence level = 98.98%

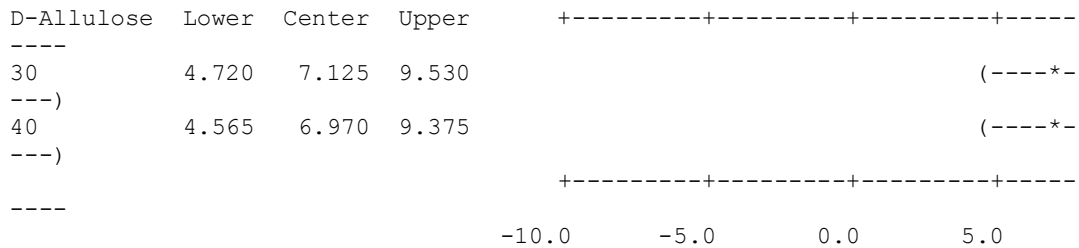
D-Allulose = 0 subtracted from:



D-Allulose = 10 subtracted from:

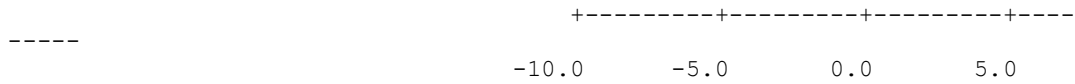


D-Allulose = 20 subtracted from:



D-Allulose = 30 subtracted from:

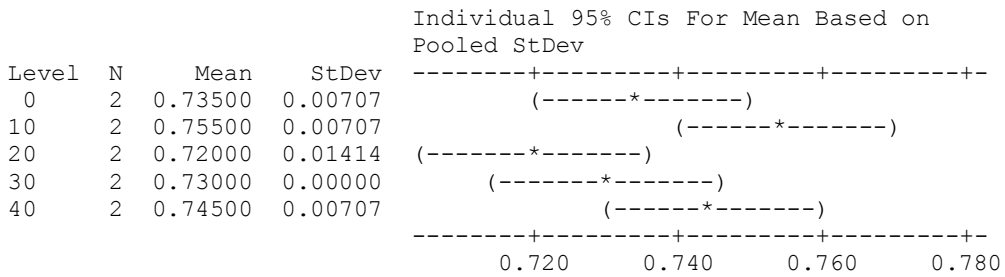




**2) One-way ANOVA: aw versus D-Allulose**

Source	DF	SS	MS	F	P
D-Allulose	4	0.0014600	0.0003650	5.21	0.050
Error	5	0.0003500	0.0000700		
Total	9	0.0018100			

S = 0.008367 R-Sq = 80.66% R-Sq(adj) = 65.19%



Pooled StDev = 0.00837

Grouping Information Using Tukey Method

D-Allulose	N	Mean	Grouping
10	2	0.755000	A
40	2	0.745000	A B
0	2	0.735000	A B
30	2	0.730000	A B
20	2	0.720000	B

Means that do not share a letter are significantly different.

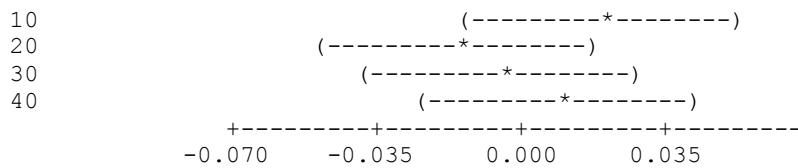
Tukey 95% Simultaneous Confidence Intervals  
All Pairwise Comparisons among Levels of D-Allulose

Individual confidence level = 98.98%

D-Allulose = 0 subtracted from:

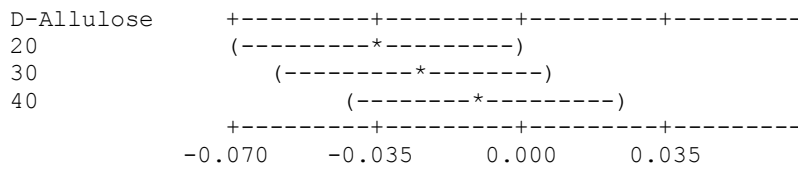
D-Allulose	Lower	Center	Upper
10	-0.013544	0.020000	0.053544
20	-0.048544	-0.015000	0.018544
30	-0.038544	-0.005000	0.028544
40	-0.023544	0.010000	0.043544

D-Allulose +-----+-----+-----+-----



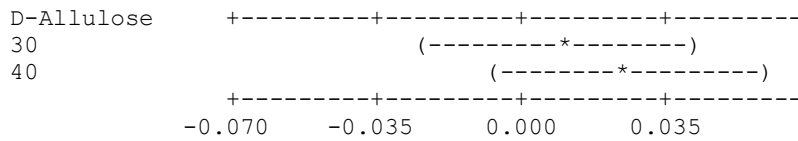
D-Allulose = 10 subtracted from:

D-Allulose	Lower	Center	Upper
20	-0.068544	-0.035000	-0.001456
30	-0.058544	-0.025000	0.008544
40	-0.043544	-0.010000	0.023544



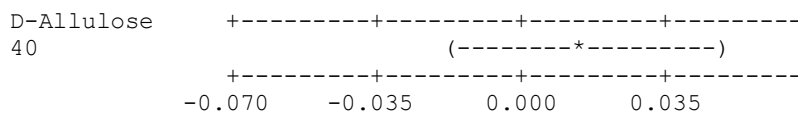
D-Allulose = 20 subtracted from:

D-Allulose	Lower	Center	Upper
30	-0.023544	0.010000	0.043544
40	-0.008544	0.025000	0.058544



D-Allulose = 30 subtracted from:

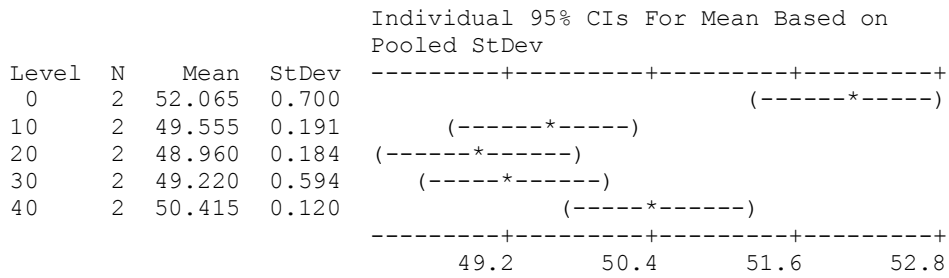
D-Allulose	Lower	Center	Upper
40	-0.018544	0.015000	0.048544



### 3) One-way ANOVA: L versus D-Allulose

Source	DF	SS	MS	F	P
D-Allulose	4	12.630	3.158	17.02	0.004
Error	5	0.928	0.186		
Total	9	13.558			

S = 0.4307    R-Sq = 93.16%    R-Sq(adj) = 87.69%



Pooled StDev = 0.431

Grouping Information Using Tukey Method

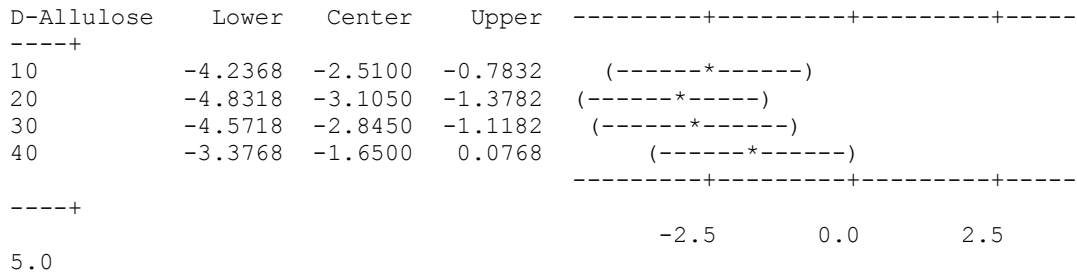
D-Allulose	N	Mean	Grouping
0	2	52.0650	A
40	2	50.4150	A B
10	2	49.5550	B
30	2	49.2200	B
20	2	48.9600	B

Means that do not share a letter are significantly different.

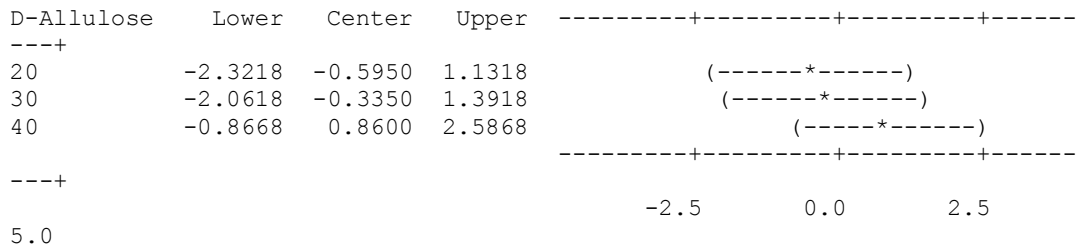
Tukey 95% Simultaneous Confidence Intervals  
All Pairwise Comparisons among Levels of D-Allulose

Individual confidence level = 98.98%

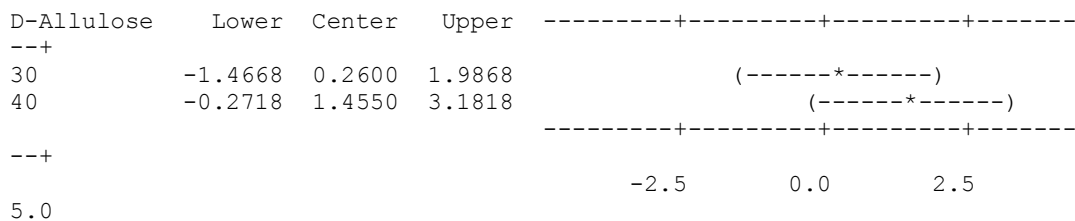
D-Allulose = 0 subtracted from:



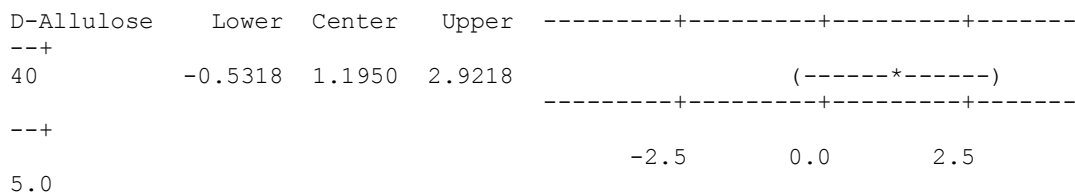
D-Allulose = 10 subtracted from:



D-Allulose = 20 subtracted from:



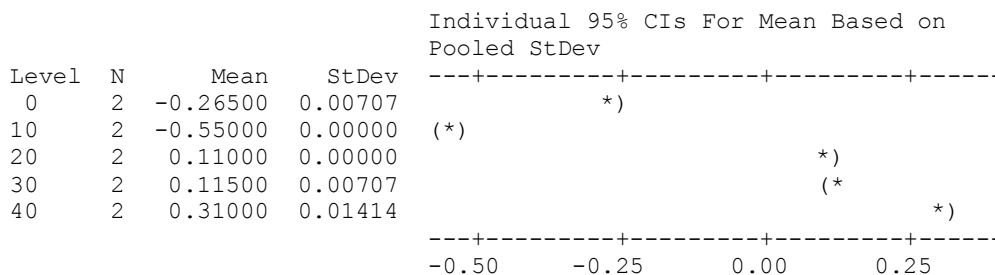
D-Allulose = 30 subtracted from:



### One-way ANOVA: a versus D-Allulose

Source	DF	SS	MS	F	P
D-Allulose	4	0.9569400	0.2392350	3987.25	0.000
Error	5	0.0003000	0.0000600		
Total	9	0.9572400			

S = 0.007746 R-Sq = 99.97% R-Sq(adj) = 99.94%



Pooled StDev = 0.00775

### Grouping Information Using Tukey Method

D-Allulose	N	Mean	Grouping
40	2	0.31000	A
30	2	0.11500	B
20	2	0.11000	B
0	2	-0.26500	C
10	2	-0.55000	D

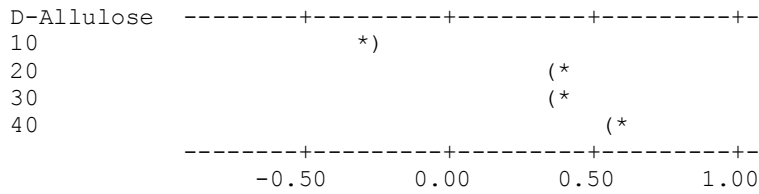
Means that do not share a letter are significantly different.

Tukey 95% Simultaneous Confidence Intervals  
All Pairwise Comparisons among Levels of D-Allulose

Individual confidence level = 98.98%

D-Allulose = 0 subtracted from:

D-Allulose	Lower	Center	Upper
10	-0.31606	-0.28500	-0.25394
20	0.34394	0.37500	0.40606
30	0.34894	0.38000	0.41106
40	0.54394	0.57500	0.60606



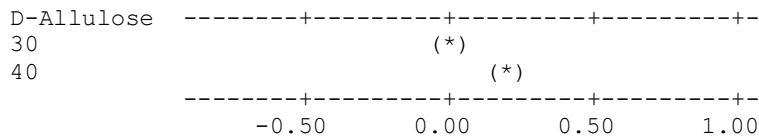
D-Allulose = 10 subtracted from:

D-Allulose	Lower	Center	Upper
20	0.62894	0.66000	0.69106
30	0.63394	0.66500	0.69606
40	0.82894	0.86000	0.89106



D-Allulose = 20 subtracted from:

D-Allulose	Lower	Center	Upper
30	-0.02606	0.00500	0.03606
40	0.16894	0.20000	0.23106



D-Allulose = 30 subtracted from:

D-Allulose	Lower	Center	Upper
40	0.16394	0.19500	0.22606

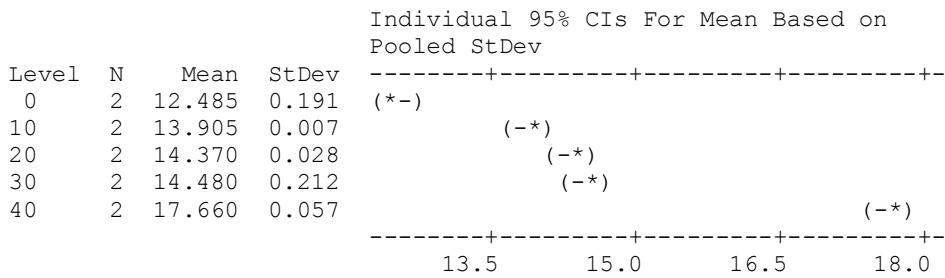




**One-way ANOVA: b versus D-Allulose**

Source	DF	SS	MS	F	P
D-Allulose	4	28.7703	7.1926	420.62	0.000
Error	5	0.0855	0.0171		
Total	9	28.8558			

S = 0.1308    R-Sq = 99.70%    R-Sq(adj) = 99.47%



Pooled StDev = 0.131

Grouping Information Using Tukey Method

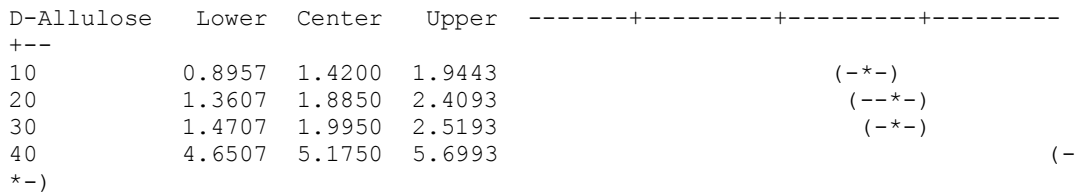
D-Allulose	N	Mean	Grouping
40	2	17.6600	A
30	2	14.4800	B
20	2	14.3700	B C
10	2	13.9050	C
0	2	12.4850	D

Means that do not share a letter are significantly different.

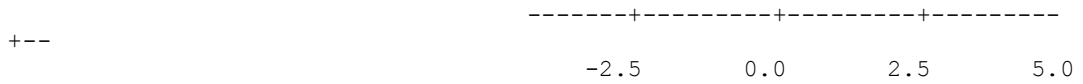
Tukey 95% Simultaneous Confidence Intervals  
All Pairwise Comparisons among Levels of D-Allulose

Individual confidence level = 98.98%

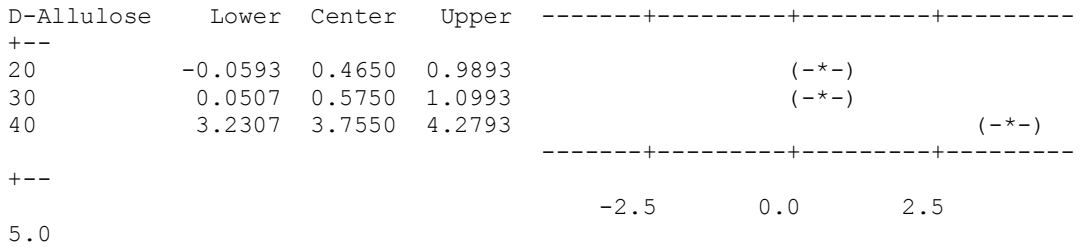
D-Allulose = 0 subtracted from:



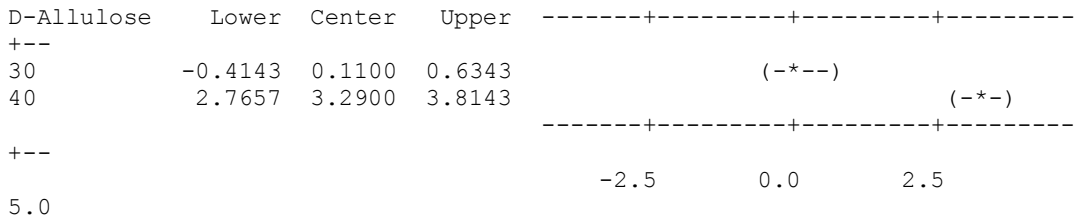




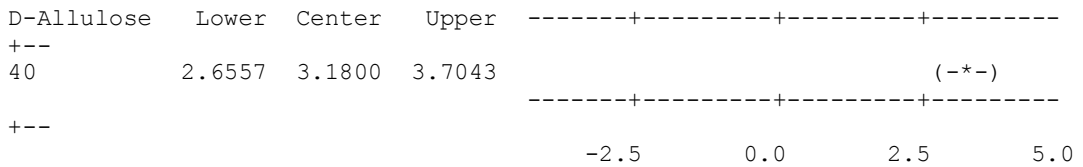
D-Allulose = 10 subtracted from:



D-Allulose = 20 subtracted from:



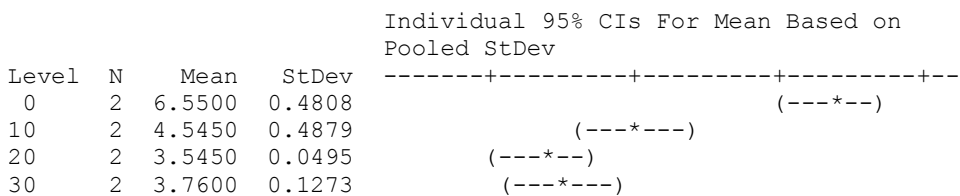
D-Allulose = 30 subtracted from:



#### 4) One-way ANOVA: hardness versus D-Allulose

Source	DF	SS	MS	F	P
D-Allulose	4	18.1705	4.5426	46.08	0.000
Error	5	0.4929	0.0986		
Total	9	18.6634			

S = 0.3140    R-Sq = 97.36%    R-Sq(adj) = 95.25%



```

40      2  2.5200  0.0707  (---*---)
-----+-----+-----+-----+
          3.0      4.5      6.0      7.5

```

Pooled StDev = 0.3140

Grouping Information Using Tukey Method

D-Allulose	N	Mean	Grouping
0	2	6.5500	A
10	2	4.5450	B
30	2	3.7600	B C
20	2	3.5450	B C
40	2	2.5200	C

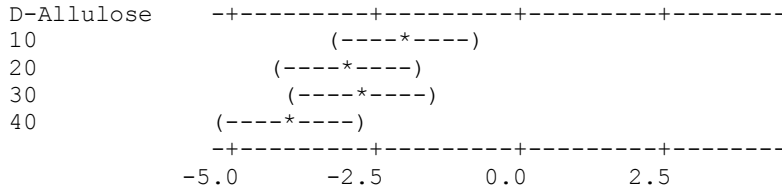
Means that do not share a letter are significantly different.

Tukey 95% Simultaneous Confidence Intervals  
All Pairwise Comparisons among Levels of D-Allulose

Individual confidence level = 98.98%

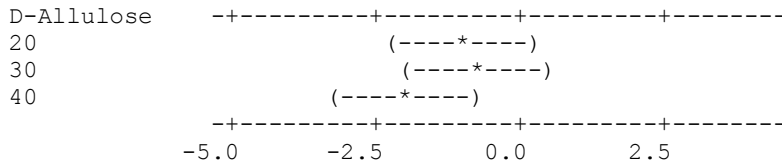
D-Allulose = 0 subtracted from:

D-Allulose	Lower	Center	Upper
10	-3.2638	-2.0050	-0.7462
20	-4.2638	-3.0050	-1.7462
30	-4.0488	-2.7900	-1.5312
40	-5.2888	-4.0300	-2.7712



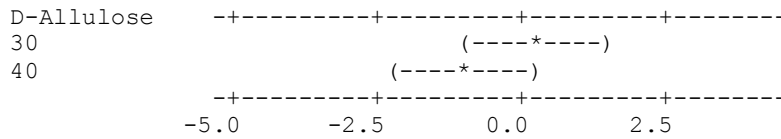
D-Allulose = 10 subtracted from:

D-Allulose	Lower	Center	Upper
20	-2.2588	-1.0000	0.2588
30	-2.0438	-0.7850	0.4738
40	-3.2838	-2.0250	-0.7662



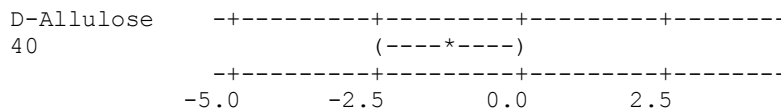
D-Allulose = 20 subtracted from:

D-Allulose	Lower	Center	Upper
30	-1.0438	0.2150	1.4738
40	-2.2838	-1.0250	0.2338



D-Allulose = 30 subtracted from:

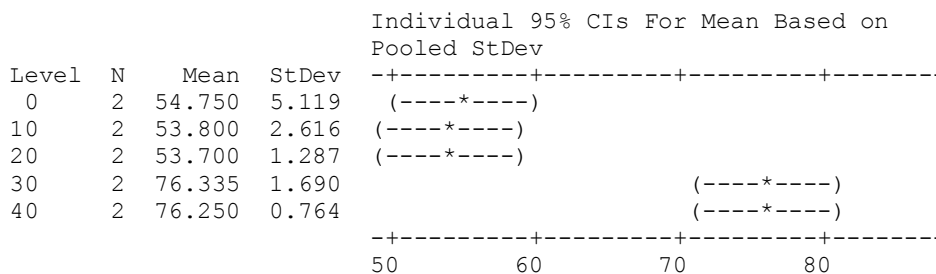
D-Allulose	Lower	Center	Upper
40	-2.4988	-1.2400	0.0188



### 5) One-way ANOVA: T1 versus D-Allulose

Source	DF	SS	MS	F	P
D-Allulose	4	1185.14	296.29	38.83	0.001
Error	5	38.15	7.63		
Total	9	1223.29			

S = 2.762    R-Sq = 96.88%    R-Sq(adj) = 94.39%



Pooled StDev = 2.762

Grouping Information Using Tukey Method

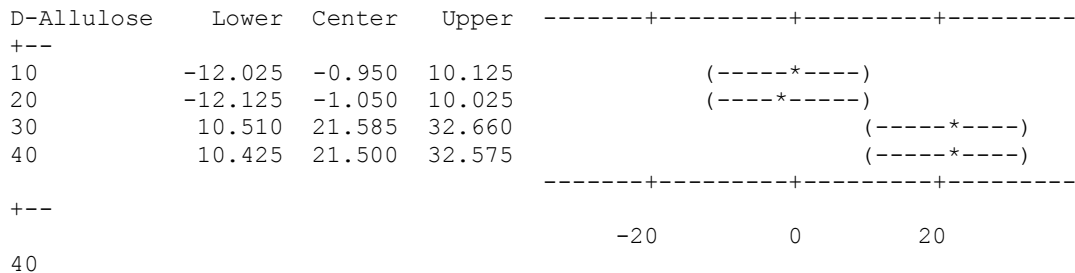
D-Allulose	N	Mean	Grouping
30	2	76.335	A
40	2	76.250	A
0	2	54.750	B
10	2	53.800	B
20	2	53.700	B

Means that do not share a letter are significantly different.

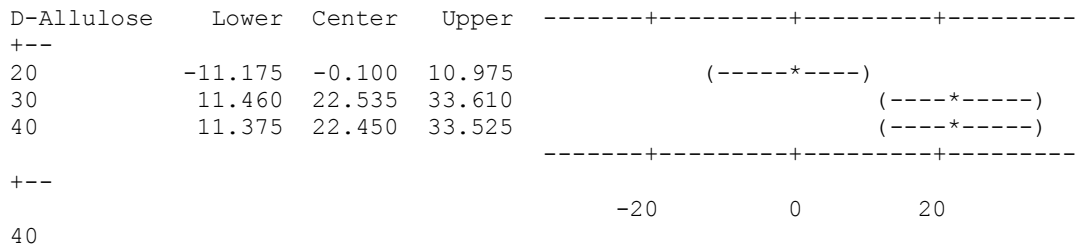
Tukey 95% Simultaneous Confidence Intervals  
 All Pairwise Comparisons among Levels of D-Allulose

Individual confidence level = 98.98%

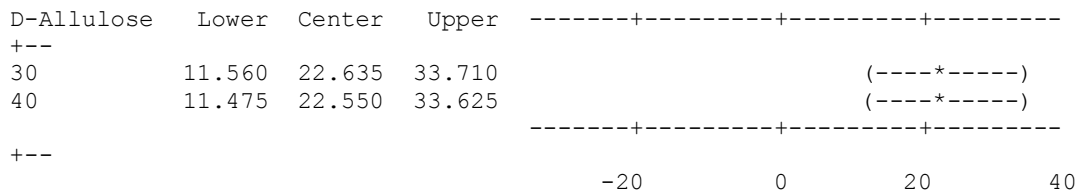
D-Allulose = 0 subtracted from:



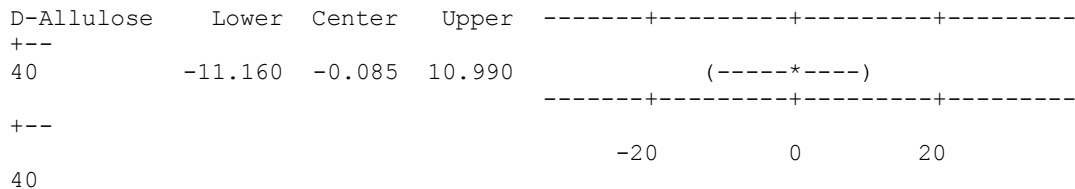
D-Allulose = 10 subtracted from:



D-Allulose = 20 subtracted from:



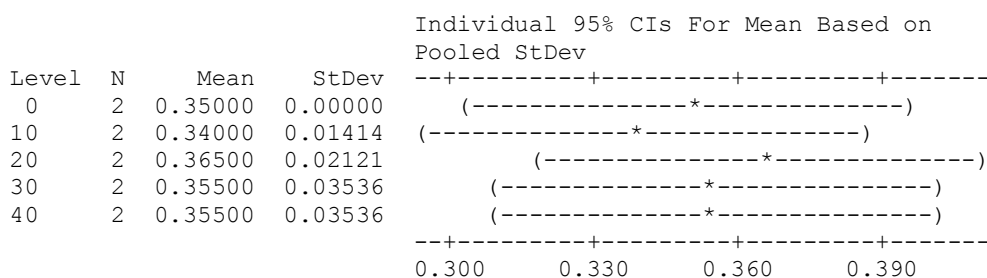
D-Allulose = 30 subtracted from:



**6) One-way ANOVA: T2 peak1 (ms) versus D-Allulose**

Source	DF	SS	MS	F	P
D-Allulose	4	0.000660	0.000165	0.26	0.891
Error	5	0.003150	0.000630		
Total	9	0.003810			

S = 0.02510 R-Sq = 17.32% R-Sq(adj) = 0.00%



Pooled StDev = 0.02510

Grouping Information Using Tukey Method

D-Allulose	N	Mean	Grouping
20	2	0.36500	A
40	2	0.35500	A
30	2	0.35500	A
0	2	0.35000	A
10	2	0.34000	A

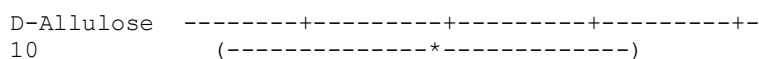
Means that do not share a letter are significantly different.

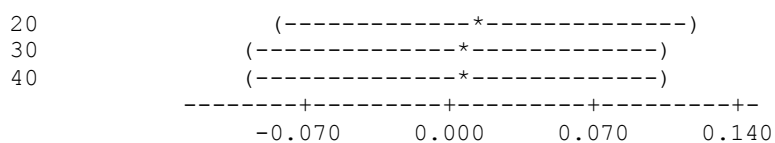
Tukey 95% Simultaneous Confidence Intervals  
All Pairwise Comparisons among Levels of D-Allulose

Individual confidence level = 98.98%

D-Allulose = 0 subtracted from:

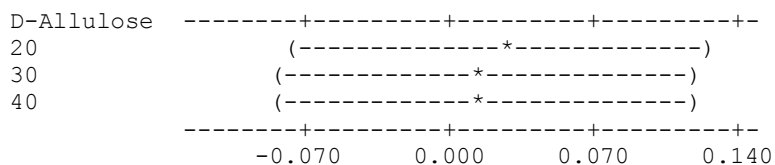
D-Allulose	Lower	Center	Upper
10	-0.11063	-0.01000	0.09063
20	-0.08563	0.01500	0.11563
30	-0.09563	0.00500	0.10563
40	-0.09563	0.00500	0.10563





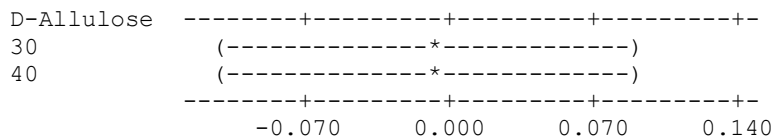
D-Allulose = 10 subtracted from:

D-Allulose	Lower	Center	Upper
20	-0.07563	0.02500	0.12563
30	-0.08563	0.01500	0.11563
40	-0.08563	0.01500	0.11563



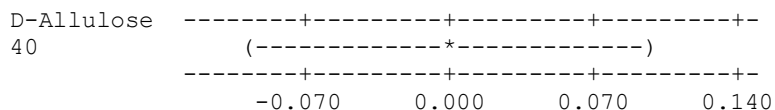
D-Allulose = 20 subtracted from:

D-Allulose	Lower	Center	Upper
30	-0.11063	-0.01000	0.09063
40	-0.11063	-0.01000	0.09063



D-Allulose = 30 subtracted from:

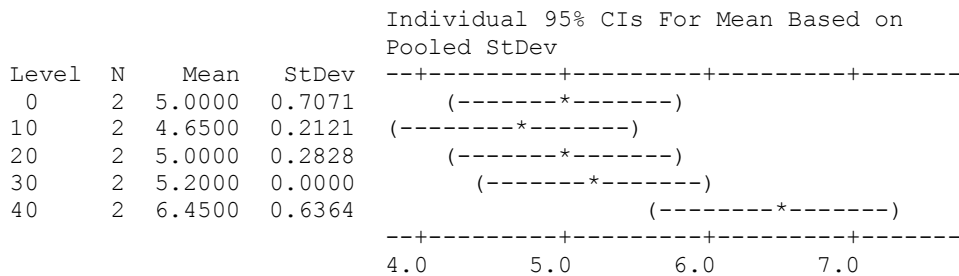
D-Allulose	Lower	Center	Upper
40	-0.10063	0.00000	0.10063



### One-way ANOVA: T2 peak 2 (ms) versus D-Allulose

Source	DF	SS	MS	F	P
D-Allulose	4	3.854	0.964	4.68	0.061
Error	5	1.030	0.206		
Total	9	4.884			

S = 0.4539    R-Sq = 78.91%    R-Sq(adj) = 62.04%



Pooled StDev = 0.4539

Grouping Information Using Tukey Method

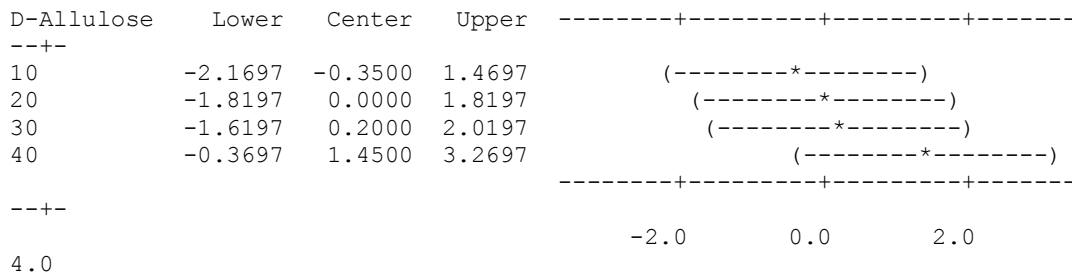
D-Allulose	N	Mean	Grouping
40	2	6.4500	A
30	2	5.2000	A
20	2	5.0000	A
0	2	5.0000	A
10	2	4.6500	A

Means that do not share a letter are significantly different.

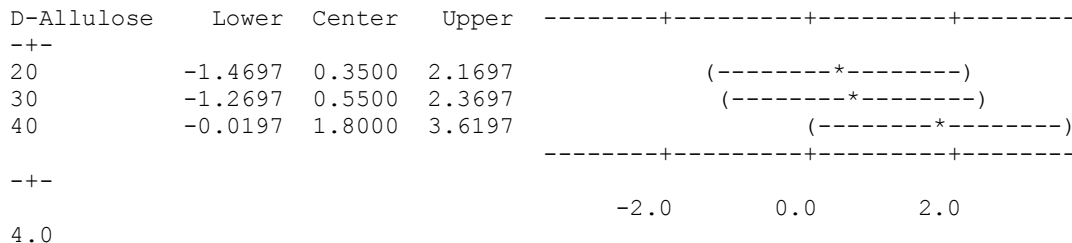
Tukey 95% Simultaneous Confidence Intervals  
All Pairwise Comparisons among Levels of D-Allulose

Individual confidence level = 98.98%

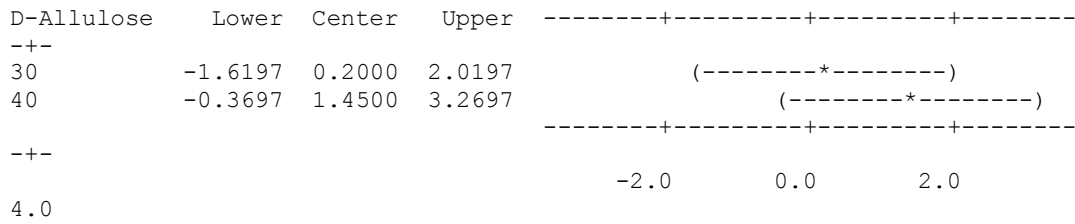
D-Allulose = 0 subtracted from:



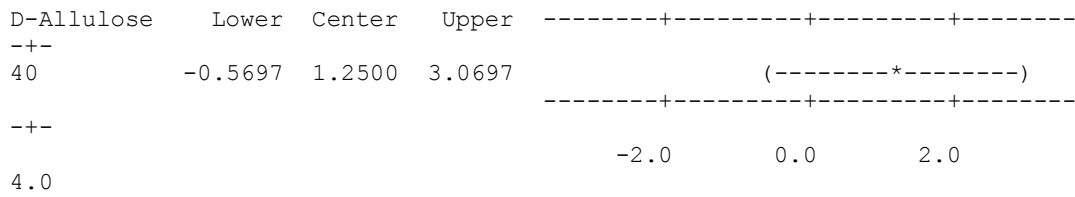
D-Allulose = 10 subtracted from:



D-Allulose = 20 subtracted from:



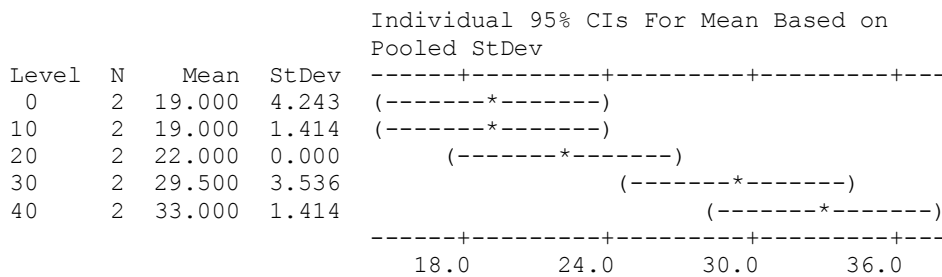
D-Allulose = 30 subtracted from:



### One-way ANOVA: T2 peak 3 (ms) versus D-Allulose

Source	DF	SS	MS	F	P
D-Allulose	4	328.00	82.00	11.88	0.009
Error	5	34.50	6.90		
Total	9	362.50			

S = 2.627 R-Sq = 90.48% R-Sq(adj) = 82.87%



Pooled StDev = 2.627

### Grouping Information Using Tukey Method

D-Allulose	N	Mean	Grouping
40	2	33.000	A
30	2	29.500	A B
20	2	22.000	B
10	2	19.000	B



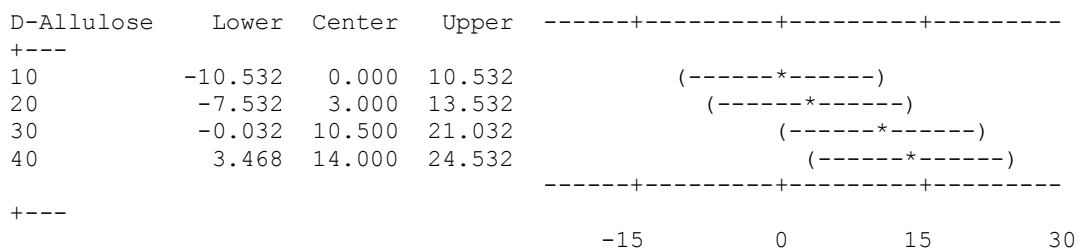
0            2   19.000    B

Means that do not share a letter are significantly different.

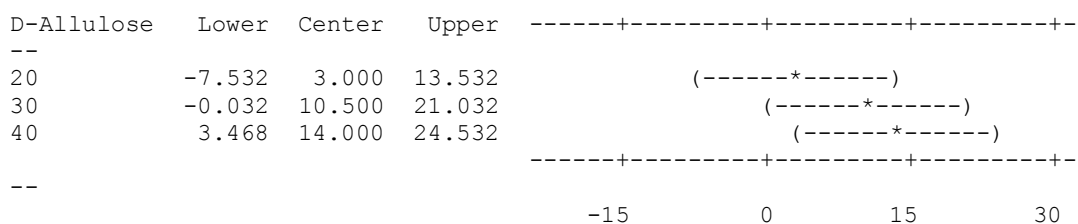
Tukey 95% Simultaneous Confidence Intervals  
All Pairwise Comparisons among Levels of D-Allulose

Individual confidence level = 98.98%

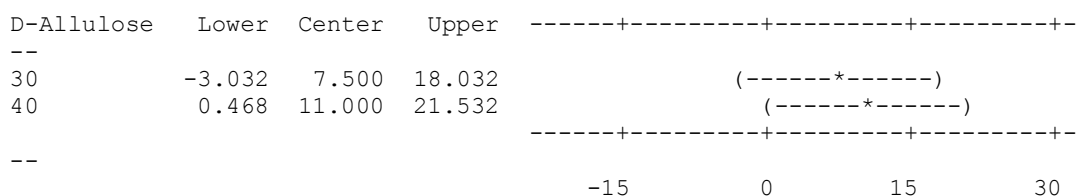
D-Allulose = 0 subtracted from:



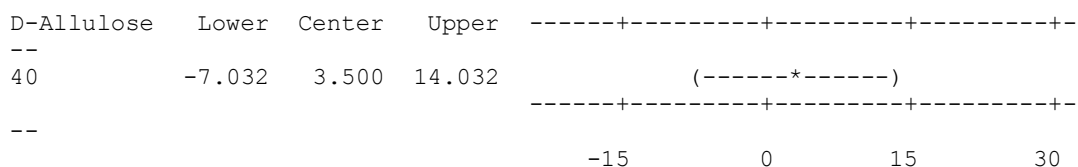
D-Allulose = 10 subtracted from:



D-Allulose = 20 subtracted from:



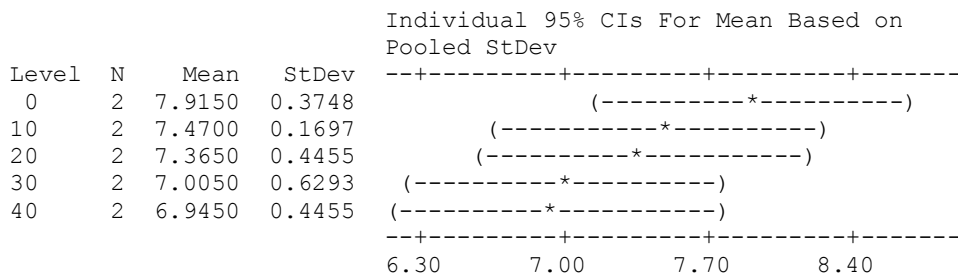
D-Allulose = 30 subtracted from:



**One-way ANOVA: RA1 (%) versus D-Allulose**

Source	DF	SS	MS	F	P
D-Allulose	4	1.233	0.308	1.60	0.306
Error	5	0.962	0.192		
Total	9	2.195			

S = 0.4387 R-Sq = 56.16% R-Sq(adj) = 21.10%



Pooled StDev = 0.4387

Grouping Information Using Tukey Method

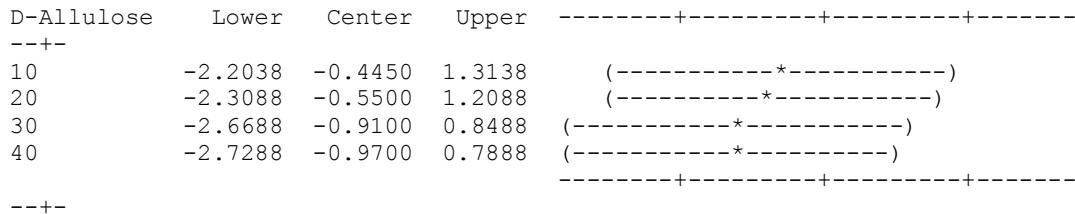
D-Allulose	N	Mean	Grouping
0	2	7.9150	A
10	2	7.4700	A
20	2	7.3650	A
30	2	7.0050	A
40	2	6.9450	A

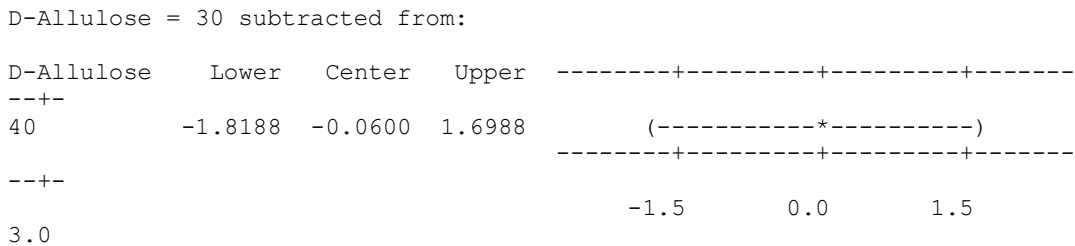
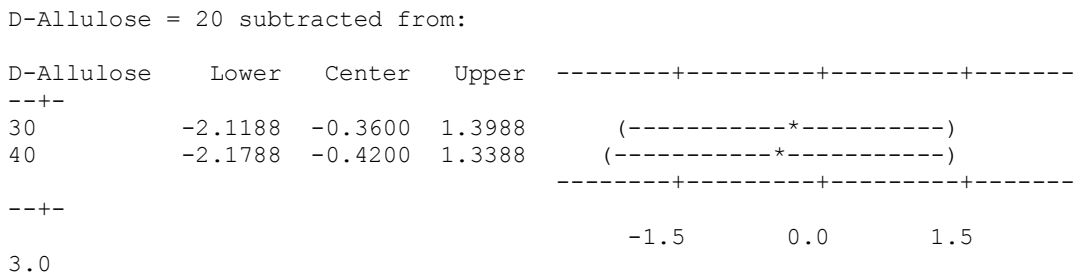
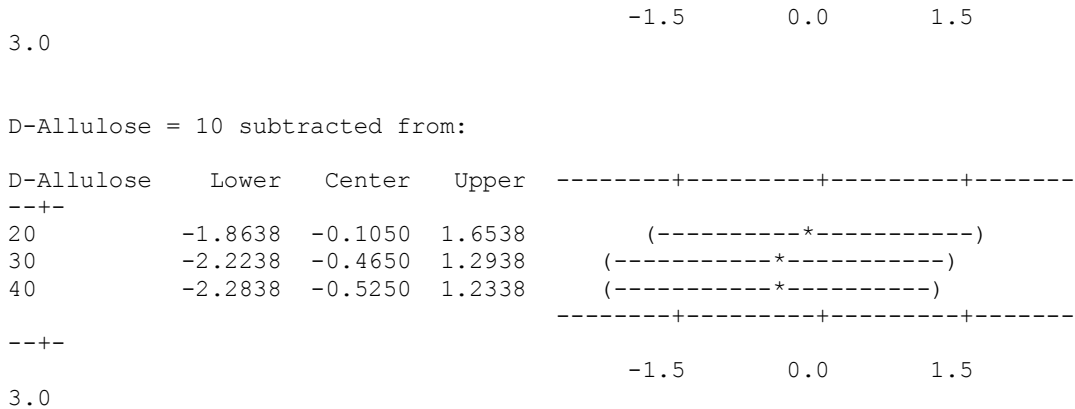
Means that do not share a letter are significantly different.

Tukey 95% Simultaneous Confidence Intervals  
All Pairwise Comparisons among Levels of D-Allulose

Individual confidence level = 98.98%

D-Allulose = 0 subtracted from:





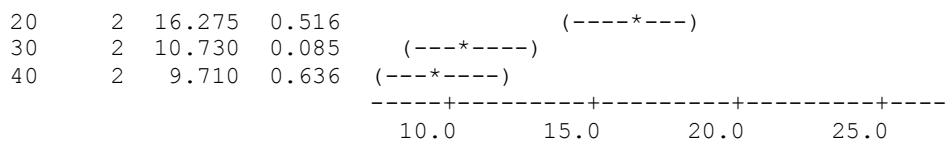
### One-way ANOVA: RA2(%) versus D-Allulose

Source	DF	SS	MS	F	P
D-Allulose	4	213.92	53.48	33.45	0.001
Error	5	7.99	1.60		
Total	9	221.91			

S = 1.265    R-Sq = 96.40%    R-Sq(adj) = 93.52%

Individual 95% CIs For Mean Based on Pooled StDev

Level	N	Mean	StDev
0	2	22.180	2.701
10	2	17.860	0.141



Pooled StDev = 1.265

Grouping Information Using Tukey Method

D-Allulose	N	Mean	Grouping
0	2	22.180	A
10	2	17.860	A B
20	2	16.275	B
30	2	10.730	C
40	2	9.710	C

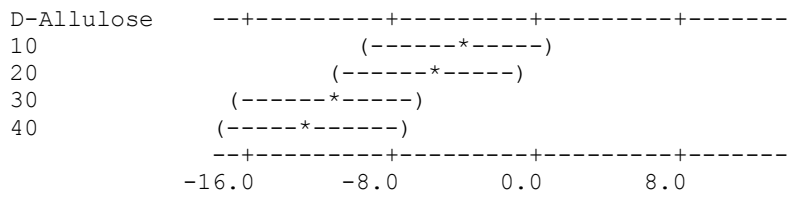
Means that do not share a letter are significantly different.

Tukey 95% Simultaneous Confidence Intervals  
All Pairwise Comparisons among Levels of D-Allulose

Individual confidence level = 98.98%

D-Allulose = 0 subtracted from:

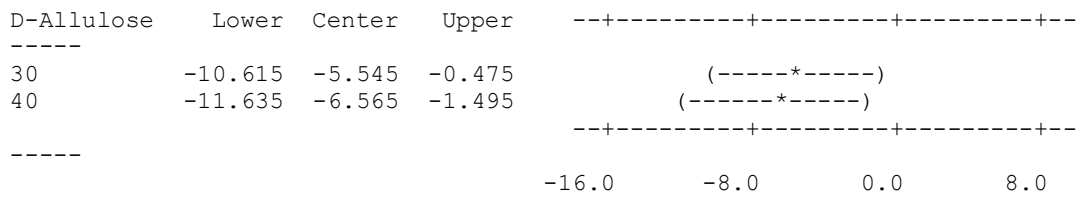
D-Allulose	Lower	Center	Upper
10	-9.390	-4.320	0.750
20	-10.975	-5.905	-0.835
30	-16.520	-11.450	-6.380
40	-17.540	-12.470	-7.400



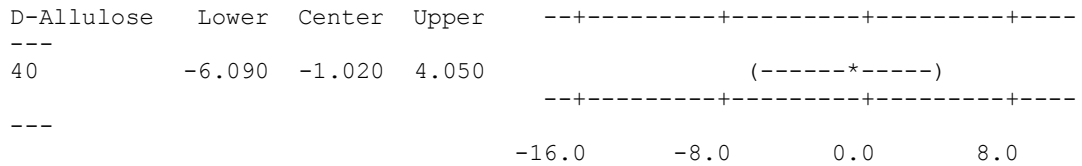
D-Allulose = 10 subtracted from:

D-Allulose	Lower	Center	Upper
20	-6.655	-1.585	3.485
30	-12.200	-7.130	-2.060
40	-13.220	-8.150	-3.080

D-Allulose = 20 subtracted from:



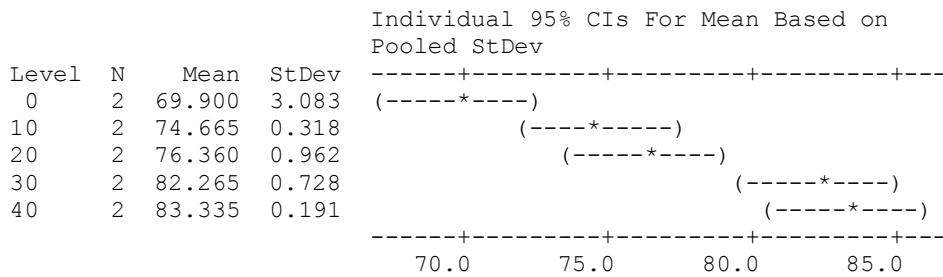
D-Allulose = 30 subtracted from:



### One-way ANOVA: RA3 (%) versus D-Allulose

Source	DF	SS	MS	F	P
D-Allulose	4	247.32	61.83	27.86	0.001
Error	5	11.10	2.22		
Total	9	258.42			

S = 1.490 R-Sq = 95.71% R-Sq(adj) = 92.27%



Pooled StDev = 1.490

Grouping Information Using Tukey Method

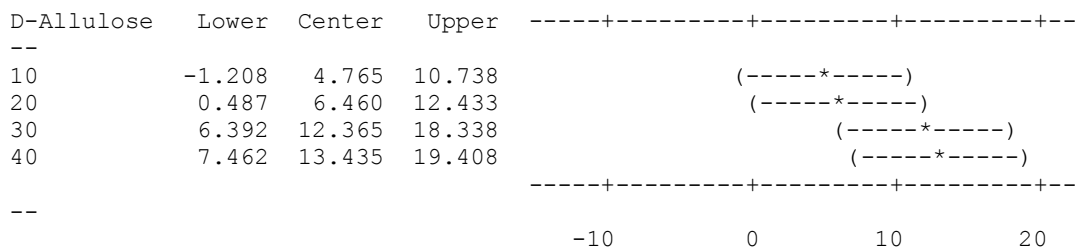
D-Allulose	N	Mean	Grouping
40	2	83.335	A
30	2	82.265	A B
20	2	76.360	B C
10	2	74.665	C D
0	2	69.900	D

Means that do not share a letter are significantly different.

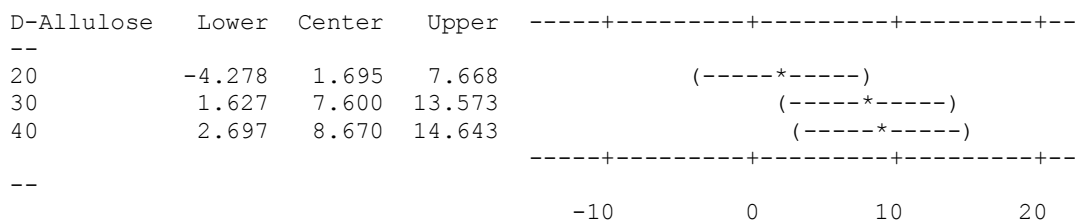
Tukey 95% Simultaneous Confidence Intervals  
 All Pairwise Comparisons among Levels of D-Allulose

Individual confidence level = 98.98%

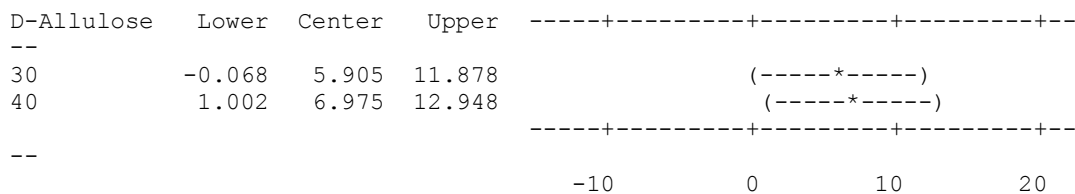
D-Allulose = 0 subtracted from:



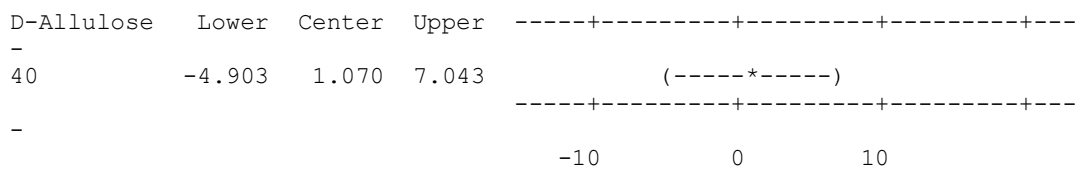
D-Allulose = 10 subtracted from:



D-Allulose = 20 subtracted from:



D-Allulose = 30 subtracted from:

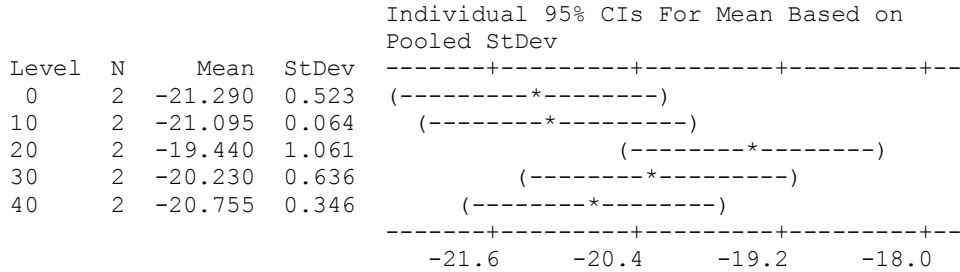


**7) One-way ANOVA: Tg versus D-Allulose**

Source	DF	SS	MS	F	P
--------	----	----	----	---	---

D-Allulose	4	4.441	1.110	2.88	0.138
Error	5	1.928	0.386		
Total	9	6.369			

S = 0.6210    R-Sq = 69.73%    R-Sq(adj) = 45.51%



Pooled StDev = 0.621

Grouping Information Using Tukey Method

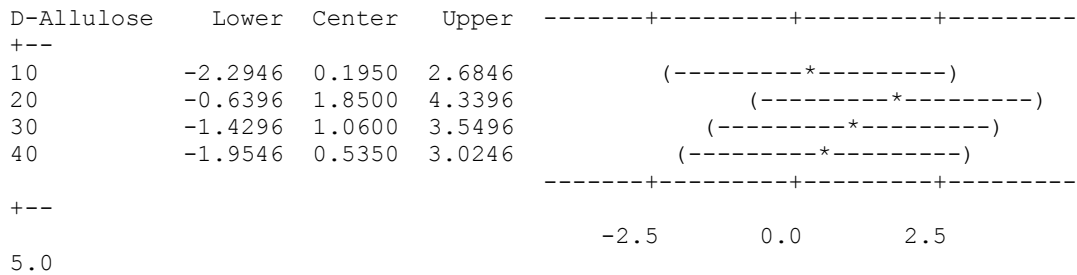
D-Allulose	N	Mean	Grouping
20	2	-19.4400	A
30	2	-20.2300	A
40	2	-20.7550	A
10	2	-21.0950	A
0	2	-21.2900	A

Means that do not share a letter are significantly different.

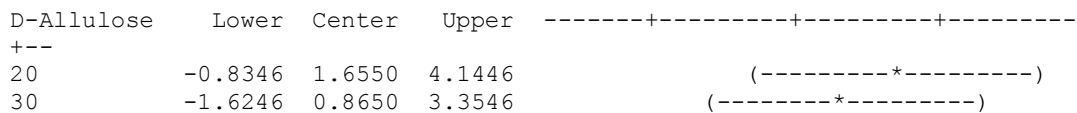
Tukey 95% Simultaneous Confidence Intervals  
All Pairwise Comparisons among Levels of D-Allulose

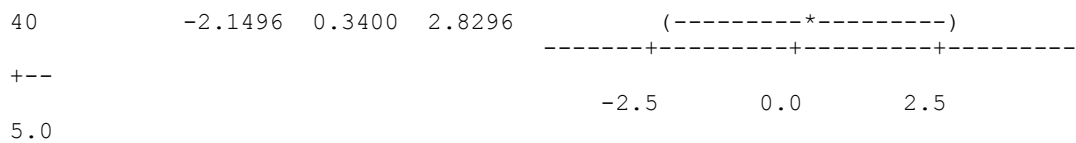
Individual confidence level = 98.98%

D-Allulose = 0 subtracted from:

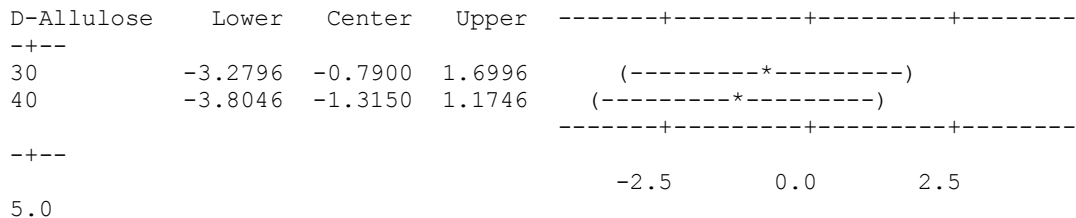


D-Allulose = 10 subtracted from:





D-Allulose = 20 subtracted from:



D-Allulose = 30 subtracted from:

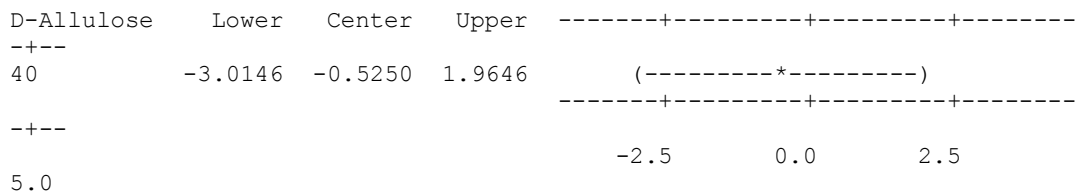
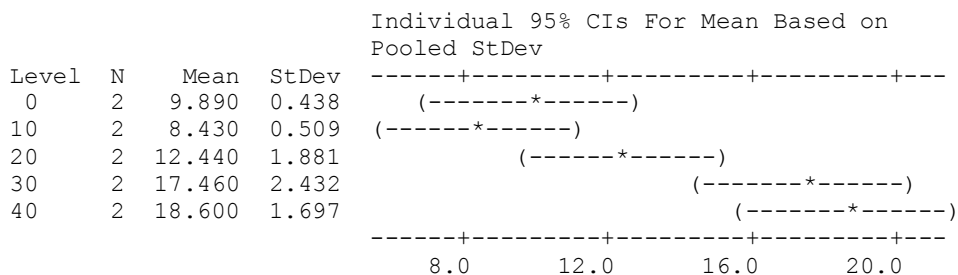


**Table A.2.** Effect of D-Allulose Substitution on the Gelatin Based Confectionery Gels for each storage day. 1) Moisture Content (MC %), 2) Water Activity (aw), 3) Hardness, 4) T<sub>1</sub>, 5) T<sub>2</sub> Spectra for Day 14.

**1) One-way ANOVA: MC (%) versus D-Allulose**

Source	DF	SS	MS	F	P
D-Allulose	4	162.92	40.73	15.93	0.005
Error	5	12.79	2.56		
Total	9	175.71			

S = 1.599 R-Sq = 92.72% R-Sq(adj) = 86.90%





Pooled StDev = 1.599

Grouping Information Using Tukey Method

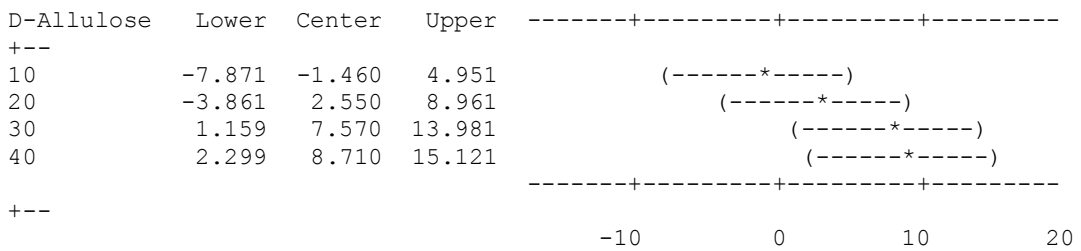
D-Allulose	N	Mean	Grouping
40	2	18.600	A
30	2	17.460	A
20	2	12.440	A B
0	2	9.890	B
10	2	8.430	B

Means that do not share a letter are significantly different.

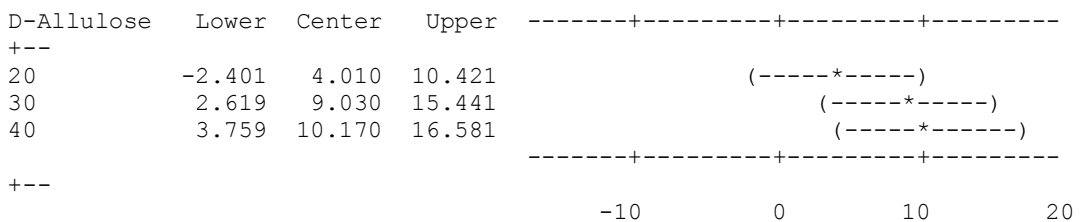
Tukey 95% Simultaneous Confidence Intervals  
All Pairwise Comparisons among Levels of D-Allulose

Individual confidence level = 98.98%

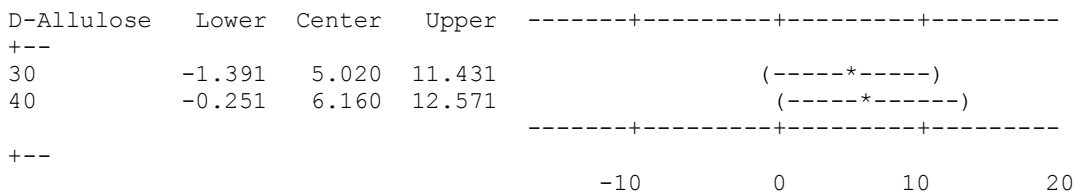
D-Allulose = 0 subtracted from:



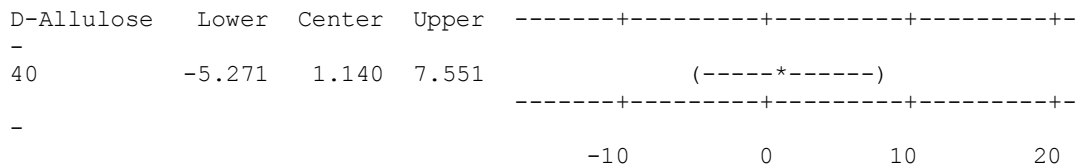
D-Allulose = 10 subtracted from:



D-Allulose = 20 subtracted from:



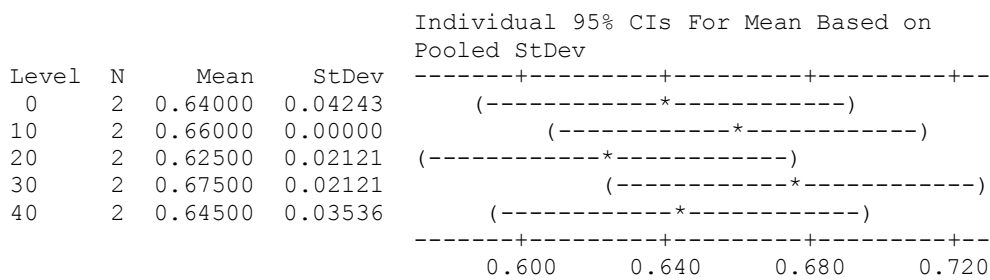
D-Allulose = 30 subtracted from:



## 2) One-way ANOVA: aw versus D-Allulose

Source	DF	SS	MS	F	P
D-Allulose	4	0.002940	0.000735	0.93	0.514
Error	5	0.003950	0.000790		
Total	9	0.006890			

S = 0.02811    R-Sq = 42.67%    R-Sq(adj) = 0.00%



Pooled StDev = 0.02811

### Grouping Information Using Tukey Method

D-Allulose	N	Mean	Grouping
30	2	0.67500	A
10	2	0.66000	A
40	2	0.64500	A
0	2	0.64000	A
20	2	0.62500	A

Means that do not share a letter are significantly different.

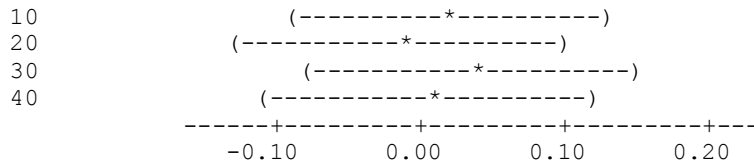
### Tukey 95% Simultaneous Confidence Intervals All Pairwise Comparisons among Levels of D-Allulose

Individual confidence level = 98.98%

D-Allulose = 0 subtracted from:

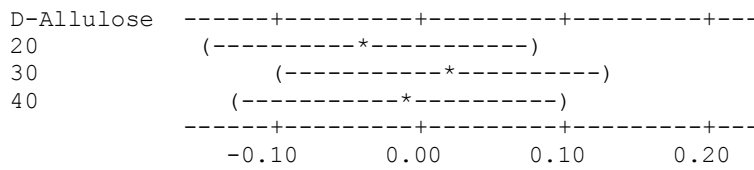
D-Allulose	Lower	Center	Upper
10	-0.09269	0.02000	0.13269
20	-0.12769	-0.01500	0.09769
30	-0.07769	0.03500	0.14769
40	-0.10769	0.00500	0.11769

D-Allulose -----+-----+-----+-----+-----+-----



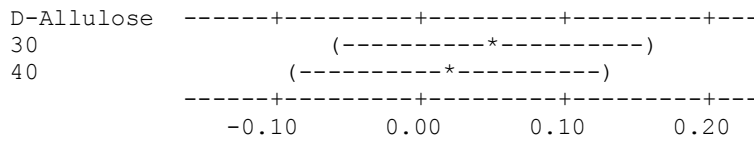
D-Allulose = 10 subtracted from:

D-Allulose	Lower	Center	Upper
20	-0.14769	-0.03500	0.07769
30	-0.09769	0.01500	0.12769
40	-0.12769	-0.01500	0.09769



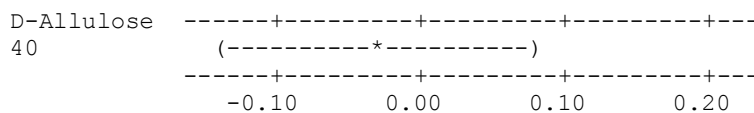
D-Allulose = 20 subtracted from:

D-Allulose	Lower	Center	Upper
30	-0.06269	0.05000	0.16269
40	-0.09269	0.02000	0.13269



D-Allulose = 30 subtracted from:

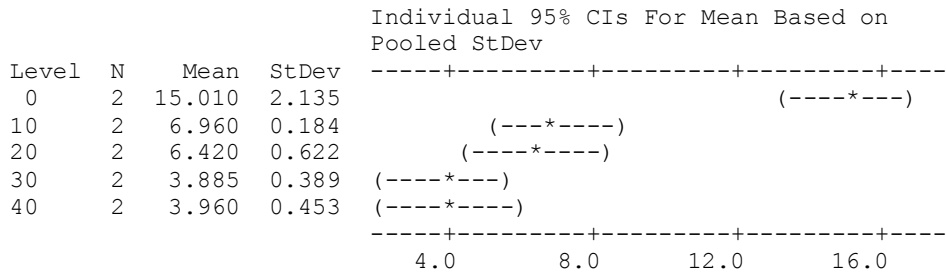
D-Allulose	Lower	Center	Upper
40	-0.14269	-0.03000	0.08269



### 3) One-way ANOVA: hardness versus D-Allulose

Source	DF	SS	MS	F	P
D-Allulose	4	166.28	41.57	38.94	0.001
Error	5	5.34	1.07		
Total	9	171.61			

S = 1.033    R-Sq = 96.89%    R-Sq(adj) = 94.40%



Pooled StDev = 1.033

Grouping Information Using Tukey Method

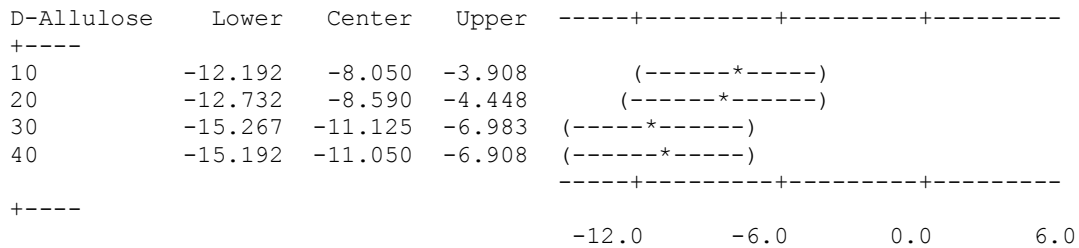
D-Allulose	N	Mean	Grouping
0	2	15.010	A
10	2	6.960	B
20	2	6.420	B
40	2	3.960	B
30	2	3.885	B

Means that do not share a letter are significantly different.

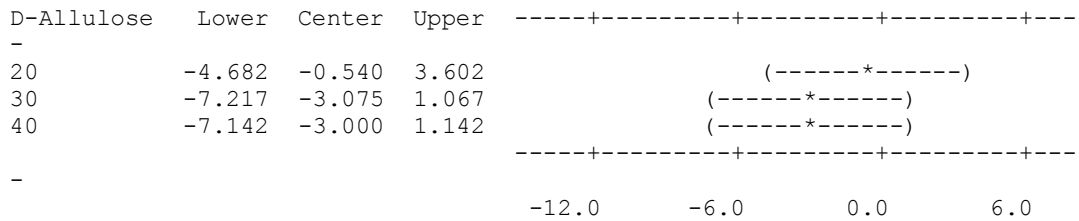
Tukey 95% Simultaneous Confidence Intervals  
All Pairwise Comparisons among Levels of D-Allulose

Individual confidence level = 98.98%

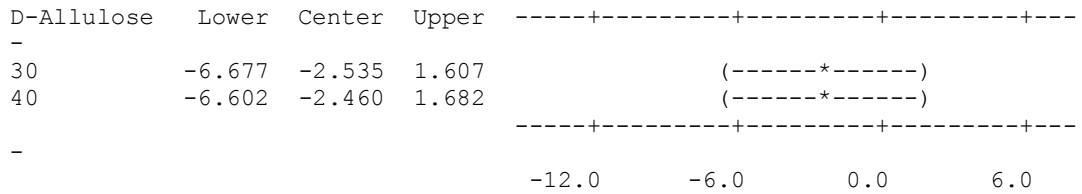
D-Allulose = 0 subtracted from:



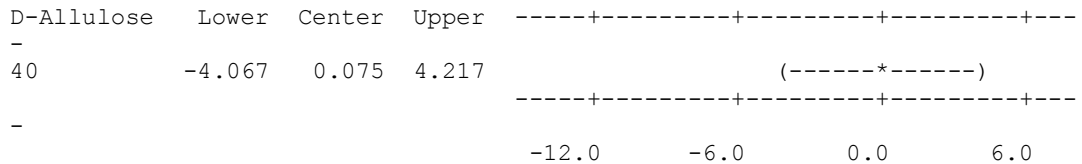
D-Allulose = 10 subtracted from:



D-Allulose = 20 subtracted from:



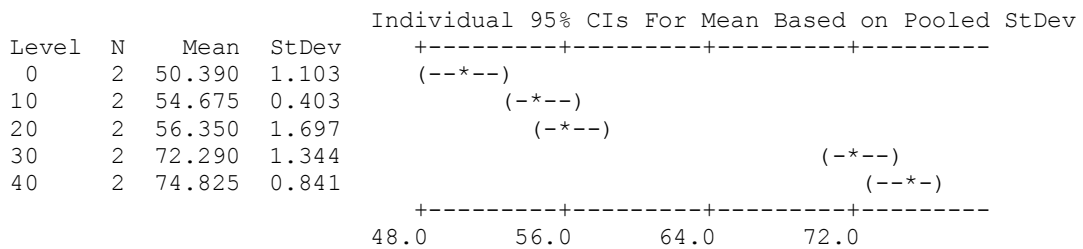
D-Allulose = 30 subtracted from:



#### 4) One-way ANOVA: T1 versus D-Allulose

Source	DF	SS	MS	F	P
D-Allulose	4	980.61	245.15	181.00	0.000
Error	5	6.77	1.35		
Total	9	987.38			

S = 1.164 R-Sq = 99.31% R-Sq(adj) = 98.77%



Pooled StDev = 1.164

Grouping Information Using Tukey Method

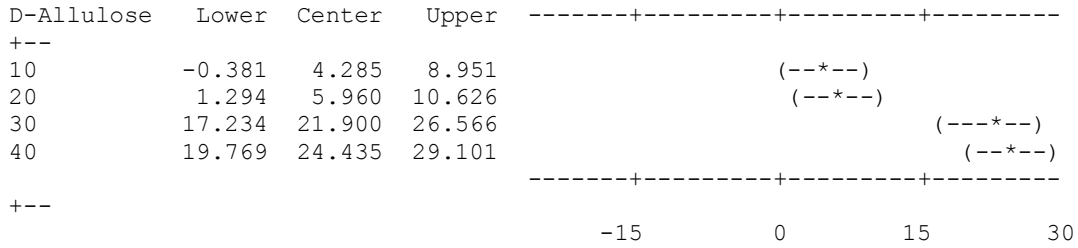
D-Allulose	N	Mean	Grouping
40	2	74.825	A
30	2	72.290	A
20	2	56.350	B
10	2	54.675	B C
0	2	50.390	C

Means that do not share a letter are significantly different.

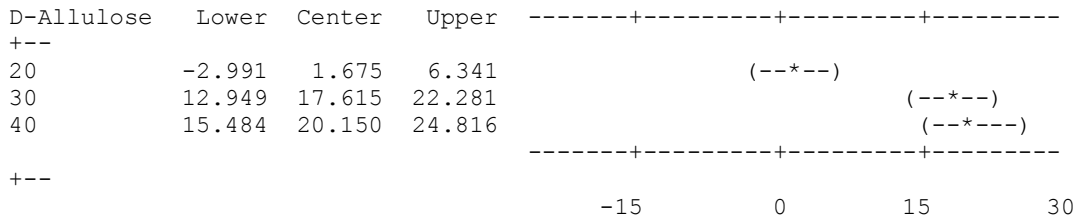
Tukey 95% Simultaneous Confidence Intervals  
All Pairwise Comparisons among Levels of D-Allulose

Individual confidence level = 98.98%

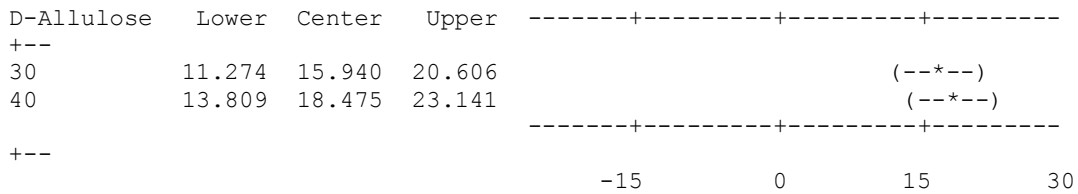
D-Allulose = 0 subtracted from:



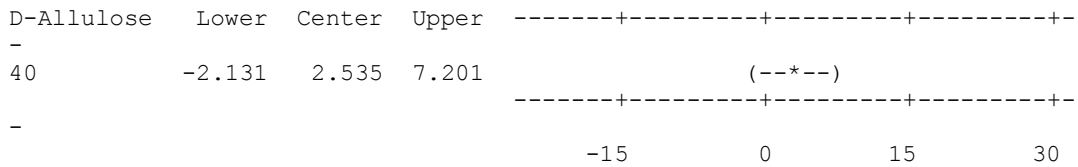
D-Allulose = 10 subtracted from:



D-Allulose = 20 subtracted from:



D-Allulose = 30 subtracted from:



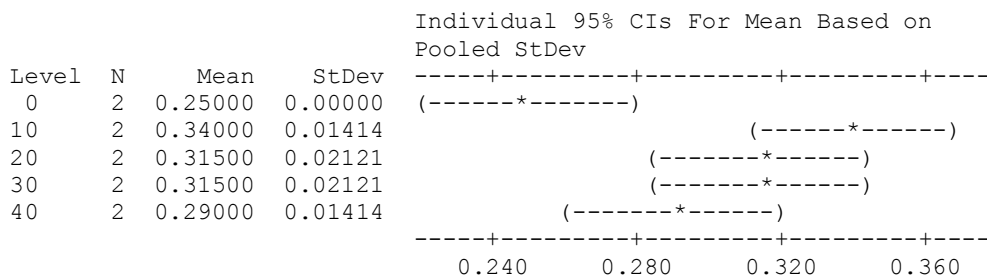
5)

**One-way ANOVA: T2 peak1 (ms) versus D-Allulose**

Source	DF	SS	MS	F	P
D-Allulose	4	0.009260	0.002315	8.90	0.017
Error	5	0.001300	0.000260		

Total 9 0.010560

S = 0.01612 R-Sq = 87.69% R-Sq(adj) = 77.84%



Pooled StDev = 0.01612

Grouping Information Using Tukey Method

D-Allulose	N	Mean	Grouping
10	2	0.34000	A
30	2	0.31500	A
20	2	0.31500	A
40	2	0.29000	A B
0	2	0.25000	B

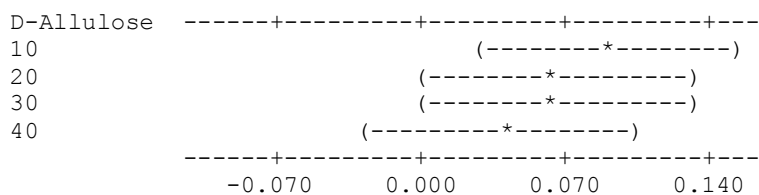
Means that do not share a letter are significantly different.

Tukey 95% Simultaneous Confidence Intervals  
All Pairwise Comparisons among Levels of D-Allulose

Individual confidence level = 98.98%

D-Allulose = 0 subtracted from:

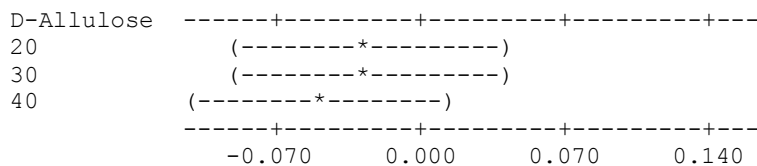
D-Allulose	Lower	Center	Upper
10	0.02535	0.09000	0.15465
20	0.00035	0.06500	0.12965
30	0.00035	0.06500	0.12965
40	-0.02465	0.04000	0.10465



D-Allulose = 10 subtracted from:

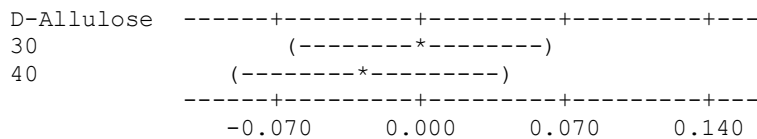
D-Allulose	Lower	Center	Upper
20	-0.08965	-0.02500	0.03965
30	-0.08965	-0.02500	0.03965

40            -0.11465   -0.05000   0.01465



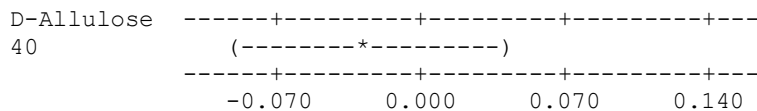
D-Allulose = 20 subtracted from:

D-Allulose	Lower	Center	Upper
30	-0.06465	0.00000	0.06465
40	-0.08965	-0.02500	0.03965



D-Allulose = 30 subtracted from:

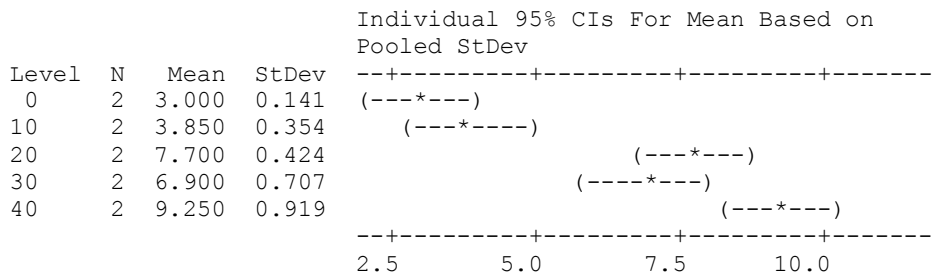
D-Allulose	Lower	Center	Upper
40	-0.08965	-0.02500	0.03965



### One-way ANOVA: T2 peak 2 (ms) versus D-Allulose

Source	DF	SS	MS	F	P
D-Allulose	4	55.574	13.894	41.60	0.000
Error	5	1.670	0.334		
Total	9	57.244			

S = 0.5779    R-Sq = 97.08%    R-Sq(adj) = 94.75%



Pooled StDev = 0.578



Grouping Information Using Tukey Method

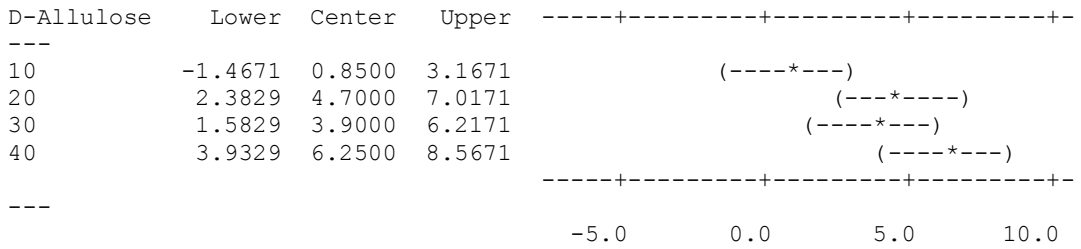
D-Allulose	N	Mean	Grouping
40	2	9.2500	A
20	2	7.7000	A B
30	2	6.9000	B
10	2	3.8500	C
0	2	3.0000	C

Means that do not share a letter are significantly different.

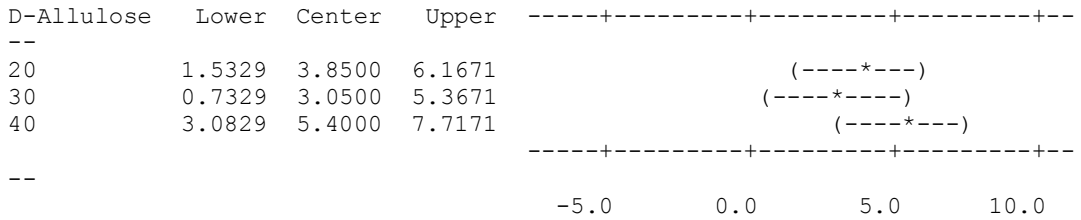
Tukey 95% Simultaneous Confidence Intervals  
All Pairwise Comparisons among Levels of D-Allulose

Individual confidence level = 98.98%

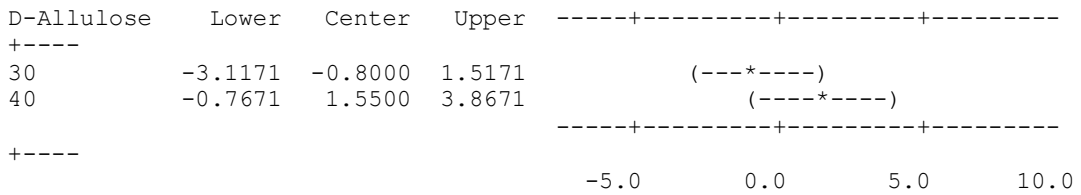
D-Allulose = 0 subtracted from:



D-Allulose = 10 subtracted from:

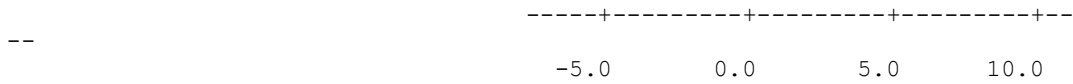


D-Allulose = 20 subtracted from:



D-Allulose = 30 subtracted from:

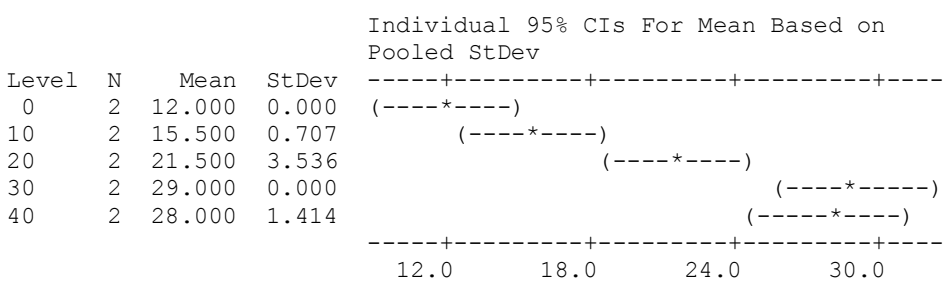




**One-way ANOVA: T2 peak 3 (ms) versus D-Allulose**

Source	DF	SS	MS	F	P
D-Allulose	4	448.60	112.15	37.38	0.001
Error	5	15.00	3.00		
Total	9	463.60			

S = 1.732    R-Sq = 96.76%    R-Sq(adj) = 94.18%



Pooled StDev = 1.732

Grouping Information Using Tukey Method

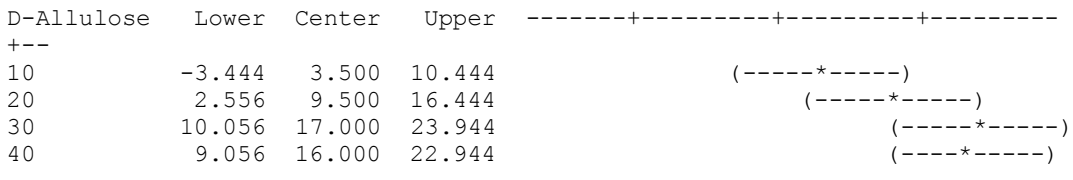
D-Allulose	N	Mean	Grouping
30	2	29.000	A
40	2	28.000	A B
20	2	21.500	B C
10	2	15.500	C D
0	2	12.000	D

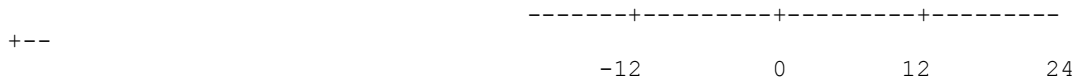
Means that do not share a letter are significantly different.

Tukey 95% Simultaneous Confidence Intervals  
All Pairwise Comparisons among Levels of D-Allulose

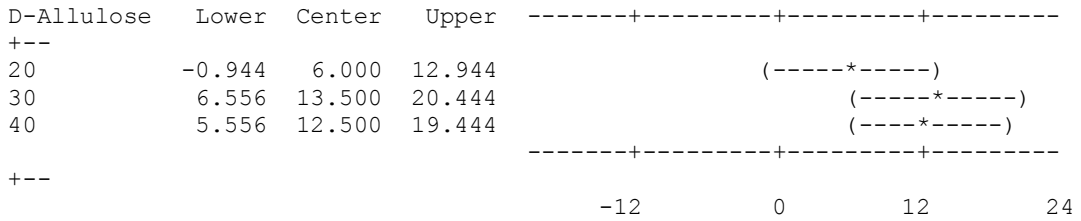
Individual confidence level = 98.98%

D-Allulose = 0 subtracted from:

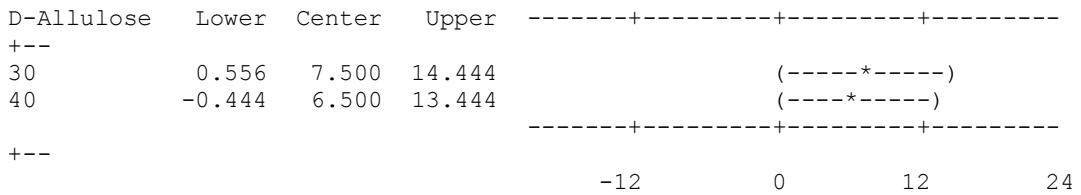




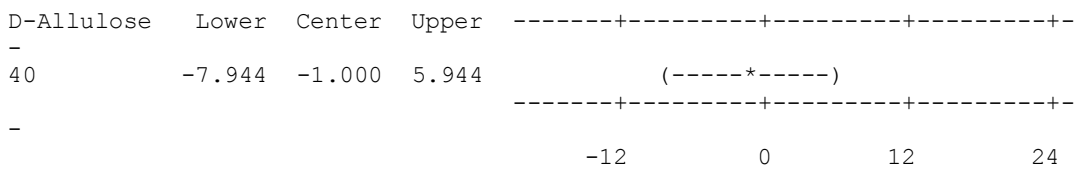
D-Allulose = 10 subtracted from:



D-Allulose = 20 subtracted from:



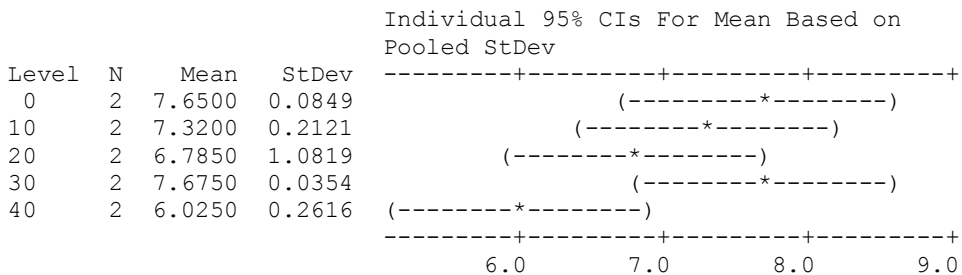
D-Allulose = 30 subtracted from:



### One-way ANOVA: RA1(%) versus D-Allulose

Source	DF	SS	MS	F	P
D-Allulose	4	3.872	0.968	3.75	0.090
Error	5	1.292	0.258		
Total	9	5.164			

S = 0.5084    R-Sq = 74.98%    R-Sq(adj) = 54.96%



Pooled StDev = 0.5084

Grouping Information Using Tukey Method

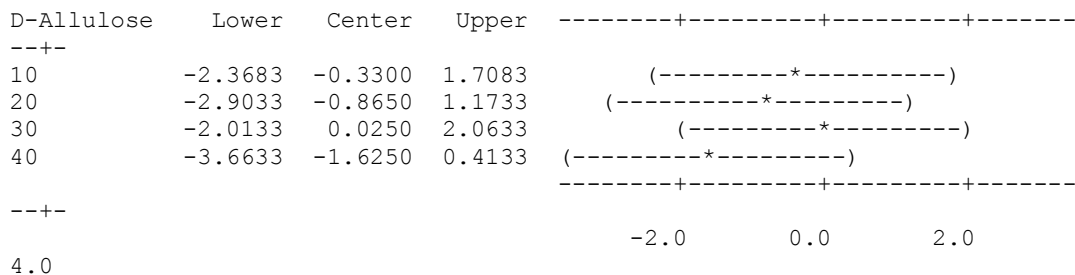
D-Allulose	N	Mean	Grouping
30	2	7.6750	A
0	2	7.6500	A
10	2	7.3200	A
20	2	6.7850	A
40	2	6.0250	A

Means that do not share a letter are significantly different.

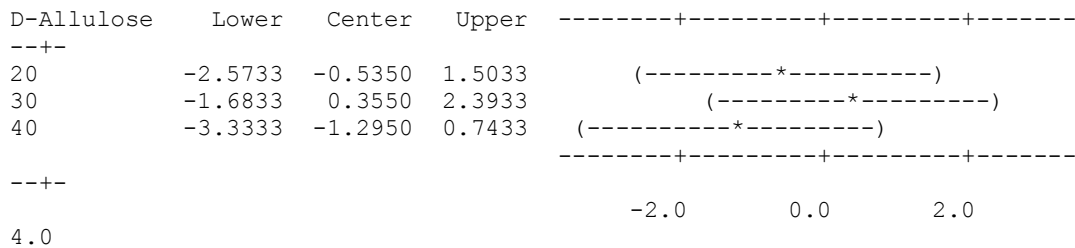
Tukey 95% Simultaneous Confidence Intervals  
All Pairwise Comparisons among Levels of D-Allulose

Individual confidence level = 98.98%

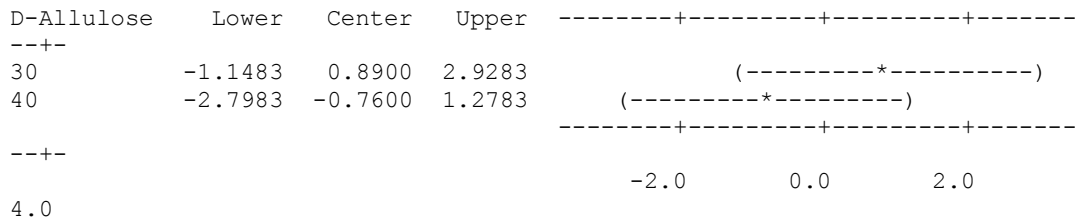
D-Allulose = 0 subtracted from:



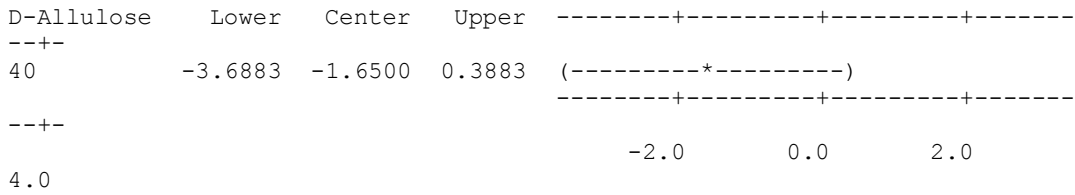
D-Allulose = 10 subtracted from:



D-Allulose = 20 subtracted from:



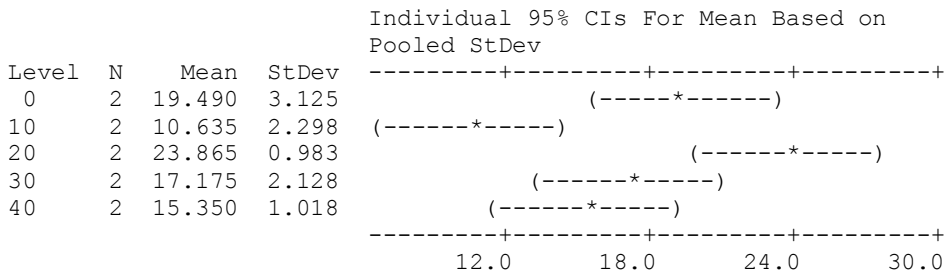
D-Allulose = 30 subtracted from:



**One-way ANOVA: RA2(%) versus D-Allulose**

Source	DF	SS	MS	F	P
D-Allulose	4	192.27	48.07	11.14	0.011
Error	5	21.58	4.32		
Total	9	213.85			

S = 2.078 R-Sq = 89.91% R-Sq(adj) = 81.83%



Pooled StDev = 2.078

Grouping Information Using Tukey Method

D-Allulose	N	Mean	Grouping
20	2	23.865	A
0	2	19.490	A B
30	2	17.175	A B C
40	2	15.350	B C
10	2	10.635	C

Means that do not share a letter are significantly different.

Tukey 95% Simultaneous Confidence Intervals  
All Pairwise Comparisons among Levels of D-Allulose

Individual confidence level = 98.98%

D-Allulose = 0 subtracted from:

D-Allulose	Lower	Center	Upper	-----+-----+-----+-----
-+-				
10	-17.185	-8.855	-0.525	(-----*-----)
20	-3.955	4.375	12.705	(-----*-----)
30	-10.645	-2.315	6.015	(-----*-----)
40	-12.470	-4.140	4.190	(-----*-----)
				-----+-----+-----+-----
-+-				
				-12            0            12
24				

D-Allulose = 10 subtracted from:

D-Allulose	Lower	Center	Upper	-----+-----+-----+-----
+--				
20	4.900	13.230	21.560	(-----*-----)
30	-1.790	6.540	14.870	(-----*-----)
40	-3.615	4.715	13.045	(-----*-----)
				-----+-----+-----+-----
+--				
				-12            0            12
24				

D-Allulose = 20 subtracted from:

D-Allulose	Lower	Center	Upper	-----+-----+-----+-----
-+-				
30	-15.020	-6.690	1.640	(-----*-----)
40	-16.845	-8.515	-0.185	(-----*-----)
				-----+-----+-----+-----
-+-				
				-12            0            12
24				

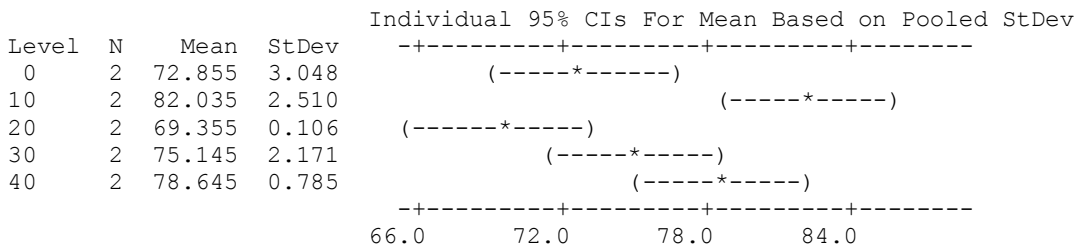
D-Allulose = 30 subtracted from:

D-Allulose	Lower	Center	Upper	-----+-----+-----+-----
+--				
40	-10.155	-1.825	6.505	(-----*-----)
				-----+-----+-----+-----
+--				
				-12            0            12
24				

**One-way ANOVA: RA3(%) versus D-Allulose**

Source	DF	SS	MS	F	P
D-Allulose	4	194.85	48.71	11.64	0.010
Error	5	20.93	4.19		
Total	9	215.78			

S = 2.046    R-Sq = 90.30%    R-Sq(adj) = 82.54%



Pooled StDev = 2.046

Grouping Information Using Tukey Method

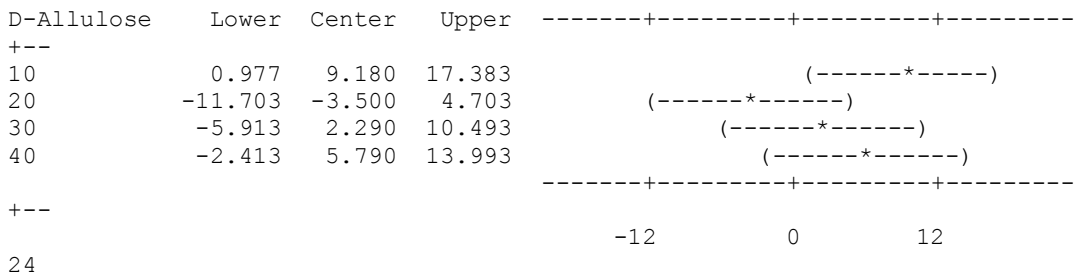
D-Allulose	N	Mean	Grouping
10	2	82.035	A
40	2	78.645	A B
30	2	75.145	A B C
0	2	72.855	B C
20	2	69.355	C

Means that do not share a letter are significantly different.

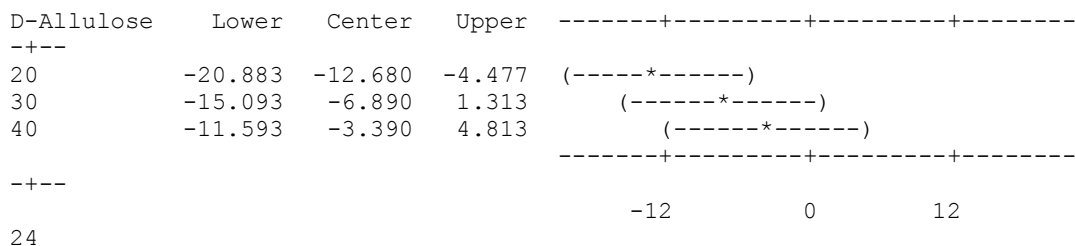
Tukey 95% Simultaneous Confidence Intervals  
All Pairwise Comparisons among Levels of D-Allulose

Individual confidence level = 98.98%

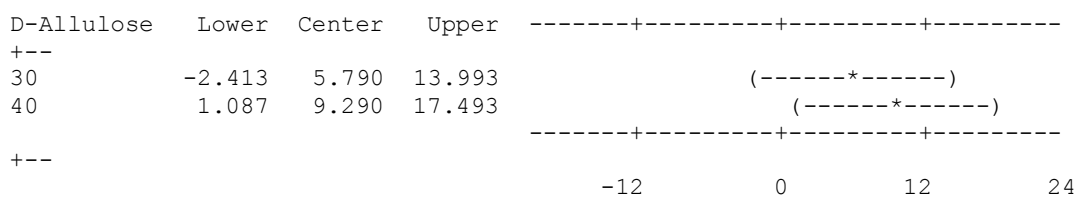
D-Allulose = 0 subtracted from:



D-Allulose = 10 subtracted from:



D-Allulose = 20 subtracted from:



D-Allulose = 30 subtracted from:

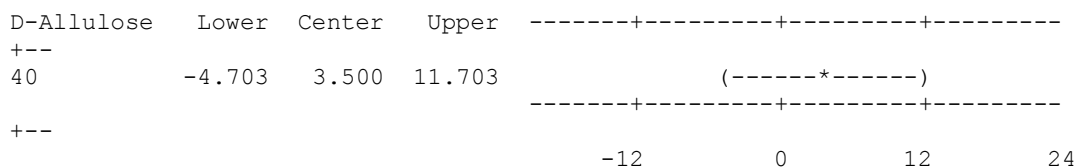


**Table A.3.** Effect of D-Allulose Substitution on the Gelatin Based Confectionery Gels for each storage day. 1) Moisture Content (MC %), 2) Water Activity (aw), 3) Hardness, 4) T<sub>1</sub>, 5) T<sub>2</sub> Spectra, 6) Glass transition Temperature (T<sub>g</sub>) for **Day 28**.

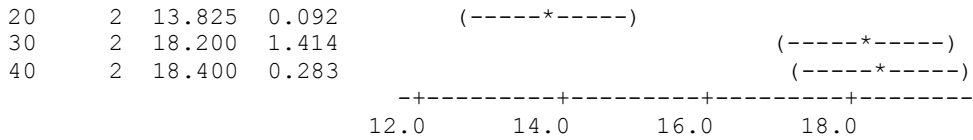
**1) One-way ANOVA: MC(%) versus D-Allulose**

Source	DF	SS	MS	F	P
D-Allulose	4	49.870	12.468	27.88	0.001
Error	5	2.236	0.447		
Total	9	52.106			

S = 0.6687    R-Sq = 95.71%    R-Sq(adj) = 92.28%

Level	N	Mean	StDev	Individual 95% CIs For Mean Based on Pooled StDev
0	2	13.070	0.042	(-----*-----)
10	2	14.710	0.382	(-----*-----)





Pooled StDev = 0.669

Grouping Information Using Tukey Method

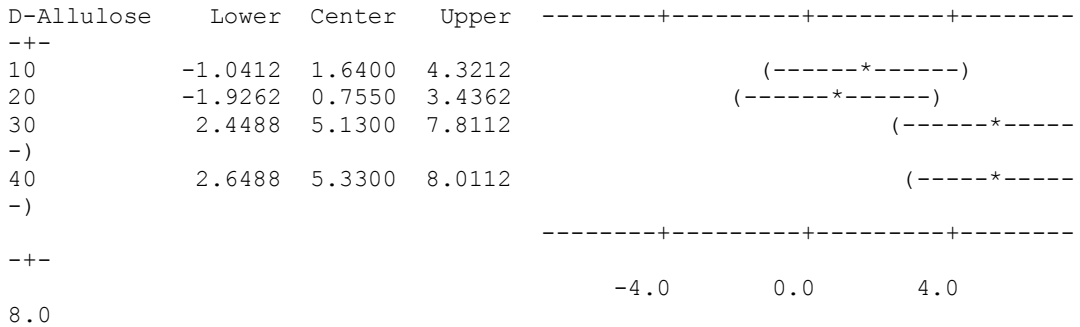
D-Allulose	N	Mean	Grouping
40	2	18.4000	A
30	2	18.2000	A
10	2	14.7100	B
20	2	13.8250	B
0	2	13.0700	B

Means that do not share a letter are significantly different.

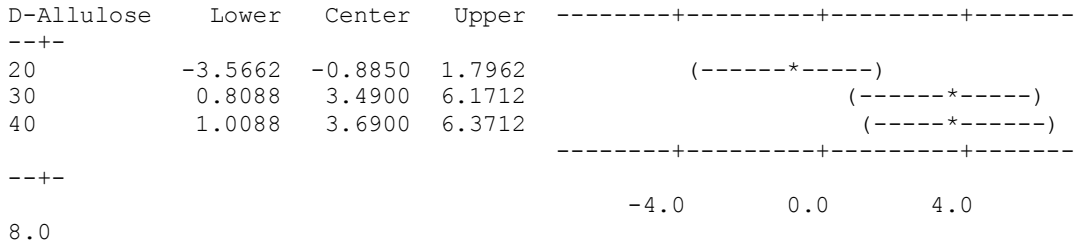
Tukey 95% Simultaneous Confidence Intervals  
All Pairwise Comparisons among Levels of D-Allulose

Individual confidence level = 98.98%

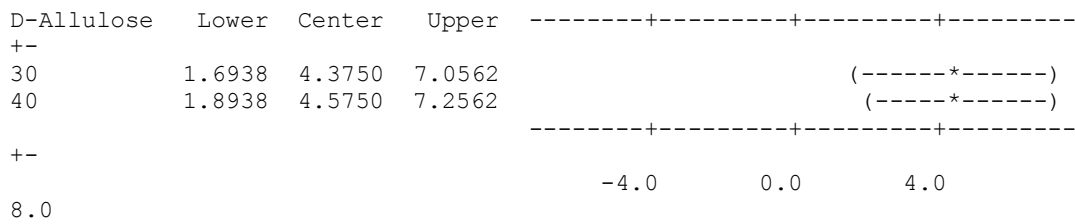
D-Allulose = 0 subtracted from:



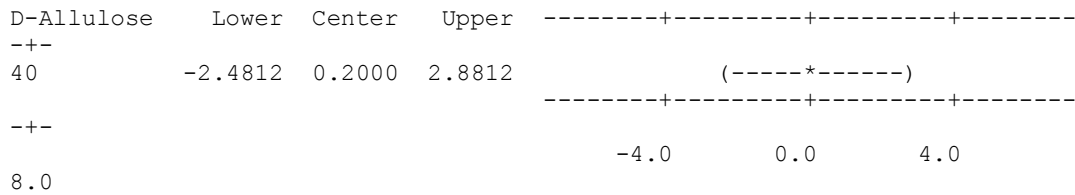
D-Allulose = 10 subtracted from:



D-Allulose = 20 subtracted from:



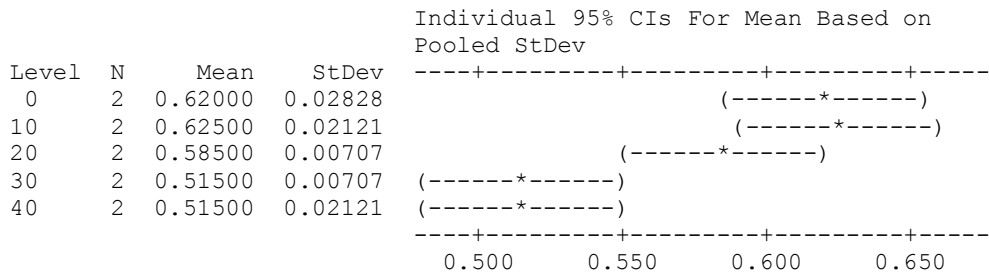
D-Allulose = 30 subtracted from:



## 2) One-way ANOVA: aw versus D-Allulose

Source	DF	SS	MS	F	P
D-Allulose	4	0.023560	0.005890	16.36	0.004
Error	5	0.001800	0.000360		
Total	9	0.025360			

S = 0.01897 R-Sq = 92.90% R-Sq(adj) = 87.22%



Pooled StDev = 0.01897

Grouping Information Using Tukey Method

D-Allulose	N	Mean	Grouping
10	2	0.62500	A
0	2	0.62000	A
20	2	0.58500	A B
40	2	0.51500	B
30	2	0.51500	B

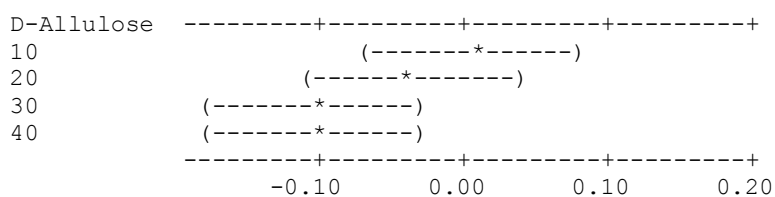
Means that do not share a letter are significantly different.

Tukey 95% Simultaneous Confidence Intervals  
 All Pairwise Comparisons among Levels of D-Allulose

Individual confidence level = 98.98%

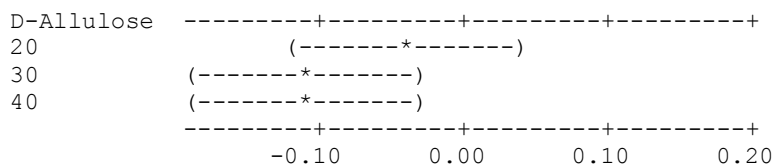
D-Allulose = 0 subtracted from:

D-Allulose	Lower	Center	Upper
10	-0.07107	0.00500	0.08107
20	-0.11107	-0.03500	0.04107
30	-0.18107	-0.10500	-0.02893
40	-0.18107	-0.10500	-0.02893



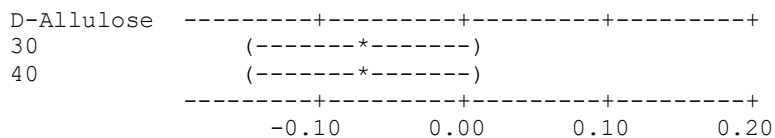
D-Allulose = 10 subtracted from:

D-Allulose	Lower	Center	Upper
20	-0.11607	-0.04000	0.03607
30	-0.18607	-0.11000	-0.03393
40	-0.18607	-0.11000	-0.03393



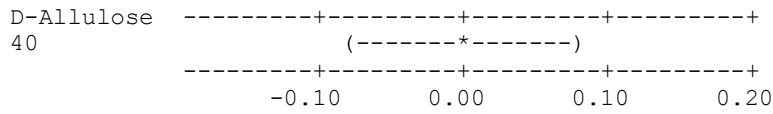
D-Allulose = 20 subtracted from:

D-Allulose	Lower	Center	Upper
30	-0.14607	-0.07000	0.00607
40	-0.14607	-0.07000	0.00607



D-Allulose = 30 subtracted from:

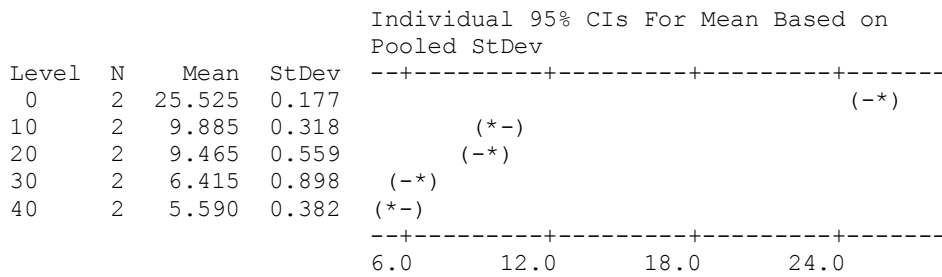
D-Allulose	Lower	Center	Upper
40	-0.07607	0.00000	0.07607



### 3) One-way ANOVA: hardness versus D-Allulose

Source	DF	SS	MS	F	P
D-Allulose	4	528.317	132.079	472.79	0.000
Error	5	1.397	0.279		
Total	9	529.714			

S = 0.5285    R-Sq = 99.74%    R-Sq(adj) = 99.53%



Pooled StDev = 0.529

#### Grouping Information Using Tukey Method

D-Allulose	N	Mean	Grouping
0	2	25.525	A
10	2	9.885	B
20	2	9.465	B
30	2	6.415	C
40	2	5.590	C

Means that do not share a letter are significantly different.

#### Tukey 95% Simultaneous Confidence Intervals All Pairwise Comparisons among Levels of D-Allulose

Individual confidence level = 98.98%

D-Allulose = 0 subtracted from:

D-Allulose	Lower	Center	Upper	
10	-17.759	-15.640	-13.521	(-***)
20	-18.179	-16.060	-13.941	(--***)

30	-21.229	-19.110	-16.991	(--*--)
40	-22.054	-19.935	-17.816	(--*--)

-----+-----+-----+-----

----+-

-16.0      -8.0      0.0

8.0

D-Allulose = 10 subtracted from:

D-Allulose	Lower	Center	Upper	-----+-----+-----+-----
+-				
20	-2.539	-0.420	1.699	(-*--)
30	-5.589	-3.470	-1.351	(--*-)
40	-6.414	-4.295	-2.176	(--*-)

-----+-----+-----+-----

+-

-16.0      -8.0      0.0

8.0

D-Allulose = 20 subtracted from:

D-Allulose	Lower	Center	Upper	-----+-----+-----+-----
+-				
30	-5.169	-3.050	-0.931	(-*--)
40	-5.994	-3.875	-1.756	(-*--)

-----+-----+-----+-----

+-

-16.0      -8.0      0.0

8.0

D-Allulose = 30 subtracted from:

D-Allulose	Lower	Center	Upper	-----+-----+-----+-----
+-				
40	-2.944	-0.825	1.294	(--*--)

-----+-----+-----+-----

+-

-16.0      -8.0      0.0      8.0

#### 4) One-way ANOVA: T1 versus D-Allulose

Source	DF	SS	MS	F	P
D-Allulose	4	991.99	248.00	67.15	0.000
Error	5	18.46	3.69		
Total	9	1010.45			

S = 1.922    R-Sq = 98.17%    R-Sq(adj) = 96.71%

Individual 95% CIs For Mean Based on  
Pooled StDev

Level	N	Mean	StDev	-----+-----+-----+-----
0	2	46.810	0.523	(----*--)

10	2	49.470	0.170	(-----*----)
20	2	52.040	1.202	(-----*----)
30	2	70.780	4.087	(-----*-----)
40	2	68.040	0.113	(-----*----)

-----+-----+-----+-----  
48.0      56.0      64.0      72.0

Pooled StDev = 1.922

Grouping Information Using Tukey Method

D-Allulose	N	Mean	Grouping
30	2	70.780	A
40	2	68.040	A
20	2	52.040	B
10	2	49.470	B
0	2	46.810	B

Means that do not share a letter are significantly different.

Tukey 95% Simultaneous Confidence Intervals  
All Pairwise Comparisons among Levels of D-Allulose

Individual confidence level = 98.98%

D-Allulose = 0 subtracted from:

D-Allulose	Lower	Center	Upper	
10	-5.045	2.660	10.365	(-----*----)
20	-2.475	5.230	12.935	(-----*-----)
30	16.265	23.970	31.675	(-----*-----)
40	13.525	21.230	28.935	(-----*-----)

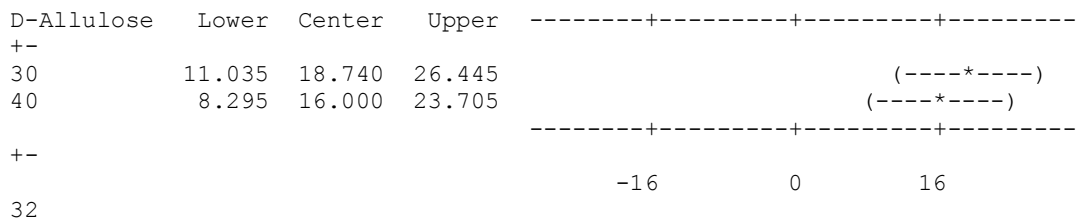
-----+-----+-----+-----  
+-  
-16      0      16  
32

D-Allulose = 10 subtracted from:

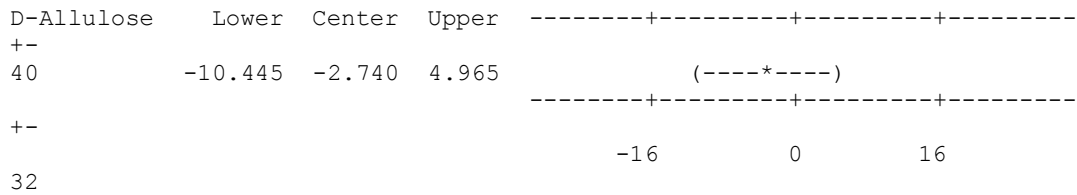
D-Allulose	Lower	Center	Upper	
20	-5.135	2.570	10.275	(-----*----)
30	13.605	21.310	29.015	(-----*-----)
40	10.865	18.570	26.275	(-----*-----)

-----+-----+-----+-----  
+-  
-16      0      16  
32

D-Allulose = 20 subtracted from:



D-Allulose = 30 subtracted from:

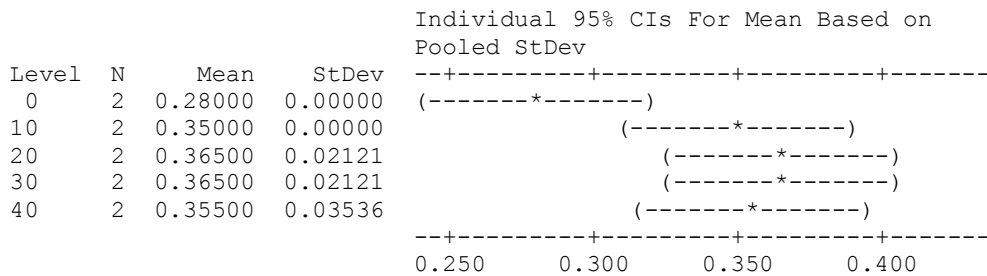


### 5)

#### One-way ANOVA: T2 peak1 (ms) versus D-Allulose

Source	DF	SS	MS	F	P
D-Allulose	4	0.010260	0.002565	5.97	0.038
Error	5	0.002150	0.000430		
Total	9	0.012410			

S = 0.02074    R-Sq = 82.68%    R-Sq(adj) = 68.82%



Pooled StDev = 0.02074

#### Grouping Information Using Tukey Method

D-Allulose	N	Mean	Grouping
30	2	0.36500	A
20	2	0.36500	A
40	2	0.35500	A B
10	2	0.35000	A B
0	2	0.28000	B

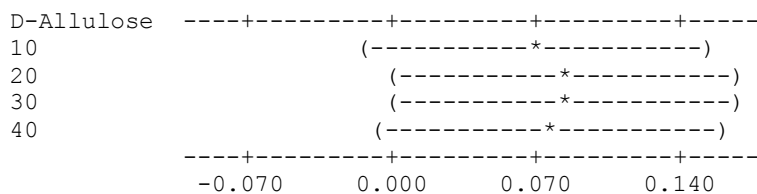
Means that do not share a letter are significantly different.

Tukey 95% Simultaneous Confidence Intervals  
 All Pairwise Comparisons among Levels of D-Allulose

Individual confidence level = 98.98%

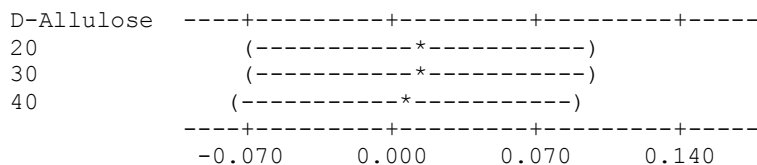
D-Allulose = 0 subtracted from:

D-Allulose	Lower	Center	Upper
10	-0.01314	0.07000	0.15314
20	0.00186	0.08500	0.16814
30	0.00186	0.08500	0.16814
40	-0.00814	0.07500	0.15814



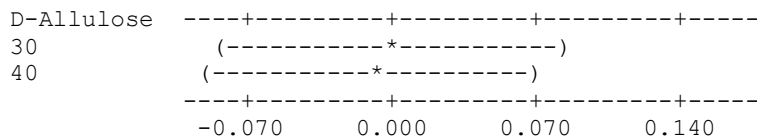
D-Allulose = 10 subtracted from:

D-Allulose	Lower	Center	Upper
20	-0.06814	0.01500	0.09814
30	-0.06814	0.01500	0.09814
40	-0.07814	0.00500	0.08814



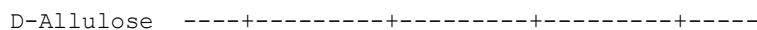
D-Allulose = 20 subtracted from:

D-Allulose	Lower	Center	Upper
30	-0.08314	0.00000	0.08314
40	-0.09314	-0.01000	0.07314

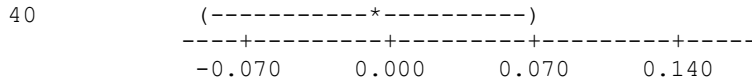


D-Allulose = 30 subtracted from:

D-Allulose	Lower	Center	Upper
40	-0.09314	-0.01000	0.07314



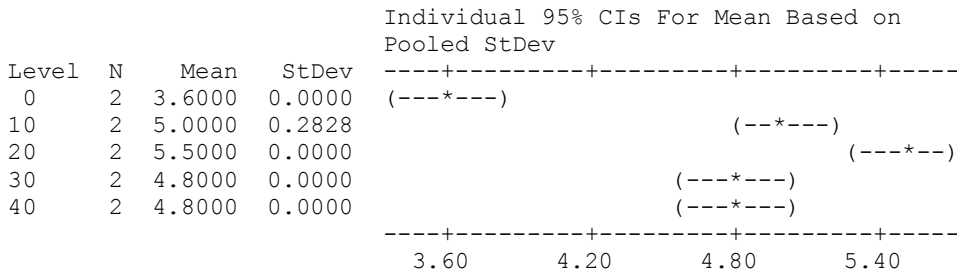




**One-way ANOVA: T2 peak 2 (ms) versus D-Allulose**

Source	DF	SS	MS	F	P
D-Allulose	4	3.9040	0.9760	61.00	0.000
Error	5	0.0800	0.0160		
Total	9	3.9840			

S = 0.1265    R-Sq = 97.99%    R-Sq(adj) = 96.39%



Pooled StDev = 0.1265

Grouping Information Using Tukey Method

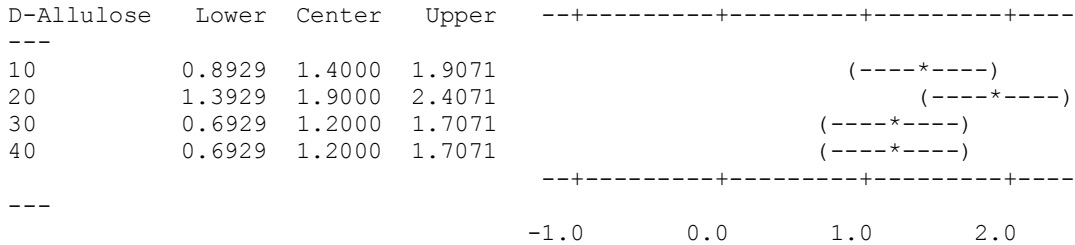
D-Allulose	N	Mean	Grouping
20	2	5.5000	A
10	2	5.0000	A B
40	2	4.8000	B
30	2	4.8000	B
0	2	3.6000	C

Means that do not share a letter are significantly different.

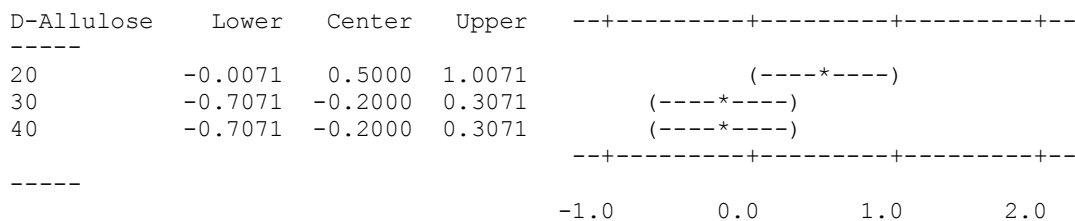
Tukey 95% Simultaneous Confidence Intervals  
All Pairwise Comparisons among Levels of D-Allulose

Individual confidence level = 98.98%

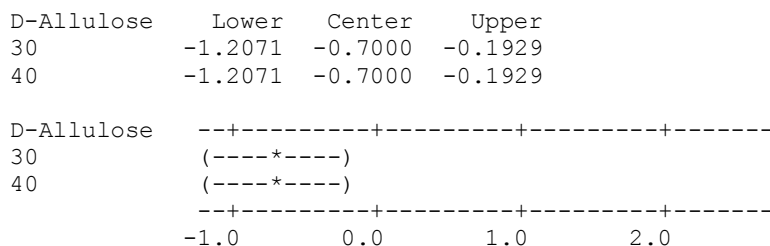
D-Allulose = 0 subtracted from:



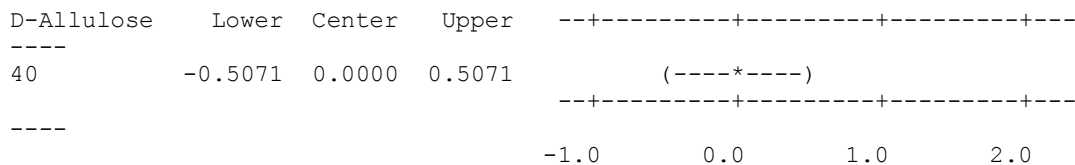
D-Allulose = 10 subtracted from:



D-Allulose = 20 subtracted from:



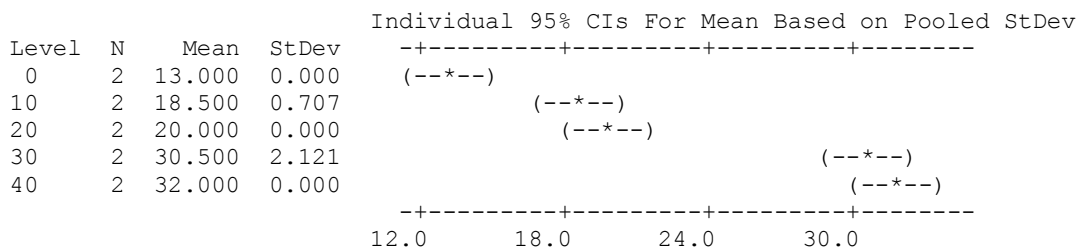
D-Allulose = 30 subtracted from:



### One-way ANOVA: T2 peak 3 (ms) versus D-Allulose

Source	DF	SS	MS	F	P
D-Allulose	4	532.60	133.15	133.15	0.000
Error	5	5.00	1.00		
Total	9	537.60			

S = 1 R-Sq = 99.07% R-Sq(adj) = 98.33%



Pooled StDev = 1.000

Grouping Information Using Tukey Method

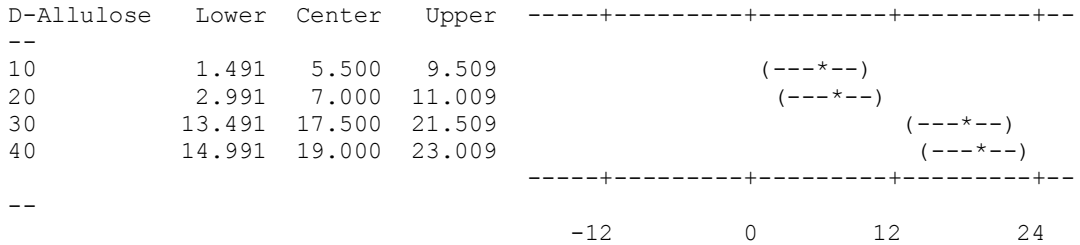
D-Allulose	N	Mean	Grouping
40	2	32.000	A
30	2	30.500	A
20	2	20.000	B
10	2	18.500	B
0	2	13.000	C

Means that do not share a letter are significantly different.

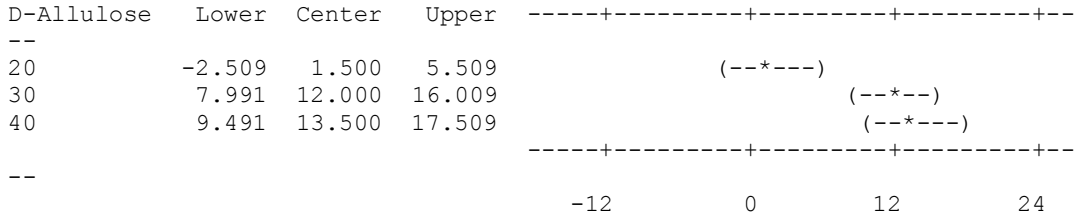
Tukey 95% Simultaneous Confidence Intervals  
All Pairwise Comparisons among Levels of D-Allulose

Individual confidence level = 98.98%

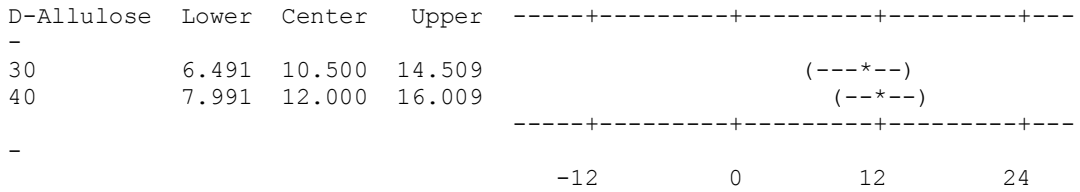
D-Allulose = 0 subtracted from:



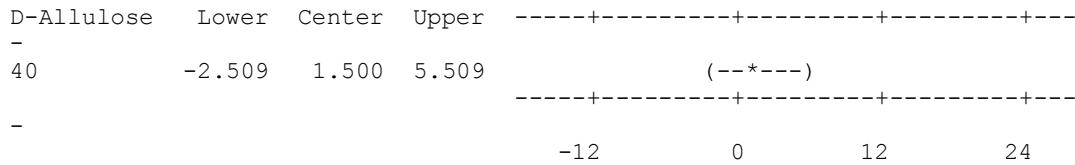
D-Allulose = 10 subtracted from:



D-Allulose = 20 subtracted from:



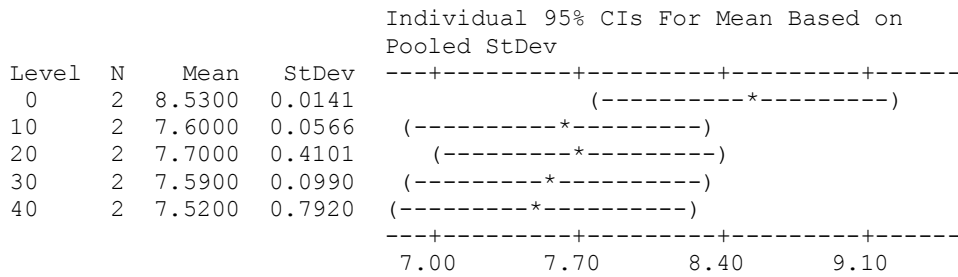
D-Allulose = 30 subtracted from:



### One-way ANOVA: RA1 (%) versus D-Allulose

Source	DF	SS	MS	F	P
D-Allulose	4	1.409	0.352	2.18	0.208
Error	5	0.809	0.162		
Total	9	2.218			

S = 0.4021 R-Sq = 63.54% R-Sq(adj) = 34.38%



Pooled StDev = 0.4021

#### Grouping Information Using Tukey Method

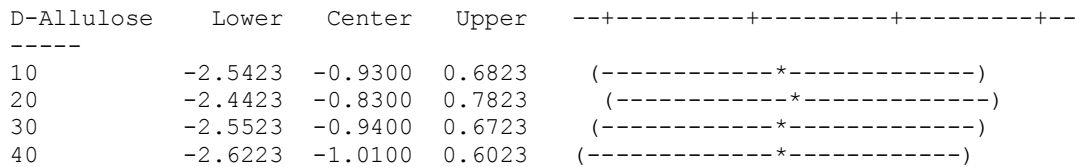
D-Allulose	N	Mean	Grouping
0	2	8.5300	A
20	2	7.7000	A
10	2	7.6000	A
30	2	7.5900	A
40	2	7.5200	A

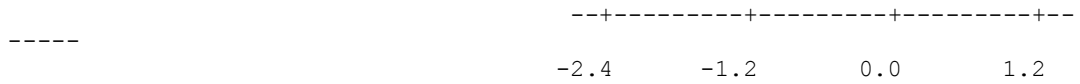
Means that do not share a letter are significantly different.

#### Tukey 95% Simultaneous Confidence Intervals All Pairwise Comparisons among Levels of D-Allulose

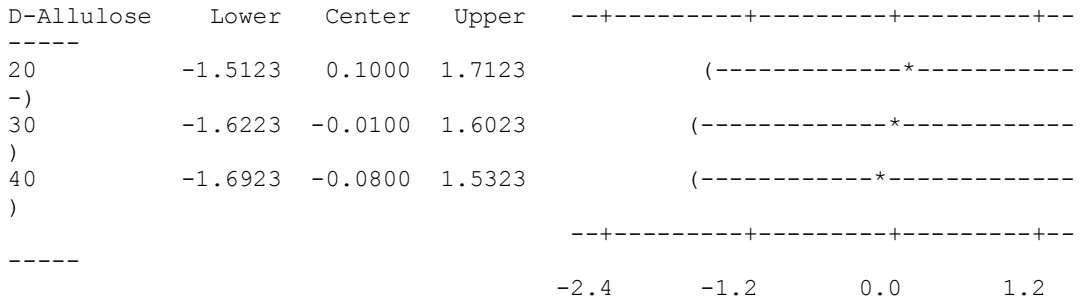
Individual confidence level = 98.98%

D-Allulose = 0 subtracted from:

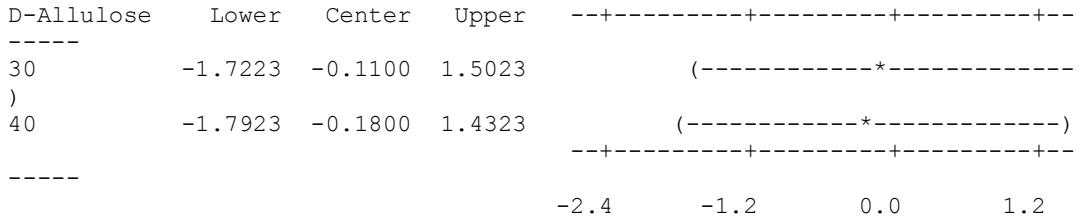




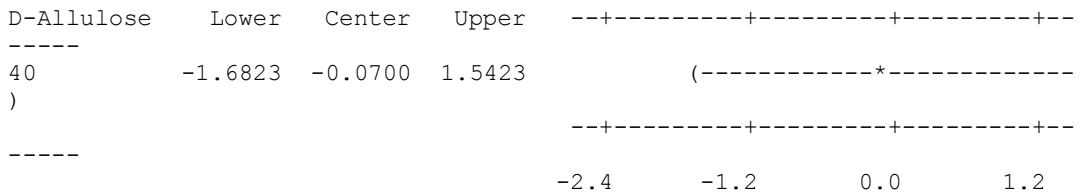
D-Allulose = 10 subtracted from:



D-Allulose = 20 subtracted from:



D-Allulose = 30 subtracted from:



### One-way ANOVA: RA2(%) versus D-Allulose

Source	DF	SS	MS	F	P
D-Allulose	4	272.487	68.122	544.15	0.000
Error	5	0.626	0.125		
Total	9	273.113			

S = 0.3538    R-Sq = 99.77%    R-Sq(adj) = 99.59%

Level	N	Mean	StDev	Individual 95% CIs For Mean Based on Pooled StDev
0	2	22.205	0.559	(-*)
10	2	20.450	0.014	(* -)

20	2	16.935	0.488		(*-)
30	2	10.425	0.191	(*-)	
40	2	9.210	0.198	(*-)	

-----+-----+-----+-----+  
12.0      16.0      20.0      24.0

Pooled StDev = 0.354

Grouping Information Using Tukey Method

D-Allulose	N	Mean	Grouping
0	2	22.205	A
10	2	20.450	B
20	2	16.935	C
30	2	10.425	D
40	2	9.210	D

Means that do not share a letter are significantly different.

Tukey 95% Simultaneous Confidence Intervals  
All Pairwise Comparisons among Levels of D-Allulose

Individual confidence level = 98.98%

D-Allulose = 0 subtracted from:

D-Allulose	Lower	Center	Upper
10	-3.174	-1.755	-0.336
20	-6.689	-5.270	-3.851
30	-13.199	-11.780	-10.361
40	-14.414	-12.995	-11.576

D-Allulose					-----+-----+-----+-----+-----
10				(*-)	
20			(*-)		
30	(*-)				
40	(*-)				

-----+-----+-----+-----+-----  
-14.0      -7.0      0.0      7.0

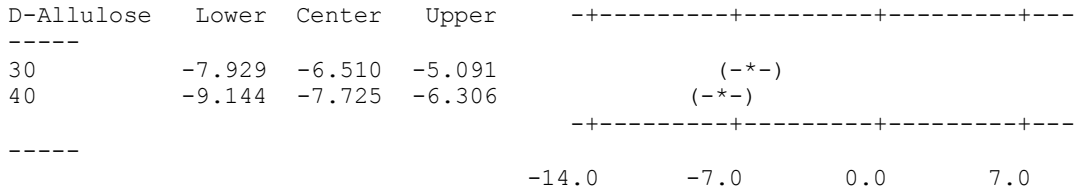
D-Allulose = 10 subtracted from:

D-Allulose	Lower	Center	Upper
20	-4.934	-3.515	-2.096
30	-11.444	-10.025	-8.606
40	-12.659	-11.240	-9.821

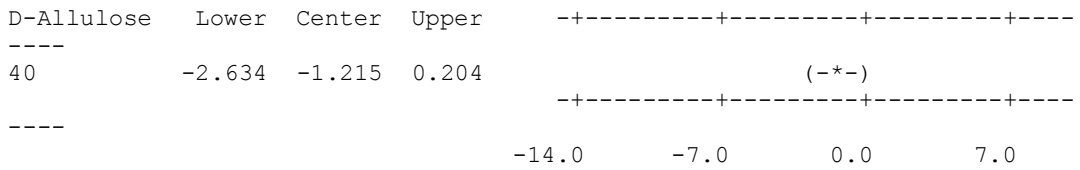
D-Allulose					-----+-----+-----+-----+-----
20			(*-)		
30	(*-)				
40	(*-)				

-----+-----+-----+-----+-----  
-14.0      -7.0      0.0      7.0

D-Allulose = 20 subtracted from:



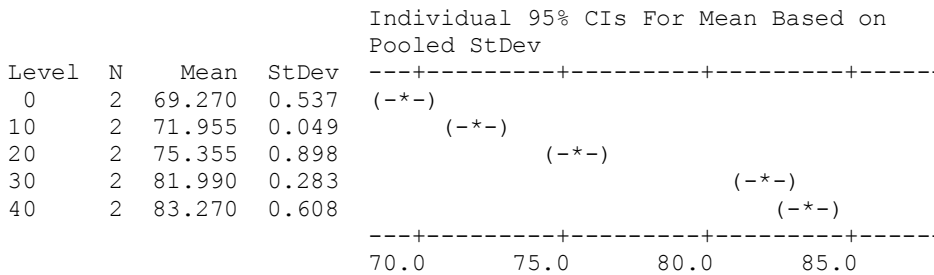
D-Allulose = 30 subtracted from:



### One-way ANOVA: RA3 (%) versus D-Allulose

Source	DF	SS	MS	F	P
D-Allulose	4	300.254	75.063	242.53	0.000
Error	5	1.547	0.309		
Total	9	301.801			

S = 0.5563 R-Sq = 99.49% R-Sq(adj) = 99.08%



Pooled StDev = 0.556

### Grouping Information Using Tukey Method

D-Allulose	N	Mean	Grouping
40	2	83.270	A
30	2	81.990	A
20	2	75.355	B
10	2	71.955	C
0	2	69.270	D

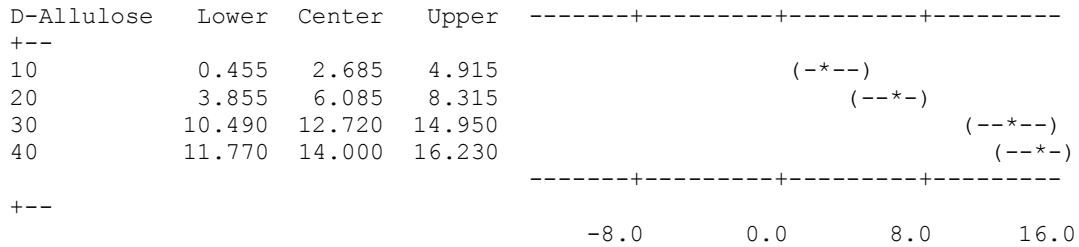
Means that do not share a letter are significantly different.

### Tukey 95% Simultaneous Confidence Intervals

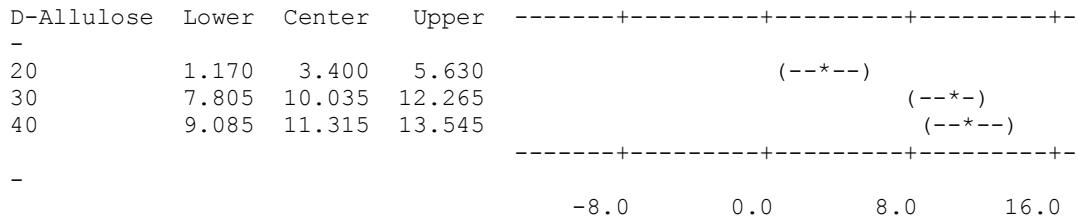
All Pairwise Comparisons among Levels of D-Allulose

Individual confidence level = 98.98%

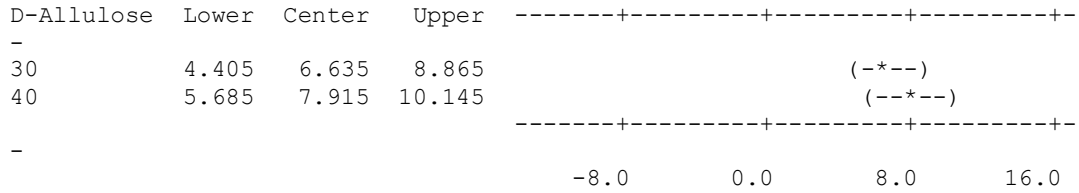
D-Allulose = 0 subtracted from:



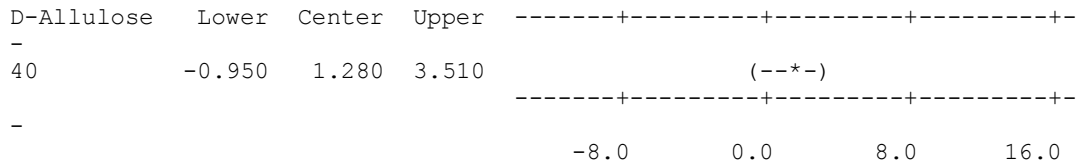
D-Allulose = 10 subtracted from:



D-Allulose = 20 subtracted from:



D-Allulose = 30 subtracted from:

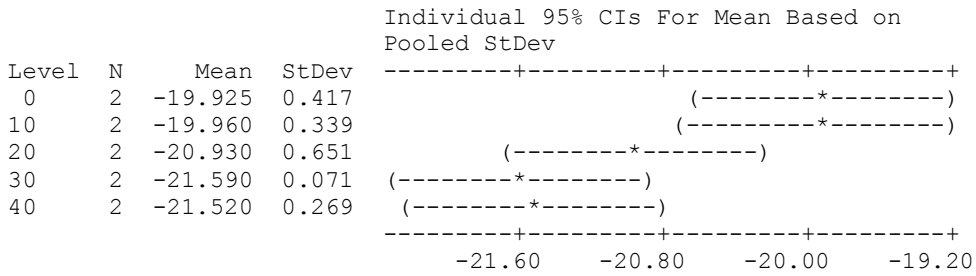


6) One-way ANOVA: Tg versus D-Allulose

Source	DF	SS	MS	F	P
D-Allulose	4	5.259	1.315	8.32	0.020
Error	5	0.790	0.158		
Total	9	6.049			



S = 0.3974 R-Sq = 86.95% R-Sq(adj) = 76.50%



Pooled StDev = 0.397

Grouping Information Using Tukey Method

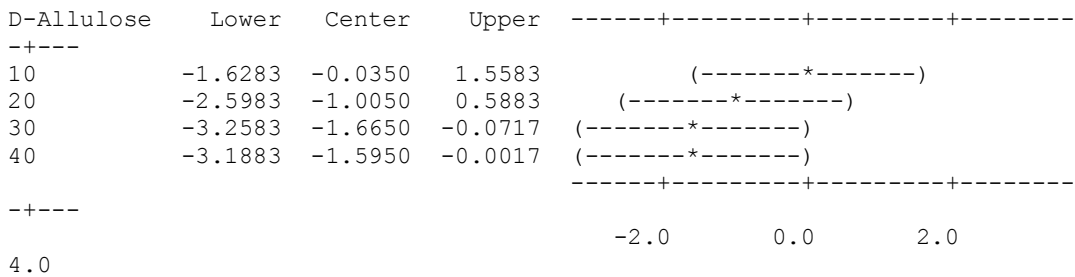
D-Allulose	N	Mean	Grouping
0	2	-19.9250	A
10	2	-19.9600	A B
20	2	-20.9300	A B C
40	2	-21.5200	B C
30	2	-21.5900	C

Means that do not share a letter are significantly different.

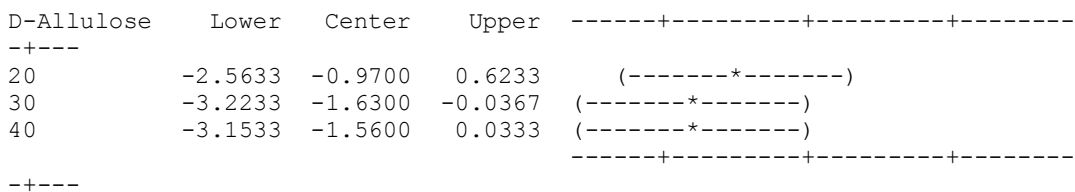
Tukey 95% Simultaneous Confidence Intervals  
All Pairwise Comparisons among Levels of D-Allulose

Individual confidence level = 98.98%

D-Allulose = 0 subtracted from:



D-Allulose = 10 subtracted from:



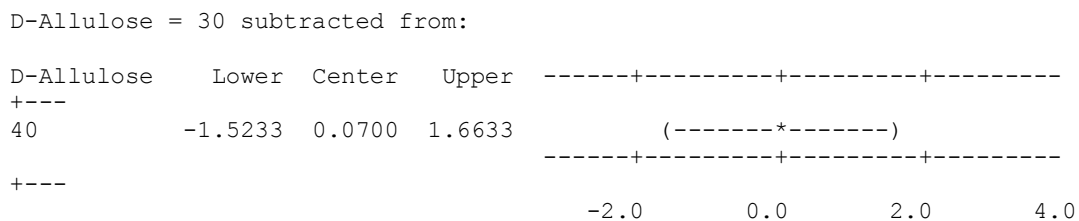
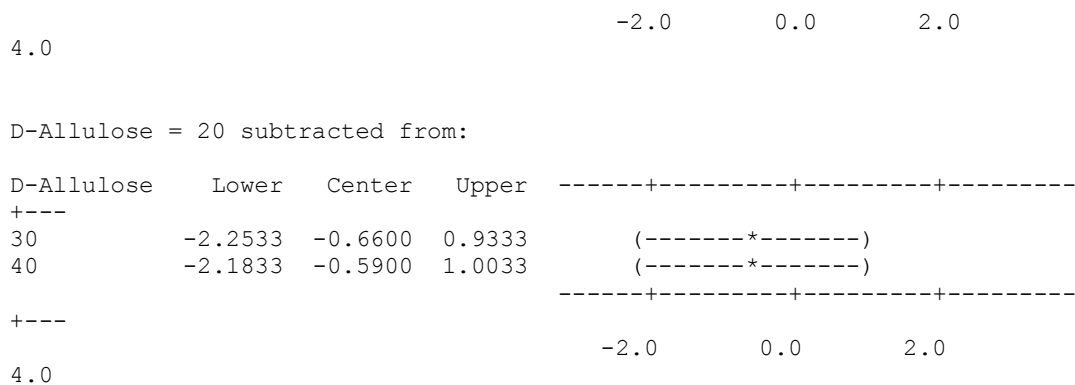
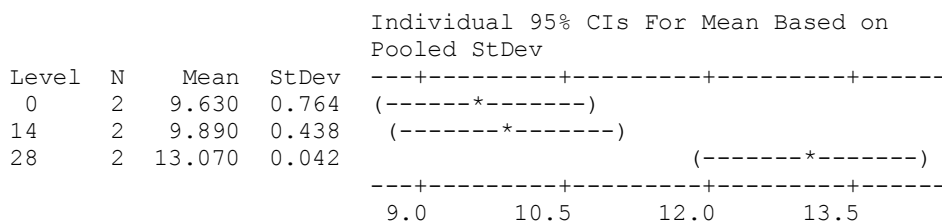


**Table A.4.** Effect of Storage Time on the Gelatin Based Confectionery Gels for each Formulation. 1) Moisture Content (MC %), 2) Water Activity (aw), 3) Hardness, 4) T<sub>1</sub>, 5) T<sub>2</sub> Spectra, 6) Glass transition Temperature (T<sub>g</sub>) for **P0**.

**1) One-way ANOVA: MC (%) - P0 versus day**

Source	DF	SS	MS	F	P
day	2	14.676	7.338	28.32	0.011
Error	3	0.777	0.259		
Total	5	15.453			

S = 0.5090    R-Sq = 94.97%    R-Sq(adj) = 91.62%



Pooled StDev = 0.509

Grouping Information Using Tukey Method

day	N	Mean	Grouping
0	2	9.630	
14	2	9.890	
28	2	13.070	

```

28  2  13.0700  A
14  2   9.8900  B
 0  2   9.6300  B

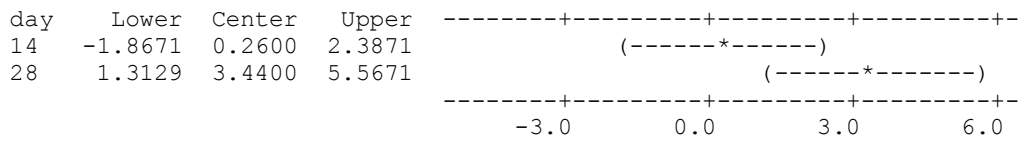
```

Means that do not share a letter are significantly different.

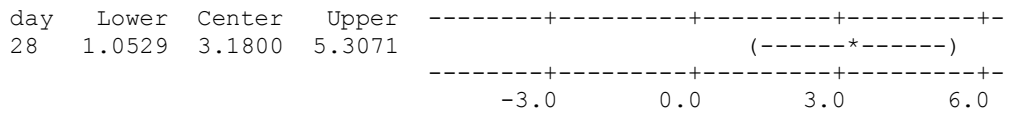
Tukey 95% Simultaneous Confidence Intervals  
All Pairwise Comparisons among Levels of day

Individual confidence level = 97.50%

day = 0 subtracted from:



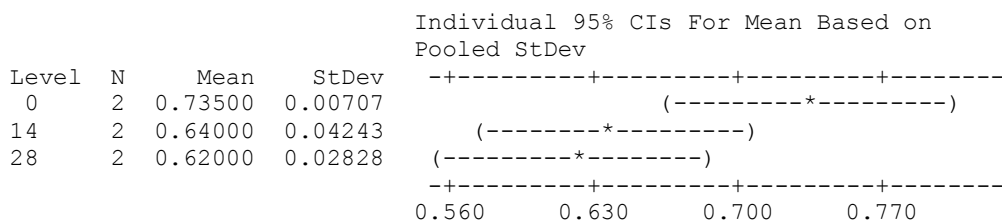
day = 14 subtracted from:



## 2) One-way ANOVA: aw-P0 versus day

Source	DF	SS	MS	F	P
day	2	0.015100	0.007550	8.55	0.058
Error	3	0.002650	0.000883		
Total	5	0.017750			

S = 0.02972 R-Sq = 85.07% R-Sq(adj) = 75.12%



Pooled StDev = 0.02972

Grouping Information Using Tukey Method

day	N	Mean	Grouping
0	2	0.73500	A
14	2	0.64000	A
28	2	0.62000	A

Means that do not share a letter are significantly different.

Tukey 95% Simultaneous Confidence Intervals  
All Pairwise Comparisons among Levels of day

Individual confidence level = 97.50%

day = 0 subtracted from:

day	Lower	Center	Upper	
14	-0.21920	-0.09500	0.02920	(-----*-----)
28	-0.23920	-0.11500	0.00920	(-----*-----)

-----+-----+-----+-----+-----  
-0.20      -0.10      -0.00      0.10

day = 14 subtracted from:

day	Lower	Center	Upper	
28	-0.14420	-0.02000	0.10420	(-----*-----)

-----+-----+-----+-----+-----  
-0.20      -0.10      -0.00      0.10

### 3) One-way ANOVA: Hardness-P0 versus day

Source	DF	SS	MS	F	P
day	2	361.46	180.73	112.43	0.002
Error	3	4.82	1.61		
Total	5	366.28			

S = 1.268    R-Sq = 98.68%    R-Sq(adj) = 97.81%

Individual 95% CIs For Mean Based on  
Pooled StDev

Level	N	Mean	StDev	
0	2	6.550	0.481	(---*---)
14	2	15.010	2.135	(---*---)
28	2	25.525	0.177	(---*---)

-----+-----+-----+-----+-----  
7.0      14.0      21.0      28.0

Pooled StDev = 1.268

Grouping Information Using Tukey Method

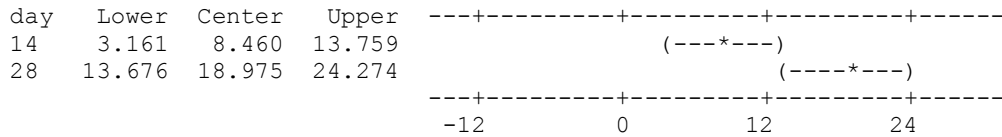
day	N	Mean	Grouping
28	2	25.525	A
14	2	15.010	B
0	2	6.550	C

Means that do not share a letter are significantly different.

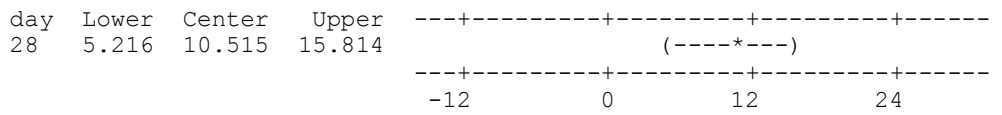
Tukey 95% Simultaneous Confidence Intervals  
 All Pairwise Comparisons among Levels of day

Individual confidence level = 97.50%

day = 0 subtracted from:



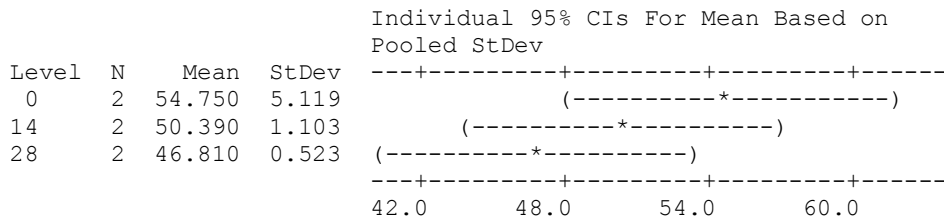
day = 14 subtracted from:



#### 4) One-way ANOVA: T1-P0 versus day

Source	DF	SS	MS	F	P
day	2	63.25	31.62	3.42	0.168
Error	3	27.70	9.23		
Total	5	90.95			

S = 3.039 R-Sq = 69.54% R-Sq(adj) = 49.24%



Pooled StDev = 3.039

Grouping Information Using Tukey Method

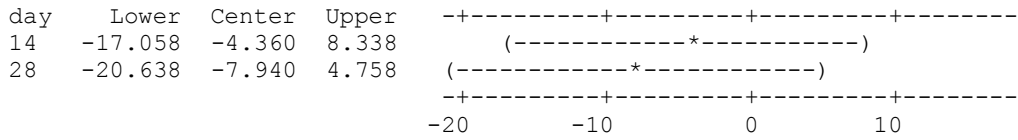
day	N	Mean	Grouping
0	2	54.750	A
14	2	50.390	A
28	2	46.810	A

Means that do not share a letter are significantly different.

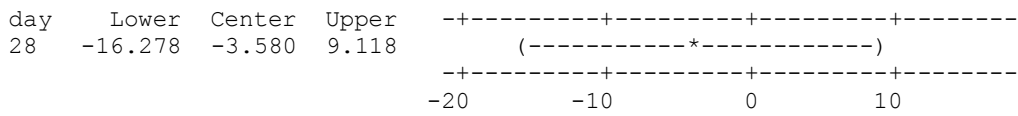
Tukey 95% Simultaneous Confidence Intervals  
 All Pairwise Comparisons among Levels of day

Individual confidence level = 97.50%

day = 0 subtracted from:



day = 14 subtracted from:

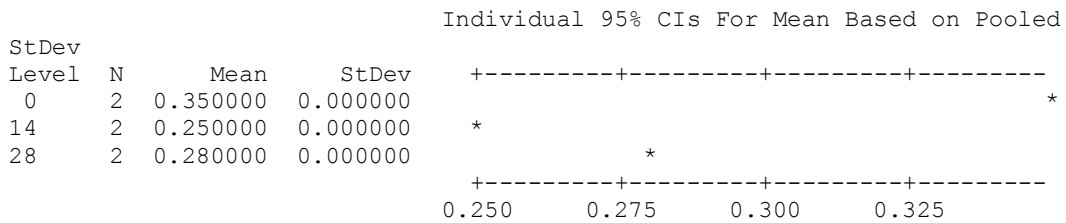


5)

### One-way ANOVA: T2 peak 1-P0 versus day

Source	DF	SS	MS	F	P
day	2	0.0105333	0.0052667	*	*
Error	3	0.0000000	0.0000000		
Total	5	0.0105333			

S = 0 R-Sq = 100.00% R-Sq(adj) = 100.00%



Pooled StDev = 0.000000

Grouping Information Using Tukey Method

day	N	Mean	Grouping
0	2	0.350000	A
28	2	0.280000	B
14	2	0.250000	C

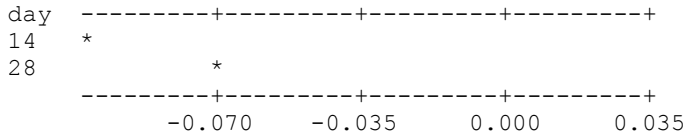
Means that do not share a letter are significantly different.

Tukey 95% Simultaneous Confidence Intervals  
All Pairwise Comparisons among Levels of day

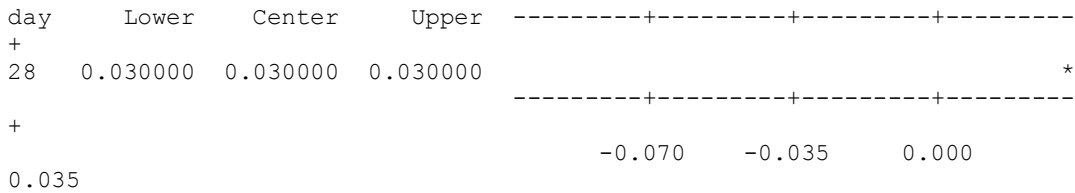
Individual confidence level = 97.50%

day = 0 subtracted from:

day	Lower	Center	Upper
14	-0.100000	-0.100000	-0.100000
28	-0.070000	-0.070000	-0.070000



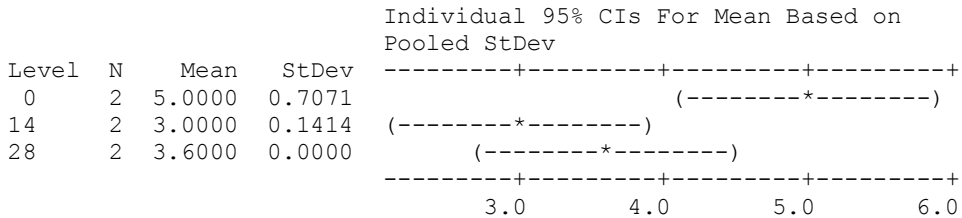
day = 14 subtracted from:



### One-way ANOVA: T2 peak2-P0 versus day

Source	DF	SS	MS	F	P
day	2	4.213	2.107	12.15	0.036
Error	3	0.520	0.173		
Total	5	4.733			

S = 0.4163 R-Sq = 89.01% R-Sq(adj) = 81.69%



Pooled StDev = 0.4163

### Grouping Information Using Tukey Method

day	N	Mean	Grouping
0	2	5.0000	A
28	2	3.6000	A B
14	2	3.0000	B

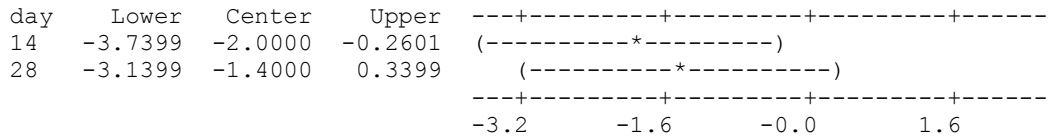
Means that do not share a letter are significantly different.

### Tukey 95% Simultaneous Confidence Intervals

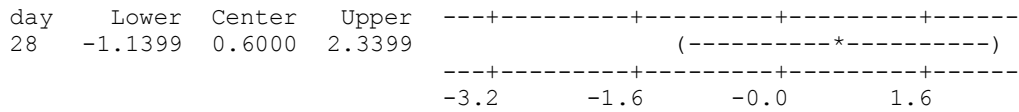
All Pairwise Comparisons among Levels of day

Individual confidence level = 97.50%

day = 0 subtracted from:



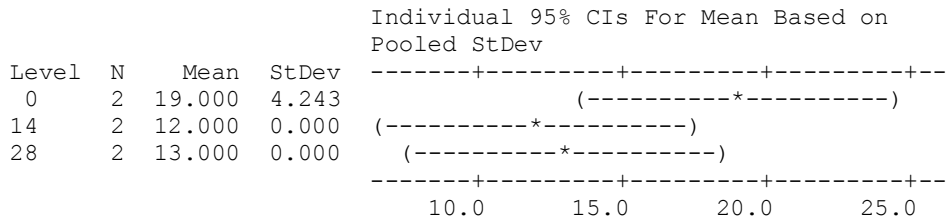
day = 14 subtracted from:



### One-way ANOVA: T2 peak 3 P0 versus day

Source	DF	SS	MS	F	P
day	2	57.33	28.67	4.78	0.117
Error	3	18.00	6.00		
Total	5	75.33			

S = 2.449 R-Sq = 76.11% R-Sq(adj) = 60.18%



Pooled StDev = 2.449

Grouping Information Using Tukey Method

day	N	Mean	Grouping
0	2	19.000	A
28	2	13.000	A
14	2	12.000	A

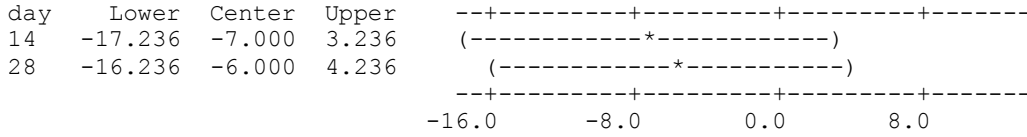
Means that do not share a letter are significantly different.

Tukey 95% Simultaneous Confidence Intervals  
All Pairwise Comparisons among Levels of day

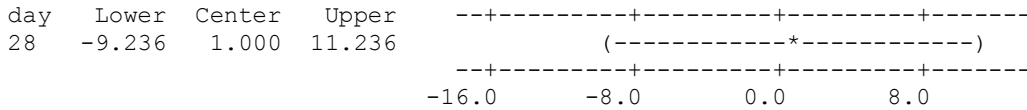
Individual confidence level = 97.50%



day = 0 subtracted from:



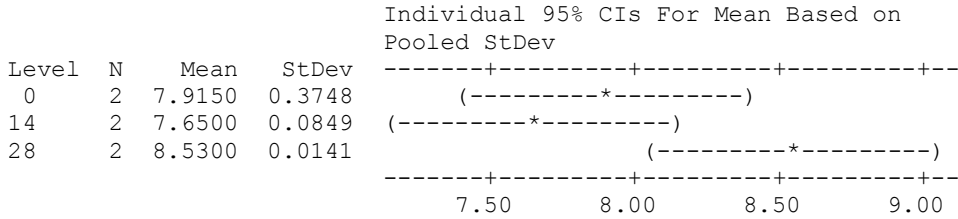
day = 14 subtracted from:



**One-way ANOVA: RA1-P0 versus day**

Source	DF	SS	MS	F	P
day	2	0.8152	0.4076	8.27	0.060
Error	3	0.1478	0.0493		
Total	5	0.9631			

S = 0.2220 R-Sq = 84.65% R-Sq(adj) = 74.41%



Pooled StDev = 0.2220

Grouping Information Using Tukey Method

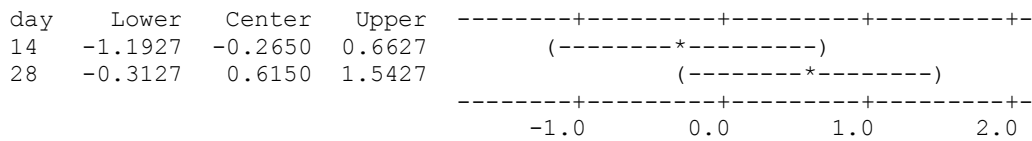
day	N	Mean	Grouping
28	2	8.5300	A
0	2	7.9150	A
14	2	7.6500	A

Means that do not share a letter are significantly different.

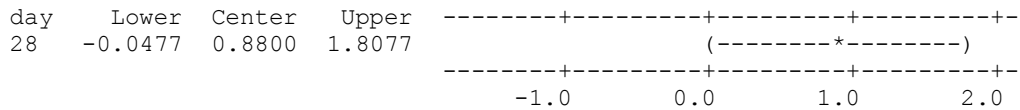
Tukey 95% Simultaneous Confidence Intervals  
All Pairwise Comparisons among Levels of day

Individual confidence level = 97.50%

day = 0 subtracted from:



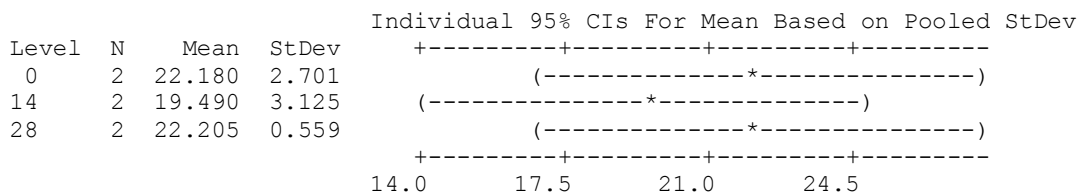
day = 14 subtracted from:



### One-way ANOVA: RA2-P0 versus day

Source	DF	SS	MS	F	P
day	2	9.74	4.87	0.84	0.513
Error	3	17.38	5.79		
Total	5	27.12			

S = 2.407 R-Sq = 35.92% R-Sq(adj) = 0.00%



Pooled StDev = 2.407

### Grouping Information Using Tukey Method

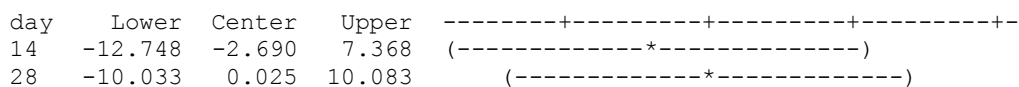
day	N	Mean	Grouping
28	2	22.205	A
0	2	22.180	A
14	2	19.490	A

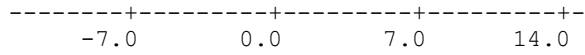
Means that do not share a letter are significantly different.

Tukey 95% Simultaneous Confidence Intervals  
All Pairwise Comparisons among Levels of day

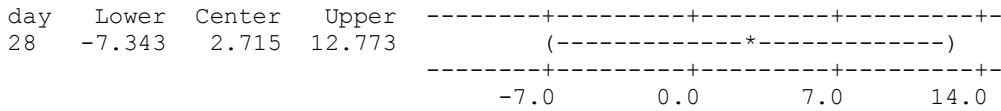
Individual confidence level = 97.50%

day = 0 subtracted from:





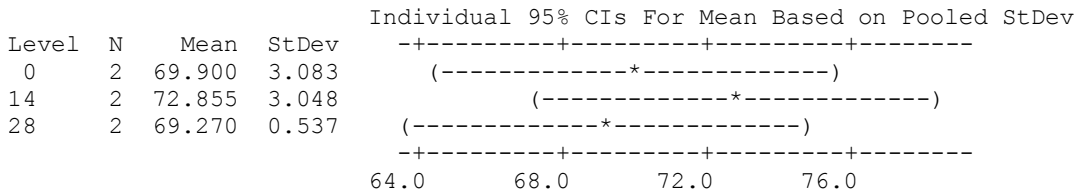
day = 14 subtracted from:



### One-way ANOVA: RA3-P0 versus day

Source	DF	SS	MS	F	P
day	2	14.65	7.33	1.15	0.425
Error	3	19.08	6.36		
Total	5	33.74			

S = 2.522 R-Sq = 43.44% R-Sq(adj) = 5.73%



Pooled StDev = 2.522

### Grouping Information Using Tukey Method

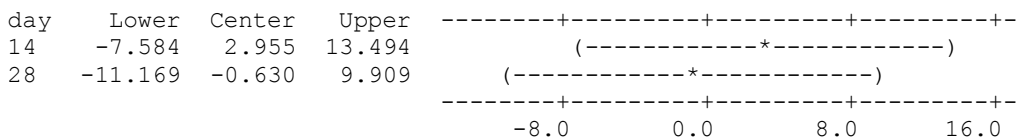
day	N	Mean	Grouping
14	2	72.855	A
0	2	69.900	A
28	2	69.270	A

Means that do not share a letter are significantly different.

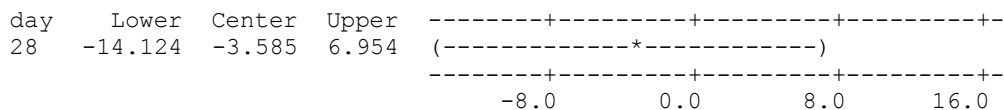
Tukey 95% Simultaneous Confidence Intervals  
All Pairwise Comparisons among Levels of day

Individual confidence level = 97.50%

day = 0 subtracted from:



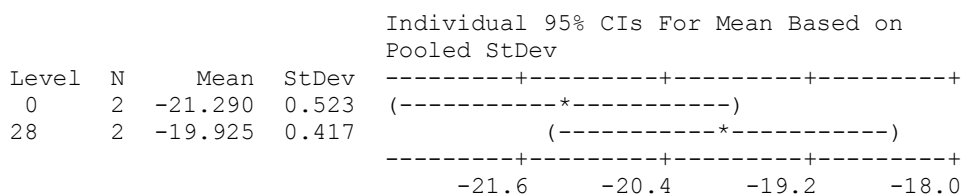
day = 14 subtracted from:



### 6) One-way ANOVA: Tg-P0 versus day

Source	DF	SS	MS	F	P
day	1	1.863	1.863	8.32	0.102
Error	2	0.448	0.224		
Total	3	2.311			

S = 0.4732    R-Sq = 80.62%    R-Sq(adj) = 70.93%



Pooled StDev = 0.473

Grouping Information Using Tukey Method

day	N	Mean	Grouping
28	2	-19.9250	A
0	2	-21.2900	A

Means that do not share a letter are significantly different.

Tukey 95% Simultaneous Confidence Intervals  
All Pairwise Comparisons among Levels of day

Individual confidence level = 95.00%

day = 0 subtracted from:

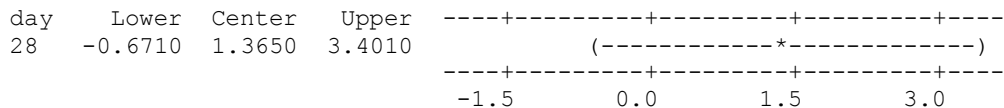
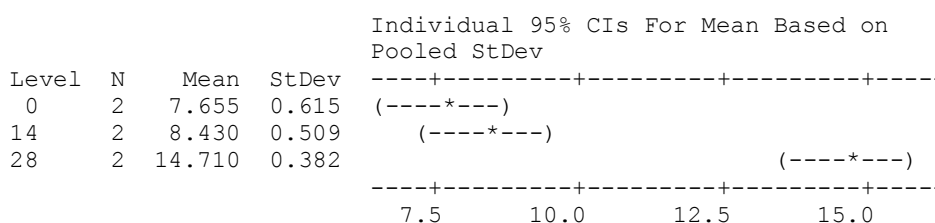


**Table A.5.** Effect of Storage Time on the Gelatin Based Confectionery Gels for each Formulation. 1) Moisture Content (MC %), 2) Water Activity (aw), 3) Hardness, 4) T<sub>1</sub>, 5) T<sub>2</sub> Spectra, 6) Glass transition Temperature (T<sub>g</sub>) for **P10**.

**1) One-way ANOVA: MC (%)-P10 versus day**

Source	DF	SS	MS	F	P
day	2	59.875	29.937	114.64	0.001
Error	3	0.783	0.261		
Total	5	60.658			

S = 0.5110    R-Sq = 98.71%    R-Sq(adj) = 97.85%



Pooled StDev = 0.511

Grouping Information Using Tukey Method

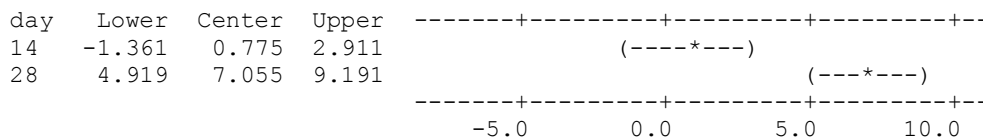
day	N	Mean	Grouping
28	2	14.710	A
14	2	8.430	B
0	2	7.655	B

Means that do not share a letter are significantly different.

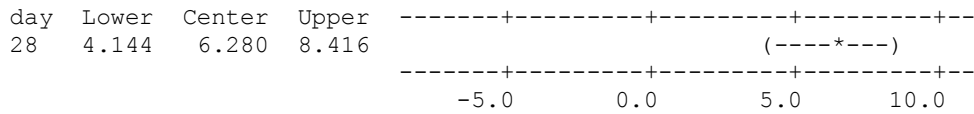
Tukey 95% Simultaneous Confidence Intervals  
All Pairwise Comparisons among Levels of day

Individual confidence level = 97.50%

day = 0 subtracted from:



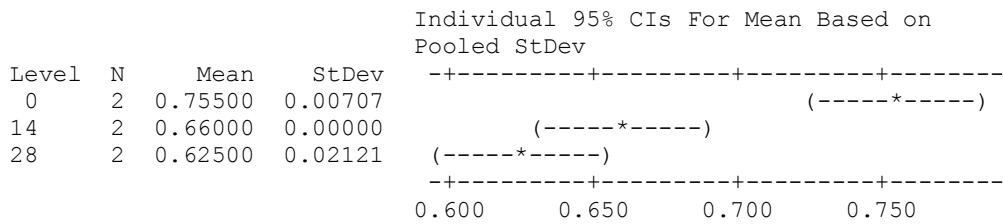
day = 14 subtracted from:



## 2) One-way ANOVA: aw-P10 versus day

Source	DF	SS	MS	F	P
day	2	0.018100	0.009050	54.30	0.004
Error	3	0.000500	0.000167		
Total	5	0.018600			

S = 0.01291    R-Sq = 97.31%    R-Sq(adj) = 95.52%



Pooled StDev = 0.01291

### Grouping Information Using Tukey Method

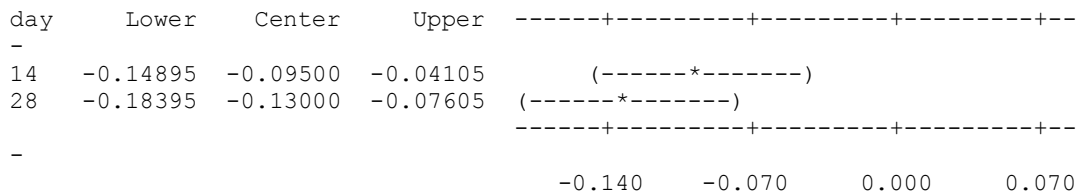
day	N	Mean	Grouping
0	2	0.75500	A
14	2	0.66000	B
28	2	0.62500	B

Means that do not share a letter are significantly different.

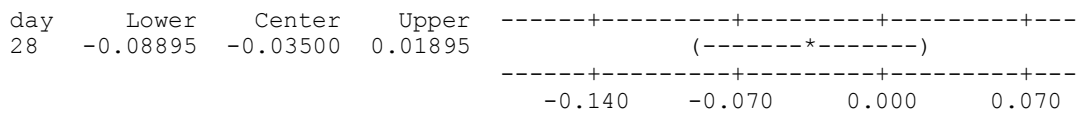
### Tukey 95% Simultaneous Confidence Intervals All Pairwise Comparisons among Levels of day

Individual confidence level = 97.50%

day = 0 subtracted from:



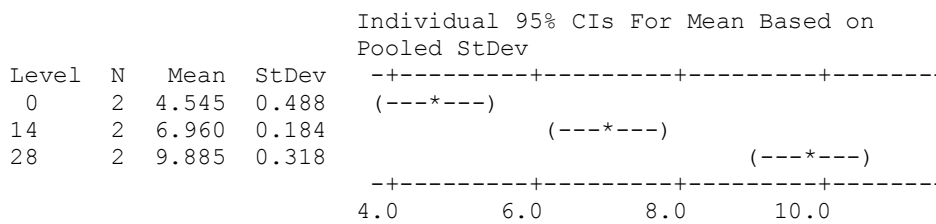
day = 14 subtracted from:



### 3) One-way ANOVA: hardness-P10 versus day

Source	DF	SS	MS	F	P
day	2	28.602	14.301	114.99	0.001
Error	3	0.373	0.124		
Total	5	28.975			

S = 0.3527    R-Sq = 98.71%    R-Sq(adj) = 97.85%



Pooled StDev = 0.353

Grouping Information Using Tukey Method

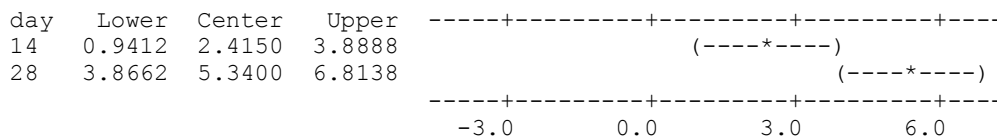
day	N	Mean	Grouping
28	2	9.8850	A
14	2	6.9600	B
0	2	4.5450	C

Means that do not share a letter are significantly different.

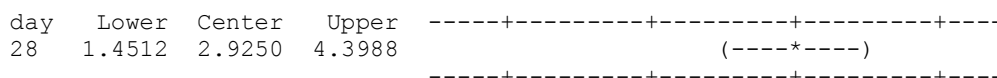
Tukey 95% Simultaneous Confidence Intervals  
All Pairwise Comparisons among Levels of day

Individual confidence level = 97.50%

day = 0 subtracted from:



day = 14 subtracted from:

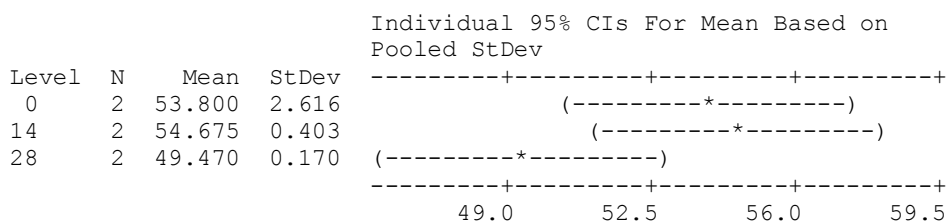


-3.0      0.0      3.0      6.0

#### 4) One-way ANOVA: T1-P10 versus day

Source	DF	SS	MS	F	P
day	2	31.07	15.54	6.62	0.079
Error	3	7.04	2.35		
Total	5	38.11			

S = 1.531    R-Sq = 81.54%    R-Sq(adj) = 69.23%



Pooled StDev = 1.531

#### Grouping Information Using Tukey Method

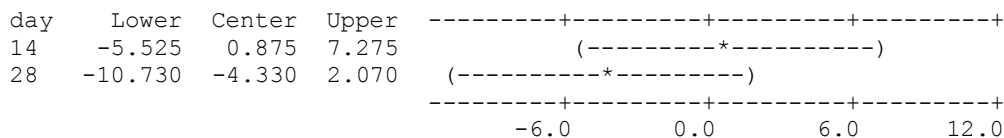
day	N	Mean	Grouping
14	2	54.675	A
0	2	53.800	A
28	2	49.470	A

Means that do not share a letter are significantly different.

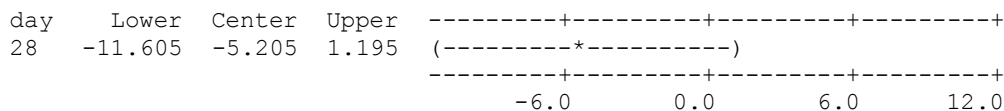
Tukey 95% Simultaneous Confidence Intervals  
All Pairwise Comparisons among Levels of day

Individual confidence level = 97.50%

day = 0 subtracted from:



day = 14 subtracted from:





5)

**One-way ANOVA: T2 peak 1-P10 versus day**

Source	DF	SS	MS	F	P
day	2	0.000133	0.000067	0.50	0.650
Error	3	0.000400	0.000133		
Total	5	0.000533			

S = 0.01155 R-Sq = 25.00% R-Sq(adj) = 0.00%

Individual 95% CIs For Mean Based on Pooled StDev

Level	N	Mean	StDev
0	2	0.34000	0.01414
14	2	0.34000	0.01414
28	2	0.35000	0.00000

0.320      0.336      0.352      0.368

Pooled StDev = 0.01155

Grouping Information Using Tukey Method

day	N	Mean	Grouping
28	2	0.35000	A
14	2	0.34000	A
0	2	0.34000	A

Means that do not share a letter are significantly different.

Tukey 95% Simultaneous Confidence Intervals  
All Pairwise Comparisons among Levels of day

Individual confidence level = 97.50%

day = 0 subtracted from:

day	Lower	Center	Upper
14	-0.04825	0.00000	0.04825
28	-0.03825	0.01000	0.05825

0.060

-0.030      0.000      0.030

day = 14 subtracted from:

day	Lower	Center	Upper
28	-0.03825	0.01000	0.05825

0.060 -0.030 0.000 0.030

**One-way ANOVA: T2 peak 1-P10 versus day**

Source	DF	SS	MS	F	P
day	2	0.000133	0.000067	0.50	0.650
Error	3	0.000400	0.000133		
Total	5	0.000533			

S = 0.01155 R-Sq = 25.00% R-Sq(adj) = 0.00%

Individual 95% CIs For Mean Based on Pooled StDev

Level	N	Mean	StDev
0	2	0.34000	0.01414
14	2	0.34000	0.01414
28	2	0.35000	0.00000

0.320 0.336 0.352 0.368

Pooled StDev = 0.01155

Grouping Information Using Tukey Method

day	N	Mean	Grouping
28	2	0.35000	A
14	2	0.34000	A
0	2	0.34000	A

Means that do not share a letter are significantly different.

Tukey 95% Simultaneous Confidence Intervals  
All Pairwise Comparisons among Levels of day

Individual confidence level = 97.50%

day = 0 subtracted from:

day	Lower	Center	Upper
14	-0.04825	0.00000	0.04825
28	-0.03825	0.01000	0.05825

0.060 -0.030 0.000 0.030

day = 14 subtracted from:

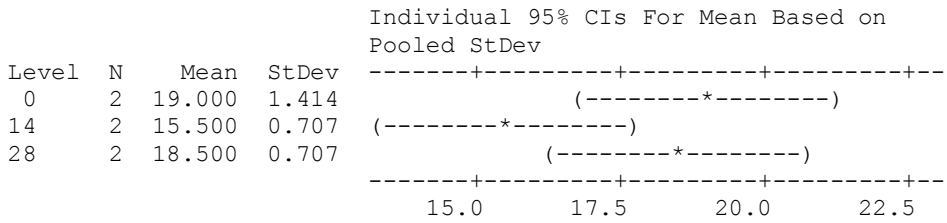
day	Lower	Center	Upper
28	-0.03825	0.01000	0.05825

0.060 -0.030 0.000 0.030

**One-way ANOVA: T2 peak 3 P10 versus day**

Source	DF	SS	MS	F	P
day	2	14.33	7.17	7.17	0.072
Error	3	3.00	1.00		
Total	5	17.33			

S = 1 R-Sq = 82.69% R-Sq(adj) = 71.15%



Pooled StDev = 1.000

Grouping Information Using Tukey Method

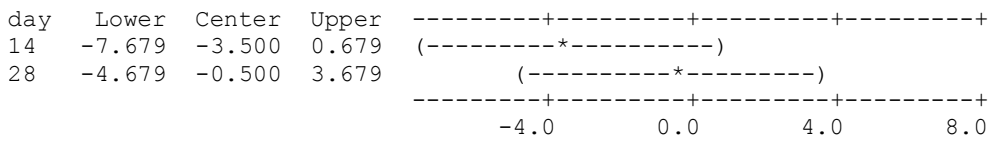
day	N	Mean	Grouping
0	2	19.000	A
28	2	18.500	A
14	2	15.500	A

Means that do not share a letter are significantly different.

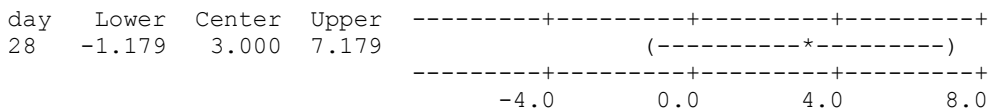
Tukey 95% Simultaneous Confidence Intervals  
All Pairwise Comparisons among Levels of day

Individual confidence level = 97.50%

day = 0 subtracted from:



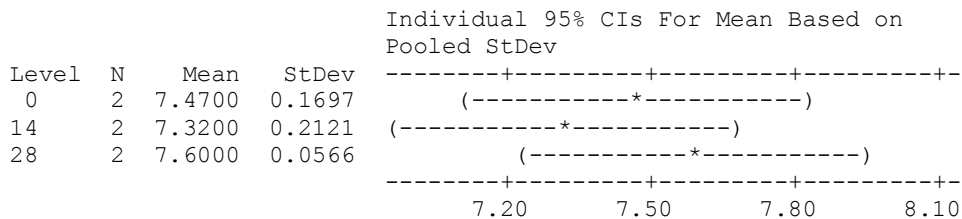
day = 14 subtracted from:



**One-way ANOVA: RA1-P10 versus day**

Source	DF	SS	MS	F	P
day	2	0.0785	0.0393	1.53	0.348
Error	3	0.0770	0.0257		
Total	5	0.1555			

S = 0.1602    R-Sq = 50.49%    R-Sq(adj) = 17.49%



Pooled StDev = 0.1602

Grouping Information Using Tukey Method

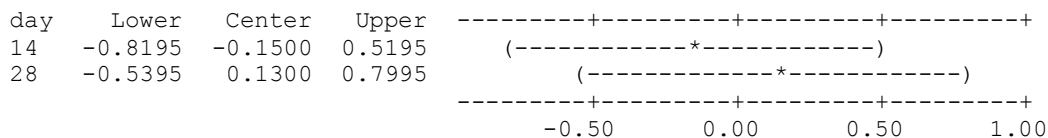
day	N	Mean	Grouping
28	2	7.6000	A
0	2	7.4700	A
14	2	7.3200	A

Means that do not share a letter are significantly different.

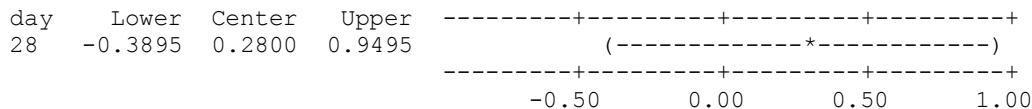
Tukey 95% Simultaneous Confidence Intervals  
All Pairwise Comparisons among Levels of day

Individual confidence level = 97.50%

day = 0 subtracted from:



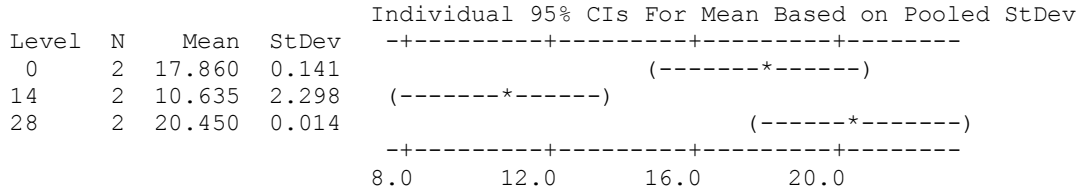
day = 14 subtracted from:



**One-way ANOVA: RA2-P10 versus day**

Source	DF	SS	MS	F	P
day	2	103.50	51.75	29.28	0.011
Error	3	5.30	1.77		
Total	5	108.80			

S = 1.329 R-Sq = 95.13% R-Sq(adj) = 91.88%



Pooled StDev = 1.329

Grouping Information Using Tukey Method

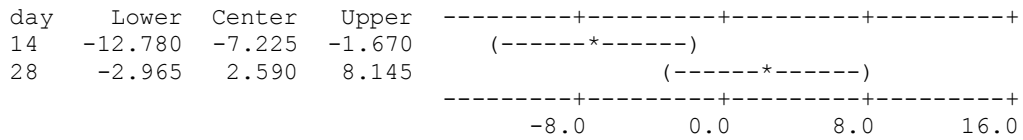
day	N	Mean	Grouping
28	2	20.450	A
0	2	17.860	A
14	2	10.635	B

Means that do not share a letter are significantly different.

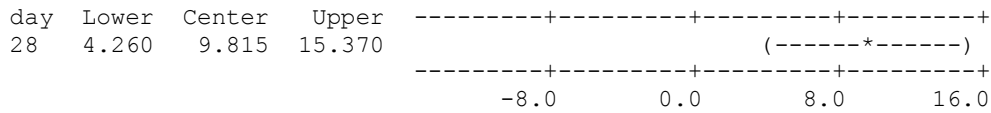
Tukey 95% Simultaneous Confidence Intervals  
All Pairwise Comparisons among Levels of day

Individual confidence level = 97.50%

day = 0 subtracted from:



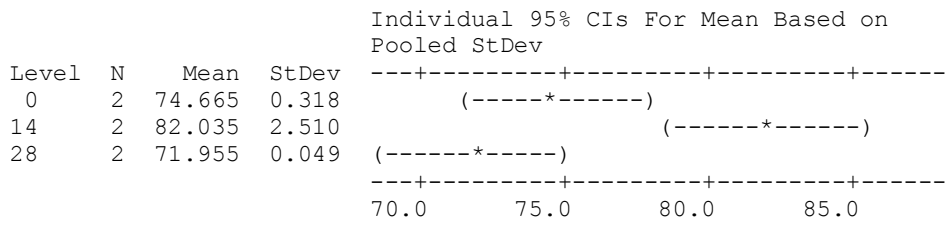
day = 14 subtracted from:



**One-way ANOVA: RA3-P10 versus day**

Source	DF	SS	MS	F	P
day	2	108.84	54.42	25.49	0.013
Error	3	6.40	2.13		
Total	5	115.25			

S = 1.461 R-Sq = 94.44% R-Sq(adj) = 90.74%



Pooled StDev = 1.461

Grouping Information Using Tukey Method

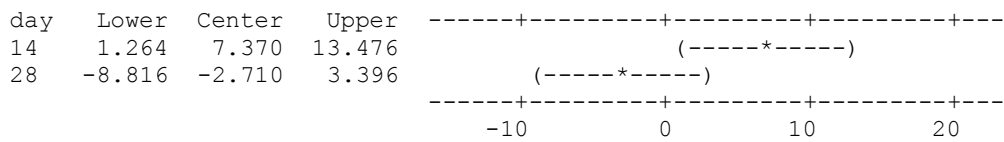
day	N	Mean	Grouping
14	2	82.035	A
0	2	74.665	B
28	2	71.955	B

Means that do not share a letter are significantly different.

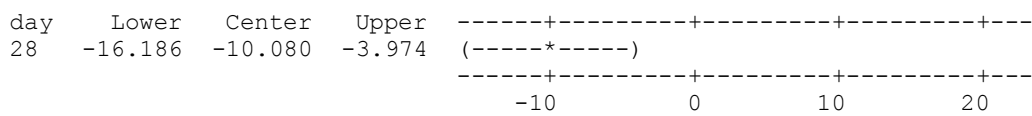
Tukey 95% Simultaneous Confidence Intervals  
All Pairwise Comparisons among Levels of day

Individual confidence level = 97.50%

day = 0 subtracted from:



day = 14 subtracted from:



6) One-way ANOVA: Tg-P10 versus day

Source	DF	SS	MS	F	P
day	1	1.2882	1.2882	21.61	0.043
Error	2	0.1193	0.0596		
Total	3	1.4075			

S = 0.2442 R-Sq = 91.53% R-Sq(adj) = 87.29%

Individual 95% CIs For Mean Based on Pooled

Level	N	Mean	StDev
0	2	-21.095	0.064
28	2	-19.960	0.339

-21.70      -21.00      -20.30      -19.60

Pooled StDev = 0.244

Grouping Information Using Tukey Method

day	N	Mean	Grouping
28	2	-19.9600	A
0	2	-21.0950	B

Means that do not share a letter are significantly different.

Tukey 95% Simultaneous Confidence Intervals  
All Pairwise Comparisons among Levels of day

Individual confidence level = 95.00%

day = 0 subtracted from:

day	Lower	Center	Upper
28	0.0844	1.1350	2.1856

-1.0      0.0      1.0      2.0

**Table A.6.** Effect of Storage Time on the Gelatin Based Confectionery Gels for each Formulation. 1) Moisture Content (MC %), 2) Water Activity (aw), 3) Hardness, 4) T<sub>1</sub>, 5) T<sub>2</sub> Spectra, 6) Glass transition Temperature (T<sub>g</sub>) for **P20**.

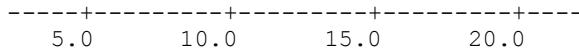
**1) One-way ANOVA: MC (%)-P20 versus day**

Source	DF	SS	MS	F	P
day	2	70.93	35.47	5.67	0.096
Error	3	18.78	6.26		
Total	5	89.71			

S = 2.502      R-Sq = 79.07%      R-Sq(adj) = 65.12%

Individual 95% CIs For Mean Based on Pooled StDev

Level	N	Mean	StDev
0	2	8.060	0.665
14	2	12.440	1.881
28	2	16.480	3.847



Pooled StDev = 2.502

Grouping Information Using Tukey Method

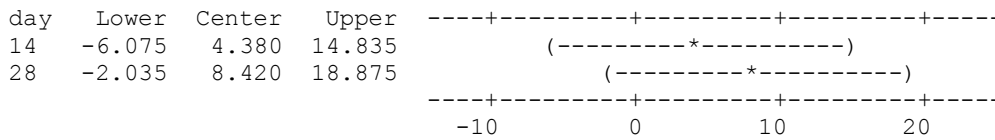
day	N	Mean	Grouping
28	2	16.480	A
14	2	12.440	A
0	2	8.060	A

Means that do not share a letter are significantly different.

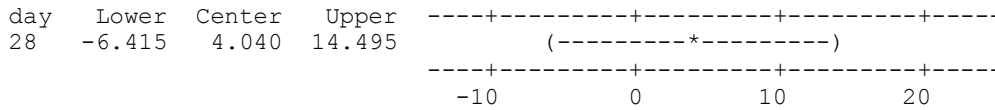
Tukey 95% Simultaneous Confidence Intervals  
All Pairwise Comparisons among Levels of day

Individual confidence level = 97.50%

day = 0 subtracted from:



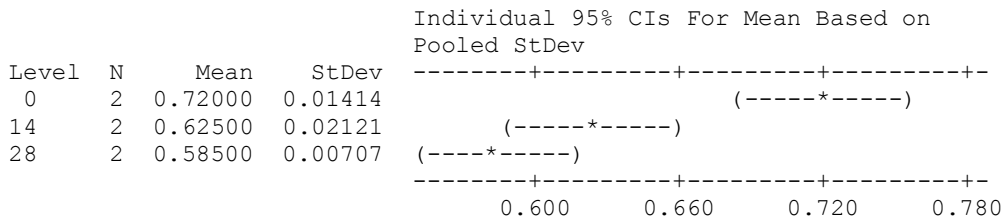
day = 14 subtracted from:



## 2) One-way ANOVA: aw-P20 versus day

Source	DF	SS	MS	F	P
day	2	0.019233	0.009617	41.21	0.007
Error	3	0.000700	0.000233		
Total	5	0.019933			

S = 0.01528 R-Sq = 96.49% R-Sq(adj) = 94.15%





Pooled StDev = 0.01528

Grouping Information Using Tukey Method

day	N	Mean	Grouping
0	2	0.72000	A
14	2	0.62500	B
28	2	0.58500	B

Means that do not share a letter are significantly different.

Tukey 95% Simultaneous Confidence Intervals  
All Pairwise Comparisons among Levels of day

Individual confidence level = 97.50%

day = 0 subtracted from:

day	Lower	Center	Upper	
14	-0.15884	-0.09500	-0.03116	(-----*-----)
28	-0.19884	-0.13500	-0.07116	(-----*-----)

-----+-----+-----+-----+-----  
-0.160    -0.080    0.000    0.080

day = 14 subtracted from:

day	Lower	Center	Upper	
28	-0.10384	-0.04000	0.02384	(-----*-----)

-----+-----+-----+-----+-----  
-0.160    -0.080    0.000    0.080

### 3) One-way ANOVA: hardness-P20 versus day

Source	DF	SS	MS	F	P
day	2	35.056	17.528	74.94	0.003
Error	3	0.702	0.234		
Total	5	35.758			

S = 0.4836    R-Sq = 98.04%    R-Sq(adj) = 96.73%

Individual 95% CIs For Mean Based on Pooled StDev

Level	N	Mean	StDev	
0	2	3.545	0.049	(---*---)
14	2	6.420	0.622	(-----*-----)
28	2	9.465	0.559	(-----*-----)

-----+-----+-----+-----+-----  
2.5    5.0    7.5    10.0

Pooled StDev = 0.484

Grouping Information Using Tukey Method

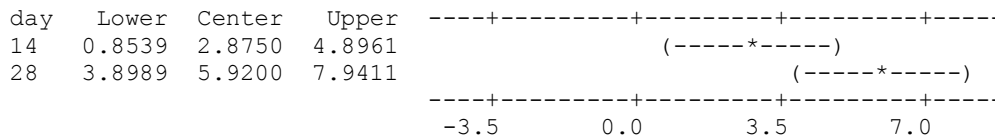
day	N	Mean	Grouping
28	2	9.4650	A
14	2	6.4200	B
0	2	3.5450	C

Means that do not share a letter are significantly different.

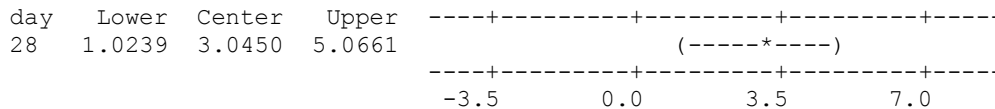
Tukey 95% Simultaneous Confidence Intervals  
All Pairwise Comparisons among Levels of day

Individual confidence level = 97.50%

day = 0 subtracted from:



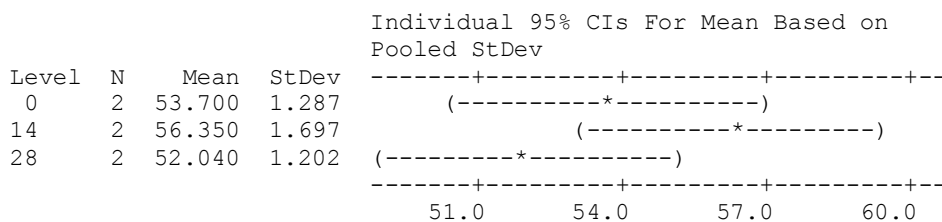
day = 14 subtracted from:



**4) One-way ANOVA: T1-P20 versus day**

Source	DF	SS	MS	F	P
day	2	18.90	9.45	4.74	0.118
Error	3	5.98	1.99		
Total	5	24.88			

S = 1.412 R-Sq = 75.96% R-Sq(adj) = 59.94%



Pooled StDev = 1.412

Grouping Information Using Tukey Method

day	N	Mean	Grouping
14	2	56.350	A
0	2	53.700	A
28	2	52.040	A

Means that do not share a letter are significantly different.

Tukey 95% Simultaneous Confidence Intervals  
All Pairwise Comparisons among Levels of day

Individual confidence level = 97.50%

day = 0 subtracted from:

day	Lower	Center	Upper
14	-3.251	2.650	8.551
28	-7.561	-1.660	4.241

day = 14 subtracted from:

day	Lower	Center	Upper
28	-10.211	-4.310	1.591

5)

### One-way ANOVA: T2 peak 1 P20 versus day

Source	DF	SS	MS	F	P
day	2	0.003333	0.001667	3.70	0.155
Error	3	0.001350	0.000450		
Total	5	0.004683			

S = 0.02121 R-Sq = 71.17% R-Sq(adj) = 51.96%

Individual 95% CIs For Mean Based on Pooled StDev

Level	N	Mean	StDev
0	2	0.36500	0.02121
14	2	0.31500	0.02121
28	2	0.36500	0.02121

Pooled StDev = 0.02121

Grouping Information Using Tukey Method

day	N	Mean	Grouping
28	2	0.36500	A

```

0 2 0.36500 A
14 2 0.31500 A

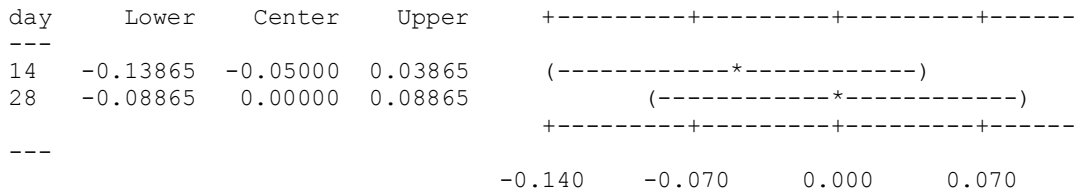
```

Means that do not share a letter are significantly different.

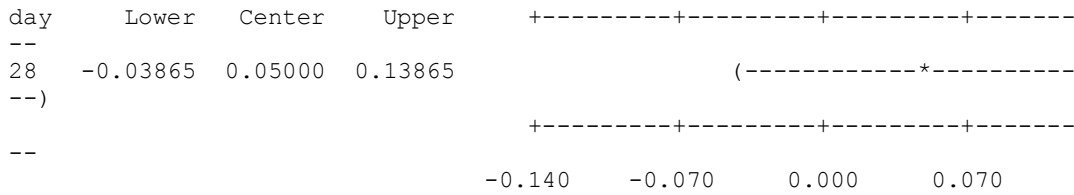
Tukey 95% Simultaneous Confidence Intervals  
All Pairwise Comparisons among Levels of day

Individual confidence level = 97.50%

day = 0 subtracted from:



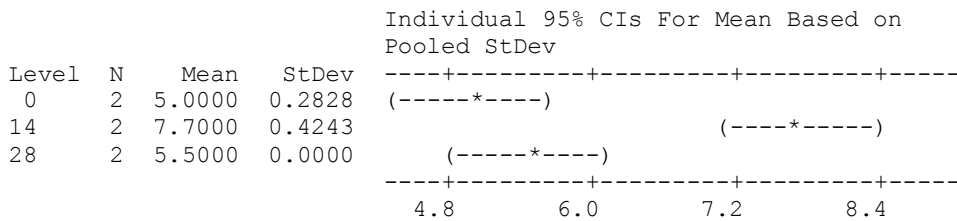
day = 14 subtracted from:



### One-way ANOVA: T2 peak 2 P20 versus day

Source	DF	SS	MS	F	P
day	2	8.2533	4.1267	47.62	0.005
Error	3	0.2600	0.0867		
Total	5	8.5133			

S = 0.2944 R-Sq = 96.95% R-Sq(adj) = 94.91%



Pooled StDev = 0.2944

Grouping Information Using Tukey Method

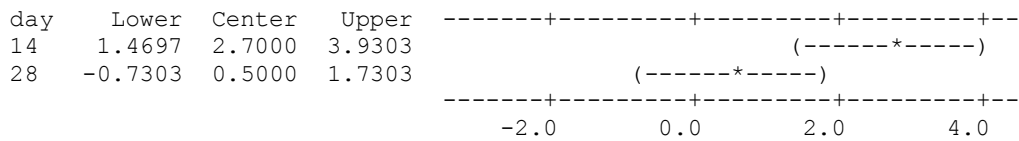
day	N	Mean	Grouping
14	2	7.7000	A
28	2	5.5000	B
0	2	5.0000	B

Means that do not share a letter are significantly different.

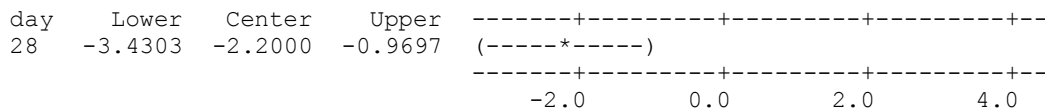
Tukey 95% Simultaneous Confidence Intervals  
All Pairwise Comparisons among Levels of day

Individual confidence level = 97.50%

day = 0 subtracted from:



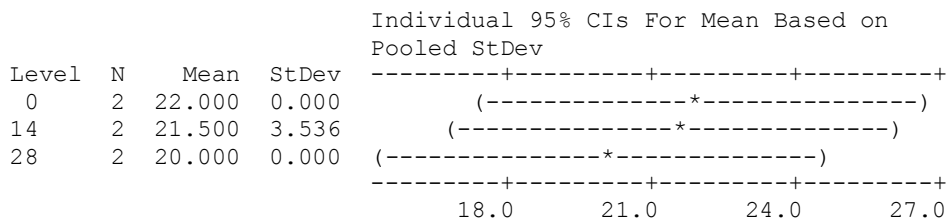
day = 14 subtracted from:



### One-way ANOVA: T2 peak 3 P20 versus day

Source	DF	SS	MS	F	P
day	2	4.33	2.17	0.52	0.640
Error	3	12.50	4.17		
Total	5	16.83			

S = 2.041 R-Sq = 25.74% R-Sq(adj) = 0.00%



Pooled StDev = 2.041

Grouping Information Using Tukey Method

day	N	Mean	Grouping
0	2	22.000	A
14	2	21.500	A

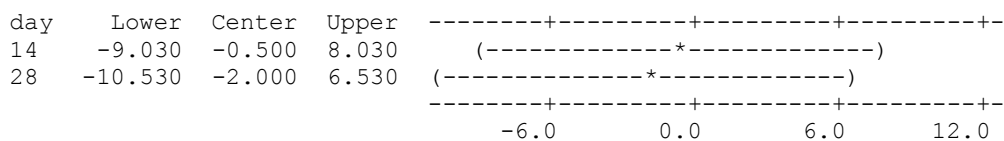
28 2 20.000 A

Means that do not share a letter are significantly different.

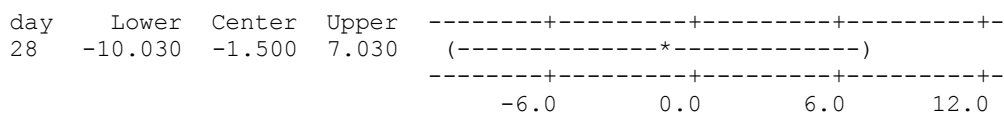
Tukey 95% Simultaneous Confidence Intervals  
All Pairwise Comparisons among Levels of day

Individual confidence level = 97.50%

day = 0 subtracted from:



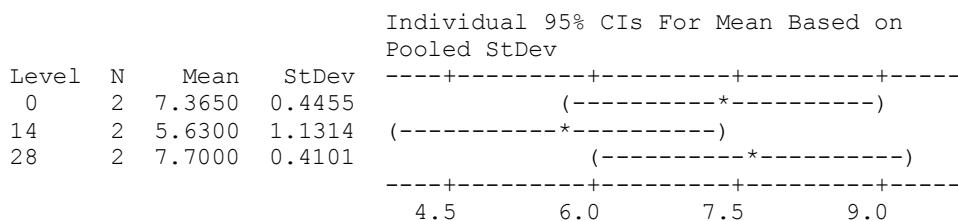
day = 14 subtracted from:



### One-way ANOVA: RA1-P20 versus day

Source	DF	SS	MS	F	P
day	2	4.938	2.469	4.50	0.125
Error	3	1.647	0.549		
Total	5	6.585			

S = 0.7409 R-Sq = 74.99% R-Sq(adj) = 58.32%



Pooled StDev = 0.7409

Grouping Information Using Tukey Method

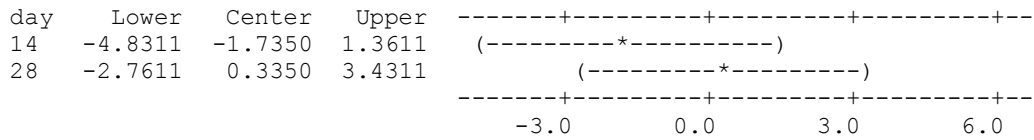
day	N	Mean	Grouping
28	2	7.7000	A
0	2	7.3650	A
14	2	5.6300	A

Means that do not share a letter are significantly different.

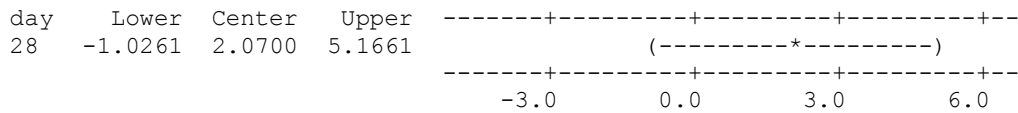
Tukey 95% Simultaneous Confidence Intervals  
 All Pairwise Comparisons among Levels of day

Individual confidence level = 97.50%

day = 0 subtracted from:



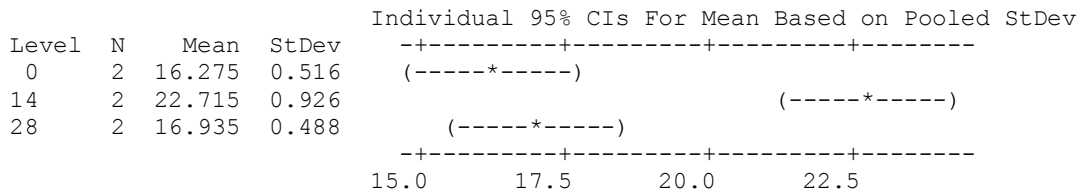
day = 14 subtracted from:



### One-way ANOVA: RA2-P20 versus day

Source	DF	SS	MS	F	P
day	2	50.212	25.106	55.28	0.004
Error	3	1.363	0.454		
Total	5	51.574			

S = 0.6739 R-Sq = 97.36% R-Sq(adj) = 95.60%



Pooled StDev = 0.674

Grouping Information Using Tukey Method

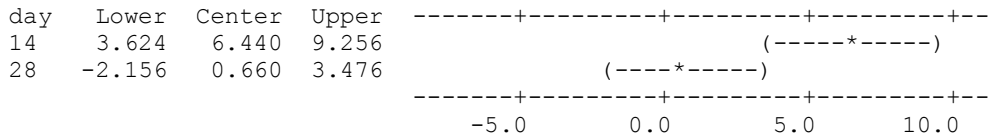
day	N	Mean	Grouping
14	2	22.715	A
28	2	16.935	B
0	2	16.275	B

Means that do not share a letter are significantly different.

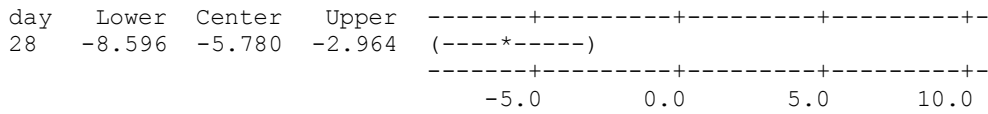
Tukey 95% Simultaneous Confidence Intervals  
 All Pairwise Comparisons among Levels of day

Individual confidence level = 97.50%

day = 0 subtracted from:



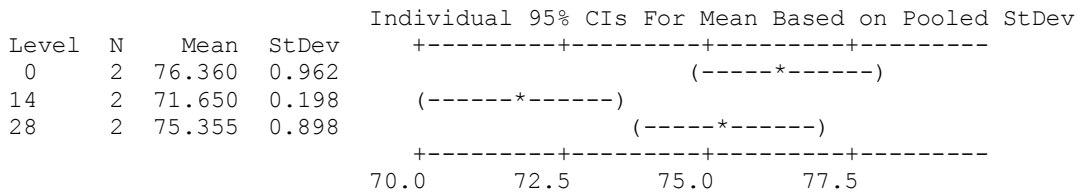
day = 14 subtracted from:



### One-way ANOVA: RA3-P20 versus day

Source	DF	SS	MS	F	P
day	2	24.614	12.307	20.85	0.017
Error	3	1.770	0.590		
Total	5	26.385			

S = 0.7682 R-Sq = 93.29% R-Sq(adj) = 88.82%



Pooled StDev = 0.768

Grouping Information Using Tukey Method

day	N	Mean	Grouping
0	2	76.3600	A
28	2	75.3550	A
14	2	71.6500	B

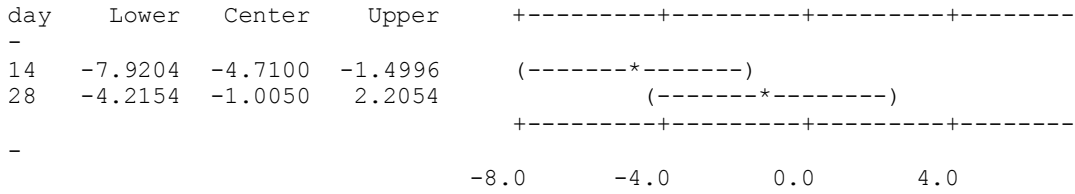
Means that do not share a letter are significantly different.

Tukey 95% Simultaneous Confidence Intervals  
All Pairwise Comparisons among Levels of day

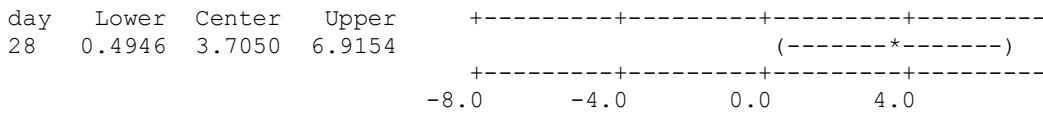
Individual confidence level = 97.50%



day = 0 subtracted from:



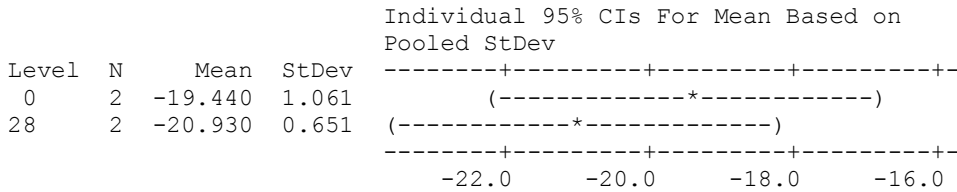
day = 14 subtracted from:



### 6) One-way ANOVA: Tg-P20 versus day

Source	DF	SS	MS	F	P
day	1	2.220	2.220	2.87	0.232
Error	2	1.548	0.774		
Total	3	3.768			

S = 0.8798    R-Sq = 58.92%    R-Sq(adj) = 38.37%



Pooled StDev = 0.880

Grouping Information Using Tukey Method

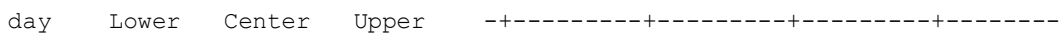
day	N	Mean	Grouping
0	2	-19.4400	A
28	2	-20.9300	A

Means that do not share a letter are significantly different.

Tukey 95% Simultaneous Confidence Intervals  
All Pairwise Comparisons among Levels of day

Individual confidence level = 95.00%

day = 0 subtracted from:



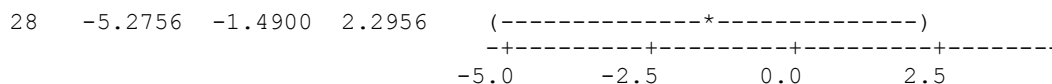
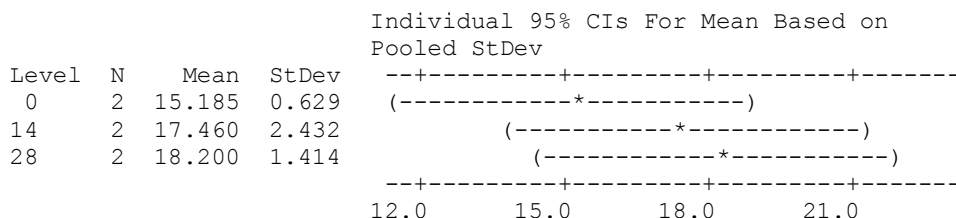


**Table A.7.** Effect of Storage Time on the Gelatin Based Confectionery Gels for each Formulation. 1) Moisture Content (MC %), 2) Water Activity ( $a_w$ ), 3) Hardness, 4)  $T_1$ , 5)  $T_2$  Spectra, 6) Glass transition Temperature ( $T_g$ ) for **P30**.

**1) One-way ANOVA: MC (%)-P30 versus day**

Source	DF	SS	MS	F	P
day	2	9.88	4.94	1.78	0.309
Error	3	8.31	2.77		
Total	5	18.19			

S = 1.665 R-Sq = 54.30% R-Sq(adj) = 23.83%



Pooled StDev = 1.665

Grouping Information Using Tukey Method

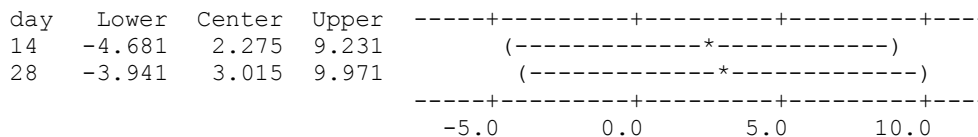
day	N	Mean	Grouping
28	2	18.200	A
14	2	17.460	A
0	2	15.185	A

Means that do not share a letter are significantly different.

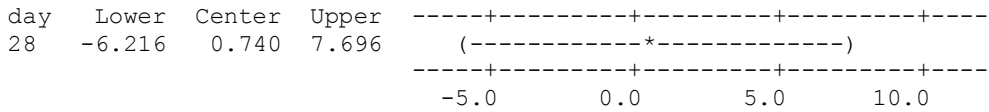
Tukey 95% Simultaneous Confidence Intervals  
All Pairwise Comparisons among Levels of day

Individual confidence level = 97.50%

day = 0 subtracted from:



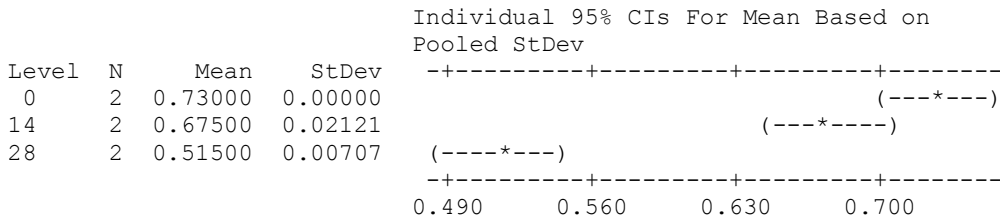
day = 14 subtracted from:



## 2) One-way ANOVA: aw-P30 versus day

Source	DF	SS	MS	F	P
day	2	0.049900	0.024950	149.70	0.001
Error	3	0.000500	0.000167		
Total	5	0.050400			

S = 0.01291 R-Sq = 99.01% R-Sq(adj) = 98.35%



Pooled StDev = 0.01291

Grouping Information Using Tukey Method

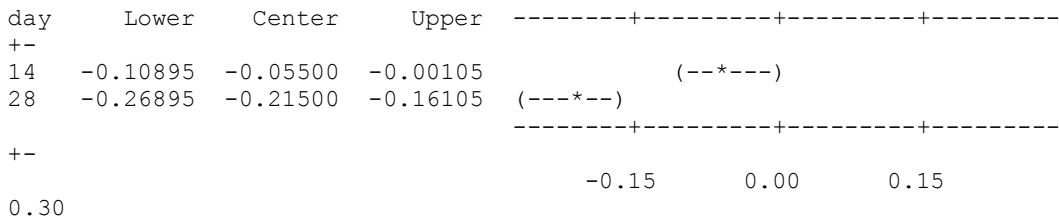
day	N	Mean	Grouping
0	2	0.73000	A
14	2	0.67500	B
28	2	0.51500	C

Means that do not share a letter are significantly different.

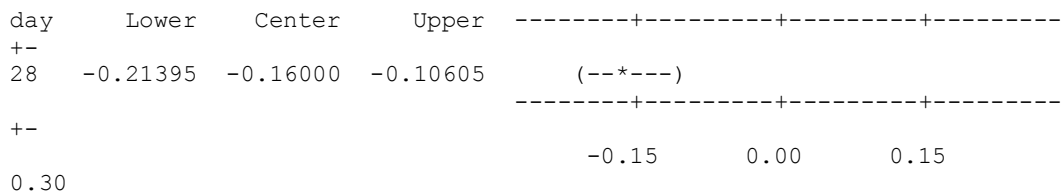
Tukey 95% Simultaneous Confidence Intervals  
All Pairwise Comparisons among Levels of day

Individual confidence level = 97.50%

day = 0 subtracted from:



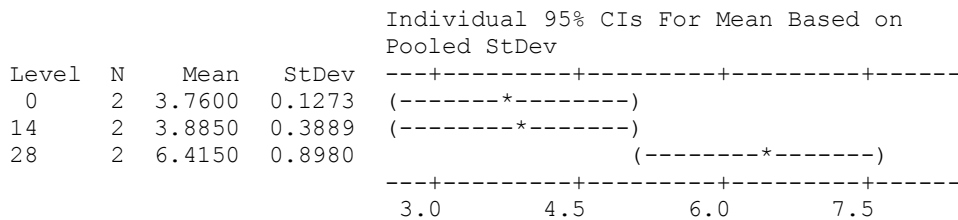
day = 14 subtracted from:



### 3) One-way ANOVA: hardness-P30 versus day

Source	DF	SS	MS	F	P
day	2	8.977	4.489	13.83	0.031
Error	3	0.974	0.325		
Total	5	9.951			

S = 0.5698 R-Sq = 90.21% R-Sq(adj) = 83.69%



Pooled StDev = 0.5698

Grouping Information Using Tukey Method

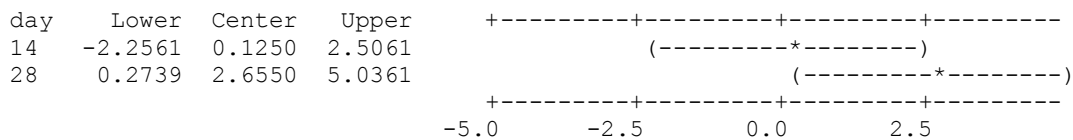
day	N	Mean	Grouping
28	2	6.4150	A
14	2	3.8850	B
0	2	3.7600	B

Means that do not share a letter are significantly different.

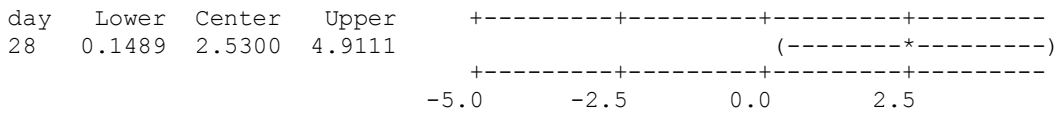
Tukey 95% Simultaneous Confidence Intervals  
All Pairwise Comparisons among Levels of day

Individual confidence level = 97.50%

day = 0 subtracted from:



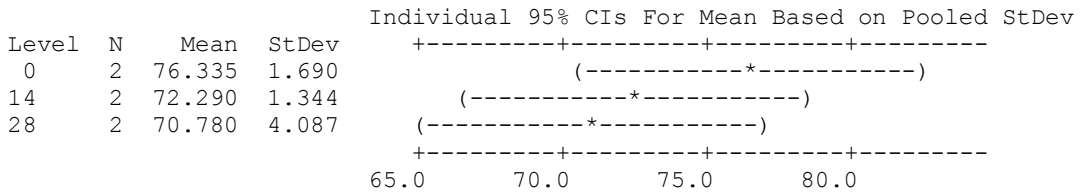
day = 14 subtracted from:



#### 4) One-way ANOVA: T1-P30 versus day

Source	DF	SS	MS	F	P
day	2	33.00	16.50	2.32	0.246
Error	3	21.37	7.12		
Total	5	54.37			

S = 2.669 R-Sq = 60.70% R-Sq(adj) = 34.50%



Pooled StDev = 2.669

Grouping Information Using Tukey Method

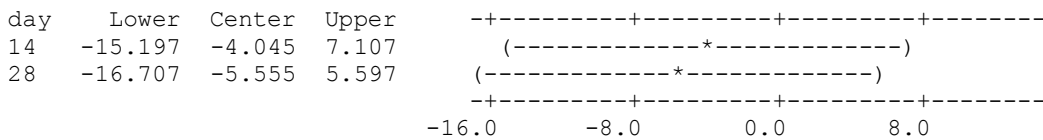
day	N	Mean	Grouping
0	2	76.335	A
14	2	72.290	A
28	2	70.780	A

Means that do not share a letter are significantly different.

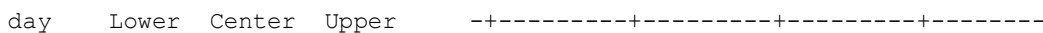
Tukey 95% Simultaneous Confidence Intervals  
All Pairwise Comparisons among Levels of day

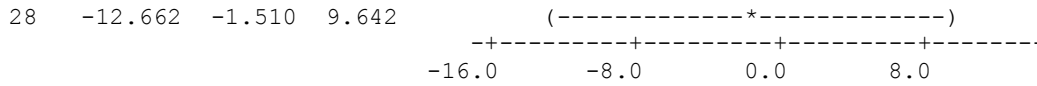
Individual confidence level = 97.50%

day = 0 subtracted from:



day = 14 subtracted from:



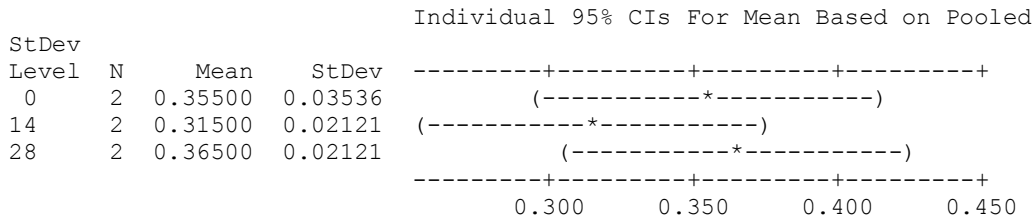


5)

**One-way ANOVA: T2 peak 1 P30 versus day**

Source	DF	SS	MS	F	P
day	2	0.002800	0.001400	1.95	0.286
Error	3	0.002150	0.000717		
Total	5	0.004950			

S = 0.02677    R-Sq = 56.57%    R-Sq(adj) = 27.61%



Pooled StDev = 0.02677

Grouping Information Using Tukey Method

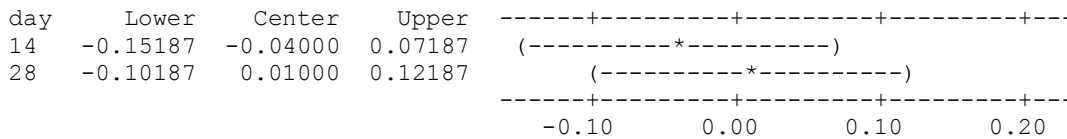
day	N	Mean	Grouping
28	2	0.36500	A
0	2	0.35500	A
14	2	0.31500	A

Means that do not share a letter are significantly different.

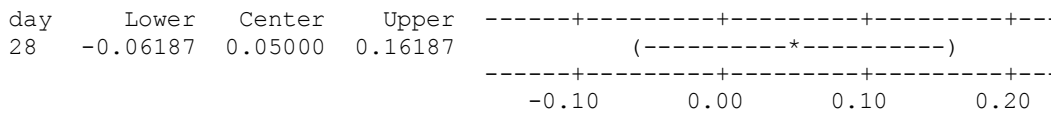
Tukey 95% Simultaneous Confidence Intervals  
All Pairwise Comparisons among Levels of day

Individual confidence level = 97.50%

day = 0 subtracted from:



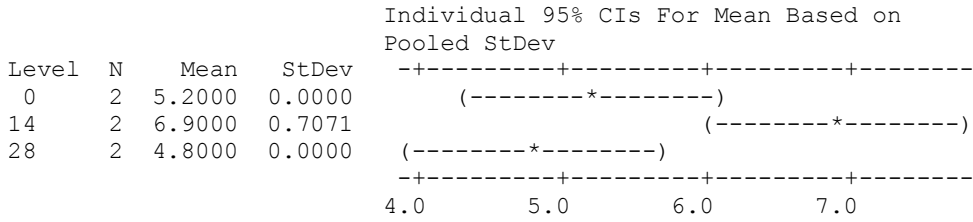
day = 14 subtracted from:



**One-way ANOVA: T2 peak 2 P30 versus day**

Source	DF	SS	MS	F	P
day	2	4.973	2.487	14.92	0.028
Error	3	0.500	0.167		
Total	5	5.473			

S = 0.4082    R-Sq = 90.86%    R-Sq(adj) = 84.77%



Pooled StDev = 0.4082

Grouping Information Using Tukey Method

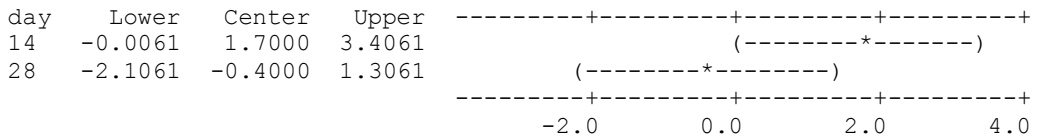
day	N	Mean	Grouping
14	2	6.9000	A
0	2	5.2000	A B
28	2	4.8000	B

Means that do not share a letter are significantly different.

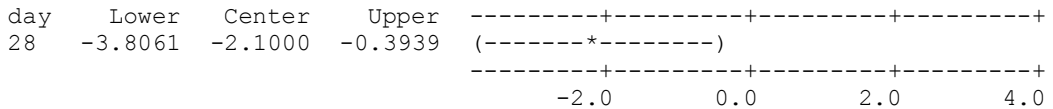
Tukey 95% Simultaneous Confidence Intervals  
All Pairwise Comparisons among Levels of day

Individual confidence level = 97.50%

day = 0 subtracted from:



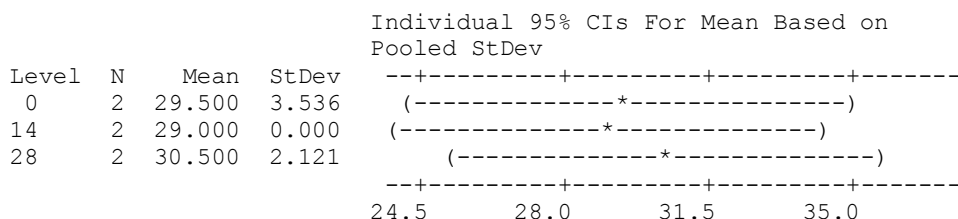
day = 14 subtracted from:



### One-way ANOVA: T2 peak 3 P30 versus day

Source	DF	SS	MS	F	P
day	2	2.33	1.17	0.21	0.825
Error	3	17.00	5.67		
Total	5	19.33			

S = 2.380    R-Sq = 12.07%    R-Sq(adj) = 0.00%



Pooled StDev = 2.380

#### Grouping Information Using Tukey Method

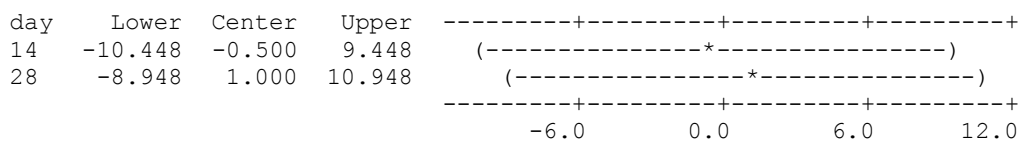
day	N	Mean	Grouping
28	2	30.500	A
0	2	29.500	A
14	2	29.000	A

Means that do not share a letter are significantly different.

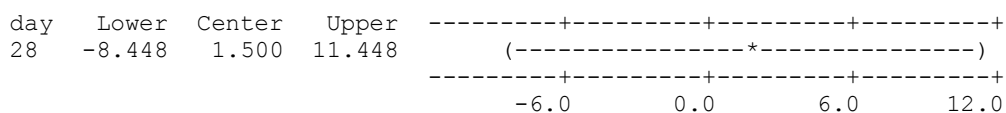
#### Tukey 95% Simultaneous Confidence Intervals All Pairwise Comparisons among Levels of day

Individual confidence level = 97.50%

day = 0 subtracted from:



day = 14 subtracted from:

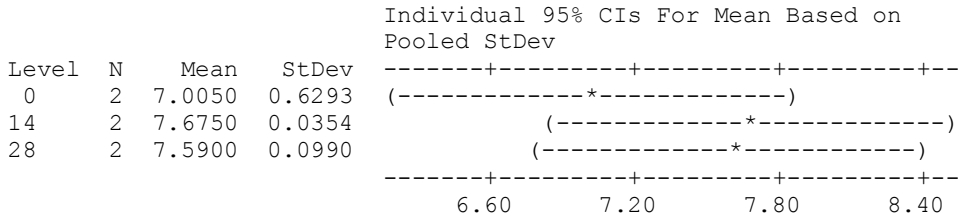




**One-way ANOVA: RA1-P30 versus day**

Source	DF	SS	MS	F	P
day	2	0.532	0.266	1.96	0.285
Error	3	0.407	0.136		
Total	5	0.939			

S = 0.3684    R-Sq = 56.66%    R-Sq(adj) = 27.77%



Pooled StDev = 0.3684

Grouping Information Using Tukey Method

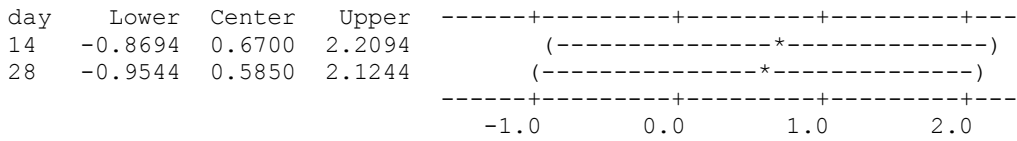
day	N	Mean	Grouping
14	2	7.6750	A
28	2	7.5900	A
0	2	7.0050	A

Means that do not share a letter are significantly different.

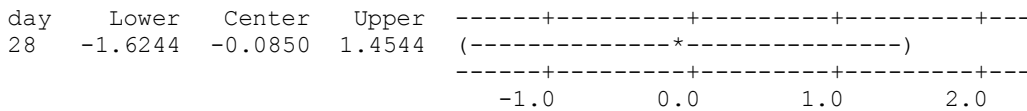
Tukey 95% Simultaneous Confidence Intervals  
All Pairwise Comparisons among Levels of day

Individual confidence level = 97.50%

day = 0 subtracted from:



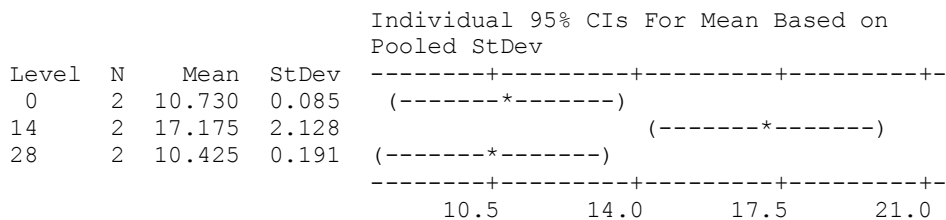
day = 14 subtracted from:



### One-way ANOVA: RA2-P30 versus day

Source	DF	SS	MS	F	P
day	2	58.13	29.06	19.06	0.020
Error	3	4.57	1.52		
Total	5	62.70			

S = 1.235    R-Sq = 92.71%    R-Sq(adj) = 87.84%



Pooled StDev = 1.235

#### Grouping Information Using Tukey Method

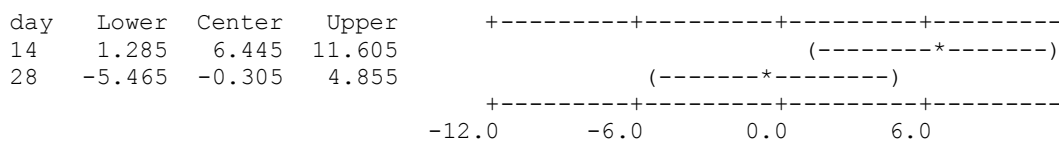
day	N	Mean	Grouping
14	2	17.175	A
0	2	10.730	B
28	2	10.425	B

Means that do not share a letter are significantly different.

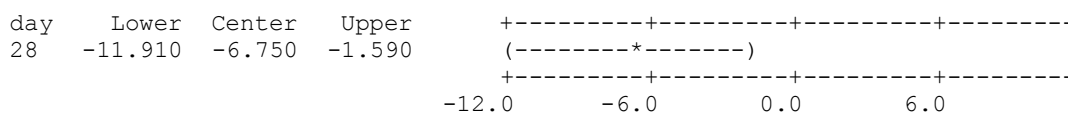
#### Tukey 95% Simultaneous Confidence Intervals All Pairwise Comparisons among Levels of day

Individual confidence level = 97.50%

day = 0 subtracted from:



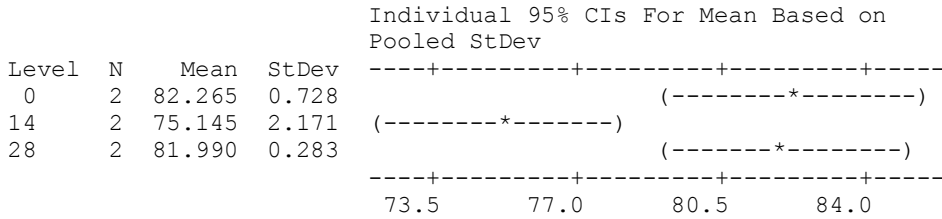
day = 14 subtracted from:



**One-way ANOVA: RA3-P30 versus day**

Source	DF	SS	MS	F	P
day	2	65.08	32.54	18.34	0.021
Error	3	5.32	1.77		
Total	5	70.41			

S = 1.332    R-Sq = 92.44%    R-Sq(adj) = 87.40%



Pooled StDev = 1.332

Grouping Information Using Tukey Method

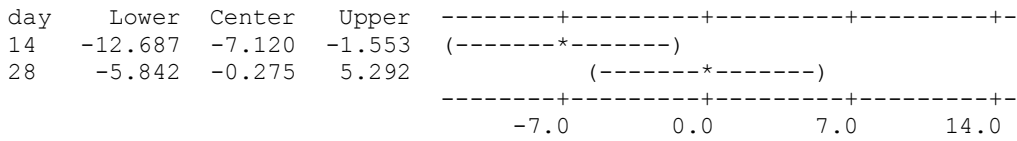
day	N	Mean	Grouping
0	2	82.265	A
28	2	81.990	A
14	2	75.145	B

Means that do not share a letter are significantly different.

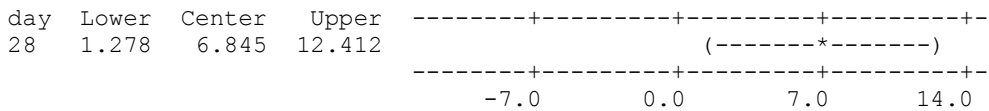
Tukey 95% Simultaneous Confidence Intervals  
All Pairwise Comparisons among Levels of day

Individual confidence level = 97.50%

day = 0 subtracted from:



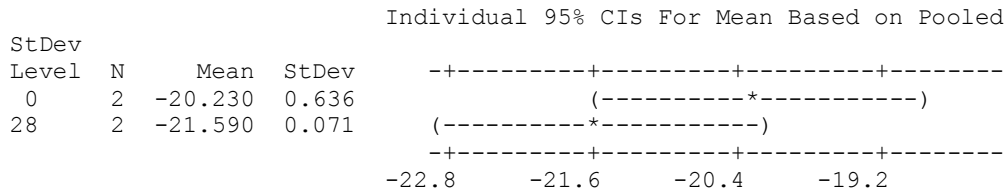
day = 14 subtracted from:



**6) One-way ANOVA: Tg-P30 versus day**

Source	DF	SS	MS	F	P
day	1	1.850	1.850	9.02	0.095
Error	2	0.410	0.205		
Total	3	2.260			

S = 0.4528    R-Sq = 81.86%    R-Sq(adj) = 72.78%



Pooled StDev = 0.453

Grouping Information Using Tukey Method

day	N	Mean	Grouping
0	2	-20.2300	A
28	2	-21.5900	A

Means that do not share a letter are significantly different.

Tukey 95% Simultaneous Confidence Intervals  
All Pairwise Comparisons among Levels of day

Individual confidence level = 95.00%

day = 0 subtracted from:

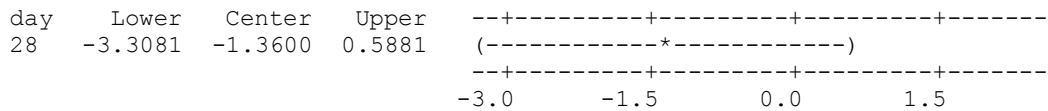
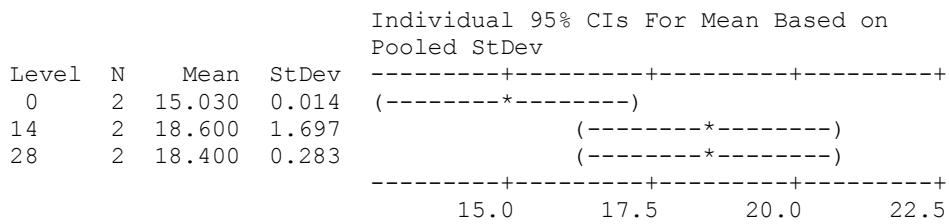


**Table A.8.** Effect of Storage Time on the Gelatin Based Confectionery Gels for each Formulation. 1) Moisture Content (MC %), 2) Water Activity (aw), 3) Hardness, 4) T<sub>1</sub>, 5) T<sub>2</sub> Spectra, 6) Glass transition Temperature (T<sub>g</sub>) for **P40**.

**1) One-way ANOVA: MC(%)-P40 versus day**

Source	DF	SS	MS	F	P
day	2	16.095	8.047	8.16	0.061
Error	3	2.960	0.987		
Total	5	19.055			

S = 0.9933    R-Sq = 84.46%    R-Sq(adj) = 74.11%



Pooled StDev = 0.993

Grouping Information Using Tukey Method

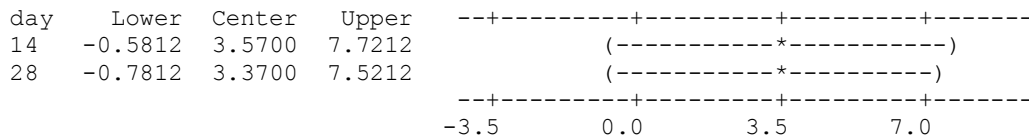
day	N	Mean	Grouping
14	2	18.6000	A
28	2	18.4000	A
0	2	15.0300	A

Means that do not share a letter are significantly different.

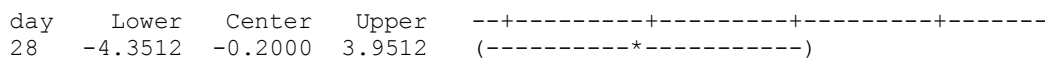
Tukey 95% Simultaneous Confidence Intervals  
All Pairwise Comparisons among Levels of day

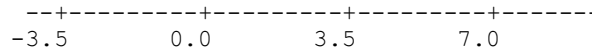
Individual confidence level = 97.50%

day = 0 subtracted from:



day = 14 subtracted from:

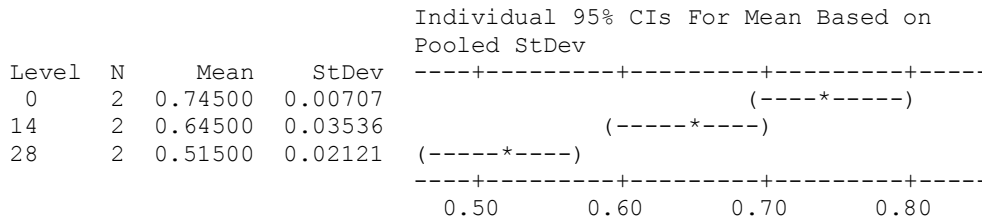




**2) One-way ANOVA: aw-P40 versus day**

Source	DF	SS	MS	F	P
day	2	0.053200	0.026600	45.60	0.006
Error	3	0.001750	0.000583		
Total	5	0.054950			

S = 0.02415    R-Sq = 96.82%    R-Sq(adj) = 94.69%



Pooled StDev = 0.02415

Grouping Information Using Tukey Method

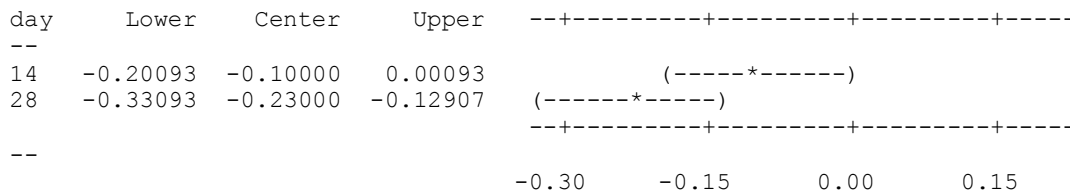
day	N	Mean	Grouping
0	2	0.74500	A
14	2	0.64500	A
28	2	0.51500	B

Means that do not share a letter are significantly different.

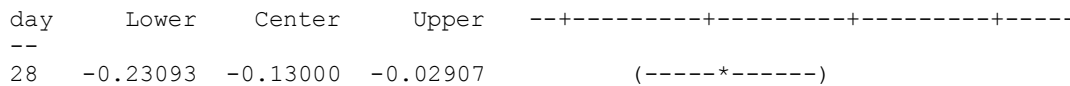
Tukey 95% Simultaneous Confidence Intervals  
All Pairwise Comparisons among Levels of day

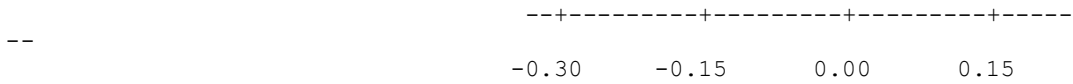
Individual confidence level = 97.50%

day = 0 subtracted from:



day = 14 subtracted from:

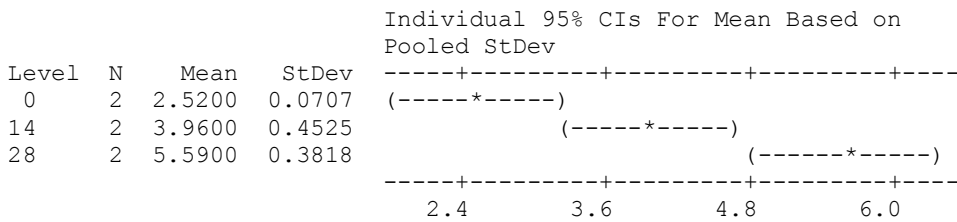




**3) One-way ANOVA: hardness-P40 versus day**

Source	DF	SS	MS	F	P
day	2	9.437	4.718	39.81	0.007
Error	3	0.356	0.119		
Total	5	9.793			

S = 0.3443    R-Sq = 96.37%    R-Sq(adj) = 93.95%



Pooled StDev = 0.3443

Grouping Information Using Tukey Method

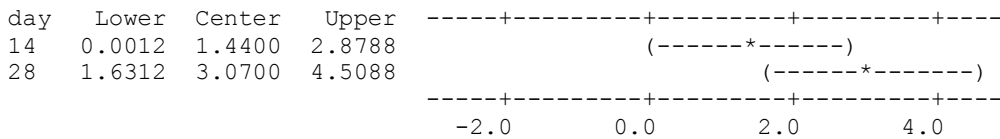
day	N	Mean	Grouping
28	2	5.5900	A
14	2	3.9600	B
0	2	2.5200	C

Means that do not share a letter are significantly different.

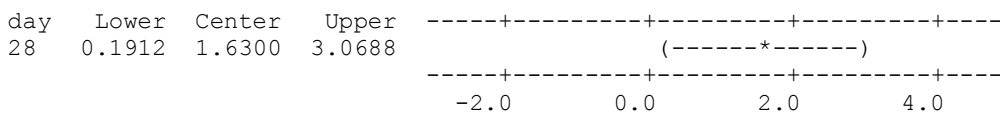
Tukey 95% Simultaneous Confidence Intervals  
All Pairwise Comparisons among Levels of day

Individual confidence level = 97.50%

day = 0 subtracted from:



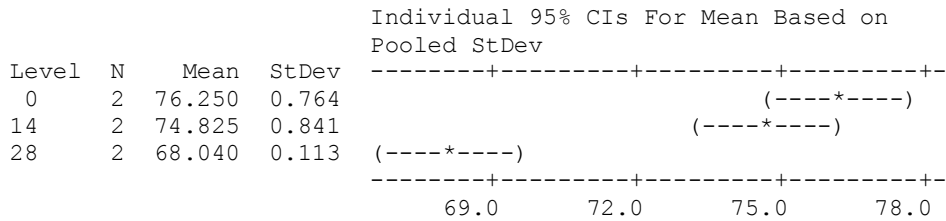
day = 14 subtracted from:



#### 4) One-way ANOVA: T1-P40 versus day

Source	DF	SS	MS	F	P
day	2	76.981	38.490	88.55	0.002
Error	3	1.304	0.435		
Total	5	78.285			

S = 0.6593    R-Sq = 98.33%    R-Sq(adj) = 97.22%



Pooled StDev = 0.659

#### Grouping Information Using Tukey Method

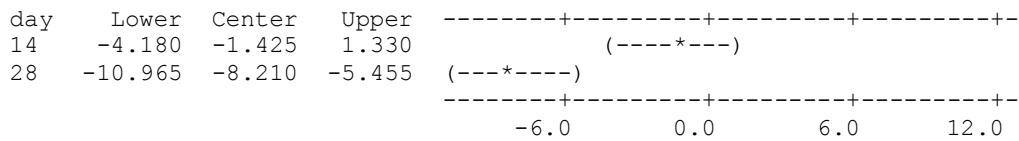
day	N	Mean	Grouping
0	2	76.250	A
14	2	74.825	A
28	2	68.040	B

Means that do not share a letter are significantly different.

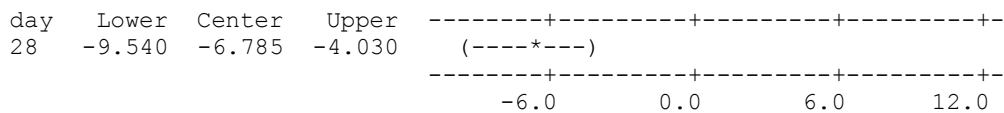
#### Tukey 95% Simultaneous Confidence Intervals All Pairwise Comparisons among Levels of day

Individual confidence level = 97.50%

day = 0 subtracted from:



day = 14 subtracted from:



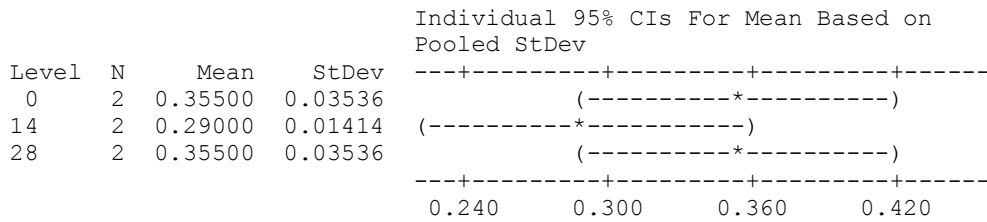


5)

**One-way ANOVA: T2 peak 1 P40 versus day**

Source	DF	SS	MS	F	P
day	2	0.005633	0.002817	3.13	0.184
Error	3	0.002700	0.000900		
Total	5	0.008333			

S = 0.03    R-Sq = 67.60%    R-Sq(adj) = 46.00%



Pooled StDev = 0.03000

Grouping Information Using Tukey Method

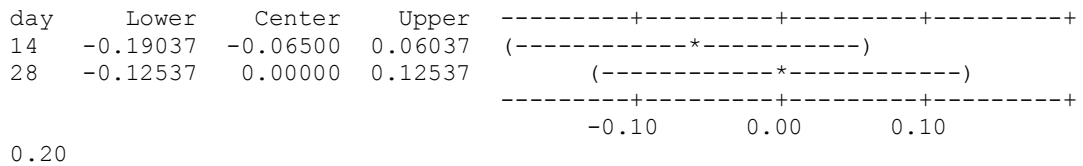
day	N	Mean	Grouping
28	2	0.35500	A
0	2	0.35500	A
14	2	0.29000	A

Means that do not share a letter are significantly different.

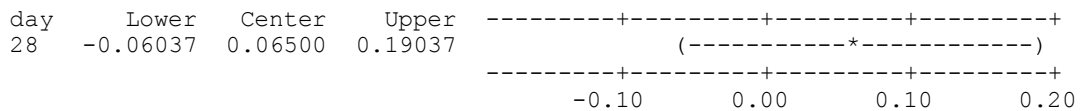
Tukey 95% Simultaneous Confidence Intervals  
All Pairwise Comparisons among Levels of day

Individual confidence level = 97.50%

day = 0 subtracted from:



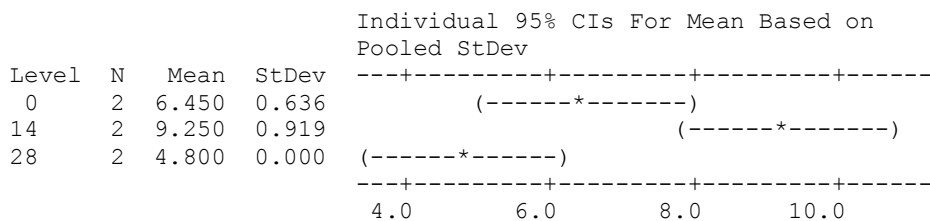
day = 14 subtracted from:



### One-way ANOVA: T2 peak 2 P40 versus day

Source	DF	SS	MS	F	P
day	2	20.243	10.122	24.29	0.014
Error	3	1.250	0.417		
Total	5	21.493			

S = 0.6455    R-Sq = 94.18%    R-Sq(adj) = 90.31%



Pooled StDev = 0.645

#### Grouping Information Using Tukey Method

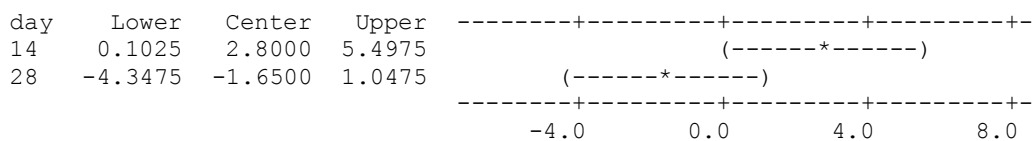
day	N	Mean	Grouping
14	2	9.2500	A
0	2	6.4500	B
28	2	4.8000	B

Means that do not share a letter are significantly different.

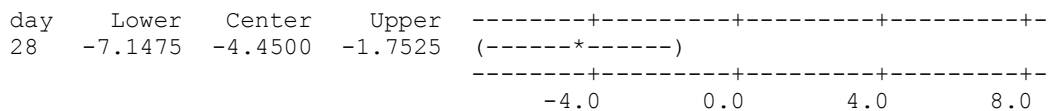
#### Tukey 95% Simultaneous Confidence Intervals All Pairwise Comparisons among Levels of day

Individual confidence level = 97.50%

day = 0 subtracted from:



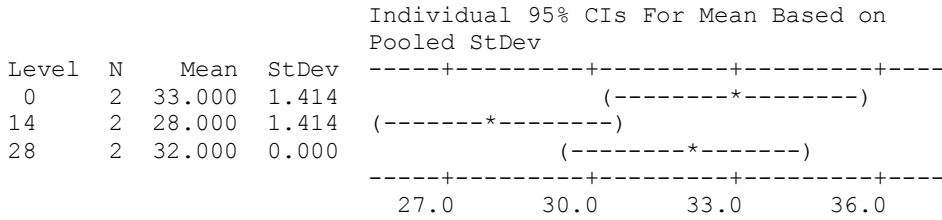
day = 14 subtracted from:



**One-way ANOVA: T2 peak 3 P40 versus day**

Source	DF	SS	MS	F	P
day	2	28.00	14.00	10.50	0.044
Error	3	4.00	1.33		
Total	5	32.00			

S = 1.155    R-Sq = 87.50%    R-Sq(adj) = 79.17%



Pooled StDev = 1.155

Grouping Information Using Tukey Method

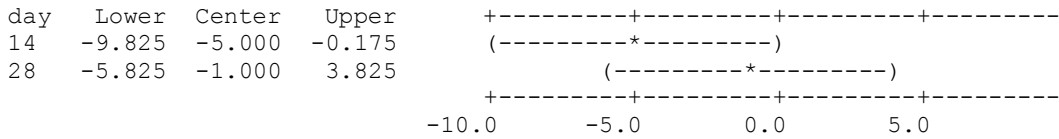
day	N	Mean	Grouping
0	2	33.000	A
28	2	32.000	A B
14	2	28.000	B

Means that do not share a letter are significantly different.

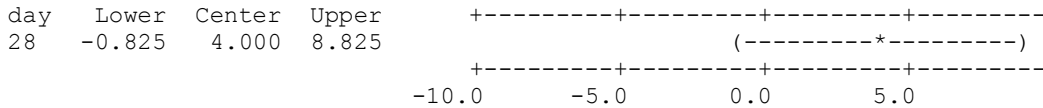
Tukey 95% Simultaneous Confidence Intervals  
All Pairwise Comparisons among Levels of day

Individual confidence level = 97.50%

day = 0 subtracted from:



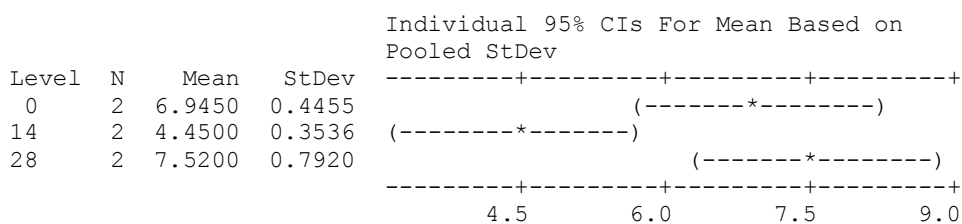
day = 14 subtracted from:



### One-way ANOVA: RA1-P40 versus day

Source	DF	SS	MS	F	P
day	2	10.654	5.327	16.81	0.023
Error	3	0.951	0.317		
Total	5	11.604			

S = 0.5629    R-Sq = 91.81%    R-Sq(adj) = 86.35%



Pooled StDev = 0.5629

#### Grouping Information Using Tukey Method

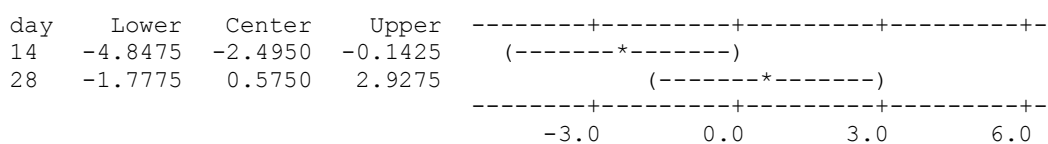
day	N	Mean	Grouping
28	2	7.5200	A
0	2	6.9450	A
14	2	4.4500	B

Means that do not share a letter are significantly different.

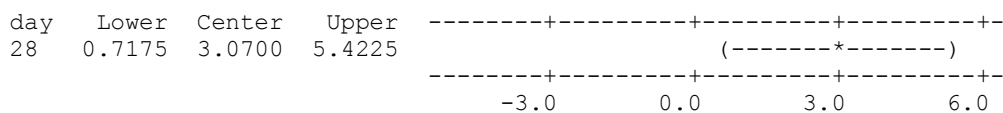
#### Tukey 95% Simultaneous Confidence Intervals All Pairwise Comparisons among Levels of day

Individual confidence level = 97.50%

day = 0 subtracted from:



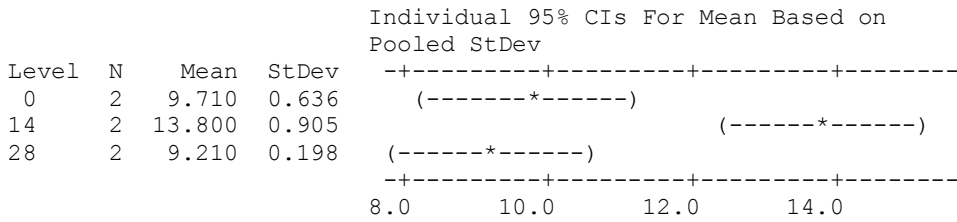
day = 14 subtracted from:



**One-way ANOVA: RA2-P40 versus day**

Source	DF	SS	MS	F	P
day	2	25.364	12.682	30.11	0.010
Error	3	1.263	0.421		
Total	5	26.628			

S = 0.6489    R-Sq = 95.26%    R-Sq(adj) = 92.09%



Pooled StDev = 0.649

Grouping Information Using Tukey Method

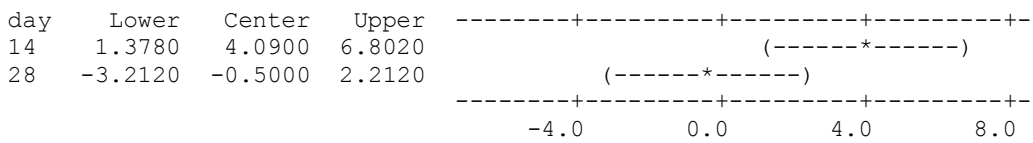
day	N	Mean	Grouping
14	2	13.8000	A
0	2	9.7100	B
28	2	9.2100	B

Means that do not share a letter are significantly different.

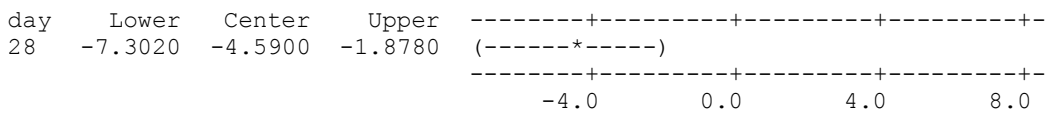
Tukey 95% Simultaneous Confidence Intervals  
All Pairwise Comparisons among Levels of day

Individual confidence level = 97.50%

day = 0 subtracted from:



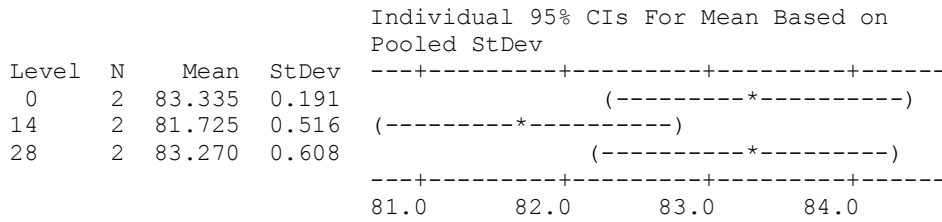
day = 14 subtracted from:



### One-way ANOVA: RA3-P40 versus day

Source	DF	SS	MS	F	P
day	2	3.322	1.661	7.41	0.069
Error	3	0.673	0.224		
Total	5	3.995			

S = 0.4735    R-Sq = 83.16%    R-Sq(adj) = 71.94%



Pooled StDev = 0.474

#### Grouping Information Using Tukey Method

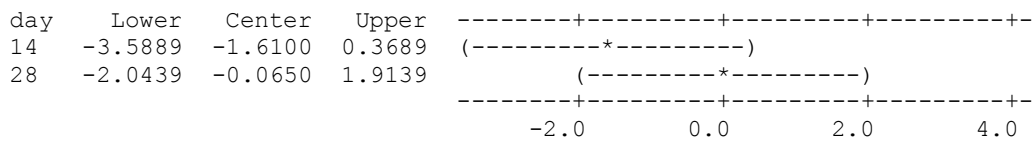
day	N	Mean	Grouping
0	2	83.3350	A
28	2	83.2700	A
14	2	81.7250	A

Means that do not share a letter are significantly different.

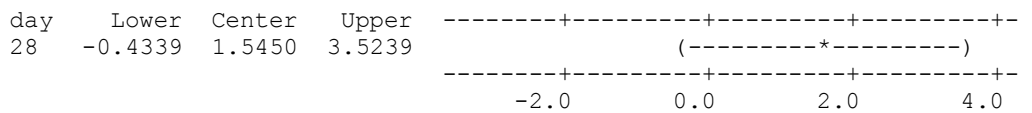
#### Tukey 95% Simultaneous Confidence Intervals All Pairwise Comparisons among Levels of day

Individual confidence level = 97.50%

day = 0 subtracted from:



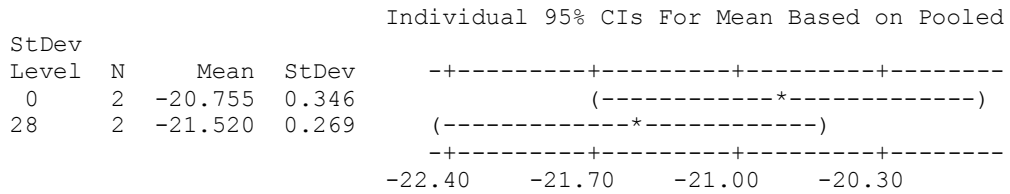
day = 14 subtracted from:



### 6) One-way ANOVA: Tg-P40 versus day

Source	DF	SS	MS	F	P
day	1	0.5852	0.5852	6.09	0.132
Error	2	0.1923	0.0961		
Total	3	0.7775			

S = 0.3100    R-Sq = 75.27%    R-Sq(adj) = 62.91%



Pooled StDev = 0.310

#### Grouping Information Using Tukey Method

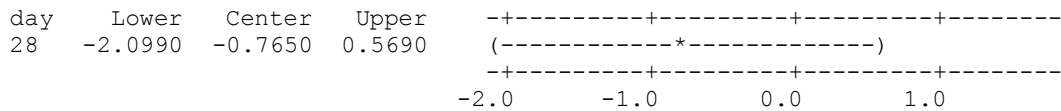
day	N	Mean	Grouping
0	2	-20.7550	A
28	2	-21.5200	A

Means that do not share a letter are significantly different.

#### Tukey 95% Simultaneous Confidence Intervals All Pairwise Comparisons among Levels of day

Individual confidence level = 95.00%

day = 0 subtracted from:



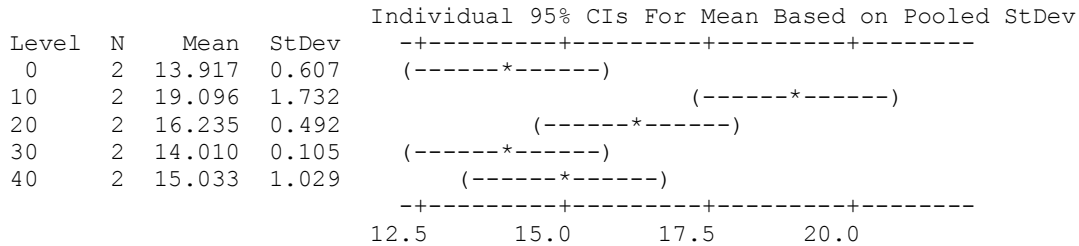
## B. Statistical Analysis Results of the TGA Experiments for the Gelatin Based Confectionery Gels

**Table B.1.** Effect of D-Allulose Substitution on the Gelatin Based Confectionery Gels at Day 0 for 1) Moisture loss (%) 2) Peak Temperature (°C)

### 1) One-way ANOVA: Moisture loss(%) versus D-Allulose

Source	DF	SS	MS	F	P
D-Allulose	4	36.585	9.146	9.77	0.014
Error	5	4.679	0.936		
Total	9	41.265			

S = 0.9674 R-Sq = 88.66% R-Sq(adj) = 79.59%



Pooled StDev = 0.967

#### Grouping Information Using Tukey Method

D-Allulose	N	Mean	Grouping
10	2	19.096	A
20	2	16.235	A B
40	2	15.033	B
30	2	14.010	B
0	2	13.917	B

Means that do not share a letter are significantly different.

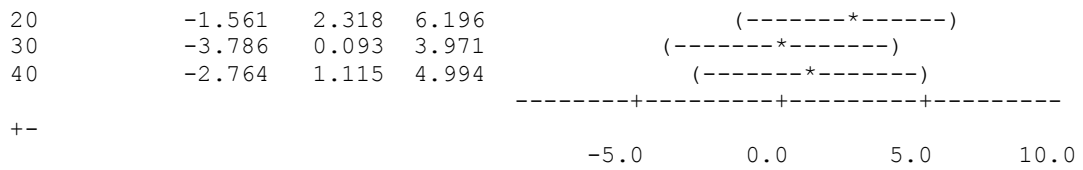
Tukey 95% Simultaneous Confidence Intervals  
All Pairwise Comparisons among Levels of D-Allulose

Individual confidence level = 98.98%

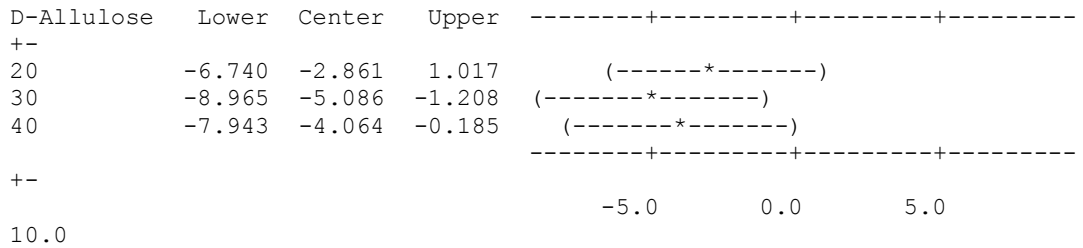
D-Allulose = 0 subtracted from:

D-Allulose	Lower	Center	Upper
10	1.300	5.179	9.058

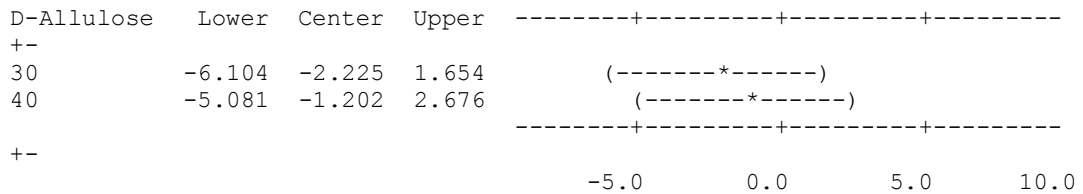




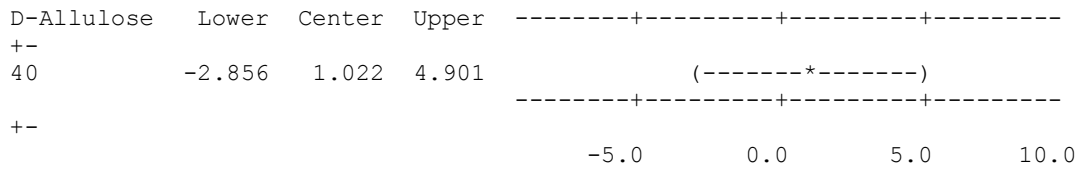
D-Allulose = 10 subtracted from:



D-Allulose = 20 subtracted from:



D-Allulose = 30 subtracted from:

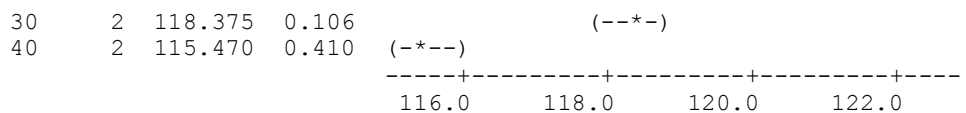


## 2) One-way ANOVA: Peak Temperature versus D-Allulose

Source	DF	SS	MS	F	P
D-Allulose	4	59.2671	14.8168	201.92	0.000
Error	5	0.3669	0.0734		
Total	9	59.6340			

S = 0.2709 R-Sq = 99.38% R-Sq(adj) = 98.89%

				Individual 95% CIs For Mean Based on Pooled StDev	
Level	N	Mean	StDev	-----+-----+-----+-----	
0	2	122.260	0.127		(-*-)
10	2	121.550	0.226		(--*-)
20	2	118.765	0.346	(--*-)	



Pooled StDev = 0.271

Grouping Information Using Tukey Method

D-Allulose	N	Mean	Grouping
0	2	122.2600	A
10	2	121.5500	A
20	2	118.7650	B
30	2	118.3750	B
40	2	115.4700	C

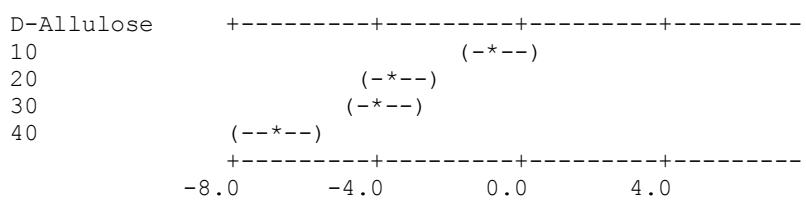
Means that do not share a letter are significantly different.

Tukey 95% Simultaneous Confidence Intervals  
All Pairwise Comparisons among Levels of D-Allulose

Individual confidence level = 98.98%

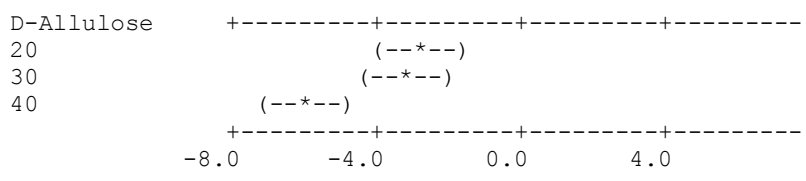
D-Allulose = 0 subtracted from:

D-Allulose	Lower	Center	Upper
10	-1.7961	-0.7100	0.3761
20	-4.5811	-3.4950	-2.4089
30	-4.9711	-3.8850	-2.7989
40	-7.8761	-6.7900	-5.7039



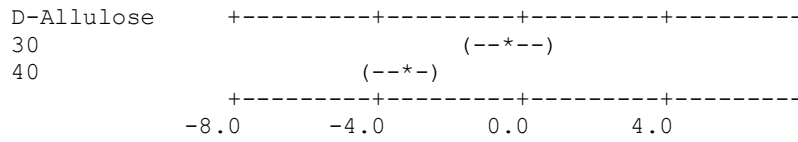
D-Allulose = 10 subtracted from:

D-Allulose	Lower	Center	Upper
20	-3.8711	-2.7850	-1.6989
30	-4.2611	-3.1750	-2.0889
40	-7.1661	-6.0800	-4.9939



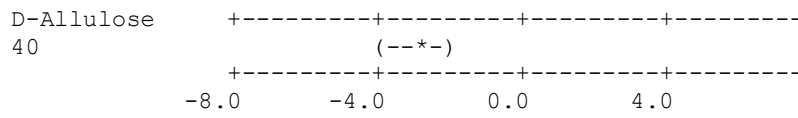
D-Allulose = 20 subtracted from:

D-Allulose	Lower	Center	Upper
30	-1.4761	-0.3900	0.6961
40	-4.3811	-3.2950	-2.2089



D-Allulose = 30 subtracted from:

D-Allulose	Lower	Center	Upper
40	-3.9911	-2.9050	-1.8189



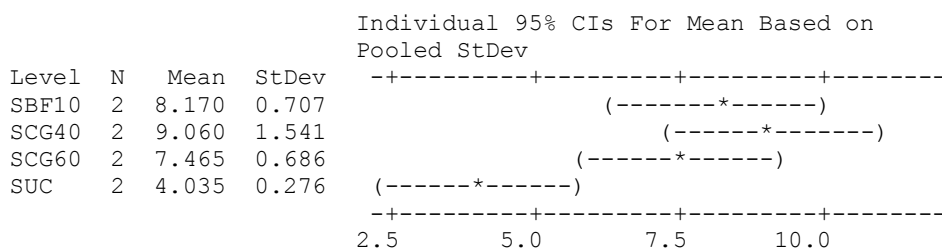
### C. Statistical Analysis Results for the Turkish Delights

**Table C.1.** Effect of sucrose / corn syrup type (SBF10, SCG40 and SCG60) on the 1) Moisture Content (%), 2) Color (L, a, b), 3) TPA (Hardness, Adhesiveness, Cohesiveness, Springiness, Gumminess and Chewiness) and 4) T2 Relaxation Spectra (T<sub>2a</sub>, T<sub>2b</sub>, RA1 (%) and RA2(%))

#### 1) One-way ANOVA: moisture versus type

Source	DF	SS	MS	F	P
type	3	28.973	9.658	11.29	0.020
Error	4	3.423	0.856		
Total	7	32.396			

S = 0.9250    R-Sq = 89.43%    R-Sq(adj) = 81.51%



Pooled StDev = 0.925

#### Grouping Information Using Tukey Method

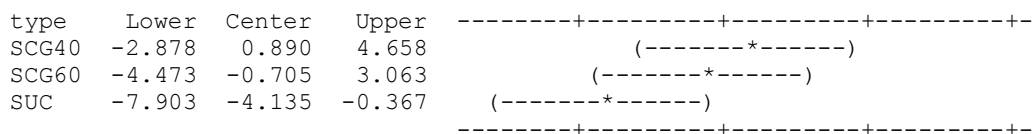
type	N	Mean	Grouping
SCG40	2	9.060	A
SBF10	2	8.170	A
SCG60	2	7.465	A B
SUC	2	4.035	B

Means that do not share a letter are significantly different.

Tukey 95% Simultaneous Confidence Intervals  
All Pairwise Comparisons among Levels of type

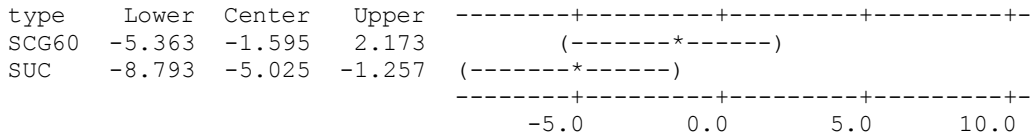
Individual confidence level = 98.48%

type = SBF10 subtracted from:

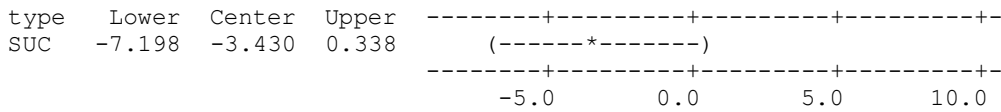


-5.0            0.0            5.0            10.0

type = SCG40 subtracted from:



type = SCG60 subtracted from:

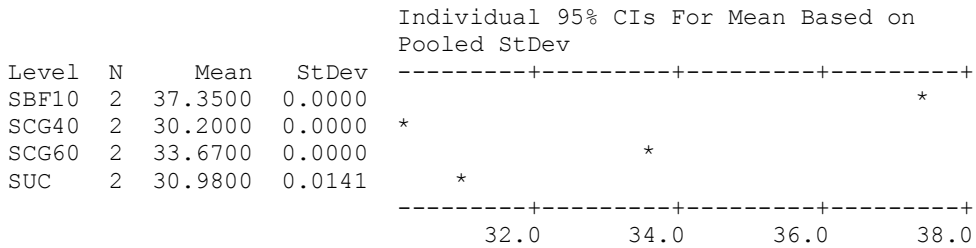


**2)**

**One-way ANOVA: L versus type**

Source	DF	SS	MS	F	P
type	3	62.56360	20.85453	417090.67	0.000
Error	4	0.00020	0.00005		
Total	7	62.56380			

S = 0.007071    R-Sq = 100.00%    R-Sq(adj) = 100.00%



Pooled StDev = 0.0071

Grouping Information Using Tukey Method

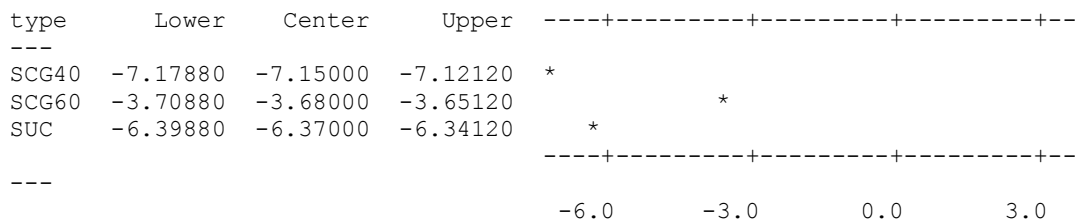
type	N	Mean	Grouping
SBF10	2	37.35000	A
SCG60	2	33.67000	B
SUC	2	30.98000	C
SCG40	2	30.20000	D

Means that do not share a letter are significantly different.

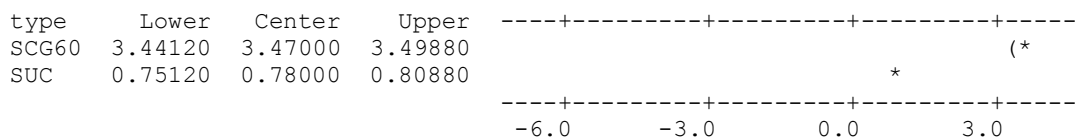
Tukey 95% Simultaneous Confidence Intervals  
All Pairwise Comparisons among Levels of type

Individual confidence level = 98.48%

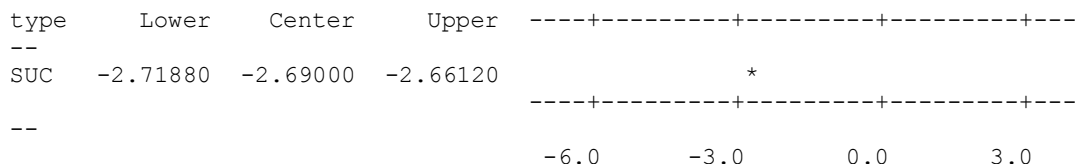
type = SBF10 subtracted from:



type = SCG40 subtracted from:



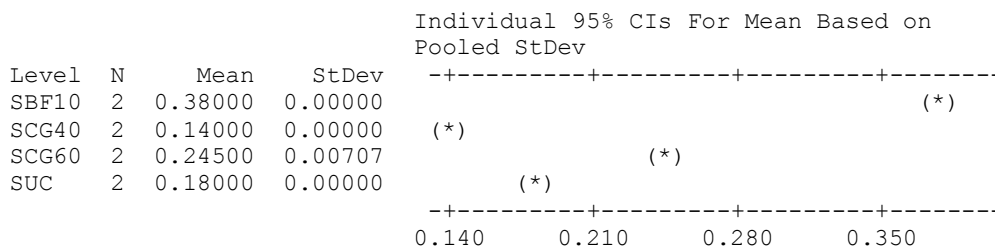
type = SCG60 subtracted from:



### One-way ANOVA: a versus type

Source	DF	SS	MS	F	P
type	3	0.0663375	0.0221125	1769.00	0.000
Error	4	0.0000500	0.0000125		
Total	7	0.0663875			

S = 0.003536 R-Sq = 99.92% R-Sq(adj) = 99.87%



Pooled StDev = 0.00354

Grouping Information Using Tukey Method

type	N	Mean	Grouping
SBF10	2	0.38000	A
SCG60	2	0.24500	B
SUC	2	0.18000	C

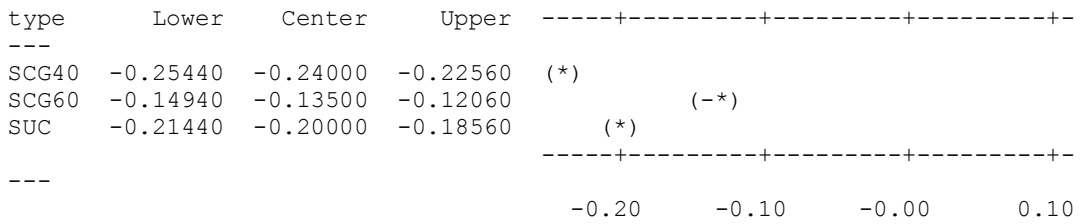
SCG40 2 0.14000 D

Means that do not share a letter are significantly different.

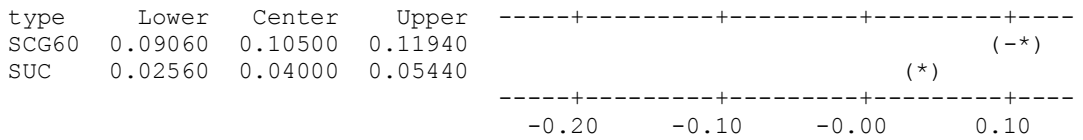
Tukey 95% Simultaneous Confidence Intervals  
All Pairwise Comparisons among Levels of type

Individual confidence level = 98.48%

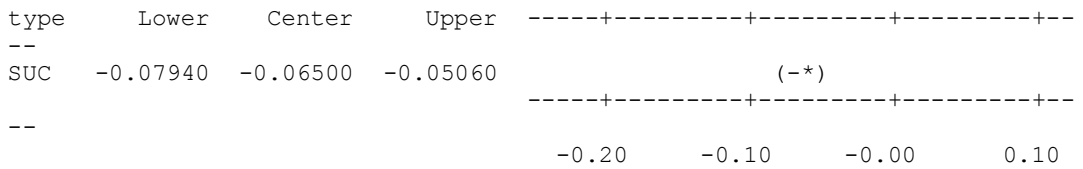
type = SBF10 subtracted from:



type = SCG40 subtracted from:



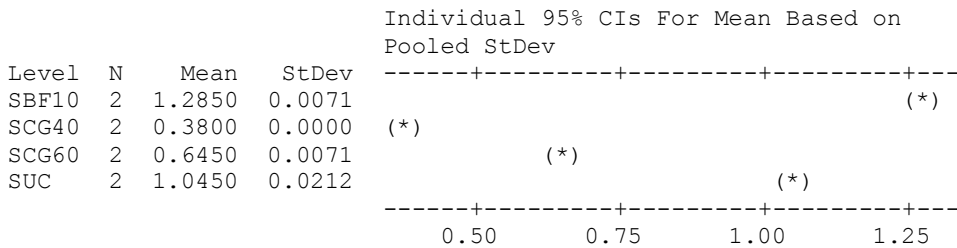
type = SCG60 subtracted from:



### One-way ANOVA: b versus type

Source	DF	SS	MS	F	P
type	3	0.979338	0.326446	2374.15	0.000
Error	4	0.000550	0.000138		
Total	7	0.979888			

S = 0.01173 R-Sq = 99.94% R-Sq(adj) = 99.90%



Pooled StDev = 0.0117

Grouping Information Using Tukey Method

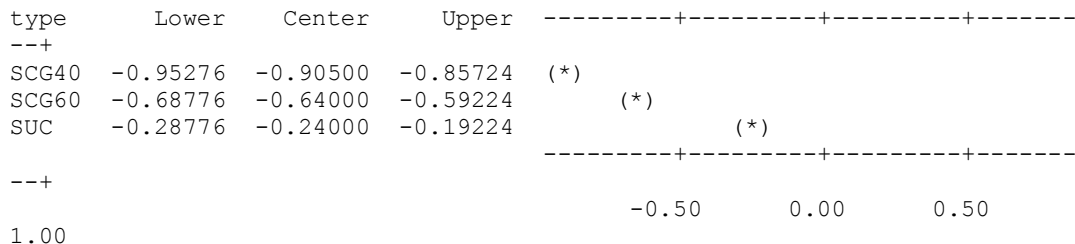
type	N	Mean	Grouping
SBF10	2	1.28500	A
SUC	2	1.04500	B
SCG60	2	0.64500	C
SCG40	2	0.38000	D

Means that do not share a letter are significantly different.

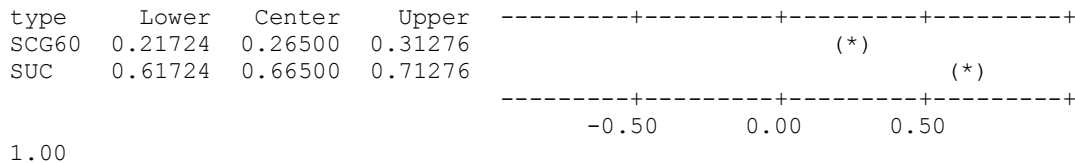
Tukey 95% Simultaneous Confidence Intervals  
All Pairwise Comparisons among Levels of type

Individual confidence level = 98.48%

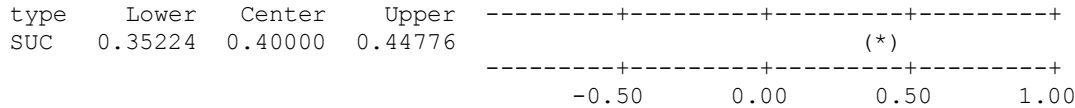
type = SBF10 subtracted from:



type = SCG40 subtracted from:



type = SCG60 subtracted from:



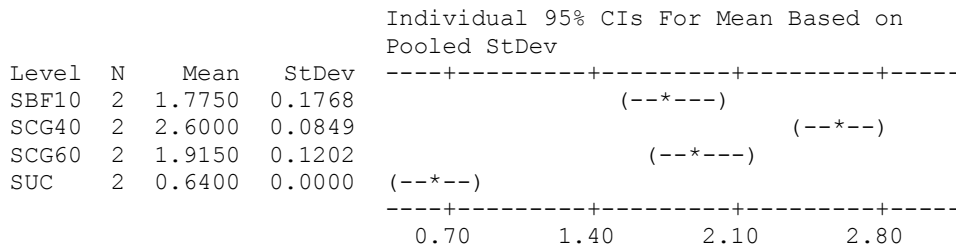


3)

**One-way ANOVA: hardness versus type**

Source	DF	SS	MS	F	P
type	3	3.9625	1.3208	99.87	0.000
Error	4	0.0529	0.0132		
Total	7	4.0153			

S = 0.115    R-Sq = 98.68%    R-Sq(adj) = 97.69%



Pooled StDev = 0.1150

Grouping Information Using Tukey Method

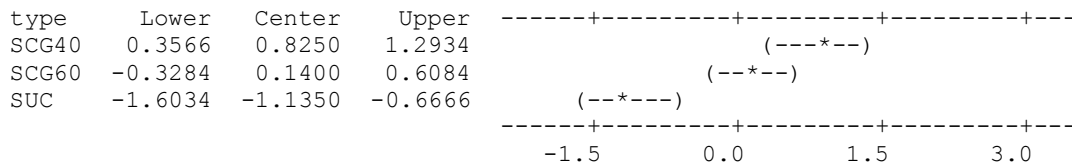
type	N	Mean	Grouping
SCG40	2	2.6000	A
SCG60	2	1.9150	B
SBF10	2	1.7750	B
SUC	2	0.6400	C

Means that do not share a letter are significantly different.

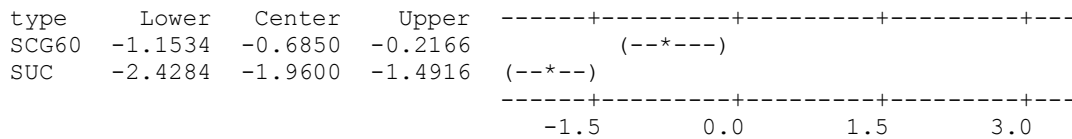
Tukey 95% Simultaneous Confidence Intervals  
All Pairwise Comparisons among Levels of type

Individual confidence level = 98.48%

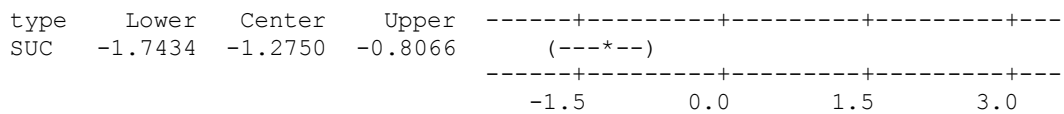
type = SBF10 subtracted from:



type = SCG40 subtracted from:



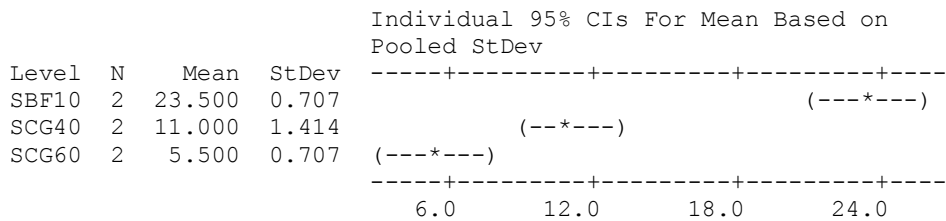
type = SCG60 subtracted from:



### One-way ANOVA: adhesiveness versus type

Source	DF	SS	MS	F	P
type	2	340.33	170.17	170.17	0.001
Error	3	3.00	1.00		
Total	5	343.33			

S = 1 R-Sq = 99.13% R-Sq(adj) = 98.54%



Pooled StDev = 1.000

#### Grouping Information Using Tukey Method

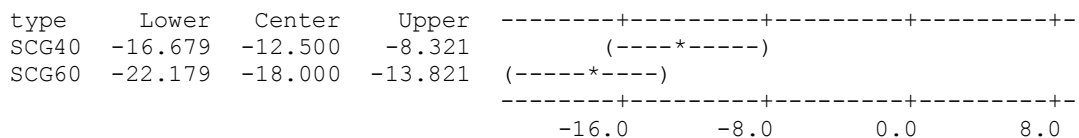
type	N	Mean	Grouping
SBF10	2	23.500	A
SCG40	2	11.000	B
SCG60	2	5.500	C

Means that do not share a letter are significantly different.

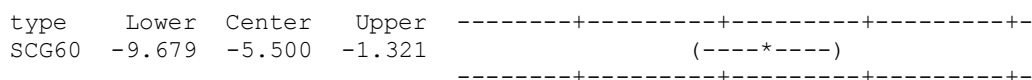
Tukey 95% Simultaneous Confidence Intervals  
All Pairwise Comparisons among Levels of type

Individual confidence level = 97.50%

type = SBF10 subtracted from:



type = SCG40 subtracted from:

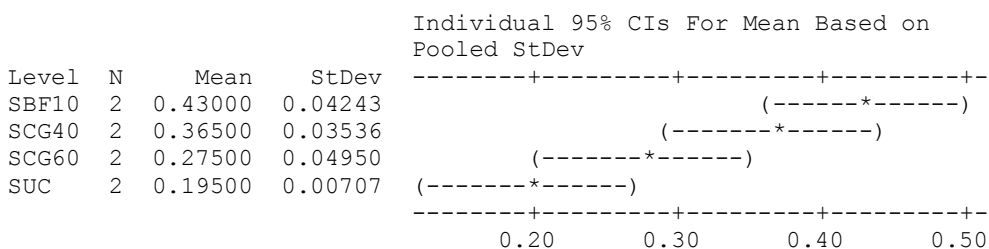


-16.0      -8.0      0.0      8.0

**One-way ANOVA: cohesiveness versus type**

Source	DF	SS	MS	F	P
type	3	0.06344	0.02115	15.24	0.012
Error	4	0.00555	0.00139		
Total	7	0.06899			

S = 0.03725    R-Sq = 91.96%    R-Sq(adj) = 85.92%



Pooled StDev = 0.03725

Grouping Information Using Tukey Method

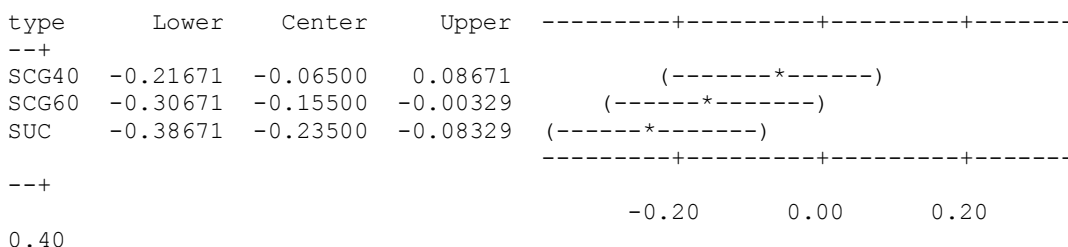
type	N	Mean	Grouping
SBF10	2	0.43000	A
SCG40	2	0.36500	A B
SCG60	2	0.27500	B C
SUC	2	0.19500	C

Means that do not share a letter are significantly different.

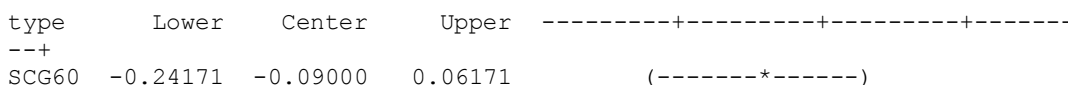
Tukey 95% Simultaneous Confidence Intervals  
All Pairwise Comparisons among Levels of type

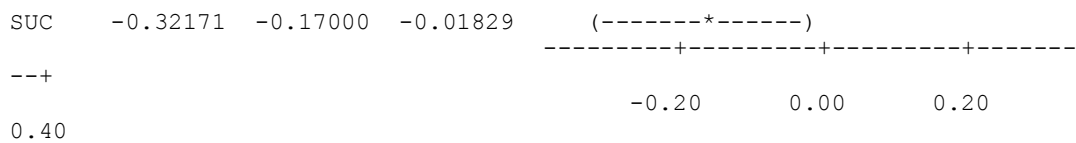
Individual confidence level = 98.48%

type = SBF10 subtracted from:

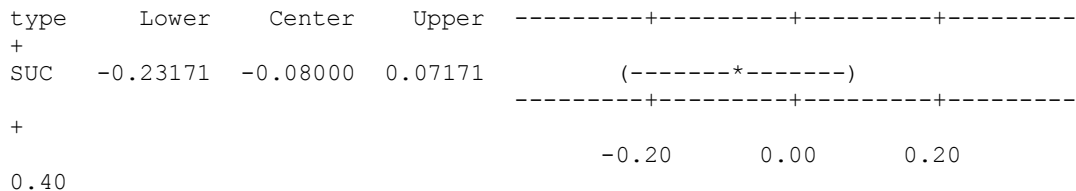


type = SCG40 subtracted from:





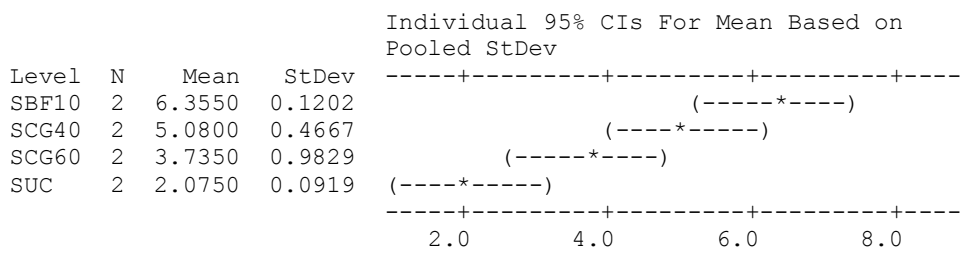
type = SCG60 subtracted from:



### One-way ANOVA: springiness versus type

Source	DF	SS	MS	F	P
type	3	20.202	6.734	22.32	0.006
Error	4	1.207	0.302		
Total	7	21.408			

S = 0.5493 R-Sq = 94.36% R-Sq(adj) = 90.14%



Pooled StDev = 0.5493

Grouping Information Using Tukey Method

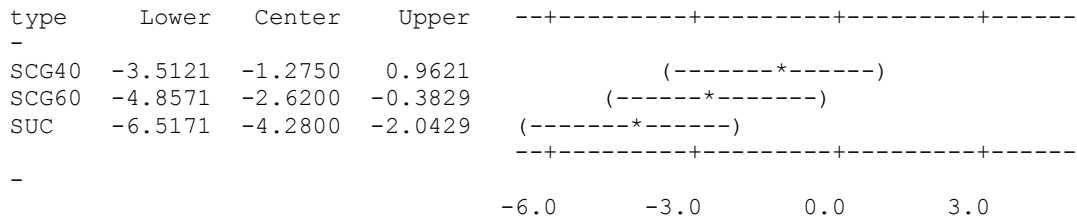
type	N	Mean	Grouping
SBF10	2	6.3550	A
SCG40	2	5.0800	A B
SCG60	2	3.7350	B C
SUC	2	2.0750	C

Means that do not share a letter are significantly different.

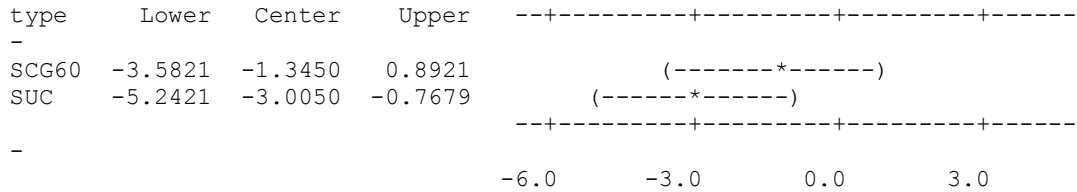
Tukey 95% Simultaneous Confidence Intervals  
All Pairwise Comparisons among Levels of type

Individual confidence level = 98.48%

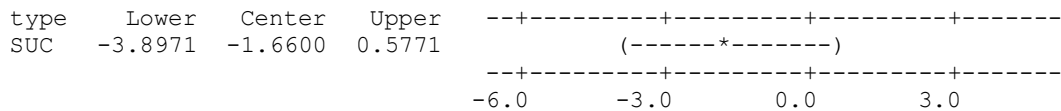
type = SBF10 subtracted from:



type = SCG40 subtracted from:



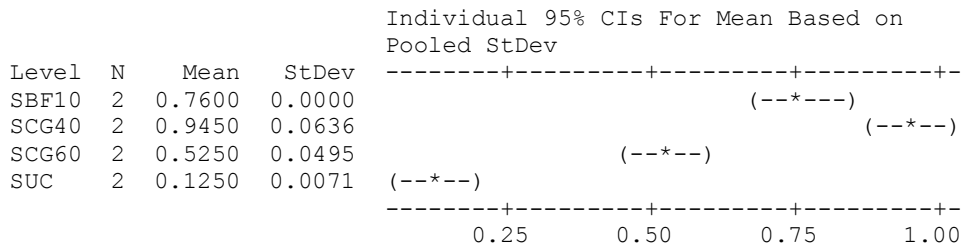
type = SCG60 subtracted from:



### One-way ANOVA: gumminess versus type

Source	DF	SS	MS	F	P
type	3	0.75074	0.25025	152.82	0.000
Error	4	0.00655	0.00164		
Total	7	0.75729			

S = 0.04047 R-Sq = 99.14% R-Sq(adj) = 98.49%



Pooled StDev = 0.0405

### Grouping Information Using Tukey Method

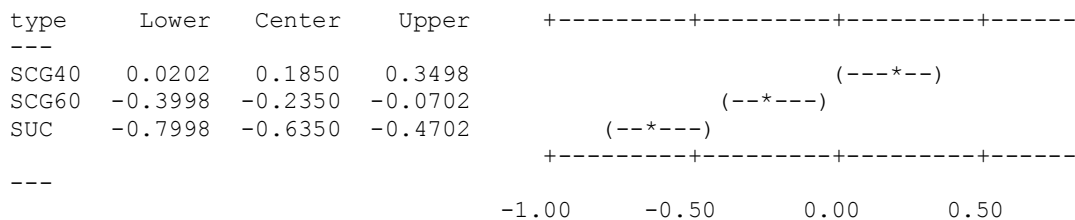
type	N	Mean	Grouping
SCG40	2	0.9450	A
SBF10	2	0.7600	B
SCG60	2	0.5250	C
SUC	2	0.1250	D

Means that do not share a letter are significantly different.

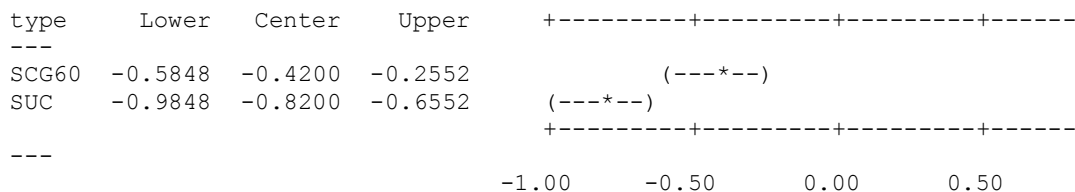
Tukey 95% Simultaneous Confidence Intervals  
 All Pairwise Comparisons among Levels of type

Individual confidence level = 98.48%

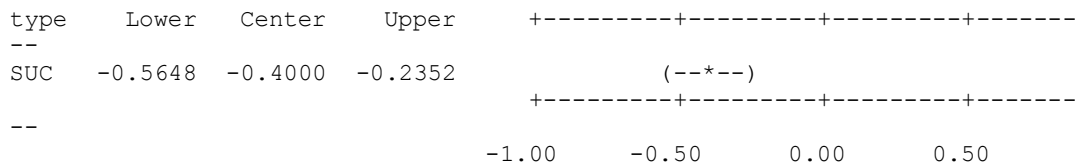
type = SBF10 subtracted from:



type = SCG40 subtracted from:



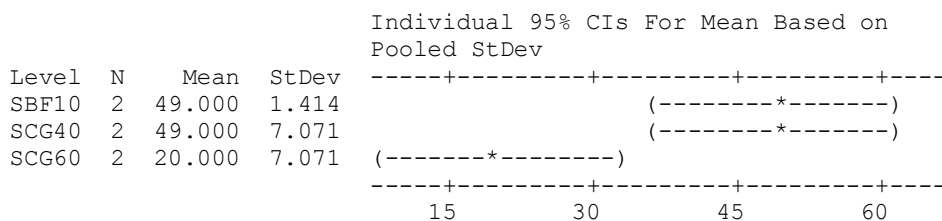
type = SCG60 subtracted from:



### One-way ANOVA: chewiness versus type

Source	DF	SS	MS	F	P
type	2	1121.3	560.7	16.49	0.024
Error	3	102.0	34.0		
Total	5	1223.3			

S = 5.831 R-Sq = 91.66% R-Sq(adj) = 86.10%



Pooled StDev = 5.831

Grouping Information Using Tukey Method

type	N	Mean	Grouping
SCG40	2	49.000	A
SBF10	2	49.000	A
SCG60	2	20.000	B

Means that do not share a letter are significantly different.

Tukey 95% Simultaneous Confidence Intervals  
All Pairwise Comparisons among Levels of type

Individual confidence level = 97.50%

type = SBF10 subtracted from:

type	Lower	Center	Upper	
SCG40	-24.368	0.000	24.368	(-----*-----)
SCG60	-53.368	-29.000	-4.632	(-----*-----)

-----+-----+-----+-----+-----+  
-30                    0                    30                    60

type = SCG40 subtracted from:

type	Lower	Center	Upper	
SCG60	-53.368	-29.000	-4.632	(-----*-----)

-----+-----+-----+-----+-----+  
-30                    0                    30                    60

#### 4) T2 Relaxation Spectra

##### One-way ANOVA: T2a versus type

Source	DF	SS	MS	F	P
type	3	4.18214	1.39405	336.93	0.000
Error	4	0.01655	0.00414		
Total	7	4.19869			

S = 0.06432    R-Sq = 99.61%    R-Sq(adj) = 99.31%

Individual 95% CIs For Mean Based on Pooled StDev

Level	N	Mean	StDev	
SBF10	2	1.1350	0.0919	(-*-)
SCG40	2	0.5050	0.0212	(-*--)
SCG60	2	0.5750	0.0212	(--*-)
SUC	2	2.3100	0.0849	(--*-)

-----+-----+-----+-----+-----+  
0.60                    1.20                    1.80                    2.40

Pooled StDev = 0.0643

Grouping Information Using Tukey Method

type	N	Mean	Grouping
SUC	2	2.3100	A
SBF10	2	1.1350	B
SCG60	2	0.5750	C
SCG40	2	0.5050	C

Means that do not share a letter are significantly different.

Tukey 95% Simultaneous Confidence Intervals  
All Pairwise Comparisons among Levels of type

Individual confidence level = 98.48%

type = SBF10 subtracted from:

type	Lower	Center	Upper	
SCG40	-0.8920	-0.6300	-0.3680	(-*-)
SCG60	-0.8220	-0.5600	-0.2980	(-***)
SUC	0.9130	1.1750	1.4370	(-*-)

-----+-----+-----+-----+-----+-----+-----  
-1.2                    0.0                    1.2                    2.4

type = SCG40 subtracted from:

type	Lower	Center	Upper	
SCG60	-0.1920	0.0700	0.3320	(--*-)
SUC	1.5430	1.8050	2.0670	(-*-)

-----+-----+-----+-----+-----+-----+-----  
-1.2                    0.0                    1.2                    2.4

type = SCG60 subtracted from:

type	Lower	Center	Upper	
SUC	1.4730	1.7350	1.9970	(-***)

-----+-----+-----+-----+-----+-----+-----  
-1.2                    0.0                    1.2                    2.4

**One-way ANOVA: T2b versus type**

Source	DF	SS	MS	F	P
type	3	82.0927	27.3642	275.26	0.000
Error	4	0.3976	0.0994		
Total	7	82.4904			

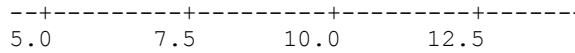
S = 0.3153    R-Sq = 99.52%    R-Sq(adj) = 99.16%

Individual 95% CIs For Mean Based on Pooled StDev

Level	N	Mean	StDev	
SBF10	2	7.180	0.396	(--*-)
SCG40	2	5.590	0.226	(-***)
SCG60	2	5.165	0.233	(--*-)
SUC	2	13.170	0.368	(--*-)

---+-----+-----+-----+-----+-----+-----





Pooled StDev = 0.315

Grouping Information Using Tukey Method

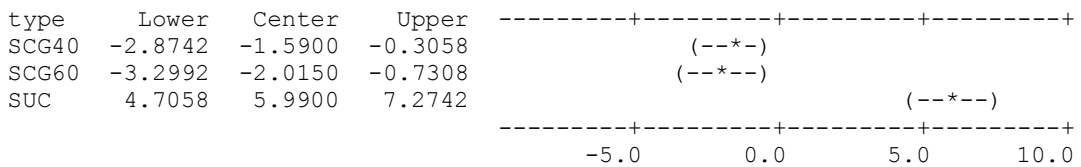
type	N	Mean	Grouping
SUC	2	13.1700	A
SBF10	2	7.1800	B
SCG40	2	5.5900	C
SCG60	2	5.1650	C

Means that do not share a letter are significantly different.

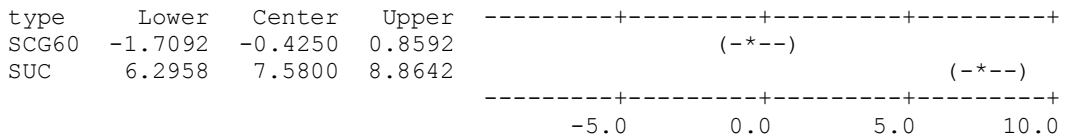
Tukey 95% Simultaneous Confidence Intervals  
All Pairwise Comparisons among Levels of type

Individual confidence level = 98.48%

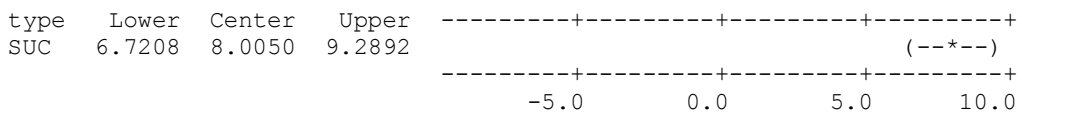
type = SBF10 subtracted from:



type = SCG40 subtracted from:



type = SCG60 subtracted from:



### One-way ANOVA: RA1 versus type

Source	DF	SS	MS	F	P
type	3	466.00	155.33	103.56	0.000
Error	4	6.00	1.50		
Total	7	472.00			

S = 1.225 R-Sq = 98.73% R-Sq(adj) = 97.78%

Individual 95% CIs For Mean Based on

Level	N	Mean	StDev	Pooled StDev
SBF10	2	59.500	0.707	(--*--)
SCG40	2	67.500	0.707	(--*--)
SCG60	2	74.500	0.707	(--*--)
SUC	2	54.500	2.121	(---*--)

-----+-----+-----+-----+-----  
56.0      63.0      70.0      77.0

Pooled StDev = 1.225

Grouping Information Using Tukey Method

type	N	Mean	Grouping
SCG60	2	74.500	A
SCG40	2	67.500	B
SBF10	2	59.500	C
SUC	2	54.500	D

Means that do not share a letter are significantly different.

Tukey 95% Simultaneous Confidence Intervals  
All Pairwise Comparisons among Levels of type

Individual confidence level = 98.48%

type = SBF10 subtracted from:

type	Lower	Center	Upper
SCG40	3.012	8.000	12.988
SCG60	10.012	15.000	19.988
SUC	-9.988	-5.000	-0.012

-----+-----+-----+-----+-----  
-15      0      15      30

type = SCG40 subtracted from:

type	Lower	Center	Upper
SCG60	2.012	7.000	11.988
SUC	-17.988	-13.000	-8.012

-----+-----+-----+-----+-----  
-15      0      15      30

type = SCG60 subtracted from:

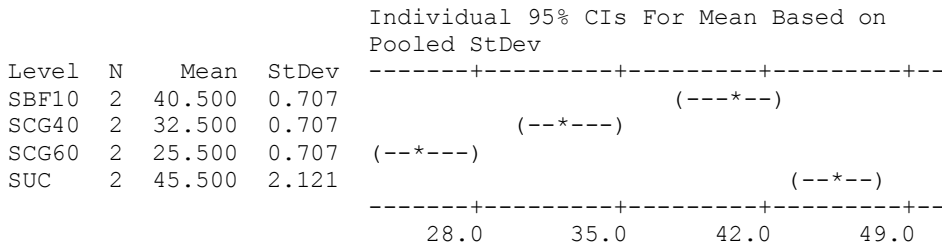
type	Lower	Center	Upper
SUC	-24.988	-20.000	-15.012

-----+-----+-----+-----+-----  
-15      0      15      30

### One-way ANOVA: RA2 versus type

Source	DF	SS	MS	F	P
type	3	466.00	155.33	103.56	0.000
Error	4	6.00	1.50		
Total	7	472.00			

S = 1.225 R-Sq = 98.73% R-Sq(adj) = 97.78%



Pooled StDev = 1.225

#### Grouping Information Using Tukey Method

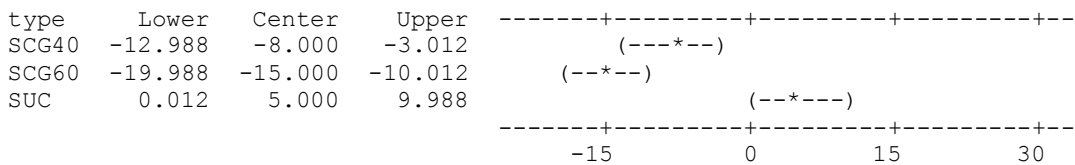
type	N	Mean	Grouping
SUC	2	45.500	A
SBF10	2	40.500	B
SCG40	2	32.500	C
SCG60	2	25.500	D

Means that do not share a letter are significantly different.

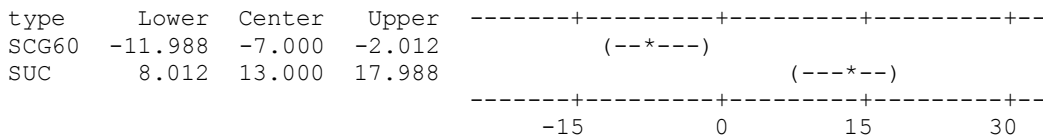
#### Tukey 95% Simultaneous Confidence Intervals All Pairwise Comparisons among Levels of type

Individual confidence level = 98.48%

type = SBF10 subtracted from:



type = SCG40 subtracted from:



type = SCG60 subtracted from:

type	Lower	Center	Upper
SUC	15.012	20.000	24.988

-----+-----+-----+-----+--  
 (--\*---)  
 -----+-----+-----+-----+--  
 -15            0            15            30

## CURRICULUM VITAE

### PERSONAL INFORMATION

Surname, Name: Poçan, Pelin  
Nationality: Turkish (TC)  
Date and Place of Birth: 17 January 1988, Konya  
Marital Status: Single  
Phone: +90 312 210 73 27  
email: pelin.pocan@metu.edu.tr

### EDUCATION

Degree	Institution	Year of Graduation
MS	METU Food Engineering	2015
BS	METU Food Engineering	2013
High School	Karatay Anadolu High School, Konya	2007

### WORK EXPERIENCE

Year	Place	Enrollment
2018-Present	METU Dept. of Food Eng.	YÖK 100/2000 Scholar
2018-2021	METU Dept. of Food Eng.	TÜBİTAK 2211/C Scholar
2013-2015	H2Biyotek Ltd. Şti.	Project Assistant

### FOREIGN LANGUAGES

Advanced English, Beginner German

### PUBLICATIONS

(1) Poçan, P.; Knapkiewicz, M.; Rachocki, A.; Oztop, M. H. Detection of Authenticity and Quality of the Turkish Delights (Lokum) by Means of Conventional and Fast Field Cycling Nuclear Magnetic Resonance Relaxometry.

Journal of Agricultural and Food Chemistry 2021.

<https://doi.org/10.1021/acs.jafc.1c00943>.

(2) Pocan, P.; Ilhan, E.; Florek–Wojciechowska, M.; Masiewicz, E.; Kruk, D.; Oztop, M. H. Exploring the Water Mobility in Gelatin Based Soft Candies by Means of Fast Field Cycling (FFC) Nuclear Magnetic Resonance Relaxometry. *Journal of Food Engineering* 2021, 294, 110422.

<https://doi.org/10.1016/j.jfoodeng.2020.110422>.

(3) Pocan, P.; Kaya, D.; Mert, B.; Oztop, M. H. Determination of the Best Drying Conditions for Gelatin Based Candies. *Gıda/ The Journal of Food* 2021, 46 (2), 279–295. <https://doi.org/10.15237/gida.GD20093>.

(4) Ilhan, E.; Pocan, P.; Ogawa, M.; Oztop, M. H. Role of ‘D-Allulose’ in a Starch Based Composite Gel Matrix. *Carbohydrate Polymers* 2020, 228, 115373. <https://doi.org/10.1016/j.carbpol.2019.115373>.

(5) Pocan, P.; Ilhan, E.; Oztop, M. H. Characterization of Emulsion Stabilization Properties of Gum Tragacanth, Xanthan Gum and Sucrose Monopalmitate: A Comparative Study. *Journal of Food Science* 2019, 84 (5), 1087–1093. <https://doi.org/10.1111/1750-3841.14602>.

(6) Pocan, P.; Ilhan, E.; Oztop, M. H. Effect of D-Psicose Substitution on Gelatin Based Soft Candies: A TD-NMR Study. *Magnetic Resonance in Chemistry* 2019, 57 (9), 661–673. <https://doi.org/10.1002/mrc.4847>.

(7) Pocan, P.; Bahcegul, E.; Oztop, M.; Hamamcı, H. Enzymatic Hydrolysis of Fruit Peels and Other Lignocellulosic Biomass as a Source of Sugar. *Waste and Biomass Valorization* 2017, 0 (0), 0. <https://doi.org/10.1007/s12649-017-9875-3>.

(8) Kilercioğlu, M.; Özel, B.; Karaçam, C. H.; Poçan, P.; Öztop, M. H. Investigating of the Effect of High Temperature and Humidity on Water and Fat Distribution in Hazelnuts By Magnetic Resonance Imaging (Mri) and Nmr Relaxometry Techniques. *Gıda / the Journal of Food* 2015, 40, 141–148.

<https://doi.org/10.15237/gida.gd14062>

## **HOBBIES**

Swimming, History, Turkish Folk Music